RELAXATION PROCESSES IN ELECTRONICALLY EXCITED MOLECULES (A) INTRAMOLECULAR EXCIMERS (B) EXCITED STATE PROTON TRANSFER

Dissertation for the Degree of Ph. D.

MICHIGAN STATE UNIVERSITY
PHAEDON AVOURIS

1974

This is to certify that the

thesis entitled
RELAXATION PROCESSES IN
ELECTRONICALLY EXCITED MOLECULES
(A) INTRAMOLECULAR EXCIMERS
(B) EXCITED STATE PROTON TRANSFER

presented by

PHAEDON AVOURIS

has been accepted towards fulfillment
of the requirements for

Ph.D. degree in Chemistry

M. Kasha El-Bayoumi
Major professor

Date Oct 22 / 74

O-7639

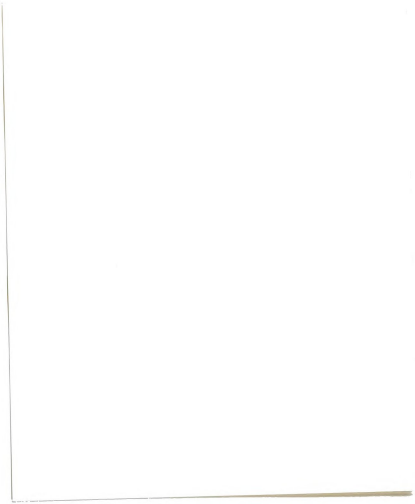

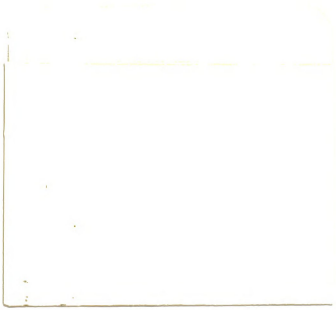

ABSTRACT

RELAXATION PROCESSES IN ELECTRONICALLY EXCITED MOLECULES

(A) INTRAMOLECULAR EXCIMERS

(B) EXCITED STATE PROTON TRANSFER

By

Phaedon Avouris

In the FIRST PART of the thesis various aspects of intramolecular excimer and exciplex behavior are investigated. The technique of time resolved fluorescence spectroscopy is used to study the dynamics of the association and dissociation processes of the intramolecular excimer formed in the excited state of 1,3-Bis(alpha-naphthyl)propane (1,3DNP). The specific rate constants of these processes are determined in media of different viscosity. It is found that the intramolecular excimer equilibrium is characterized by a high equilibrium constant ($\sim 10^4$) and that both the association and dissociation rates are viscosity dependent. Through coupling of transient kinetic data with steady illumination data and model calculations, various thermodynamic quantities describing the intramolecular excimer interaction are determined. A method for obtaining the radiative lifetime τ_F° of the excimer is developed, and the τ_F° value is discussed in terms of the excimer geometry. Other factors like the effects of oxygen and solvent polarity are investigated in the system 1,3DNP and also in 1,3-diphenylpropane (1,3DPP). Evidence is presented for intramolecular triplet excimers in viscous solutions and microcrystalline aggregates of 1,3DPP.

Other intramolecular systems studied are the systems 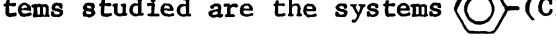 n = 1 ($PyCH_2P$), n = 3 (1,3PyPP). These systems, under various conditions, display a variety of interactions. In neutral alcohol solutions, the absorption spectra of 1,3PyPP do not show signs of ground state interactions while the room temperature fluorescence spectrum shows intramolecular mixed-excimer formation completely analogous to the 1,3DPP case. As the hydrogen bonding ability or acidity of the solvent increases, strong hydrogen bonding or protonation of the pyridinic nitrogen changes the interaction drastically. Under these conditions the absorption spectra of 1,3PyPP and $PyCH_2P$ show ground state interactions while the broad emission bands show extremely large Stokes shifts (14,000-15,000 cm^{-1}). These emissions are interpreted as charge-transfer emissions. This is supported by the out of plane polarization of the fluorescence and by thermodynamic arguments. Evidence is also presented that the emitting charge-transfer and exciplex states are not identical in these intramolecular systems. In low temperature rigid glasses the Stokes shifts are much smaller, demonstrating the importance of molecular and solvent Franck-Condon state relaxation. Phosphorescence arises from a localized excited state of the phenyl group. More subtle manifestations of the exciplex interaction (no exciplex emission) are observed in the case of rigid and non-rigid phenylcarboxylic acids. From the study of fluorescence and phosphorescence quantum yields and lifetimes, it appears that in the flexible molecules interaction of the carboxyl group and the aromatic ring results in enhanced intersystem crossing.

The SECOND PART of the thesis is devoted to the study of excited state proton transfer reactions, especially the various acid-base reactions in which 7-azaindole (7AI) is involved. Initially, the excited state

acid-base properties of 7AI are investigated through absorption and emission studies and the excited state pK_a^* and pK_b^* are determined. Time resolved spectroscopy is used to study the kinetics of double proton transfer in 7AI hydrogen bonded dimers. 7AI deuterated in the N_1 position is studied in a frozen 3-methylpentane matrix at 77°K. The analysis of the non-exponential character of the decay curves gives the forward and backward reaction rate constants. The phenomenon is clearly demonstrated through time resolved spectra in the nanosecond time range. The effect of isotopic substitution on the emission spectra is used to obtain the rate constant for proton transfer in non-deuterated 7AI. From the kinetic data at 77°K and the effect of temperature on the fluorescence spectra down to 4.2°K, it is concluded that quantum mechanical tunneling must be the mechanism by which the proton transfer occurs at very low temperatures. When 7AI is dissolved in alcohols, a new emission band appears in addition to the molecular fluorescence. The intensity ratio of the molecular band and the new emission is concentration independent. Through the effect of solvent deuteration on the fluorescence quantum yield of 7AI and other model compounds strong evidence is found that the new emission results from a tautomeric species resulting from double proton transfer between the excited 7AI and an alcohol molecule. Finally, the various mechanisms deactivating the lowest excited singlet state of 7AI in H_2O are studied through solvent isotope effects, temperature and pH studies.

RELAXATION PROCESSES IN ELECTRONICALLY EXCITED MOLECULES

(A) INTRAMOLECULAR EXCIMERS

(B) EXCITED STATE PROTON TRANSFER

By

Phaedon Avouris

A DISSERTATION

Submitted to

Michigan State University

in partial fulfillment of the requirements

for the degree of

DOCTOR OF PHILOSOPHY

Department of Chemistry

1974

TO MY MOTHER AND IN MEMORY OF MY FATHER

The author w
M. Ashraf El-Bay
the course of th
I would als
whose lectures
understanding.
on my committee
Finally s
Liedtke for nu
Miss Li Yang f

ACKNOWLEDGEMENTS

The author would like to express sincere appreciation to Professor M. Ashraf El-Bayoumi for his guidance, encouragement and friendship during the course of this investigation.

I would also like to express my gratitude to Professor J. F. Harrison whose lectures and informal discussions greately contributed to my scientific understanding. I also thank Professors G. Leroi and A. U. Khan for serving on my committee.

Finally special thanks go to my good friends and colleagues Dr. R. Liedtke for numerous discussions and help with computer programing and Miss Li Yang for encouragement and help with the proton transfer experiments.

TABLE OF CONTENTS

TABLE OF CONTENTS

TABLE OF CONTENTS---continued

TABLE OF CONTENTS-

ABLE OF CONTENTS---continued

BLE OF CONTENTS---continued

APTER 4---continued

LIST OF TABLES

LIST OF TABLES---

IST OF TABLES---continued

Figure 1a. Sche
in M

Figure 1b. Fors
Aro

Figure 2. Room
(1.2

Figure 3. The

Figure 4. The
Flu

Figure 5. Qua
Gro

Figure 6. The
Mo
Et

Figure 7. Th
Mo

Figure 8. De
Ex

Figure 9. T
(
A

Figure 10.

Figure 11.

Figure 12.

Figure 13.

Figure 14.

LIST OF FIGURES

LIST OF FIGURES--

T OF FIGURES---contined

LIST OF FIGURES-

ST OF FIGURES---continued

LIST OF FIGURES-

OF FIGURES---continued

E

A molecul

ent molecular

state. Such a

aggregate) is

dissociates a

inverse case

This case is

bound-excited

(excited sta

the main phe

Probabl

in 1924[1] who

discharge o

helium mole

of mercury.

leigh in 19

Beside

large orga

mers. In

of pyrene

CHAPTER 1

EXCIMERS-EXCIPLEXES-CHARGE TRANSFER COMPLEXES

INTRODUCTION

A molecule in an electronically excited state may behave as a differ-
molecular species. This can lead to associations unique to the excited
te. Such a case is the "excimer" association where the dimer (or higher
regate) is stable only during the lifetime of the excited state and
sociates after the emission of the photon. The excimer represents the
erse case of absorption followed by dissociation of the excited state.
s case is manifested by continuous absorption spectra (ground state
nd-excited unbound) while excimers show continuous emission spectra
:ited state bound-ground unbound). Continuous emission spectra provide
main phenomenological manifestation of excimer formation.

Probably the first observation of the excimer emission was that of Lyman
.924[1] who observed a diffuse-appearing band at 600.3 Å in a transformer
harge of helium. Sommer in 1927[2] attributed this emission to the
.um molecule, He_2*. Another of the early discovered excimers was that
ercury. The excimeric emission of mercury was discovered by Lord Ray-
h in 1929[3] and the assignment to Hg_2* was done by S. Mrozowski in 1937[4].

Besides the excimers found between excited and ground state atoms,
e organic molecules (e.g. aromatic hydrocarbons) form molecular exci-
. In 1954 Forster and Kasper[5] were studying the concentration dependence
yrene fluorescence when they observed that by increasing the concentration

of pyrene, the

while a new bro

intensity red s

to an excited

years this beh

the phenomenon

Excited s

called "excip

where it was

carbons by ar

5000 cm^{-1} to

to an excite

simple atomi

The obs

manifestatio

we mention

(1) The app

changes in

change is

that the n

(2) The em

state equi

(3) From

the dimer

tion; thi

observed

(4) The

pyrene, the fluorescence emission band (0,0 ~27,000 cm^{-1}) was quenched, le a new broad and structureless emission started appearing with a peak tensity red shifted by ~ 6000 cm^{-1}. The authors ascribed this new emission an excited state association between two pyrene molecules. For several rs this behavior was considered somehow unique to pyrene. Birks[6] showed phenomenon is common to most aromatic hydrocarbons and their derivatives.

Excited state associations between different kind of molecules are lled "exciplexes". They were discovered by Leonhardt and Weller[7] in 1963, re it was found that upon quenching the fluorescence of aromatic hydro-bons by aromatic amines, like anilines, a new broad band appeared about 00 cm^{-1} to the red of the hydrocarbon emission. This emission was assigned an excited complex of the hydrocarbon and the amine. Exciplexes between mple atomic systems like (KrAr)* were also reported recently[8].

The observation of a broad strutureless emission band is not the only nifestation of excimer formation. There are several criteria from which mention the following:

) The appearance of the broad emission band is not associated with any anges in the absorption spectra. Even after prolonged irradiation no ange is detected in the absorption spectrum. This supports the idea at the new emission is not due to photoproducts.

) The emission spectra show an "isostilbic" point indicative of the excited ate equilibrium.

) From Stern-Volmer relations the ratio of fluorescence intensities of dimer and monomer is expected to be proportional to monomer concentra-n; this is actually observed. No concentration-dependent changes are erved in the absorption spectrum.

The excimer formation is viscosity dependent and shows the characteristics

of diffusion controlle

(5) The decay of the m

If the excimer dissoci

described by a sum of

lished in the excited

a common lifetime.

(6) Thermodynamic dat

of association proces

Several other results

and we will talk abou

Excimer formatio

molecular crystals.

fluorescence and cr

molecules like napht

of an A type, in whi

dicular to one anoth

structures of a B ty

pairs (pyrene, benzo

(β-perylene , corone

crystals of the B t

interactions (sligh

further relaxation

formation to occur.

at very low tempera

10-50 kbar show par

and polyvinylnaphth

Excimers and

ffusion controlled reactions.

he decay of the monomer is usually described by a single exponential.

e excimer dissociation rate is significant then the monomer decay is

ibed by a sum of two exponentials. Finally if equilibrium is estab-

d in the excited state then both monomer and excimer will decay with

mon lifetime.

hermodynamic data always yield negative entropy changes characteristic

sociation processes.

al other results point to an excited state reversible association

e will talk about them in the text.

Excimer formation is not unique to fluid phases but is common in

ular crystals. Stevens[9] proposed a general relationship between

escence and crystal structure of aromatic compounds. "Elongated"

ules like naphthalene, anthracene, phenanthrene, favor structures

A type, in which adjacent molecules are oriented almost perpen-

ar to one another. "Disk-Shaped" molecules on the other hand, favor

tures of a B type, in which the molecules are either arranged in

(pyrene, benzo [g,h,i] perylene, α-perylene) or stacked in columns

rylene , coronene, ovalene). Excimer fluorescence occurs only in

als of the B type. The absorption spectra do not show any strong

actions (slight Davydov splitting may be observed). In the crystal,

er relaxation is needed from the ground state arrangement for excimer

tion to occur. Thus α-perylene no longer exhibits excimer fluorescence

y low temperatures[10], while crystals of type A under pressures of

kbar show partially excimeric emission[11]. Polymers like polystyrene

lyvinylnaphthalene exhibit excimeric emission[12].

xcimers and exciplexes can be formed in a variety of other situations,

for example:

a. Radical ion annihi

b. Triplet-Triplet an

c. Photodecomposition

The literature

Birks[14] and Stevens[1

While experimen

well established, th

complete. The most

a mixture of "excit

following the molec

discussed together

transfer interacti

and ground state i

discussed.

GRO

Consider two

and B) that are w

system is describ

Intermolecular el

symmetric with re

of the dimer is

where V_{ab} is the

xample:

dical ion annihilations (Chemiluminescence)

$$A\cdot^- + A\cdot^+ \longrightarrow (AA)^*$$

iplet-Triplet annihilation

$$^3A^* + {}^3A^* \longrightarrow {}^1(AA)^*$$

otodecomposition of dimers, like dianthracene.

The literature on excimers has been reviewed extensively by Forster[13], [14] and Stevens[15].

While experimentally the phenomenon of excimer association appears established, the theoretical description of the phenomenon is not lete. The most commonly used description of the excimer state is as ture of "exciton resonance and charge-transfer states". In the wing the molecular exciton and the charge-transfer models will be ssed together with a model which considers both exciton and charge-fer interactions. Since excimer luminescence reflects both excited round state interactions, the forces present in both cases will be ssed.

GROUND STATE INTERACTIONS-DISPERSION FORCES

Consider two ground state molecules of the same kind (labeled as A) that are weakly interacting. The ground state wave function of the m is described by:

$$\Psi_G = \phi_a\phi_b$$

molecular electronic overlap is neglected so $\phi_a\phi_b$ need not be anti-tric with respect to intermolecular electron exchange. The Hamiltonian e dimer is given by:

$$H = H_a + H_b + V_{ab}$$

V_{ab} is the intermolecular perturbation potential (electrostatic

interactions). The e

A and B is then

$$E_G = \langle \phi_a$$

where $E_a = E_b$ is the

element on the left

V_{ab} is expressed as

$$V = V_{\text{mono-mono}} + V_{\text{mo}}$$

This point-multipole

molecules a few Å a

multipole expansion

shown by Dalgarno a

truncated at some c

and better when R

For neutral m

the only important

circumstances the

The interact

dipole approximat

where X_a is the s

A and in the same

is

$$E^{(}$$

where $\langle X_a \rangle$, $\langle X_b \rangle$

coordinates in t

the X component

eractions). The energy of the ground state of the system of molecules
d B is then

$$E_G = \langle \phi_a\phi_b \,|H|\, \phi_a\phi_b \rangle = E_a + E_b + \langle \phi_a\phi_b | V_{ab} | \phi_a\phi_b \rangle$$

e $E_a = E_b$ is the energy of the isolated molecule while the matrix
ent on the left gives the van der Waals interaction energy. Usually
is expressed as a point-multipole expansion:

$$= V_{\text{mono-mono}} + V_{\text{mono-di}} + V_{\text{di-di}} + V_{\text{quad-quad}} + V_{\text{di-quad}} + V_{\text{octu-octu}} + \cdots\cdots$$

point-multipole expansion does not strictly apply to the case of
ecules a few Å apart. As a result of this the use of the complete
ipole expansion will lead to a divergent series in (R^{-1}) as has been
n by Dalgarno and Lewis[16]. This series is asymptotic, so that, when
cated at some order, it gives an approximate value which becomes better
better when R increases.

For neutral molecules the monopole interactions are zero. Usually
only important term is the dipole-dipole interaction term, in these
umstances the point dipole approximation is used.

The interaction energy between two molecules A and B in the point
ole approximation is

$$V = e^2/R^3 (X_a X_b + Y_a Y_b - 2Z_a Z_b) \qquad (1)$$

e X_a is the sum of the X coordinates of all the electrons in molecule
d in the same way for X_b, Y_a etc. The first order perturbation energy

$$E^{(1)} = e^2/R^3 (\langle X_a\rangle\langle X_b\rangle + \langle Y_a\rangle\langle Y_b\rangle - 2\langle Z_a\rangle\langle Z_b\rangle) \qquad (2)$$

e $\langle X_a\rangle$, $\langle X_b\rangle$ etc. are the expectation values of the sums of the
rdinates in the respective molecules $\langle \phi_a | X_a | \phi_a \rangle$ etc. By definition
X component of the dipole moment of molecule A is

$$\mu_{xa} = e\langle X_a \rangle \qquad (3)$$

So the first order er

For centrosymmetric

lene (D_{2h}) the matri

odd parity of the di

To get an inter

$$E^{(2)} = e^4/R^6 \sum_{i,j\neq 0} ($$

where ϕ_a^i is the i

the ground state wa

orientations of the

vanish so (5) is w

$$E^{(2)} = e^4/R^6 \sum_{i,j\neq 0} ($$

For isotropic mole

$$|X$$

$$|X$$

So (6) can be wri

$$E^{(2)} = 2$$

London[17] sir

for the static po

From studies of

found that the m

for which $E_k - E_0$

mately (9) is

o the first order energy can be written

$$E^{(1)} = 1/R^3(\mu_{xa}\mu_{xb} + \mu_{ya}\mu_{yb} - 2\mu_{za}\mu_{zb}) \qquad (4)$$

or centrosymmetric aromatic hydrocarbons like benzene (D_{6h}) and naphtha-
ene (D_{2h}) the matrix elements of the form of (3) vanish because of the
dd parity of the dipole operator.

To get an interaction energy we have to go to second order, then

$$E^{(2)} = e^4/R^6 \sum_{i,j\neq 0} (X_a^{io}X_b^{jo} + Y_a^{io}Y_b^{jo} - 2Z_a^{io}Z_b^{jo})^2/(E_{ao} + E_{bo} - E_{ai} - E_{bj}) \qquad (5)$$

$$X_a^{io} = \langle \phi_a^i | X_a | \phi_a^o \rangle \qquad \text{etc.}$$

here ϕ_a^i is the i excited state wavefunction of molecule A and ϕ_a^o is
he ground state wavefunction. If the interaction is averaged for all
rientations of the molecules, cross products involving XY, YZ and XZ
anish so (5) is written:

$$E^{(2)} = e^4/R^6 \sum_{i,j\neq 0} (X_a^{io\,2} X_b^{jo\,2} + Y_a^{io\,2} Y_b^{jo\,2} + 4 Z_a^{io\,2} Z_b^{jo\,2})/(E_{ao}+E_{bo}-E_{ai}-E_{bj}) \qquad (6)$$

or isotropic molecules (not aromatic hydrocarbons)

$$\begin{aligned} |X_a^{io}|^2 &= |Y_a^{io}|^2 = |Z_a^{io}|^2 = 1/3\,|F_a^{io}|^2 \\ |X_b^{jo}|^2 &= |Y_b^{jo}|^2 = |Z_b^{jo}|^2 = 1/3\,|F_b^{jo}|^2 \end{aligned} \qquad (7)$$

o (6) can be written:

$$E^{(2)} = 2e^4/3R^6 \sum_{i,j\neq 0} (|F_a^{io}|^2 |F_b^{jo}|^2)/(E_{ao} + E_{bo} - E_{ai} - E_{bj}) \qquad (8)$$

London[17] simplified further the above expression through the expression
or the static polarizability

$$\alpha = 2e^2/3 \sum_k (|F^{ko}|^2)/(E_k - E_o) \qquad (9)$$

rom studies of the frequency dependence of the polarizability it was
ound that the most important terms (contributions) arise from states
or which $E_k - E_o \approx I$ the ionization potential of that molecule. So approxi-
ately (9) is

$$\alpha = (2e^2/3I) \sum_k |F^{ko}|^2 \qquad (10)$$

and (8) may be writte

$$E^{(2}$$

Expression (11) gives

and B, while α_A and α

forces are always att

to the case of aniso

$$E^{(2)}$$

For an anisotro

a second order tenso

As the cooridinates

an optically inacti

Geometrically $\bar{\bar{\alpha}}$ is

be transformed by

quasi-scalar tenso

gonal elements (α_x

α_{xx}, α_{yy}, and α_{zz} a

and the directions

of the molecular

comes from the ex

$\vec{R}$.

$$\vec{E} = 1$$

which leads to de

the matrix repres

Two cases a

(1) Random orien

(8) may be written as

$$E^{(2)} = -3I_A I_B/2(I_A+I_B)\cdot(\alpha_A\alpha_B/R^6) \qquad (11)$$

ession (11) gives the dispersion energy for two isotropic molecules A
B, while α_A and α_B are the isotropic polarizabilities. The dispersion
es are always attractive. This expression can be easily generalized
he case of anisotropic molecules[18]

$$E^{(2)} = -\tfrac{1}{2}(I_A I_B \mathrm{tr}[\overline{\overline{T}}\overline{\overline{\alpha}}_A\overline{\overline{T}}\overline{\overline{\alpha}}_B])/(I_A+I_B)R^6 \qquad (12)$$

For an anisotropic molecule the polarizability is not a scalar but
cond order tensor

$$\overline{\overline{\alpha}} = \begin{vmatrix} \alpha_{xx} & \alpha_{xy} & \alpha_{xz} \\ \alpha_{yx} & \alpha_{yy} & \alpha_{yz} \\ \alpha_{zx} & \alpha_{zy} & \alpha_{zz} \end{vmatrix}$$

he cooridinates are rectangular $\overline{\overline{\alpha}}$ becomes a symmetrical tensor for
ptically inactive molecule, i.e., six independent elements are required.
etrically $\overline{\overline{\alpha}}$ is a polarizability ellipsoid. The symmetric tensor can
ransformed by appropriate rotation of its coordinate system into a
i-scalar tensor in the matrix of which the three pairs of non-dia-
l elements (α_{xy},α_{yx},α_{zx} etc.) are all zero. The diagonal components
α_{yy}, and α_{zz} are then the principal polarizabilities of the molecule
the directions along which that are measured are the principal axes
he molecular polarizability ellipsoid. $\overline{\overline{T}}$ which appears in equation (12)
s from the expression for the field $\vec{E}$ created by a dipole $\vec{\mu}$ at a point

$$\vec{E} = 1/R^3\vec{\nabla}\vec{R}/R[(\vec{R}/R)\vec{\mu}]- \vec{\mu})= 1/R^3(3\vec{R}/R \otimes \vec{R}/R-\overline{\overline{1}})$$

h leads to define $T = 3(\vec{R}/R \otimes \vec{R}/R) - \overline{\overline{1}}$. In an orthogonal basis xyz
matrix representing $\vec{R}/R \otimes \vec{R}/R$ is easy to obtain.

Two cases are important for us

Random orientation of the two interacting molecules,

(2) Stacked aromatic

In the first case we

is the isotropic pola

we can get the intera

$$\overline{\overline{T}} = 3(\vec{R} \otimes \vec{R})/$$

So $\mathrm{Trace}(T\alpha_A T\alpha_B) = ($

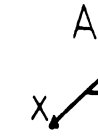

If the stacking is

Tr

So (12) becomes

$$E_d$$

For aromatic hydr

polarized, the α_{xx}

out of plane pola

tions that lie hi

the following val

2) Stacked aromatic molecules

n the first case we can use equation (11) where $\alpha = (\alpha_{xx} + \alpha_{yy} + \alpha_{zz})/3$ s the isotropic polarizability. In the case of stacked configuration e can get the interaction as follows:

$$\bar{\bar{T}} = 3(\vec{R} \otimes \vec{R})/R^2 - \bar{\bar{1}} = 3/R^2 \begin{vmatrix} xx & xy & xz \\ yx & yy & yz \\ zx & zy & zz \end{vmatrix} - \begin{vmatrix} 1 & 0 & 0 \\ 0 & 1 & 0 \\ 0 & 0 & 1 \end{vmatrix}$$

$$\text{Trace}(\bar{\bar{T}}\alpha_A \bar{\bar{T}}\alpha_B) = (3x^2-1)^2 \alpha_{A_{xx}} \alpha_{B_{xx}}/R^2 + (3y^2-1)^2 \alpha_{A_{yy}} \alpha_{B_{yy}}/R^2 + (3z^2-1)\alpha_{A_{zz}} \alpha_{B_{zz}}/R^2$$

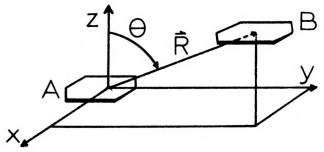

f the stacking is vertical then x=y=0 and

$$\text{Trace}\,(\bar{\bar{T}}\alpha_A \bar{\bar{T}}\alpha_B) = (3\cos^2\theta - 1)^2 \alpha_{A_{zz}} \alpha_{B_{zz}} = 4\alpha_{A_{zz}} \alpha_{B_{zz}} \quad (\theta = 90^\circ)$$

o (12) becomes

$$E_{disp} = -I_A I_B \alpha_{A_{zz}} \alpha_{B_{zz}}/(I_A+I_B)R^6 \qquad (13)$$

or aromatic hydrocarbons with $\pi\pi^*$low excited states, which are in plane olarized, the α_{xx} and α_{yy} principal polarizabilities are larger than the ut of plane polarizability α_{zz} which is determined mainly by $\pi\sigma^*$ transi- ions that lie higher in energy. For example LeFevre and Sundaram[19] give he following values

Compound	$\alpha_{xx} = \alpha_{yy}(\times 10^{23})$	$\alpha_{zz}(\times 10^{23})$ in cm^3
Benzene	1.12	0.73
Triphenylene	3.89	1.54
Coronene	5.68	2.07

In conclusion we see th

(1) For nonpolar ground

second order and depend

(2) For planar aromatic

favorable orientation f

figuration repulsive fo

one would expect that

wich configuration to

EXCITED STATE

The exciton conce

in 1931[20] in connectio

heat in rare-gas solid

exciton model to the

tals. Since that tim

book "Theory of Molec

area of molecular and

cally using exciton t

and its applications

to consider in the

and an unexcited mol

we have the two mole

tance/$\lambda_{emission}$ <1).

and becomes excited,

On the other hand if

be

nclusion we see that:

or nonpolar ground state molecules the interaction appears in the
d order and depends on the polarizability

or planar aromatic hydrocarbons the stacked orientation is the least
able orientation from the dispersion energy standpoint. In this con-
ation repulsive forces (closed-shell interactions) are maximal. Thus
ould expect that ground state interactions particularly in the sand-
configuration to be repulsive as it is usually assumed.

EXCITED STATE INTERACTION—THE MOLECULAR EXCITON MODEL

The exciton concept was introduced into solid state physics by Frenkel
[20] in connection with the transformation of excitation energy into
in rare-gas solids. In 1948 A. S. Davydov[21] applied the molecular
on model to the problem of the electronic states of naphthalene crys-
Since that time and especially after the publication of Davydov's
"Theory of Molecular Excitons"[22], a great variety of problems in the
of molecular and solid state physics have been approached theoreti-
using exciton theory. For a recent review of the exciton theory
s applications see the article by Philpott[23]. Here we are going
sider in the most simplified form the interaction of an excited
unexcited molecule on the basis of the exciton model. Say again
e the two molecules A and B (of the same kind) in proximity (Dis-
$\lambda_{emission} < 1$). Now we consider that molecule A absorbs a photon
comes excited, then we can write the wavefunction of the system as

$$\Psi_1 = \phi_a^* \phi_b$$

other hand if the excitation is localized on b the wavefunction will

$$\Psi_2 = \phi_a \phi_b^*$$

Ψ_1 and Ψ_2 are degenerat

the system. Proper lin

stationary states of th

sentations of the dimer

perturbation theory.

terminant:

where

H_{aa}

H_{ab}

(* denotes electronic

the determinant are

and the eigenvectors

In both stationary e

molecules, A and B,

The node correspond

an excitation node.

transition moments

Evaluating E' and E

$E' = E_a^* +$

$E'' = E_a^* -$

In equations 16&17

Waals forces and a

d Ψ_2 are degenerate states and do not describe stationary states of ystem. Proper linear combinations of these two localized states are onary states of the dimer and belong to different irreducible repre- tions of the dimer point group. This is a simple case of degenerate rbation theory. The first order energies can be found from the de- nant:

$$\begin{vmatrix} H_{aa} - E & H_{ab} \\ H_{ab} & H_{bb} - E \end{vmatrix} = 0$$

$$H_{aa} = H_{bb} = \langle \phi_a^* \phi_b \,|H|\, \phi_a^* \phi_b \rangle$$

$$H_{ab} = H_{ba} = \langle \phi_a^* \phi_b \,|H|\, \phi_a \phi_b^* \rangle$$

notes electronic excitation, not complex conjugates), the roots of eterminant are

$$E' = H_{aa} + H_{ab}$$

$$E'' = H_{aa} - H_{ab}$$

he eigenvectors

$$\Psi' = 2^{-\frac{1}{2}}(\phi_a^* \phi_b + \phi_a \phi_b^*) \tag{14}$$

$$\Psi'' = 2^{-\frac{1}{2}}(\phi_a^* \phi_b - \phi_a \phi_b^*) \tag{15}$$

th stationary exciton states Ψ' and Ψ'' the excitation is on both ules, A and B, i.e., the excitation is collective or delocalized. ode corresponding to the minus sign in the exciton wavefunction is citation node. At the excitation node, the phase relation between ition moments on the respective molecular centers changes sign. ating E' and E" we get:

$$E' = E_a^* + E_b + \langle \phi_a^* \phi_b \,|V_{ab}|\, \phi_a^* \phi_b \rangle + \langle \phi_a^* \phi_b \,|V_{ab}|\, \phi_a \phi_b^* \rangle \tag{16}$$

$$E'' = E_a^* + E_b + \langle \phi_a^* \phi_b \,|V_{ab}|\, \phi_a^* \phi_b \rangle - \langle \phi_a^* \phi_b \,|V_{ab}|\, \phi_a \phi_b^* \rangle \tag{17}$$

uations 16&17, the term $\langle \phi_a^* \phi_b |V_{ab}| \phi_a^* \phi_b \rangle$ represents again the van der forces and almost always results in a lowering of the energy of the

system. If energy leve

photon resonance and th

term leads to repulsion

always attractive. The

splitting"

$$\Delta$$

and describes the effe

the dipole approximati

$$\langle \phi_a | X_a | \phi_a^* \rangle = M_a^X$$

$$\langle \phi_b | X_b | \phi_b^* \rangle = M_b^X$$

the exciton splitting

$$\Delta\varepsilon = - |M_a|^2$$

where M_a represents t

$\cos\theta_a^y$, $\cos\theta_a^z$ represen

moment of a, M_a makes

maximum exciton inter

in a perfect way, "p

will be given then b

Experimentally M is

the compound under

ε is the molar ext

e.s.u.. Figure 1a

though in the molec

the exciton splitt

allowed spectral t

by evaluating the

em. If energy levels exist betwen the two states involved in the
on resonance and the ground state then a situation may arise that this
leads to repulsion[24]. In the ground state van der Waals forces are
ys attractive. The last term in equations 16&17 gives the "exciton
tting"

$$\Delta\varepsilon = \langle \phi_a^* \phi_b | V_{ab} | \phi_a \phi_b^* \rangle$$

describes the effect of photon exchange between A and B. Using again
dipole approximation for V_{ab} and recognizing that

$\langle \phi_a | X_a | \phi_a^* \rangle = M_a^x$: x component of the transition moment of A

$\langle \phi_b | X_b | \phi_b^* \rangle = M_b^x$: x component of the transition moment of B, etc.,

xciton splitting term is given by the general expression

$$\Delta\varepsilon = - |M_a|^2 / R_{ab}^3 (2\cos\theta_a^z \cos\theta_b^z - \cos\theta_a^y \cos\theta_b^y - \cos\theta_a^x \cos\theta_b^x)$$

M_a represents the transition moment in the free molecule, and $\cos\theta_a^x$,
, $\cos\theta_a^z$ represent the cosines of the angles which the transition
t of a, M_a makes with the x, y, z axes of the coordinate frame. The
um exciton interaction will appear when the two molecules are stacked
perfect way, "perfect sandwich" configuration. The exciton splitting
be given then by

$$\Delta\varepsilon = - M_a^2 / R_{ab}^3$$

imentally M is obtained from the absorption of a dilute solution of
ompound under consideration using the equation

$$M^2 = 3.97 \times 10^{-20} e^2 \int \varepsilon d\tilde{\nu} / \tilde{\nu}$$

the molar extinction coefficient and e is the electronic charge in
.. Figure 1a describes the case of a "perfect sandwich" dimer. Al-
h in the molecular dimer two exciton states theoretically result from
xciton splitting, both of these may not necessarily be observed as
ed spectral transitions. Let us examine the spectral selection rules
aluating the matrix elements of the electric dipole operator between

the ground state and the

the transition moment ve

M

M

or $M^{1,"} = [\langle \phi_a \phi_b | M_a + M_b | ($

Orthogonality and norma

or

Similarly

For the "perfect sandw

and

Thus, the transition

the transition moment

strength (f) for elec

transition to $\Psi"$ is

f

In conclusion we see

interaction energy w

lated molecule energ

correction is in fi

guration is the lea

In our discuss

for simplicity tha

there is no electr

spin free, photon

e ground state and the stationary exciton states of the dimer. Thus,

e transition moment vector of the dimer is given by

$$M' = \langle \Psi_G | M_a + M_b | \Psi' \rangle$$

$$M'' = \langle \Psi_G | M_a + M_b | \Psi'' \rangle$$

$$M','' = [\langle \phi_a \phi_b | M_a + M_b | (\phi_a^* \phi_b \pm \phi_a \phi_b^*) \rangle]/2^{\frac{1}{2}}$$

thogonality and normalization properties of the wavefunctions lead to:

$$M' = \langle \phi_a | M_a | \phi_a^* \rangle / 2^{\frac{1}{2}} + \langle \phi_a | M_a | \phi_a^* \rangle / 2^{\frac{1}{2}}$$

$$M' = (M_a + M_b)/2^{\frac{1}{2}}$$

milarly $$M'' = (M_a - M_b)/2^{\frac{1}{2}}$$

r the "perfect sandwich" dimer

$$M' = 2^{-\frac{1}{2}}(M_a - M_b) = 0$$

d $$M'' = 2^{-\frac{1}{2}}(M_a + M_b) = 2M_a/2^{\frac{1}{2}}$$

us, the transition moments for the dimer are given as superpositions of e transition moments for the individual molecules. The oscillator rength (f) for electric dipole transitions to Ψ' is zero, while the ansition to Ψ'' is equal to

$$f'' \propto |M''^2| = |2M_a^2| \quad \text{or} \quad f'' = 2f_{monomer}$$

conclusion we see that for non-polar molecules in the ground state, the teraction energy will be given as a second order correction to the iso- ted molecule energy. In the excited-ground state case, however, the rrection is in first order. For aromatic hydrocarbons the stacked confi- ration is the least favored in the ground state.

TRIPLET MOLECULAR EXCITONS

In our discussion of the simple molecular exciton theory we assumed simplicity that there was no electronic overlap between A and B. If ere is no electronic overlap and since the Hamiltonian is practically n free, photon resonance of the form

is not allowed because

allow electronic overl

cribing the interactio

$$H_{ab} = \int \phi_a^*(1)\phi_b(2$$

$$-\int \phi_a^*(1)\phi_b(2$$

where $H(1,2) = 1/r_{1,2}$

spin wavefunctions.

is the same integral

i.e., it is the Coul

and $\phi_b(2)\phi_b^*(2)$. Si

ordinates of electro

has non-zero value

this Coulomb term va

exchange integral wh

the "overlap charge

has a non-zero valu

dition is satisfied

overlap decreases

tegral will be sig

The concept o

explain certain mu

crystals[25]. Since

ionic and molecul

exciton propertie

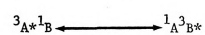

I II

is not allowed because it involves a spin forbidden transition. If we allow electronic overlap the picture is changed. The matrix element describing the interaction between states I and II is given by

$$H_{ab} = \int \phi_a^*(1)\phi_b(2)H(1,2)\phi_a(1)\phi_b^*(2)\chi_a(1)\chi_b(2)\chi_a(1)\chi_b^*(2)dv(1,2)$$
$$-\int \phi_a^*(1)\phi_b(2)H(1,2)\phi_b^*(1)\phi_a(2)\chi_a^*(1)\chi_b(2)\chi_b^*(1)\chi_a(2)dv(1,2) \quad (18)$$

where $H(1,2) = 1/r_{1,2}$, ϕ's are the spatial wavefunctions and x's are the spin wavefunctions. The first term in the right-hand side of equation 18 is the same integral as the one which arises in the absence of exchange, i.e., it is the Coulomb integral between the charge distributions $\phi_a^*(1)\phi_a(1)$ and $\phi_b(2)\phi_b^*(2)$. Since H(1,2), being the function of only the space coordinates of electrons, does not affect the spin function, the first term has non-zero value only when $\chi_a^*(1) = \chi_a(1)$ and $\chi_b(1) = \chi_b^*(2)$. Therefore this Coulomb term vanishes in the present case. The second term is the exchange integral which represents the electrostatic interaction between the "overlap charge distributions" $\phi_a^*(1)\phi_b^*(1)$ and $\phi_a(1)\phi_b(1)$, and which has a non-zero value when $\chi_a^*(1) = \chi_b^*(2)$ and $\chi_a(1) = \chi_b(2)$. The last condition is satisfied in the present case. However, since the electronic overlap decreases rapidly with intermolecular distance, the exchange integral will be significant only if the molecules are very close.

The concept of the spin multiplet state exciton has been introduced to explain certain multiplet structures occuring in the optical spectra of ionic crystals[25]. Since that time numerous investigations of triplet excitons in ionic and molecular crystals have appeared. For a description of the triplet exciton properties see for example the work by Avakian and Merrifield[26].

The theory of cha
veloped by Mulliken in
of this theory with en
of the subject see the
Mulliken and Pearson[3]

The quantum-mech
molecular complex in
for normal state), th
of the Schroedinger w

Mulliken represe
state wavefunctions ϕ
acceptor (A) with co
and interacting. For

In the case tha
writes ψ

Here the no-bond wav
wavefunctions ϕ_D and
due to possible clas
attractive (dispersi
in ϕ_D and ϕ_A which
upon complexing.

The function ϕ
pair obtained by re
previously unoccupi
between the odd ele
The ψ_N function is

CHARGE-TRANSFER INTERACTIONS

The theory of charge transfer complexes in its present form was de-
oped by Mulliken in 1952[27]. Here we are going to discuss some aspects
this theory with emphasis on electronic spectra. For excellent reviews
the subject see the articles of McGlynn[28], Briegleb[29], Murrel[30] and
liken and Pearson[31].

The quantum-mechanical description for the electronic structure of a
ecular complex in its ground electronic state is given by ψ_N(N stands
normal state), the wavefunction which is the lowest-energy solution
the Schroedinger wave equation for all the electrons in the complex.

Mulliken represented ψ_N for a 1:1 complex in terms of the normal-
te wavefunctions ϕ_D and ϕ_A of the electron donor (D) and the electron
eptor (A) with corrections because the two partners are close together
interacting. For this purpose, ϕ_D and ϕ_A need not actually be known.

In the case that donor and acceptor are even-electron systems Mulliken
es

$$\psi_N = a\phi_0(D,A) + b\phi_1(D^+\text{-}A^-)$$

no-bond dative

the no-bond wavefunction $\phi_0(D,A)$ is an antisymmetrized product of the
functions ϕ_D and ϕ_A each first corrected for any polarization effects
to possible classical electrostatic forces and to quantum mechanical
active (dispersion) and repulsive (exchange) forces together with changes
$_D$ and ϕ_A which result from changes in the internal geometry of D and A
complexing.

The function ϕ_1 is of Heitler-London type for the hypothetical $D^+\text{-}A^-$
obtained by removing one electron from an MO in D, putting it into a
lously unoccupied MO of A, and possibly forming a weak chemical binding
een the odd electrons now situated on the two components of the complex.
$'_N$ function is normalized to unity which means that $a^2+b^2+2abS_{01} = 1$

where $S_{01} = \langle \phi_0 | \phi_1 \rangle$. A

they should belong to t

If the ground stat

to quantum theory princ

can be called a charge-

$$\psi_V$$

The coefficients b* an

cited-state wavefuncti

ψ_V is normalized so a*

quirement $\langle \psi_N | \psi_V \rangle = 0$

and b* = b. Since fo

($a^2 \gg b^2$) and so (bec

is mostly dative (a^{*2}

essentially amounts t

THE ENERGIES

To obtain the e

complex is of course

approximate expressi

Since both ψ_N and ψ_V

problem is reduced s

mantal equation:

where

Noting that $H_{10} =$

roots which are to

ere $S_{01} = \langle \Phi_0 | \Phi_1 \rangle$. An important property of Φ_0 and Φ_1 is of course that ey should belong to the same group theoretical symmetry species.

If the ground state of the complex is described by ψ_N, then according quantum theory principles there must be also an excited state ψ_V which n be called a charge-transfer (CT) state given by

$$\psi_V = -b^*\Phi_0(D,A) + a^*\Phi_1(D^+A^-)$$

ie coefficients b* and a* are determined by the requirement that the ex- .ted-state wavefunction be orthogonal to the ground state wavefunction. , is normalized so $a^{*2}+b^{*2}-2a^*b^*S_{01} = 1$ and from the orthogonality re- iirement $\langle \psi_N | \psi_V \rangle = 0$ follows that $a^* \simeq a$, $b^* \simeq b$. If $S_{01} = 0$ then $a^* = a$ id $b^* = b$. Since for loose complexes the ground state is mostly no -bond $a^2 >> b^2$) and so (because of the orthogonality requirement) the excited state s mostly dative ($a^{*2} >> b^{*2}$). Excitation of an electron from ψ_N to ψ_V ssentially amounts to the transfer of an electron from D to A.

THE ENERGIES OF THE NORMAL AND CHARGE-TRANSFER STATES

To obtain the exact solution of the Schroedinger equation for the mplex is of course not feasible. For this reason we have to use the pproximate expression for ψ_N and ψ_V and apply the variation principle. nce both ψ_N and ψ_V are two component linear variation functions the roblem is reduced simply to the solution of a two dimentional determi- ntal equation:

$$\begin{vmatrix} H_{00} - E & H_{01} - S_{01}E \\ H_{10} - S_{01}E & H_{11} - E \end{vmatrix} = 0$$

ere

$$H_{00} = E_0 = \langle \Phi_0 | H | \Phi_0 \rangle$$

$$H_{11} = E_1 = \langle \Phi_1 | H | \Phi_1 \rangle$$

$$H_{01} = E_{01} = \langle \Phi_0 | H | \Phi_1 \rangle$$

$$H_{10} = E_{10} = \langle \Phi_1 | H | \Phi_0 \rangle$$

ting that $H_{10} = H_{01}$ the solution of this determinant for for E has two ots which are to be identified as E_N and E_V

$$E = \{$$

Here $\beta_$

β

and $\Delta \equiv E_1 - E_0$ ($\Delta > 0$ u

The lower energy

is E_V, even if $\Delta < 0$. A

the appearance of a ne

band. The frequency

$$h\nu_{CT} =$$

Knowing the energies

cients b/a and b^*/a^*

$$\lambda \equiv b/a =$$

and $\lambda^* \equiv b^*/a^*$

In this way the wavef

If $(\Delta/2)^2 \gg \beta_0\beta_1$, and

for weak complexes,

then

The position of the

and $\beta_0^2 + \beta_1^2$. Clas

is the energy of fo

of formation of the

For a series o

equation 19 can be

$$E = (\tfrac{1}{2}(E_0+E_1)-S_{01}E_{01}\pm[(\tfrac{1}{2}\Delta)^2+\beta_0\beta_1]^{\frac{1}{2}})/(1-S_{01}^2)$$

Here $\beta_0 \equiv E_{01} - E_0S_{01}$ $(\beta_0 < 0)$

$\beta_1 \equiv E_{01} - E_1S_{01}$ $(\beta_1 < 0)$

and $\Delta \equiv E_1 - E_0$ ($\Delta > 0$ usually but sometimes $\Delta < 0$).

The lower energy root is always called E_N (normal state), the upper is E_V, even if $\Delta < 0$. As we said the complex formation is associated with the appearance of a new absorption band the so called charge-transfer (CT) band. The frequency of the CT band is

$$h\nu_{CT} = E_V - E_N = 2[(\Delta/2)^2 + \beta_0\beta_1]^{\frac{1}{2}}/(1 - S_{01}^2)$$

Knowing the energies E_N and E_V we can now obtain the ratio of the coefficients b/a and b*/a*

$$\lambda \equiv b/a = -(E_0-E_N)/(E_{01}-S_{01}E_N) = -(E_{01}-S_{01}E_N)/(E_1-E_N)$$

and $$\lambda^* \equiv b^*/a^* = (E_{01}-S_{01}E_V)/(E_0-E_V) = (E_1-E_V)/(E_{01}-S_{01}E_V)$$

In this way the wavefunctions can be written

$$\Psi_N = (\phi_0 + \lambda\phi_1)/(1 + 2\lambda S_{01} + \lambda^2)^{\frac{1}{2}}$$

$$\Psi_V = (\phi_1 - \lambda^*\phi_0)/(1 - 2\lambda^*S_{01} + \lambda^{*2})^{\frac{1}{2}}$$

If $(\Delta/2)^2 \gg \beta_0\beta_1$, and if $S_{01}^2 \ll 1$ as is expected to be more or less true for weak complexes, the exact expressions above reduce to the following

$$E_N = E_0 - \beta_0^2/\Delta + \text{small correction terms}$$

$$E_V = E_1 + \beta_1^2/\Delta + \text{small correction terms}$$

then $$h\nu_{CT} = \Delta + (\beta_0^2 + \beta_1^2)/\Delta + \ldots \qquad (19)$$

The position of the CT band is sometimes used to empirically estimate Δ and $\beta_0^2 + \beta_1^2$. Classically $E_1 - E_0 = I_D - A_A - (\Delta E_{D^+A^-} - \Delta E_{DA})$ where I_D is the energy of formation of the D^+A^- structure and E_{DA} is the energy of formation of the DA structure.

For a series of closely related weak complexes with a single acceptor equation 19 can be written in the form

Briegleb[29] showed that

fitted with curves of

curve-fitting is moder

types of complexes, b

Pearson[33].

Alternatively

where ΔE_V and ΔE_N are

excited and ground s

The discussion

two different chemic

similar we reach the

two molecules A whic

$$\Psi_N = a\phi_0($$

THE DETAILED FORM

The no-bond st

where the D and A r

fication of their

tions they have in

spins of the elect

$$\phi_0^{[N]}(D,A) = \sqrt{}$$

where the donor co

mod means that the

by the presence o

$$h\nu_{CT} = I_D - C_1 + C_2/(I_D - C_1) \qquad (20)$$

Briegleb[29] showed that experimental ν_{CT} values plotted against I_D and fitted with curves of the form (20) can give values of C_1 and C_2. The curve-fitting is moderate (scattered points) and has been applied to various types of complexes, besides Briegleb, by Becker and Chen[32] and Mulliken and Pearson[33].

Alternatively

$$\begin{aligned} h\nu_{CT} &= E_V - E_N \\ &= I_D - A_A - (\Delta E_V - \Delta E_N) \\ &= I_D - A_A - C \end{aligned}$$

where ΔE_V and ΔE_N are the energies of formation of the DA complex in the excited and ground states, respectively, and C is their difference.

The discussion above was describing the situation where D and A are two different chemical species. When D and A are becoming more and more similar we reach the case of a self-complex. In this case the Ψ_N between two molecules A which we label as 1 and 2 can be written as

$$\Psi_N = a\phi_0(A_1,A_2) + b[\phi_1(A_1^+ - A_2^-) + \phi_1(A_1^- - A_2^+)]$$

THE DETAILED FORM OF THE WAVEFUNCTIONS-THE CHARGE TRANSFER TRIPLET STATE

The no-bond structure ϕ_0 is defined as we said for a hypothetical state where the D and A molecules are pressed together, with more or less modification of their original geometrical configurations, into the configurations they have in the complex. ϕ_0 is a function of the coordinates and spins of the electrons in the complex. It can be expressed as follows:

$$\phi_0^{[N]}(D,A) = \mathcal{A}\,\Psi_{mod}[1\ldots M]_{(D)}\,\Psi_{mod}[M+1\ldots N]_{(A)}$$

where the donor contains M electrons and the acceptor N-M. The subscript mod means that the electronic wavefunction of the, say, donor is modified by the presence of the acceptor and vice versa. The donor wavefunction

$\Psi_{mod}(D)$ is antisymmetr

M electrons, whereas

Besides this "lo

antisymmetric in all

can be written in ter

the presence of each

$$\phi_0(D,A) = \mathcal{A}[\omega_d($$

Here ω_d refers to on

while ω_a and ω_a' ref

ω_d which supplies th

trons, while the acc

The dative fun

$$\Psi' = \mathcal{A}_{\Psi_{mod}}(\alpha)\phi_1($$

in Ψ' the electron

and placed in the

dative and no-bond

$$\Psi'' = \mathcal{A}_{\Psi_{mod}}(\beta)$$

here electron 1 fr

electrons 1 and 2

on D+ and one on

(S=0). Besides t

be a triplet stat

$\psi_{mod}(D)$ is antisymmetric with respect to the exchange of any two of its M electrons, whereas $\psi_{mod}(A)$ is antisymmetric in its N-M electrons.

Besides this "local" antisymmetrization the operator $\mathcal{A}$ makes $\phi_0(D,A)$ antisymmetric in all the N electrons of the complex. The above wavefunction can be written in terms of the MO's of the donor and acceptor (modified by the presence of each other, but only slightly in weak complexes)

$$\phi_0(D,A) = \mathcal{A}[\omega_d(1)\alpha(1)\omega_d(2)\beta(2)\omega_d'(3)\alpha(3)\ldots\omega_a(M+1)\alpha(M+1)$$
$$\omega_a(M+2)\beta(M+2)\omega_a'(M+3)\alpha(M+3)\ldots\ ]$$

Here ω_d refers to one of the MO's on the donor, ω_d' to another, and so on, while ω_a and ω_a' refer to MO's on the acceptor. In $\phi_0(D,A)$ the donor MO ω_d which supplies the electron in donor-acceptor action contains two electrons, while the acceptor MO into which the electron will go is unoccupied.

The dative function $\phi_1(D^+\text{-}A^-)$ can be written as:

$$\phi_1(D^+\text{-}A^-) = (\psi' + \psi'')/[2(1+S'')]^{\frac{1}{2}}$$

$$\psi' = \mathcal{A}\psi_{mod}^{(\alpha)}(D+)\psi_{mod}^{(\beta)}(A^-) = \mathcal{A}[\omega_d(1)\alpha(1)\omega_{a-}(2)\beta(2)\omega_d'(3)\alpha(3)\ldots$$
$$\omega_a(M+1)\alpha(M+1)\omega_a(M+2)\beta(M+2)\omega_a'(M+3)\alpha(M+3)\ldots\ ]$$

In ψ' the electron number 2 has been removed from the spinorbital $\omega_d\beta$ and placed in the spin-orbital $\omega_{a-}\beta$ (strictly of course the MO's in the dative and no-bond structure are not the same)

$$\psi'' = \mathcal{A}\psi_{mod}^{(\beta)}(D^+)\psi_{mod}^{(\alpha)}(A^-) = \mathcal{A}[\omega_{a-}(1)\alpha(1)\omega_d(2)\beta(2)\omega_d'(3)\alpha(3)\ldots$$
$$\omega_a(M+1)\alpha(M+1)\omega_a(M+2)\beta(M+2)\omega_a'(M+3)\alpha(M+3)]$$

Here electron 1 from ω_d is placed into the orbital ω_{a-}. If we consider electrons 1 and 2 only, the dative function ϕ_1 has two odd electrons (one on D+ and one on A^-). The combination $\psi' + \psi''$ gives a singlet wavefunction (S=0). Besides the state with S=0 we can have a state with S=1 which will be a triplet state.

$$\psi_T = \phi_1'(D^+\text{-}A^-)$$

Ψ_T is pure dative, sinc

triplet has three subst

For $M_S=0$, Ψ_T is exactly

$$\Psi_T$$

and $M_S = \pm 1$ functions

$$\Psi_T$$

and Ψ_T

THEORETI

In this section

excimer state. We wi

of immediate interest

excimer theoretically

binding to be due to

formation process in

(1) The lowest excit

which has a small t

long lifetime of th

monomer concentrati

(2) The ^1L_b state s

has a large transi

of the ^1L_a state i

state results in t

the lowest ^1L_b com

energy ^1L_a compone

fluorescence. Sh

not account for t

in order to accou

Ψ_T is pure dative, since ϕ_1', being triplet, cannot mix with ϕ_0. Every triplet has three substates (approximately degenerate) with $M_S = -1, 0, +1$. For $M_S=0$, Ψ_T is exactly like Ψ_1 except for a change from $\Psi' + \Psi''$ to $\Psi' - \Psi''$

$$\Psi_{T,0} = (\Psi' - \Psi'')/[2(1-S'^2)]^{\frac{1}{2}}$$

and $M_S = \pm 1$ functions can be described as

$$\Psi_{T,+1} = \mathcal{A}\Psi_{D+}^{(\alpha)}\Psi_{A-}^{(\alpha)}$$

and

$$\Psi_{T,-1} = \mathcal{A}\Psi_{D+}^{(\beta)}\Psi_{A-}^{(\beta)}$$

THEORETICAL DESCRIPTION OF THE EXCIMER STATE

In this section we will outline the usual approach in describing the excimer state. We will consider the case of naphthalene excimer which is of immediate interest to us. The first to consider the case of naphthalene excimer theoretically was Th. Forster in 1962[34]. He attributed the excimer binding to be due to exciton coupling. His general model for the excimer formation process in the case of aromatic hydrocarbons was as follows:

(1) The lowest excited singlet state of the monomer should be a ^1L_b state, which has a small transition moment to the ground state ^1A. The relatively long lifetime of this state allows excimer formation to occur at reasonable monomer concentration.

(2) The ^1L_b state should be adjacent to a higher energy ^1L_a state, which has a large transition moment to the ground state. The large splitting of the ^1L_a state in contrast to the usually small splitting of the ^1L_b state results in the lowering of one of the ^1L_a exciton components below the lowest ^1L_b component, figure 1b. It is the transition from this lowest energy ^1L_a component to the ground state which Forster attributed the excimer fluorescence. Shortly after it was realized that the exciton coupling can not account for the excimer binding energy. For the naphthalene excimer in order to account for the binding energy using $\Delta\varepsilon = |M^2|/R^3$, the physically

$\phi_a^*\phi_b$ ϕ

Figure 1a. Schem
Molec

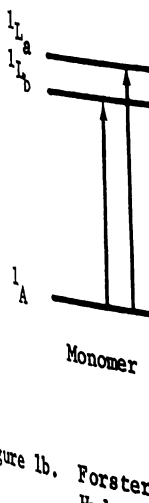

Figure 1b. Forster
Hydroca

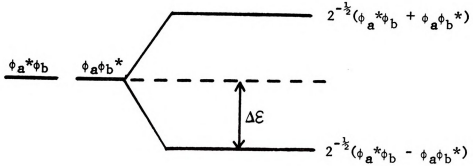

Figure 1a. Schematic Energy Diagram Showing Exciton Splitting in Molecular Dimers.

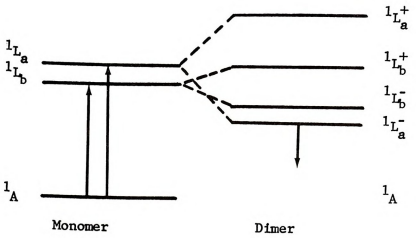

gure 1b. Forster's[34] Exciton Model of Excimer Formation in Aromatic Hydrocarbons.

unacceptable R of 1.8Å

Slifkin[35] conside

in the excimer emissi

hydrocarbons he found

the excimer emission

charge transfer state

A=electron affinity,

and R is a term resul

charge resonance sta

In the case of

approximation[38], C i

than the energy of e

high to be accounted

and $A^{*}A^{\perp}$ and the gr

The failure of

explain excimer beh

figuration interact

adopted by most sub

a "mixed" state pr

and exciton-resona

Murrel[41] and

excimer.

In the follow

The MO picture of

we consider only

unacceptable R of 1.8Å must be used.

Slifkin[35] considered the possible implication of charge resonance states in the excimer emission. By plotting I-A-^1L_b vs $h\nu_D$ for a number of aromatic hydrocarbons he found a linear relationship which made him to suggest that the excimer emission is a charge-transfer emission. The energy of such a charge transfer state can be expressed as I-A-C$\pm$R (I=ionization potential, A=electron affinity, C=Coulombic interaction between the resulting charges and R is a term resulting from the interaction of the two possible degenerate charge resonance states).

In the case of naphthalene I-A=8.50[36] or 8.74[37]. Using the point charge approximation[38], C is approximately 3 eV at 3 Å. So I-A is over 2 eV higher than the energy of excimer fluorescence 3.13 eV[39] an energy which is too high to be accounted by the resonance energy between the structures A^+A^- and A^-A^+ and the ground state repulsion.

The failure of either the exciton or the charge-resonance model to explain excimer behavior in general led to the introduction of the configuration interaction model by Konijnenberg[40]. This model which has been adopted by most subsequent authors, considers the singlet excimer state as a "mixed" state produced by configuration interaction of charge-resonance and exciton-resonance state.

Murrel[41] and McGlynn[42] used this approach to study the naphthalene excimer.

In the following we will just outline how such a treatment goes. The MO picture of naphthalene molecule (D_{2h} symmetry) is as follows if we consider only the most important MO's

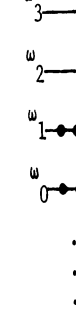

Molecule A

Let us consider the

one charge resonance

^1L_a monomer state an

produced by the exci

to the lowest vacant

of the two zeroth-or

Molecular exciton s

two wavefunctions

where the bar denot

can be expressed as

Finally for the ch

Linear combination

irreducible repres

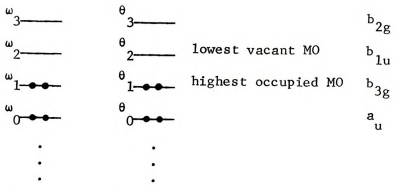

Let us consider the three lowest energy excited states of the excimer: one charge resonance state and two molecular exciton state, one due to ^1L_a monomer state and one due to ^1L_b monomer state. The ^1L_a state is produced by the excitation of an electron from the highest occupied orbital to the lowest vacant orbital $\omega_1 \rightarrow \omega_2$ while the ^1L_b state is a resultant of the two zeroth-order degenerate excitation: $\omega_1 \rightarrow \omega_3$ and $\omega_0 \rightarrow \omega_2$. Molecular exciton states of ^1L_a parentage may be expressed by the following two wavefunctions

$$\Psi_A = |\omega_1\bar{\omega}_1\theta_1\bar{\theta}_2| - |\omega_1\bar{\omega}_1\bar{\theta}_1\theta_2|$$

$$\Psi_B = |\omega_1\bar{\omega}_2\theta_1\bar{\theta}_1| - |\bar{\omega}_1\omega_2\theta_1\bar{\theta}_1|$$

where the bar denotes β spin. Molecular exciton states of ^1L_b parentage can be expressed as

$$\Psi_C = |\omega_1\bar{\omega}_1\theta_0\bar{\theta}_2| - |\omega_1\bar{\omega}_1\bar{\theta}_0\theta_2| + |\omega_1\bar{\omega}_1\theta_1\bar{\theta}_3| - |\omega_1\bar{\omega}_1\bar{\theta}_1\theta_3|$$

$$\Psi_D = |\theta_1\bar{\theta}_1\omega_0\bar{\omega}_2| - |\theta_1\bar{\theta}\,\bar{\omega}_0\omega_2| + |\theta_1\bar{\theta}_1\omega_1\bar{\omega}_3| - |\theta_1\bar{\theta}_1\bar{\omega}_1\omega_3|$$

Finally for the charge resonance states

$$\Psi_E = |\omega_1\bar{\theta}_2\theta_1\bar{\theta}_1| - |\bar{\omega}_1\theta_2\theta_1\bar{\theta}_1|$$

$$\Psi_F = |\omega_1\bar{\omega}_1\omega_2\bar{\theta}_1| - |\omega_1\bar{\omega}_1\omega_2\theta_1|$$

Linear combinations of the above wavefunctions transform according to irreducible representations of the D_{2h} group

^1L_a

B_{3g}: $\Psi_A - \Psi_B$

B_{2u}: $\Psi_A + \Psi_B$

Charge resonance state

From these results one

transform in the same

exciton states transf

resonance states.

To determine the

separability approxi

Hamiltonian of the s

where $1/r_{\nu\mu}$ is the

$H_{core} = \sum_{\nu} H_{core}(\nu)$ wh

electron ν.

For the D_{2h} ex

vanishing configura

and between $|B_{3g}(e$

the solution of se

where for example

McGlynn and Murre

involved and espe

both concluded t

the other excime

	^1L_b	B_{2g}: $\Psi_C - \Psi_D$
		B_{3u}: $\Psi_C - \Psi_D$
Charge resonance states		B_{3g}: $\Psi_E - \Psi_F$
		B_{2u}: $\Psi_E + \Psi_F$

From these results one sees that for a D_{2h} excimer the ^1L_a exciton states transform in the same way as the charge-resonance state while the ^1L_b exciton states transform differently from both ^1L_a exciton and charge-resonance states.

To determine the energy of the excimer state the validity of the σ-π separability approximation is usually assumed. In this approximation the Hamiltonian of the system can be written as

$$H = H_{core} + \sum_{\nu<\mu} 1/r_{\nu\mu}$$

where $1/r_{\nu\mu}$ is the electrostatic repulsion between π-electrons ν and μ and $H_{core} = \sum_{\nu} H_{core}(\nu)$ where $H_{core}(\nu)$ represents the effect of the core on electron ν.

For the D_{2h} excimer, from our previous considerations, there is non-vanishing configuration interaction between $|B_{2u}(exc)\rangle$ and $|B_{2u}(CR)\rangle$ and between $|B_{3g}(exc)\rangle$ and $|B_{3g}(CR)\rangle$ states. So the problem reduces to the solution of secular equations of the form

$$\begin{vmatrix} H_{11} - E & H_{12} - S_{12}E \\ H_{12} - S_{12}E & H_{22} - E \end{vmatrix} = 0$$

where for example

$$H_{12} = \langle (exc) | H | (CR) \rangle$$

$$S_{12} = \langle (exc) | (CR) \rangle$$

McGlynn and Murrel used different methods to evaluate the matrix elements involved and especially matrix elements of the type $\langle (exc) | H | (exc) \rangle$ but both concluded that the lowest excimer state is of B_{3g}^- symmetry and that the other excimer states in order of increasing energy are B_{2u}^-, B_{2u}^+ and

$^1\Sigma_g^+$. Both calculation
semiempirical techniqu
concepts do not give r

A "supermolecule"
entity, molecule, with
Moreover the ab initi
appears technically u
initio calculations c
5p/3s, 1p) and H(5s/
or two-electron inte
molecules" of von Ni
structed from the wa
molecule may be usef

Up to now only
performed. In this
naphthalene excimer
tion interaction ar
was again 3 Å.

B_{3g}^{+}. Both calculations give an interplanar distance of about 3 Å. These semiempirical techniques although useful in providing us with "physical" concepts do not give results of quantitative significance.

A "supermolecule" approach where the whole excimer is treated as one entity, molecule, with the technique of molecular orbitals would be desirable. Moreover the ab initio approach is needed. At this moment this approach appears technically unrealistic. Buenker and Peyerimhoff[43] performed ab initio calculations on naphthalene. Even with an inflexible basis C(10s, 5p/3s, 1p) and H(5s/1s) they had to compute 0.89 billion electron repulsion or two-electron integrals. Probably an approach like the "molecule in molecules" of von Niessen[44]; where the wavefunction of a molecule is constructed from the wavefunctions of fragments structurally related to the molecule may be useful for constructing excimer states.

Up to now only semiempirical supermolecule calculations have been performed. In this way Azumi[45] used a simple Huckel treatment for the naphthalene excimer while Lim[46] used Huckel orbitals and limited configuration interaction among several states. The calculated interplanar distance was again 3 Å.

STUDY OF

IN 1,3-D

The first intra

styrene in liquid so

polystyrene shows mo

tensities of the two

These findings led

styrene occurs intr

phenyl groups. Lat

the form (phenyl)-(

nolecular excimer f

pene chain (n = 3)

and does not have

CHAPTER 2

STUDY OF THE INTRAMOLECULAR EXCIMER INTERACTIONS IN 1,3-DINAPHTHYLPROPANE AND 1,3-DIPHENYLPROPANE

INTRODUCTION

The first intramolecular excimer reported was the one formed by polystyrene in liquid solutions[47,48]. Under these conditions the spectrum of polystyrene shows monomer and excimer bands except that the relative intensities of the two bands are independent of polystyrene concentration. These findings led the authors to conclude that excimer formation in polystyrene occurs intramolecularly by the association of excited and unexcited phenyl groups. Later Hirayama[49] studied a series of diphenylalkanes of the form (phenyl)-$(CH_2)_n$-(phenyl) and showed that only when n = 3 intramolecular excimer formation can take place (The "n = 3 rule"). The propane chain (n = 3) allows for parallel sandwich excimer configuration and does not have the configurational instability of n = 4,5, and 6 alkane chains. Since that time several cases of intramolecular excimer formation have been reported in aromatic polymers like polyvinylnaphthalene[12] and polyvinylcarbazole[50] and simpler compounds like (4,4)-paracyclophane[12].

Intramolecular excimer fluorescence has also been observed in various biological and model systems. The dinucleotides of cytosine (CpC) and thymine (TpT) and also polycytosine (poly C) all show excimer emission in solid solution at 85°K, when the pH of the solution is such that the bases are stacked, as determined by optical rotatary dispersion[51]. Synthetic

nables of the form (nc
used through their exc
stacking interactions
(calf thymus) is stru
spectrum of the dinuc
adenine-thymine excip
namely the thymine di
(excimer) as the init
this case the import
intersystem crossing
that will be studied

Intramolecular

preferred configura
is a transient spec
not susceptible to
his study of the py
tion with an interp

3.5 A. Conclusion

generalized to the

models of the form (adenine)-$(CH_2)_3$-(N-isopentanyl-adenine) have been used through their excimer properties to obtain information about the stacking interactions in tRNA[52]. Finally the fluorescence spectrum of DNA (calf thymus) is structureless and closely represents the fluorescence spectrum of the dinucleotide ApT and is accordingly identified[51] with the adenine-thymine exciplex $^1AT^*$. One of the most important photomutations namely the thymine dimerization is considered to involve selfassociation (excimer) as the initial step or involvement of the $^1AT^*$ exciplex[53]. In this case the important photophysical result is the enhancement of $S_1 \rightarrow T_1$ intersystem crossing because of the excimer/exciplex interaction a subject that will be studied further in Chapter 3.

Intramolecular excimer have been used to get information about the preferred configuration of the excimer in fluid solutions. Since the excimer is a transient species existing only during the excited state lifetime is not susceptible to the usual methods of structural analysis. Ferguson[54] in his study of the pyrene crystal fluorescence suggested a sandwich configuration with an interplanar spacing less that the normal graphite distance of 3.5 Å. Conclusions drawn from study of excimers in crystals cannot be generalized to the solution cases because of the constrains imposed by the lattice. Others like Birks[55] have suggested that the excimer geometry may be one where one molecule is displaced considerably from the other, along one of the molecular axes, so as to minimize the repulsion between corresponding carbon atoms. Chandross and Dempster[56] studied a series of 1,3-dinaphthylpropanes and showed that only the symmetrical $\alpha\alpha$- and $\beta\beta$-dinaphthylpropanes which allow for perfect sandwich configuration of the naphthyl groups, show significant excimer formation. This appears as a strong support of the "perfect sandwich" excimer configuration in fluid media.

The use of intram
under various conditi
case:(1) The geometry
theoretical predictio
radiative properties,
unimolecular process
be used. The high c
like to study the ex
Recently excimers fo
micelles[57] and biol
be promising in this
possibility is the
expected to be obse
quenching), (3) Fin
information about t
rotational relaxat
in the study of po

In this chapt

excimer and excip

The use of intramolecular excimers to study the properties of excimers under various conditions has several advantages over the intermolecular case:(1) The geometry of the excimer is known and this is important for theoretical predictions about the excimer state and its radiative and non-radiative properties, (2) Since the intramolecular excimer formation is a unimolecular process (independent of concentration) a dilute solution can be used. The high concentration poses solubility problems if one would like to study the excimer behavior in viscous media or at lower temperatures. Recently excimers found an important use as probes of the microfluidity of micelles[57] and biological membranes[58]. Intramolecular excimers appear to be promising in this area because of the concentration problem. Another possibility is the search for triplet intramolecular excimers which are expected to be observable in viscous/low temperature media (collisional quenching), (3) Finally the study of intramolecular excimers will provide information about the effect of the connecting chain on the translational-rotational relaxation of the interacting chromophores which is important in the study of polymers and biopolymers.

In this chapter we are going to study various aspects of intramolecular excimer and exciplex behavior. The technique of time resolved spectroscopy is used initially to study the dynamics of the association and dissociation processes of the intramolecular excimer formed in the excited state of 1,3-Bis(α-naphthyl)propane (1,3DNP). The specific rate constants of these processes are determined in media of different viscosity and the translational relaxation nature of the phenomenon is demonstrated. Through coupling of transient kinetic data with photostationary data and model calculations, various thermodynamic quantities describing the intramolecular excimer interaction are determined. The behavior of the intramolecular excimer in

a wider viscosity r
with the aim of usi
for obtaining the r
metry of the excim
diative deactivati
nolecular oxygen i
and the results ar
quenching action.

The excimer i
dependent of othe
another intramole
that the monomer/
energies of the a
with the polarity
viscosity and the
vation energies

Finally the
possibility of t
exist in viscous

a wider viscosity range is studied through steady illumination techniques with the aim of using 1,3DNP as viscosity probe of biomembranes. A method for obtaining the radiative lifetime is developed and the fact that the geometry of the excimer is known allows speculation on the mechanism of radiative deactivation of the excimer state. The relative efficiency by which molecular oxygen is quenching the monomer and excimer fluorescence is studied and the results are discussed in terms of the proposed mechanisms of oxygen's quenching action.

The excimer interaction has been considered in the literature as independent of other solvent properties besides the solvent viscosity. In another intramolecular excimer system 1,3-diphenylpropane (1,3DPP) we found that the monomer/excimer fluorescence intensity ratios and the activation energies of the association process are solvent dependent and correlate with the polarity of the solvent. The relative contribution of the solvent viscosity and the methylene chain rotational barriers to the observed activation energies is also analyzed.

Finally the system 1,3-diphenylpropane is used to investigate the possibility of triplet excimers. Indeed triplet excimers are shown to exist in viscous solutions and in microcrystalline aggregates.

1,3-DINAPHTHYLPROPANE

Kinetic Treatment of the Excimer Formation and Dissociation Process

In our kinetic treatment we consider the following reaction scheme:

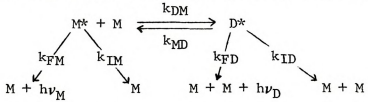

Where M signifies the "monomer", in this case a single naphthalene ring and D* the intramolecular excimer. The meaning of the rate constants is as

follows:

Obviously

where τ_M and τ_D ar
respectively. For

Let us assume tha
δ-function at tim
and at a subseque
$[M^*]$ and $[D^*]$ res
$[M^*]$ and $[D^*]$ ar

This system of t
and $[D^*]$ can be
form

where A and B a
substitute equa

or

follows:

k_{FM}: fluorescence of monomer

k_{IM}: internal quenching of monomer

k_{DM}: excimer formation

k_{FD}: fluorescence of excimer

k_{MD}: dissociation of excimer

k_{ID}: internal quenching of excimer

Obviously

$$k_{FM} + k_{IM} = k_M = 1/\tau_M$$

$$k_{FD} + k_{ID} = k_D = 1/\tau_D$$

where τ_M and τ_D are the experimental lifetimes of the monomer and excimer respectively. For convenience we group the rate constants as follows:

$$k_{FM} + k_{IM} + k_{DM} = X$$

$$k_{FD} + k_{ID} + k_{MD} = Y$$

Let us assume that the solution is excited by a light pulse which is a δ-function at time t = 0. The pulse produces $[M^*]_0$ excited "monomers" and at a subsequent time t the concentration of monomer and excimer is $[M^*]$ and $[D^*]$ respectively. $[D^*]$ at t = 0 is zero. The rates of change of $[M^*]$ and $[D^*]$ are as follows:

$$\begin{aligned} d[M^*]/dt &= -X[M^*] + k_{MD}[D^*] \\ d[D^*]/dt &= -Y[D^*] + k_{DM}[M^*] \end{aligned} \tag{21}$$

This system of two differential equations in two dependent variables $[M^*]$ and $[D^*]$ can be easily solved. Let us assume a particular solution of the form

$$[M^*] = Ae^{-\lambda t} \quad \text{and} \quad [D^*] = Be^{-\lambda t} \tag{22}$$

where A and B are constants and λ is a parameter to be determined. If we substitute equation 22 into 21, we get:

$$\begin{aligned} -\lambda Ae^{-\lambda t} &= -XAe^{-\lambda t} + k_{MD}Be^{-\lambda t} \\ -\lambda Be^{-\lambda t} &= -YBe^{-\lambda t} + k_{DM}Ae^{-\lambda t} \end{aligned}$$

or

$$\begin{aligned} A(X-\lambda) - k_{MD}B &= 0 \\ B(Y-\lambda) - k_{DM}A &= 0 \end{aligned} \tag{23}$$

The system of equat

determinant is zero

From the above det

$$\lambda_1,$$

The particular sol

satisfy the initia

is necessary to ha

combination of pa

The system of equ

the secular deter

and

From equations

$$[$$

At $t = 0$, $[D^*]$

of M^*, $[M^*]_0$ is

Solving equati

Then the conce

Now let us fi

The system of equations23 has a nontrivial solution for A and B if the determinant is zero

$$\begin{vmatrix} X-\lambda & -k_{MD} \\ -k_{DM} & Y-\lambda \end{vmatrix} = 0 \qquad (24)$$

From the above determinant, we get

$$\lambda_{1,2} = \tfrac{1}{2}\left[X + Y \mp \sqrt{(Y-X)^2 + 4k_{DM}k_{MD}}\right] \qquad (25)$$

The particular solution is not an acceptable solution because it does not satisfy the initial conditions of concentration, at t = 0, $[D^*] \neq 0$. It is necessary to have a general solution which may be written as a linear combination of particular solutions

$$[M^*] = c_1A_1e^{-\lambda_1 t} + c_2A_2e^{-\lambda_2 t} \qquad (26a)$$

$$[D^*] = c_1B_1e^{-\lambda_1 t} + c_2B_2e^{-\lambda_2 t} \qquad (26b)$$

The system of equations 23 splits to two systems one for each root of the secular determinant 24

$$A_1(X-\lambda_1) - B_1k_{MD} = 0 \qquad (27a)$$

$$B_1(Y-\lambda_1) - A_1k_{DM} = 0 \qquad (27b)$$

and

$$A_2(X-\lambda_2) - B_2k_{MD} = 0 \qquad (28a)$$

$$B_2(Y-\lambda_2) - A_2k_{DM} = 0 \qquad (28b)$$

From equations 26a, 27a and 28a:

$$[M^*] = c_1k_{MD}B_1e^{-\lambda_1 t}/(X-\lambda_1) + c_2k_{MD}B_2e^{-\lambda_2 t}/(X-\lambda_2) \qquad (29)$$

At t = 0, $[D^*] = 0$ so $c_1B_1 = -c_2B_2$ or $c_1' = -c_2'$. The initial concentration of M*, $[M^*]_0$ is then

$$[M^*]_0 = c_1'k_{MD}/(X-\lambda_1) - c_1'k_{MD}/(X-\lambda_2) \qquad (30)$$

Solving equation 30 for c_1' we get

$$c_1' = -(X-\lambda_1)(X-\lambda_2)[M^*]_0/\ k_{MD}(\lambda_2-\lambda_1) \qquad (31)$$

Then the concentration of M* at any time t will be:

$$[M^*] = c_1'k_{MD}e^{-\lambda_1 t}/(X-\lambda_1) - c_1'k_{MD}e^{-\lambda_2 t}/(X-\lambda_2) \qquad (32)$$

Now let us find an expression for $[D^*]$. From equations 27b and 28b, we

get that

$$A_1 = (Y$$

So $[M^*]_0$

or $c_1' =$

$[P^*]$ from equati

$$[D^*]$$

by using the exp

$$[D^*]$$

Equations 32 and

time t. The qu

molecule of M)

Using equations

$$I_M(t) =$$

or $I_M(t) =$

Defining the q

and using equa

The solution

are two ways

I. From our e

is not a δ-fu

Because

given by the

where I(t) i

get that

$$A_1 = (Y - \lambda_1)B_1/k_{DM} \quad \text{and} \quad A_2 = (Y-\lambda_2)B_2/k_{DM}$$

So $$[M^*]_0 = c_1'(Y - \lambda_1)/k_{DM} - c_1'(Y - \lambda_2)/k_{DM}$$

or $$c_1' = k_{DM}[M^*]_0/(\lambda_2 - \lambda_1) \tag{33}$$

$[D^*]$ from equation 26b is given by

$$[D^*] = c_1'e^{-\lambda_1 t} - c_1'e^{-\lambda_2 t} \tag{34}$$

by using the expression for c_1' from equation 34, we get

$$[D^*] = k_{DM}[M^*]_0(e^{-\lambda_1 t} - e^{-\lambda_2 t})/(\lambda_2 - \lambda_1) \tag{35}$$

Equations 32 and 33 give the concentration of monomer and excimer at any time t. The quantum intensity of monomer fluorescence (per initial excited molecule of M) at time t is

$$I_M(t) = k_{FM}[M^*]/[M^*]_0 \tag{36}$$

Using equations 30 and 32 we can write equation 36 as:

$$I_M(t) = k_{FM}(\lambda_2-X)\left[e^{-\lambda_1 t} + (X-\lambda_1)e^{-\lambda_2 t}/(\lambda_2-X)\right]/(\lambda_2-\lambda_1) \tag{37}$$

or $$I_M(t) = k_{FM}\left[(\lambda_2-X)e^{-\lambda_1 t} + (X-\lambda_1)e^{-\lambda_2 t}\right]/(\lambda_2-\lambda_1) \tag{38}$$

Defining the quantum intensity of the excimer as

$$I_D(t) = k_{FD}|D^*|/|M^*|_0$$

and using equations 30 and 33, we get

$$I_D(t) = k_{FD}k_{DM}(e^{-\lambda_1 t} - e^{-\lambda_2 t})/(\lambda_2 - \lambda_1) \tag{39}$$

The solution of the problem is now reduced in evaluating λ_1 and λ_2. There are two ways for doing that:

I. From our exciting pulse-decay plots we see that the exciting light pulse is not a δ-function but has a width at half-maximum of about 5 ns.

Because of that the observed fluorescence response function R(t) is given by the convolution integral

$$R(t) = \int_0^t I(t')P(t-t')dt' \tag{40}$$

where I(t) is given by equations 37 and 38 and P(t) is the time function of

the lamp and

pulse.

By using

and performin

observed fluc

achieved is

There a

an important

the analysis

Schuyler and

Very re

problem of

taneous equ

In the

deconvoluti

excimer flu

which can

the deriva

t_{max} can b

maxima of

occur. We

gradient

t is equa

we go bac

equation

Kno

the lamp and the detector and is given by the observed shape of the excited pulse.

By using equation 37 or 38 for I(t) with various values of λ_1 and λ_2 and performing the integration numerically we can match R(t) with the observed fluorescence decay. The pare of λ_1 and λ_2 for which this is achieved is the required solution[59].

There are several other methods for treating the convolution integral, an important one being the Method of Moments which has been applied to the analysis of multiexponential decay by Isenberg and Dyson[60] and by Schuyler and Isenberg[61].

Very recently, Ware described a least-squares method which reduces the problem of solving an integral equation to one of solving a set of simultaneous equations[62].

In the present study we use a simplified technique which avoids the deconvolution procedure. From the excimer decay plots we see that the excimer fluorescence intensity reaches a maximum after a certain time t_{max} which can be easily computed by differentiating equation 38 and equating the derivative to zero. In this way we obtain

$$t_{max} = \ln(\lambda_2/\lambda_1)/(\lambda_2 - \lambda_1) \qquad (41)$$

t_{max} can be obtained as the difference between the times at which the maxima of exciting light intensity and excimer fluorescence intensity occur. We further note from equation 38 that at large t the negative gradient of the curve of $\ln I_D(t)$ (which for large t equals $\ln R(t)$) against t is equal to λ_1. Obtaining λ_1 this way and by measuring t_{max} directly we go back to equation 40 and solve for λ_2. Equation 40 is a transendental equation and was solved with a computer iterative technique.

Knowing λ_1 and λ_2 we can use equation 25 to generate the following

system of two si

k_D in equations

of monomer in t

from decay expe

experimental co

similar to that

equations 42 g

where

and

Results

The measu

rate constant

Using th

namic quantit

quantities of

state leading

tion energy

Pane in etha

$E_{DM} = 4.0$ kc

to ethanol s

which can be

which by us

system of two simultaneous equations

$$\lambda_1 + \lambda_2 = k_M + k_D + k_{MD} + k_{DM}$$
$$\lambda_1 \cdot \lambda_2 = k_{DM} k_D + k_M k_{MD} + k_M k_D \qquad (42)$$

k_D in equations 42 is essentially λ_1 and k_M which refers to the decay of monomer in the absence of the excimer formation process, was obtained from decay experiments on α-methyl naphthalene (model) under the same experimental conditions. k_M of α-methyl naphthalene is assumed to be similar to that of k_M of dinaphthylpropane. Solution of the system as equations 42 gives

$$k_{DM} = A - k_{MD} \qquad (43)$$

$$k_{MD} = (Ak_D - B)/(k_D - k_M) \qquad (44)$$

where $A = \lambda_1 + \lambda_2 - k_M - k_D$

and $B = \lambda_1 \cdot \lambda_2 - k_M k_D$

Results

The measured values of λ_1, λ_2, k_M and k_D along with the calculated rate constants k_{DM} and k_{MD} are collected in Table 1.

Using the kinetic data thus obtained we can calculate some thermodynamic quantities for the excimer formation reaction and thermodynamic quantities of the assumed equilibrium between reactants and the transition state leading to the excimer. In our treatment we make use of the activation energy for the excimer formation process of 1,3-Bis-(α-naphthyl)propane in ethanol which has been found by Chandross and Dempster to be E_{DM} = 4.0 kcal/mole[56]. The thermodynamic quantities to be computed refer to ethanol solution at 25°C. The excimer formation is an activated process which can be represented generally by an Arrhenius form of equation

$$k_{DM} = A_{DM} \exp(-E_{DM}/RT) \qquad (45)$$

which by using the determined values of k_{DM} and E_{DM} gives us a value of

Figure 2

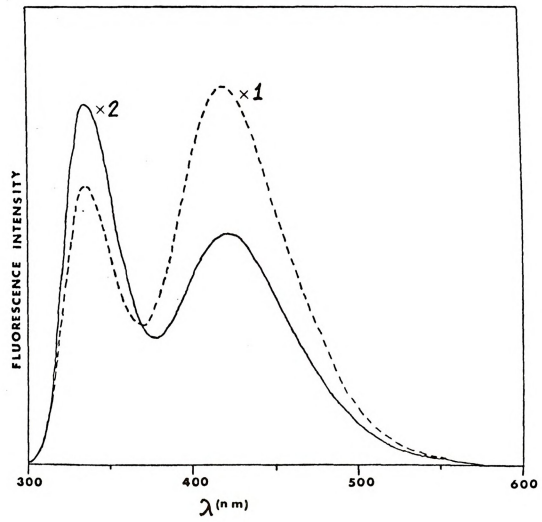

Figure 2. Room Temperature Fluorescence Spectra of 1,3DNP (1.2×10^{-4} M) in EtOH. (__) Air Equilibrated, (--) Nitrogenated Solution.

Figure 3

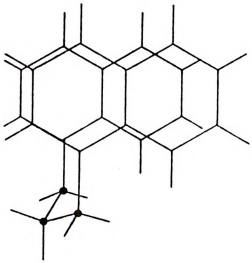

Figure 3 . The Gauche-Gauche Conformation of 1,3-dinaphthylpropane


10 ns

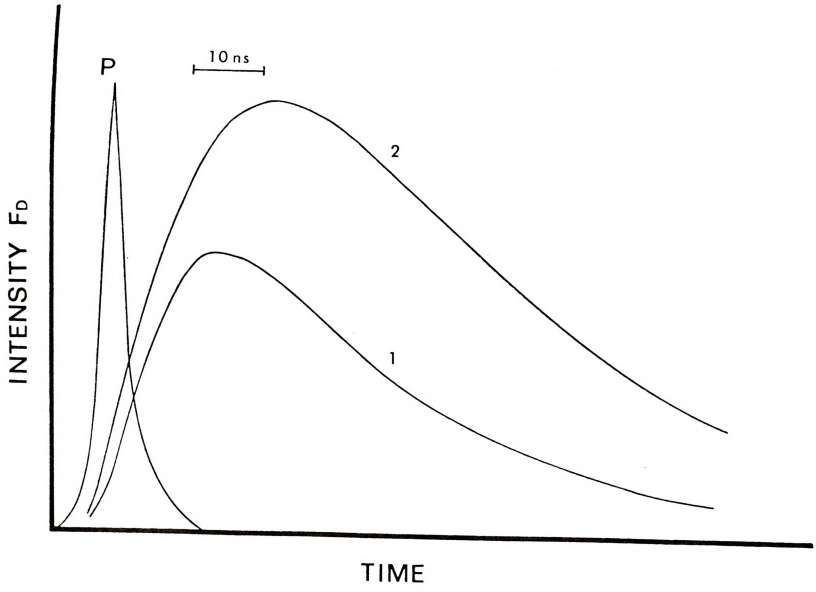

Figure 4. The Rise and Decay of the Intramolecular Excimer Fluorescence. (1) Ethanol Solution (2) 1:1 Ethanol-Glycerol Mixture.

Table 1. K
M

Solution I.

Solution I

Solution

Table 1. Kinetic Data for the 1,3DPP Excimer in Ethanol-Glycerol Mixtures at 25°C.

Solution I. Ethanol Solution 10^{-4}M at 25°C, Viscosity = 1.2 cp.

$\lambda_1 = 3.10 \times 10^7\ s^{-1}$

$\lambda_2 = 12.96 \times 10^7\ s^{-1}$ $\quad k_{DM} = 1.2 \times 10^8\ s^{-1}$

$k_M = 1.12 \times 10^7\ s^{-1}$ $\quad k_{MD} = 1.6 \times 10^4\ s^{-1}$

$k_D = 3.10 \times 10^7\ s^{-1}$

Solution II. Mixture 25% Glycerol, 75% Ethanol at 25°C, Viscosity = 3.6 cp.

$\lambda_1 = 3.17 \times 10^7\ s^{-1}$

$\lambda_2 = 8.27 \times 10^7\ s^{-1}$ $\quad k_{DM} = 6.4 \times 10^7\ s^{-1}$

$k_M = 1.89 \times 10^7\ s^{-1}$ $\quad k_{MD} = 3.0 \times 10^3\ s^{-1}$

$k_D = 3.17 \times 10^7\ s^{-1}$

Solution III. 1:1 Mixture of Ethanol-Glycerol at 25°C, Viscosity = 20 cp.

$\lambda_1 = 2.68 \times 10^7\ s^{-1}$

$\lambda_2 = 6.32 \times 10^7\ s^{-1}$ $\quad k_{DM} = 4.9 \times 10^7\ s^{-1}$

$k_M = 1.41 \times 10^7\ s^{-1}$ $\quad k_{MD} = 2.9 \times 10^3\ s^{-1}$

$k_D = 2.68 \times 10^7\ s^{-1}$

$A_{DM} = 9.8 \times 10^{10}\ s^{-1}$ for the preexponential factor.

A more informative description of the process is through the transition state theory in the form that Eyring, Evans and Polanyi put it

$$k_{DM} = kT/h \cdot \exp(\Delta S^{\ddagger}_{DM}/R) \cdot \exp(-\Delta H^{\ddagger}_{DM}/RT) \tag{46}$$

In equation 46 we have assumed that the transmission coefficient is one and we must also realize that this equation strickly applies to gas phase. A more detailed discussion of that point will be given later.

$\Delta S^{\ddagger}$ and $\Delta H^{\ddagger}$ are the entropy and enthalpy change for the process of going from the reactants to the transition state. An expression connecting the experimentally obtained activation energy to the enthalpy of activation can be easily obtained as follows. Equation 46 is valid for both constant-volume and constant temperature systems. In our case we are dealing with a constant pressure system. Differentiating the logarithm of equation 46 at constant pressure we get

$$(\partial \ln k/\partial T)_P = (\Delta H^{\ddagger}_{DM} + RT)/RT^2 \tag{47}$$

Also from the Arrhenium equation

$$(\partial \ln k/\partial T)_P = E_{DM}/RT^2 \tag{48}$$

By comparing equations 47 and 48, we see that

$$E_{DM} = \Delta H^{\ddagger}_{DM} + RT \tag{49}$$

Using equation 49 and $E_{DM} = 4.0$ kcal/mole, we obtain

$$\Delta H^{\ddagger}_{DM} = 3.5 \text{ kcal/mole}$$

with this result and k_{DM}, using equation 46 we obtain

$$\Delta S^{\ddagger}_{DM} = -10 \text{ cal mole}^{-1} \text{ deg}^{-1}$$

Let us now turn to the thermodynamics of the process $M^* + M \rightleftarrows D^*$. The equilibrium constant of that reaction is

$$K_e = k_{DM}/k_{MD} \tag{50}$$

and from thermodynamics the Gibbs free-energy change will be

$$\Delta G^{\circ}_{DM} = -RT\ln K_e \tag{51}$$

equation 51 gives in our case $\Delta G^{\circ}_{DM} = -5.3$ kcal/mole.

It would be very informative if we could determine separatly the ΔH and ΔS of the reaction. Unfortunately we do not have a value for the binding energy of the excimer which is equal to ΔH. In the following we will try to estimate this binding energy. Figure 5 is a qualitative diagram showing the excimer energy as a function of the distance between the rings. From this diagram we see that

$$hc(\tilde{\nu}^{0,0}_M - \tilde{\nu}^{max}_D) = -\Delta H + E_{Rep} \tag{52}$$

where $\tilde{\nu}^{0,0}_M$ is the frequency in cm^{-1} of the (0,0) transition in the monomer, $\tilde{\nu}^{max}_D$ is the frequency of the maximum of the excimer fluorescence and E_{Rep} is the energy of the ground state configuration generated by the vertical (Franck-Condon) emission process of the excimer.

$\tilde{\nu}^{0,0}_M$ for 1-methyl naphthalene in ethanol is 31,500 cm^{-1}[63]. $\tilde{\nu}^{max}_D$ is from our data 23,800 cm^{-1}. E_{Rep} is more difficult ot get. First we have to know the configuration of the excimer. The intramolecular excimer configuration is a stacked $\sim D_{2h}$ configuration where the two naphthalene rings are forced by the steric requirements of the methylene chain to a "sandwich" configuration with an interplanar distance of 3 Å[56] which is also in agreement with all the theoretical calculations on the naphthalene excimer. The best way to calculate E_{Rep} is by semiempirical methods using parameters that fit experimental data[64]. In this study E_{Rep} is estimated by using an interatomic potential (referred to as "6-exp") of the form

$$V_{ij} = -A_{ij}r_{ij}^{-6} + B_{ij}\exp(-c_{ij}r_{ij}) \tag{53}$$

and finally obtaining the intermolecular potential by summing the various interatomic potentials

$$V_{molecular} = \sum_{ij} V_{ij} \tag{54}$$

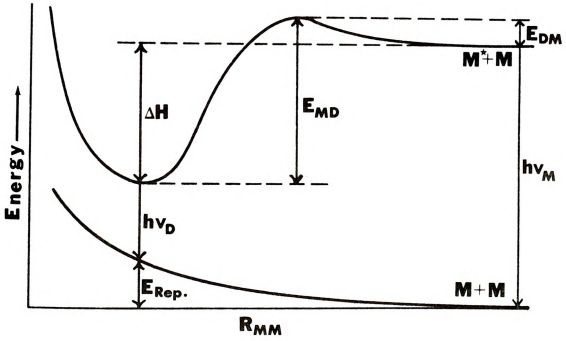

Figure 5. Qualitative Potential Energy Diagram for the Dimer in Ground and Excited States.

The values for the parameters A, B and C of the "6-exp" potential used here are those given by Rae and Mason[65] which are appropriate for aromatic hydrocarbons

$$A_{H\cdots H} = -36\ \mathring{A}^6 \text{ kcal/mole}$$

$$A_{C\cdots C} = -535\ \mathring{A}^6 \text{ kcal/mole}$$

$$A_{C\cdots H} = -139\ \mathring{A}^6 \text{ kcal/mole}$$

$$B_{H\cdots H} = 5010 \text{ kcal/mole}$$

$$B_{C\cdots C} = 74460 \text{ kcal/mole}$$

$$B_{C\cdots H} = 9411 \text{ kcal/mole}$$

$$C_{H\cdots H} = 3.74\ \mathring{A}^{-1}$$

$$C_{C\cdots C} = 3.60\ \mathring{A}^{-1}$$

$$C_{C\cdots H} = 3.67\ \mathring{A}^{-1}$$

A computer program was written to calculate the intermolecular potential as a function of the interplanar distance the result for r = 3 $\mathring{A}$ is E_{Rep} = 0.15 eV. For intermolecular excimers of aromatic hydrocarbons, the usually assumed value for E_{Rep} is between 0.2-0.3 eV[66]. It is of interest to note that a similar method by Kitaygorodsky[67] after the modification of Mantione for stacking configurations gives an even less repulsive potential $E_{Rep}(3\mathring{A})$ = 0.05 eV. This method was used extensively for predicting configurations[68] and the importance of van der Waals forces in the binding energy of "charge-transfer" complexes by Mantione[69]. This method appears to understimate the repulsive potential and so we will use the results of the "6-exp" potential.

So using the above mentioned values for $\tilde{\nu}_M^{0,0}$ and $\tilde{\nu}_D^{max}$ and E_{Rep} = 0.15 eV we obtain from equation 52

$$\Delta H = \text{Binding Energy} = -18 \text{ kcal/mole}$$

Now we can use this estimated value to try to analyse further the excimer formation and dissociation process. We understand of course that the

quantities thus to be obtained have the uncertainty of both the originally obtained data and of the above estimate of the excimer binding energy. The numbers are then only indicative.

The entropy change ΔS will be

$$\Delta S = -(\Delta G - \Delta H)/T = -21 \text{ cal mole}^{-1} \text{ deg}^{-1}$$

Let us now consider the dissociation process. If the binding energy is -18 kcal/mole then the activation energy for the dissociation process will be

$$E_{MD} = -\Delta H + E_{DM} \tag{55}$$

because the difference of the activation energies of the dissociation and association process equals the binding energy. In this way

$$E_{MD} = 22 \text{ kcal/mole}$$

Proceeding in the same way as for the association process we estimate

$$A_{MD} = 3.8 \times 10^{20} \text{ s}^{-1}$$

$$\Delta H_{MD} = 21.4 \text{ kcal/mole}$$

$$\Delta S_{MD} = +32 \text{ cal mole}^{-1} \text{ deg}^{-1}$$

A summary of the kinetic and thermodynamic results is given in Tables 2 and 3.

Table 2. Rate Constants for 1,3DNP Excimer Formation and Dissociation Processes in Ethanol-Glycerol Mixtures at 25°C.

Medium	Viscosity (cp)	$k_{DM}(s^{-1})$	$k_{MD}(s^{-1})$	Temp.(°C)
Ethanol	1.2	1.2×10^{8}	1.6×10^{4}	25
Ethanol-Glycerol (3:1)	3.6	6.4×10^{7}	3.0×10^{3}	25
Ethanol-Glycerol (1:1)	20	4.9×10^{7}	2.9×10^{3}	25

Table 3. Thermodynamic Data for the 1,3DNP Excimer Interaction.

$$\Delta H^{\ddagger}_{DM} = 3.5 \text{ kcal/mole}$$
$$\Delta S^{\ddagger}_{DM} = -10 \text{ cal mole}^{-1} \text{ deg}^{-1}$$
$$\Delta H^{\ddagger}_{MD} = +21 \text{ kcal/mole}$$
$$\Delta S_{MD} = +32 \text{ cal mole}^{-1} \text{ deg}^{-1}$$
$$\Delta H_{DM} = -18 \text{ kcal/mole}$$
$$\Delta S_{DM} = -21 \text{ cal mole}^{-1} \text{ deg}^{-1}$$

Discussion

Before discusing the data let us first understand the meaning of the equations used. The result of the classical theory of reaction rates is written in the form

$$k = \nu \exp(-E^*/RT) \qquad (56)$$

where ν is a frequency factor which is in principle calculable from spectroscopic frequencies of the normal molecule and which should lie in the range 10^{12} to 10^{14} s^{-1}. E^* is the experimental activation energy. Adapting the idea that a molecule must have an energy E^* or higher to react and that energy is localized to a particular set of normal coordinates essential for the reaction, Rice, Ramsperger[70] and Kassel[71] developed a quantum mechanical theory for unimolecular reactions. The difference between the classical and quantum mechanical rates was shown to be in the introduction of the entropy difference between the normal and activated molecule. So

$$\text{Rate quantum mechanically/Rate classically} = \exp(\Delta S^{\ddagger}/R) \qquad (57)$$

The final form of the equation for the specific rate constant of a

unimolecular process is

$$k = \gamma^* \cdot \exp(\Delta S^{\ddagger}/R) \cdot \exp(-\Delta H^{\ddagger}/RT) \qquad (58)$$

In equation 58, γ^* represents a weighted average of the internal frequencies of a species that has the configuration of the transition state. One would expect it to lie in the same range as γ for the normal molecule but such an equivalence is purely ad hoc. So although $\Delta H^{\ddagger}$ can be obtained experimentally there is no obvious way of partitioning the experimental frequency factor between γ^* and $\Delta S^{\ddagger}$. The transition state theory introduces a universal value of $\gamma = kT/h = 6 \times 10^{12}$ s^{-1} for t = 300°K or in terms of wavenumbers ~ 200 cm^{-1}, a quite low frequency. If the preexponential factor is $\sim 10^{13}$ s^{-1} then the reaction is considered as normal and in this case $\Delta S^{\ddagger} \simeq 0$. Another way to understand the deviations from normality (classical behavior) is to look to another expression for the ratio of quantum mechanical and classical rates[72]

$$R_{q.m.}/R_{clas.} \simeq Q^{\ddagger}_{vib}/Q_{vib} \qquad (59)$$

Equation 59 assumes that $(I_a^{\ddagger} I_b^{\ddagger} I_c^{\ddagger}/I_a I_b I_c)^{3/2} = 1$, where I_i is a principal moment of inertia. This assumption is not necessarily true in our case. Q_{vib} (the vibrational partition function) can be generally factored as a product of contributions from each normal coordinate

$$Q_{vib} = \prod_i q_i = \prod_i (1 - e^{-h\nu_i/kT})^{-1} \qquad (60)$$

It is only when the frequency $\nu_i \leq kT/h$ that q_i differs appreciably from unity (for $\nu_i >> kT/h$, $q_i = 1$), so that the q_i and hence Q_{vib} will be unity except for the contributions of low-frequency vibrations. If some of the frequencies of M (reactant) are lowered in changing to $M^{\ddagger}$, then $q_i^{\ddagger}/q_i > 1$ for those particular frequencies and we should expect an enhancement of the rate. If on the other hand some originally low frequencies of M are increased, then we may expect to find $q_i^{\ddagger}/q_i < 1$ and consequent falling of

the rate. According to Benson the greatest contributions may be expected from the very low frequencies arising from almost free internal rotations.

Going back to our data we see that the excimer formation process has a preexponential factor of $\sim 10^{11}$ s^{-1} and a negative $\Delta S^{\ddagger} = -10$ cal $mole^{-1}deg^{-1}$. These results indicate a significant ordering during the transition from reactant to the transition state. The loss of entropy and a low value of A can be attributed to loss of rotational degrees of freedom of both the naphthalene rings and of the methylene chain. Similar results have been found in cases where the transition state involves some kind of a cyclic intermediate. For example the isomerization of vinyl allyl ether to n-pentaldehyde-ene-4 is considered as going through a six-membered ring complex:

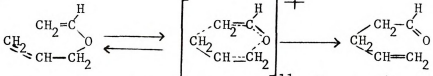

The observed preexponential factor is $\sim 10^{11}$ s^{-1} and $\Delta S^{\ddagger} = -8$cal $mole^{-1}deg^{-1}$.[73]

The excimer formation process although clearly a unimolecular process has also characteristics of a diffusional process and so is dependent on solvent properties particularly solvent viscosity. Also the observed activation energy can have contributions from the rotational barriers of the methylene chain and the diffusion process which is an activated process (solvent viscosity temperature dependence). These points will be considered later.

Turning to the estimated binding energy (0.78 eV) we see that it is considerably high compared with the already reported values for binding energies of intermolecular excimers. For example the binding energy of 1-methyl-naphthalene excimer in n-heptane was reported by Birks[74] to be 0.30 eV and by Selinger[75] in 95% EtOH solution as 0.20 eV. Pyrene in

ethanol has one of the highest binding energies 0.40 eV[76]. Although our binding energy estimate depends on the estimate of E_{Rep}, we should note that in our case the value of $\tilde{\nu}_M^{0,0} - \tilde{\nu}_D^{max} = \Delta H_{DM} + E_{Rep}$ is 7700 cm^{-1} which is higher than the value of 6500 cm^{-1} in the case of 1-methyl-naphtnalene intermolecular excimer and 6100 cm^{-1} in the case of pyrene excimer; an indication of a higher binding energy for our case. The effect of the methylene chain strain is expected to be the same in both excimer and Franck-Condon ground states. Even if we use a higher value for E_{Rep}, say, 0.3 eV, the resulting binding energy is still higher (0.48 eV) than usual.

The excimer binding energies are usually obtained by substructing the activation energy of the association process obtained at lower temperatures from the activation energy of the dissociation process obtained at elevated temperatures. This is done under the assumption that k_{FD} is independent of temperature which especially at elevated temperatures we do not believe it is true (vibronically induced emission). Cundall and Robinson[77] has shown for the case of benzene excimer that k_{FD} is indeed a function of temperature and by correcting for this dependence the binding energy was changed from 0.22 to 0.37 eV. Other reported binding energies in the literature seem to be quite low like the 9-methylanthracene in benzene 0.20 eV, $\Delta\nu$ = 6850 cm^{-1}[78] which implies a $E_{Rep} \simeq$ 0.6 eV an unusually high value. An unusually high binding energy value for 1,3-dinaphthylpropane may be associated with the steric requirements of the methylene chain which may bring the aromatic chromophores in a more favorable excimer conformation. It is interesting to note here that when pyrene was studied in viscous paraffin oil solution[79] the binding energy was found to be higher than in fluid solution (0.48 eV). In our case the methylene chain is expected to play the role of a highly viscous medium locking the molecule in the excimer configuration.

The high negative entropy of reaction ΔS = -21 cal mole^{-1} deg^{-1} seems to be characteristic of excimer formation. Compare for example the value of -21 cal mole^{-1} deg^{-1} for 2-methyl naphthalene in ether, -19 cal mole^{-1} deg^{-1} for acenaphthene in toluene[80], ΔS = -22.7 cal mole^{-1} deg^{-1} for pyrene in toluene[81]. This entropy decrease is again a result of freezing of various degrees of freedom which is expected for the association of two complex molecules and appears in other cases of association reactions like the dimerization of acetic acid (hydrogen bonding) in benzene ΔS = -22.3 eu[82].

Finally the results for the dissociation process $D^* \longrightarrow M^* + M$ of the intramolecular excimer seem to be different than in the case of intermolecular excimers. The reported values of the dissociation rate constant in the case of intermolecular excimers are in the order $\sim 10^6$ s^{-1} for example pyrene in 95% EtOH $k_{MD} = 7.0 \times 10^6$ s^{-1}[83] to be compared with 1.5×10^4 s^{-1} in our case of intramolecular excimer. The estimated preexponential factor 10^{20} s^{-1} is very high. A collection of A's for the dissociation process of excimers by Lewis and Ware[84] shows a good linear correlation between logA and E_{MD} (a kind of enthalpy-entropy compensation). Using his graph we obtain for our activation energy of 22 kcal/mole a preexponential factor of 10^{20} s^{-1} which seems to support the consistency of our kinetic data. Again viscosity seem to be important for example for pyrene in cyclohexane E_{MD} = 0.55 eV and $A_{MD} \sim 10^{16}$ s^{-1} while in paraffin oil E_{MD} = 0.76 eV and $A_{MD} \sim 10^{18}$ s^{-1}. It is obvious in our case that the methylene chain prohibits the excimer dissociation process much more effectively than a viscous solution. An anomalously high entropy of activation $\Delta S^{\ddagger}_{MD}$ = +28 cal mole^{-1} deg^{-1} for the intermolecular benzene excimer in fluid solution ($A \simeq 6 \times 10^{18}$ s^{-1}) was reported by Hirayama[85]. The authors believe that this high value is due to a partial immobilization of the aromatic rings as well as a longer range

ordering of solvent molecules accompanying the excimer formation process. In our case the high value of A or equivalently $\Delta S^{\ddagger}_{MD}$ may be due to both the methylene chain and the effect of the solvent.

The Radiative Lifetime of the Intramolecular Excimer

The lifetime of the excimer fluorescence has been a subject of dispute for a long time. Hoijtink[86] showed that if the excimer has a center of symmetry, excimer luminescence is forbidden. On the other hand the mere fact that we observe excimer fluorescence proves that the emission is not completely forbidden or it is induced by some intra- or inter-molecular mechanism. The observed fluorescence decay time of pyrene excimer in fluid solutions is much shorter (~65 ns) than that of the monomer (~380 ns). This led to some speculation whether the steric configuration of the excimers may not be the symmetrical overlapping one[87,88 89]. Unlike the case of Pyrene Mataga et al.[90] showed that the fluorescence decay time of naphthalene and α-methylnaphthalene intermolecular excimers are almost the same as the fluorescence decay times of the monomer. Mataga argues that because the probability of the radiationless transition from the fluorescent state of the excimer may not be smaller than that of the monomer, due to the smaller energy gap between the fluorescent and phosphorescent states as well as between the fluorescent and the ground state of the excimer, the radiative transition probability of the excimer fluorescence may not be larger than that of the monomer. A possible experimental support of enhanced intersystem crossing from the singlet excimer state has been discussed by Cundall et al.[91] Since the fluorescence of naphthalene is due to an approximately forbidden transition Mataga concluded that the fluorescence transition of the naphthlene excimer is also approximately forbidden. Another interesting experiment by Mataga was on the anthracene excimer. Mataga photodecomposed

the anthracene dimer in a cyclohexane matrix at 77°K and subsequently excited by a nanosecond light pulse. The excimer fluorescence decay time was 215 ns to be compared with a ~9 ns decay time of the monomer. On the other hand the fluorescence decay of the anthracene dimer produced by the controlled cooling and softening of the matrix[92] was only ~6 ns. Further the perylene excimer produced in the cyclohexane matrix at 77°K shows excimer fluorescence with a decay time of 77 ns which is much longer than the decay time of the monomer ~5 ns.

The above experiments tend to show some degree of forbidness for the excimer emission but the results are complicated by the unknown factor of non-radiative transitions. An obviously more useful quantity will be the radiative lifetime. A few radiative lifetimes have already been determined. They are of the order of 10^2-10^3 ns except for pyrene, for example ~900 ns for 1-methyl naphthalene in 95% ethanol[75], ~770 ns for 1,6-dimethylnaphthalene in 95% EtOH[75], ~550 ns toluene in hexane[93] and ~77 ns for pyrene in 95% EtOH[83].

On the basis of these results Birks supported an overlap picture of the pyrene excimer where the long axes are parallel but the short axes are displaced[88] and also proposed that k_{FD} is temperature independent[93].

There are several difficulties with the above results and interpretations. For example Mataga and coworkers[94] obtained a lifetime (observed) of 200 ns for pyrene excimer in cyclohexane matrix at 77°K while Birks reported a smaller radiative lifetime of ~86 ns in the same solvent at toom temperature[95]. Recently Cundall and Robinson[77] have found that the excimer radiative decay process of benzene is temperature dependent with an activation energy of 0.145 eV and a preexponential factor of 2.4×10^8 s^{-1}. Hirayama and Lipsky[85] also suggest that the rate constant for the radiative process

for benzene excimer may be temperature dependent.

In the following we will try to determine the radiative lifetime of the intramolecular naphthlene excimer (1,3-Bis-(α-naphtyl)-propane). The intramolecular excimer has a more or less definite steric configuration because of the restrictions put by the methylene chain. As it has been shown by Chandross this configuration must be a perfect "sandwich" configuration with an interplanar distance of 3 Å[56]. Because we feel quite confident about the excimer configuration the result may be helpful in deciding on the mechanism by which the excimer emission becomes allowed.

In order to calculate the radiative lifetime we make use of the results of our transient kinetics experiments which we couple with data from photostationary reaction kinetics.

For steady excitation with light of intensity I_0 einsteins ℓ^{-1} s^{-1} the rate equations are

$$d[{}^1M^*]/dt = I_0 - (k_M + k_{DM})[{}^1M^*] + k_{MD}[{}^1D^*] \tag{61}$$

$$d[{}^1D^*]/dt = k_{DM}[{}^1M^*] - (k_D + k_{MD})[{}^1D^*] \tag{62}$$

Under photostationary conditions $d[{}^1M^*]/dt = d[{}^1D^*]/dt = 0$. From equation 62, we get

$$k_{DM}[{}^1M^*] = (k_D + k_{MD})[{}^1D^*] \tag{63}$$

or

$$[{}^1D^*] / [{}^1M^*] = k_{DM}/(k_{MD} + k_D)$$

By definition $\Phi_{FM} = k_{FM}[{}^1M^*]/I_0$, $\Phi_{FD} = k_{FD}[{}^1D^*]/I_0$ (64)

so from equations 63 and 64,

$$\Phi_{FD}/\Phi_{FM} = k_{FD}[{}^1D^*]/(k_{FM}[{}^1M^*]) = k_{FD}k_{DM}/(k_{FM}(k_{MD} + k_D)) \tag{65}$$

or

$$k_{FD} = \Phi_{FD}k_{FM}(k_{MD} + k_D)/\Phi_{FM}k_{DM} \tag{66}$$

In equation 66, k_{FM} was obtained from quantum yield and lifetime measurements of α-methyl-naphthalene fluorescence through the relation $\tau_F = \tau_F^{\circ}\Phi_F$. The ratio of the quantum yeilds was obtained as the ratio of the integrated emission intensities of excimer and monomer after corrections for instrumental

response. Finally the lifetimes were expressed in a medium of unit static dielectric constant through the expression $k_{FD}(n^2=1)=k_{FD}/n^2$ where n is the refractive index of the solvent. The radiative lifetimes thus obtained are τ°_{FM} = 300 ns and τ°_{FD} = 720 ns.

As we see the radiative lifetime of the excimer is longer than that of the monomer. Mataga[96] argues that although α-methylnaphthalene does not have a center of symmetry the perturbation of the methyl group is not significant and so there is a center of symmetry for the electronic density of the π system and consequently the excimer emission should be forbidden. If we accept the fixed sandwich configuration for the intramolecular excimer then a possible mechanism by which the excimer emission becomes allowed is the mechanism proposed by Chandra and Lim[46]. According to their treatment the emission is induced by thermal excitation of tortional oscillations of the excimer components. During such tortional vibrations the excimer geometry is distorted and emission can occur. Due to their low frequencies several tortional levels may be populated at ambient temperatures.

Effect of Solvent Viscosity on the Intramolecular Excimer Formation Process

From our kinetic data we see that, as expected, both the rates of formation and dissociation of the intramolecular excimer depend on solvent viscosity. As has been pointed out by Melhuish and Metcalf[97] although both rates depend on viscosity their ratio, the equilibrium constant of the reaction may be independent of the viscosity. In our case the equilibrium constant is shown to be 1.7 ($\pm$ 0.3) x 10^4, approximately independent of viscosity. Besides the transient kinetic measurements we studied the intramolecular excimer system in ethanol-glycerol mixtures of variable viscosity. The results expressed on I_M/I_D (I_M = maximum intensity of monomer,

I_D = maximum intensity of excimer) vs macroscopic solvent viscosity are displaced in Figure 7. It appears that for higher viscosities (above 20 cp) there is a linear dependence of I_M/I_D on η while a more complicated dependence is found at low viscosities.

Using the results of the Einstein-Smoluchowski diffusion theory[98,99] the rate constant of a diffusion controlled reaction is given by

$$k = 4\pi N \times 10^{-3} DpR$$

where D is the sum of the diffusion coeffients of the two simultaneously moving particles, R is the sum of the interaction radii and $p(\leq 1)$ is a factor introduced to describe the reaction probability per collision.

The diffusion coefficient is usually approximated through the Einstein-Stokes equation

$$D = kT/6\pi r\eta$$

where η is the microscopic viscosity which is assumed to be the same as the macroscopic viscosity.

The intramolecular case is more complicated but if one makes the reasonable assumption that the excimer formation rate depends linearly on the diffusion coefficient then using the equation 66 derived under photostationary conditions we get that

$$I_M/I_D = C(T)\, k_{FM}k_D/k_{FD}$$

where C(T) is constant for constant temperature.

In this way a linear dependence of I_M/I_D is expected. Not excluding some trivial factor the anomalous behavior at low viscosities may be due to the implicit assumption that microviscosity = κ macroviscosity where $\kappa < 1$[100]. The difference between the radii of solute and solvent is the factor determining the above relationship[101]. Obviously the inhomogenouity and radius disparity is larger at the low glycerol content region.

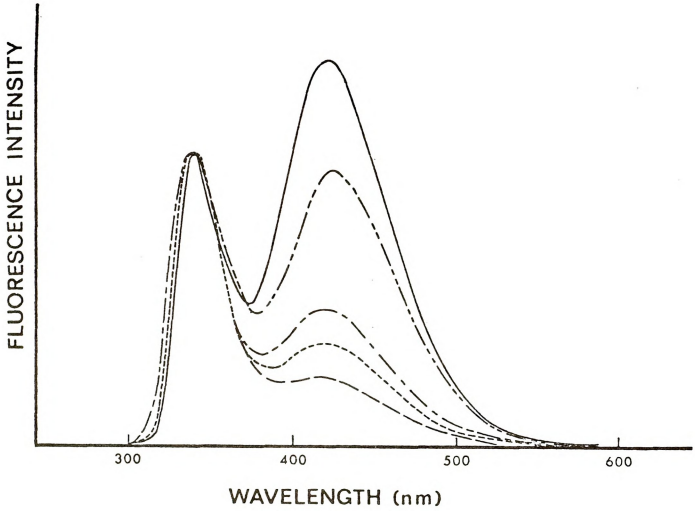

Figure 6. The Effect of Viscosity on the Relative Intensity of the Monomer and Excimer Fluorescence Bands of 1,3DNP in Ethanol-Glycerol Mixtures. The Percentage by Volume of Ethanol is Indicated: (__) 100%, (——__) 75%, (--) 50%, (----) 39%, (_ _ _) 30%.

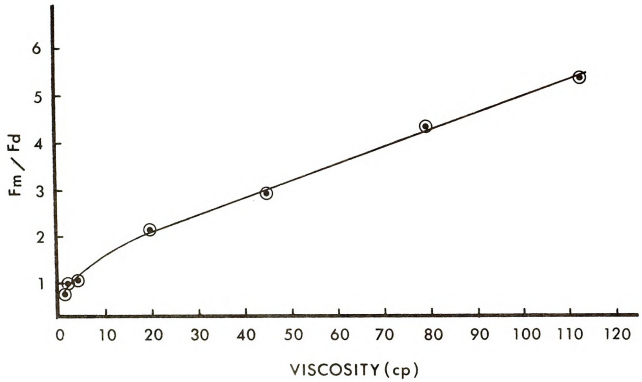

Figure 7. The Effect of Viscosity on the Relative Intensity of the Monomer and Excimer Fluorescence Bands of 1,3DNP.

The Effect of Oxygen on the Excimer-Monomer Relative Yields

During our study of the intramolecular naphthalene excimer we noticed large variations in the excimer-monomer relative yields depending on the extent of degassing of the solution. The excimer intensity being more sensitive to oxygen quenching. In the following we will try to investigate the behavior of the excimer-monomer system towards oxygen quenching more quantitatively using data we have already acquired from the transient kinetic measurements.

The rate of the monomer formation in the presence of quencher ($Q = O_2$) is

$$d\left[{}^1M^*\right]/dt = I_0 - (k_M + k_{DM} + k_{QM}[Q])\left[{}^1M^*\right] + k_{MD}\left[{}^1D^*\right] \quad (67)$$

Under stationary conditions $d\left[{}^1M^*\right]/dt = 0$

$$I_0 = (k_M + k_{DM} + k_{QM}[Q])\left[{}^1M^*\right] - k_{MD}\left[{}^1D^*\right] \quad (68)$$

From our data we see that the repopulation of the monomer through excimer dissociation is negligible so we can neglet the second term on the right hand side of equation 68 then,

$$\left[{}^1M^*\right] = I_0/(k_M + k_{DM} + k_{QM}[Q]) \quad (69)$$

If there is no quencher in the solution then,

$$\left[{}^1M^*\right] = I_0/(k_M + k_{DM}) \quad (70)$$

By definition

$$\Phi_{FM} = k_{FM}\left[{}^1M^*\right]/I_0 \quad (71)$$

so

$$\Phi^\circ_{FM}/\Phi_{FM} = (k_M+k_{DM}+k_{QM}[Q])/(k_M+k_{DM}) = 1+(k_{QM}[Q])/(k_M+k_{DM}) \quad (72)$$

since

$$(\tau_M)^{-1} = k_M + k_{DM} \quad (73)$$

lifetime of monomer emission which takes into account the additional path of excimer formation

$$\Phi^\circ_{FM}/\Phi_{FM} = 1 + \tau_M k_{QM}[Q] \quad (74)$$

Equation 74 is the familiar Stern-Volmer relation. The rate of excimer in the presence of quencher is

$$d\left[{}^1D^*\right]/dt = k_{DM}\left[{}^1M^*\right] - (k_D + k_{MD} + k_{QD}[Q])\left[{}^1D^*\right] \quad (75)$$

Under stationary conditions $d[^1D^*]/dt = 0$, so

$$[^1D^*] = k_{DM}[^1M^*]/(k_D + k_{MD} + k_{QD}[Q]) \tag{76}$$

in this equation $[^1M^*]$ is given by equation 69. By definition

$$\Phi_{FD} = k_{FD}[^1D^*]/I_0 \tag{77}$$

Using equations 76 and 69, we get

$$\Phi_{FD} = k_{FD}k_{DM}/\left[(k_D + k_{MD} + k_{QD}[Q])(k_M + k_{DM} + k_{QM}[Q])\right] \tag{78}$$

In the presence of quencher

$$[^1D^*] = k_{DM}[^1M^*]/(k_D + k_{MD}) \tag{79}$$

In equation 79, $[^1M^*]$ is now given by equation 70. So

$$\Phi^\circ_{FD} = k_{FD}k_{DM}/[(k_D + k_{MD})(k_M + k_{DM})] \tag{80}$$

and $$\Phi^\circ_{FD}/\Phi_{FD} = (k_D+k_{MD}+k_{QD}[Q])(k_M+k_{DM}+k_{QM}[Q])/[(k_D+k_{MD})(k_M+k_{DM})] \tag{81}$$

since $$(\tau_D)^{-1} = k_D + k_{DM} \tag{82}$$

$$\Phi^\circ_{FD}/\Phi_{FD} = (1 + \tau_M k_{QM}[Q])(1 + \tau_D k_{QD}[Q]) \tag{83}$$

Using equations 81 and 72, we get

$$(\Phi^\circ_{FD}/\Phi_{FD})/(\Phi^\circ_{FM}/\Phi_{FM}) = 1 + k_{QD}[Q]/(k_D + k_{MD}) = 1+ \tau_D k_{QD}[Q] \tag{84}$$

From equation 84 solving for k_{QD} we get,

$$k_{QD} = \left((\Phi^\circ_{FD}\Phi_{FM})/(\Phi_{FD}\Phi^\circ_{FM}) - 1\right)/\tau_D[Q] \tag{85}$$

In the same way from equation 72,

$$k_{QM} = (\Phi^\circ_{FM}/\Phi_{FM} - 1)/(\tau_D[Q]) \tag{86}$$

So the ratio of the quenching rate constant will be

$$k_{QD}/k_{QM} = [(\Phi^\circ_{FD}\Phi_{FM}/\Phi_{FD}\Phi^\circ_{FM}) - 1]\tau_M/(\Phi^\circ_{FM}/\Phi_{FM} - 1)\tau_D \tag{87}$$

Using our experimental data we get,

$$k_{QD}/k_{QM} = 0.48$$

So our kinetic analysis indicates that the monomer fluorescence is more susceptible to oxygen quenching and the experimentally observed preferential quenching of excimer fluorescence is due to the fact that the excimer lifetime is longer than that of the monomer*. In this way the

*The excimer lifetime is 32 ns while the monomer lifetime including the excimer forming step is about 8.5 ns.

excimer fluorescence is quenched to larger extent due to collisional quenching.

If we want to understand the difference in the quenching rates of the monomer and excimer we should consider the possible mechanisms of such a quenching.

(a) Enhanced Intersystem Crossing

During the collision of the excited naphthalene monomer with the ground state oxygen there is coupling of the spin momenta to give a triplet collision complex $^3\left[{}^1M^* + {}^3\Sigma_g^-(O_2)\right]$ so the spin prohibition of the intersystem crossing process is removed[62].

The process can be described as follows:

$$^1M^* + {}^3\Sigma_g^-(O_2) \longrightarrow {}^3M^* + {}^3\Sigma_g^-(O_2)$$

Initially both naphthalene and O_2 are in the zero vibrational state. Using the Robinson-Frosch[103] theory of non-radiative transitions the matrix element for the interaction between the initial and final state can be written as

$$\beta = H_{if} \langle 0|\nu\rangle_N \langle 0|\mu\rangle_{O_2}$$

where H_{if} is the matrix element for the exchange interaction between the initial and final states of naphthalene and the other two factors are the appropriate vibrational overlaps. The electronic state of oxygen remains the same before and after the reaction so $0 = \mu$ for oxygen because the two vibrations belong to the same orthonormal set of functions and consequently for $0 \neq \mu$ $\langle 0|\mu\rangle_{O_2} = 0$.

The vibrational overlap is known to be very sensitive to the energy gap between the states. When the vibrational quantum numbers are very different the overlap becomes extremely small.

(b) Energy Transfer to Oxygen

This process can be represented as follows[104]

$$^1M^* + {}^3\Sigma_g^-(O_2) \longrightarrow {}^3M^* + {}^1\Delta_g(O_2)$$

where during the quenching singlet oxygen is produced.

Importance of the Two Mechanisms for the Quenching of the Monomer Emission

When the total electronic energies of the initial and final states are nearly equal, very little electronic energy is converted into nuclear vibrational energy during a radiationless transition between the two states. If the total electronic energy of the final state is significantly less than that of the initial state, the difference has to be made up by vibrational excitation in the final state. Because the Franck-Condon factor for oxygen becomes exceedingly small if the initial and final vibrational states of the oxygen molecule differ by more than a few quanta[105] we can, for practical purposes, assume that most of the vibrational excitation energy goes into the large naphthalene molecule.

For mechanism (a) the energy gap between the naphthalene $^1B_{3u}$ state and the $^3B_{2u}$ state is $E = 10700\ cm^{-1}$. For mechanism (b), since the excitation energy for the process $^3\Sigma_g^-(O_2) \longrightarrow {}^1\Delta_g(O_2)$ is $\sim 7880\ cm^{-1}$ we are left with only $2800\ cm^{-1}$ to be distributed as vibrational energy. Since the Franck-Condon factors are known to dominate the nonradiative transition rate, process (b) should be favored.

In the case of excimer, the $^1D^*$ state is at $\sim 25400\ cm^{-1}$[106, 107]. The excimer singlet state can intersystem cross to the naphthalene triplet excimer state which has been placed at $\sim 18600\ cm^{-1}$ with an energy gap $\Delta E \simeq 6800\ cm^{-1}$[108,109]. On the other hand, energy transfer is energetically impossible. Although process (a) is more favorable in the excimer case, the elimination of process (b) which is the most efficient one seems to be the cause for the slower quenching rate of excimer fluorescence.

1,3-DIPHENYLPROPANE

Solvent Effects on Excimer Luminescence

In our kinetic treatment of the excimer formation process we neglected other properties of the solvent except its viscosity which obviously affects the motion of the aromatic rings.

In the course of our study of intramolecular excimer formation we found that the ratio of monomer to excimer fluorescence intensity in 1,3-diphenylpropane is solvent dependent. Table 4 shows this ratio expressed as the ratio of the intensities at the corresponding maxima.

Table 4. Effect of Solvent on the Emission Properties of 1,3DPP

Solvent	I_M/I_D	λ_D^{max} (nm)	μ[1] (Debyes)	n[2] (sodium D)
Methanol	0.56	329	1.70	1.316
Ethanol	0.56	329	1.69	1.359
n-Propanol	0.56	329	1.68	1.383
n-Butanol	0.56	329	1.66	1.397
Methylene Chloride	1.46	327	1.60	1.444
p-Dioxane	0.71	326	~0	1.420
Methyl Cyclohexane	0.77	325	~0	1.421
Hexane	0.88	325	~0	1.372

(1) Gas phase dipole moments in Debyes[110].

(2) Refractive index for sodium D line[111].

From Table 4, we see a correlation between the observed I_M/I_D ratios and the polarity of the medium as expressed by the dipole moment of the solvent

molecules. Associated is a shift of the broad maximum of the excimer emission. The above data refer to non-degassed solutions. After the effect of oxygen was realized certain results were rechecked after exhaustive freeze-pump-thaw cycles. The results are as follows:

Solvent	I_M/I_D
Ethanol	0.33
Cyclohexane	0.43
Methylene Chloride	0.86

So although the actural numbers change, the relative ratios for different solvents do not change significantly and the effect is qualitatively the same.

The excimer formation process in 1,3-diphenylpropane is a kinetically controlled process and the observed I_M/I_D ratios signify changes in the rate of the excimer formation process as a function of solvent or some special quenching phenomena.

We have previously derived the equation

$$k_{DM} = \Phi_{FD} k_{FM}(k_D + k_{MD})/\Phi_{FM} k_{FD}$$

where

$$\Phi_{FD}/\Phi_{FM} \propto I_D/I_M$$

To test the assumption that the observed different I_M/I_D signify different association rates in different solvents, we studied that excimer formation process as a function of temperature in ethanol and methyl cyclohexane trying to determine the corresponding activation energies. If the temperature dependence of I_M/I_D is determined by the temperature dependence of k_{DM} then the activation energy of the association reaction is obtained by the following equation[112]

$$\partial \ln(I_D/I_M)/\partial(1/T) = -E_{DM}/R$$

Plots of I_D/I_M against 1/T are shown in Figure 8. The plots are quite linear and the activation energies are as following:

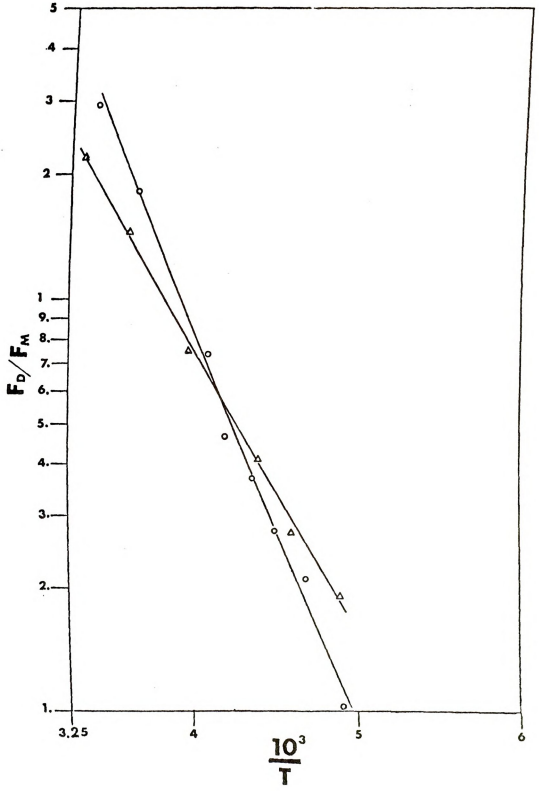

Figure 8. Determination of the Activation Energy for Intramolecular Excimer Formation in 1,3-Diphenylpropane. Circles: Methylcyclohexane, Triangles: Ethanol.

Ethanol E_{DM} = 3.3 kcal/mole

Methyl Cyclohexane E_{DM} = 4.3 kcal/mole

The activation energy in ethanol appears lower as one may have expected from the static I_D/I_M measurements. This behavior may be explained if the activated complex is polar. Polar characteristics for the benzene excimer have been suggested by Hirayama and Lipsky[85].

Chandross and Dempster[56] found an E_{DM} for 1,3-Bis-(α-naphthyl)-propane (1,3DNP) in ethanol of 4.0 kcal/mole and Itoh et al.[112] an activation energy E_{DM} = 2.0 for β, α'(9,10-dicyanoanthracene)-$(CH_2)_3$-(naphthalene) (β, α'-DCAN) and an E_{DM} = 2.2 kcal/mole for β, β'-DCAN in ethanol. Our value of 3.3 kcal/mole lies between these values. It can be argued that the transition state for DCAN is more polar as expected for an exciplex than that of an excimer and thus the lower activation energy. So 1,3DPP excimer appears more polar than the 1,3DNP excimer. We studied 1,3DNP in ethanol and hydrocarbon and we did not notice any enhancement in the polar solvent.

We would like to know if the assignment of polar character to the 1,3DPP excimer could account for the observed activation energy difference. For this reason we are going to do a very rough calculation using a theory first developed by Kirkwood[113]. This theory gives the energy of an idealized dipole (μ) in a continuous dielectric of constant ϵ compared to that in a similar medium of unit dielectric constant.

$$\Delta G_{solv} = -\mu^2/r^3\left[(\epsilon - 1)/(2\epsilon + 1)\right] \tag{88}$$

Applying this equation to the transition state theory one obtains[114]

$$\ln k/k_0 = -(\epsilon - 1)/(2\epsilon + 1)\cdot(\mu_R^2/r_R^3 - \mu_\ddagger^2/r_\ddagger^3)/kT \tag{89}$$

where k is the rate constant in a medium of dielectric constant ϵ, k_0 is the rate constant in a medium of $\epsilon = 1$, and μ_R and $\mu_\ddagger$ are the dipole moments

of the reactants and activated complex respectively.

The change of entropy appearing in the transition state theory expression for the rate constant can be decomposed as

$$\Delta S = \Delta S_{intra} + \Delta S_{solv} \tag{90}$$

where ΔS_{intra} refers to the intramolecular entropy changes during the association process and ΔS_{solv} refers to the effect of solvation.

From classical thermodynamics we know that

$$\Delta G = \Delta H - T\Delta S \qquad \text{and} \qquad (\partial \Delta G/\partial T)_p = -\Delta S$$

So $$\Delta S_{solv} = -3\epsilon/(2\epsilon + 1)^2 \cdot (\partial \ln\epsilon/\partial T)_p (\mu_R^2/r_R^3 - \mu_\pm^2/r_\pm^3) \tag{91}$$

The connection between the Arrhenius equation preexponential factor A and the preexponential factor of the transition state theory is

$$A = e(kT/h)\exp(\Delta S^{\ddagger}/R) \tag{92}$$

It further seems reasonable to assume that

$$\Delta S_{1\ intra} = \Delta S_{2\ intra}$$

where subscript 1 denotes alcohol as solvent and subscript 2 cyclohexane. Using the Arrhenius equation we can get that

$$E_2 - E_1 = \left(RT\ln(k_1/k_2)/\ln(k_2/k_0)\right) / \left(\ln(A_1/A_0)/\ln(A_2/A_0)\right) \tag{93}$$

where E_2 and E_1 are the activation energies in hydrocarbon and ethanol respectively.

From equation 92, we see that,

$$\ln(A_1/A_0)/\ln(A_2/A_0) = \Delta S^{\ddagger}_{1_{solv}}/\Delta S^{\ddagger}_{2_{solv}} \tag{94}$$

Substituting equations 94 to 93, we get

$$E_2 - E_1 = RT\left(\ln(k_1/k_0)/\ln(k_2/k_0)\right)/(\Delta S^{\ddagger}_{1_{solv}}/\Delta S^{\ddagger}_{2_{solv}}) \tag{95}$$

where the numerator can be calculated with the use of equation 89 and the denominator with the use of equation 91. Using $\epsilon^{25°C}_{ethanol} = 25$, $\epsilon^{25°C}_{cyclohexane} = 2$,

$(\partial \ln\epsilon/\partial T)_{P,ethanol} = 6.02 \times 10^{-3}$ (reference 114)

$(\partial \ln\epsilon/\partial T)_{P,cyclohexane} = 7.35 \times 10^{-4}$ (reference 115)

we obtain $E_2 - E_1 \simeq 0.8$ kcal/mole

This result is of the same order of magnitude with the experimentally observed difference of 1 kcal/mole and tents to support the idea that solvation of the excimer is important.

In the case of the non polar solvents the forces are of the dipole-induced dipole and the dispersion kind which both depend on the polarizability of the molecules. A measure of the polarizability is the refractive index. Dioxane is known to behave like a more polar solvent than its bulk dielectric properties imply. Suppan[116] showed that this anomaly is related to the polarity of the solute molecule, and suggest that the phenomenon may result from a "conformation polarization" of dioxane from the non polar chair form to two polar boat forms with dipole moments of 2.4 and 1.4 D.

Finally there is an apparent anomaly in the case of the polar dichloromethane with a very high I_M/I_D ratio. It is well known that chlorocarbons especially carbon tetrachloride are very effective quenchers of the fluorescence of aromatic hydrocarbons[117] and that the excimer fluorescence is quenched to a greater extent that the monomer fluorescence[118]. In our case the effect may be partially due to weak ground state interactions of the monomer with CH_2Cl_2 probably weak charge transfer complexes that may inhibit the excimer formation.

Polar Nature of the Intramolecular 1,3DPP Excimer

Hirayama and Lipsky[85] discussing the intermolecular benzene excimer case suggest that "the charge-transfer component in the excimer wavefunction generates an adequate electric moment to extensively orient the surrounding solvent". The excimer wavefunction can be approximated by a trial function of the type

$$a\psi(M_1^+M_2^-) + b\psi(M_1^-M_2^+) + c\psi(M_1^*M_2) + d\psi(M_1M_2^*)$$

The dipole moment due to charge-transfer interaction in the excited complex species, μ_D is proportional to $|a^2 - b^2|$. In the excimer case, unlike the exciplex, a = b and c = d and no permanent dipole moment should result, contrary to Hirayama's speculation. Weller and coworkers[119] by means of solvent shift studies concluded that the pyrene excimer has no permanent dipole moment.

A possible explanation by which a dipole moment could arise in the 1,3DPP excimer state is because the excimer is composed of two"toluene like" units arranged in a sandwich configuration. Toluene is very weakly dipolar = 0.55 D[120]. A ground state molecule with the excimer configuration will probably have a dipole moment of ~ 1 D. The lowest excited state of toluene (Group C_{2V}) is $^1B_1$ and the transition $^1B_1 \longleftarrow {}^1A_1$ is x polarized.

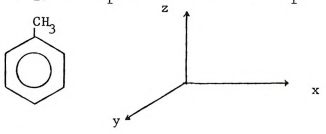

Thus it is not expected that the excitation will produce any significant charge separation along the long axis (z) of the molecule and the excited state dipole moment of toluene should be close to that of the ground state. Hence the excimer of 1,3DPP will probably have a dipole moment of ~ 1 D.

The excimer fluorescence spectral shifts from hydrocarbon to alcohol are not large corresponding to an energy difference of about 1 kcal/mole. These shifts can not be explained in terms of the dipolar character of the excimer since the lowering of the energy of the excimer state in a polar medium is expected to be compensated by a corresponding lowering of the Franck-Condon ground state. The excimer is expected to have higher polarizability and so dipole-induced dipole interactions may account for the small observed shifts.

Origin of the Activation Energy

As first pointed out by Chandross and Dempster[56] part of the activation of an intramolecular excimer may be due to the rotational barriers of the carbon chain that must be surpassed to attain the appropriate geometry for excimer formation. In fact in the case of $\alpha\alpha$- and $\beta\beta$- 1,3DNP that they studied the activation energy was attributed completely to that effect. On the other hand the observed activation energy for intermolecular excimer formation was attributed to the activation energy for viscous flow of the solvent. This activation energy was obtained by using the simplified result of the Einstein-Smoluchowski diffusion theory[76]

$$k_D = 8RT/3000\eta = A\exp(-E_a/RT) \qquad (96)$$

We have studied 1,3DPP in ethanol-glycerol mixtures and although the result can not be interpreted quantitatively because of the concurred dielectric constant changes which as we have shown influence the I_M/I_D ratio, it is obvious that the intramolecular excimer formation in 1,3DPP as also in the case of 1,3DNP is viscosity dependent. In the following we will try to estimate the importance of rotational barriers to the activation energy.

1,3DPP from energetic considerations, can exist in two stable conformations. Using the n-butane system nomenclature[121] these two conformations are the trans-trans (TT) and the trans-gauche (TG). Using molecular models we see that in the supposed stacked excimer donfiguration the methylene chain conformation is gauche-gauche (GG). The energy difference between a trans and a gauche form is about 0.8-0.9 kcal/mole[122]. A way to estimate the importance of the various conformers of a molecule is through the use of the "steric partition function" introduced by Pitzer[123]

$$Q^{st} = \sum_i \exp(-E_i/RT) \qquad (97)$$

The summation covers all conformations of the molecule; E_i is the steric

energy of the i^{th} conformation limited by the intramolecular repulsion forces. The total number of energetically favorable conformations of a normal paraffin with n carbon atoms amounts to 3^{n-3}. It would be pointed out that terminal groups (in this case ϕ groups) do not produce different conformations during innner rotation.

In this way the fraction of molecules in the (TT) conformation n_{TT}/N will be given by

$$n_{TT}/N = f_{TT} = g_{TT} \cdot \exp(-E_{TT}/RT)/Q^{st} \tag{98}$$

and the fraction of molecules in the (TG) conformation will be

$$n_{TT}/N = f_{TG} = g_{TG} \cdot \exp(-E_{TG}/RT)/Q^{st} \tag{99}$$

The degeneracy of the (TT) state is one ($g_{TT} = 1$) and the degeneracy of the (TG) state is two ($g_{TG} = 2$). So

$$f_{TT}/f_{TG} = \tfrac{1}{2}\exp\left[-(E_{TT} - E_{TG})/RT\right] \tag{100}$$

If $E_{TT} - E_{TG} = 0.9$ kcal/mole, then

$$f_{TT}/f_{TG} = 2.26 \tag{101}$$

Also

$$f_{TT} + f_{TG} \simeq 1 \tag{102}$$

Replacing the approximate sign in equation 102 by an exact equality we can get from equations 101 and 102

$$f_{TT} = 0.69 \qquad \text{and} \qquad f_{TG} = 0.31 \tag{103}$$

Then the contribution of methylene chain rotation to the observed activation energy will be given by

$$E_R = f_{TT} \times 2E_{G \leftarrow T} + f_{TG} \times E_{G \leftarrow T} \tag{104}$$

Using again $E_{G\ T} = 0.9$ kcal/mole

$$E_R = 1.5 \text{ kcal/mole}$$

In the case where the solvent does not have any specific interaction with the activated complex (solvation) as in the methylcyclohexane case one may expect that the observed activation energy is approximately the

addition of the rotation activation energy and the activation due to the solvent viscosity. Hirayama and Lipsky[85] studied the temperature dependence of the viscosity of methyl cyclohexane and got an activation energy of 2.8 kcal/mole. The observed activation energy in MCH is then expected to be

$$E_{obs} = E_R + E_{visc} = 4.3 \text{ kcal/mole}$$

which is the same value we obtained experimentally. Obviously we do not attach great significance to the closeness of the observed and estimated activation energies, however it seems that our argument is valid. So we see that the anomalous values of activation energies in ethanol[112,124] can be explained as due to specific interactions with the excimer or exciplex state.

Intramolecular Triplet Excimer Formation

Although the formation of singlet excimers is a quite general phenomenon especially between aromatic hydrocarbons there are few and conflicting reports on the existence of triplet excimers. The main phenomenological manifestation of triplet excimer formation is expected to be an additional component in the phosphorescence spectrum which is red shifted with respect to the monomer phosphorescence.

Castro and Hochstrasser[125] observed broad phosphorescence band systems having their intensity maxima about 5000 cm^{-1} lower in energy than the 0,0 monomer phosphorescence from halogenated benzene crystals at low temperatures. In these crystals translationally equivalent molecules are spaced closely along one crystal axis such that excimer type interaction is possible. Later however Lim and Chakrabarti[126] ascribed these emissions to photoproducts, and assigned a broad phosphorescence band lying at considerably longer wavelength, which they observed in concentrated solutions of chlorobenzene in rigid glass, to an excimer phosphorescence. Langelaar et al.[108]

observed a broad delayed emission band superimposed on the monomer phosphorescence of naphthalene in fluid ethanol solutions aroung 180°K and attributed it to triplet excimers. The red shift (~ 1000 cm^{-1}) of the phosphorescence spectrum of [4,4] paracyclophane in EPA at 77°K has been attributed[127] to triplet excimer interaction. In this molecule the two benzene rings are held together by methyl bridges in a sandwich structure with an inter-ring separation of ~ 3.5 Å. Emission bands are observed at $\sim 20{,}000$ cm^{-1} in liquid alkyl benzenes as a result of intense electron beam excitation. These emissions were attributed by Christophorou et al.[128] to excimer phosphorescence produced by ion-recombination processes. Finally solid benzene at 138°K excited by 1 MeV electron beam exhibits a phosphorescence spectrum which in addition to the monomer phosphorescence has a structureless component beyond 430 nm, the latter has been attributed by Phillips and Schug[50] to an emission from a "triplet charge-exchange excimer". More indirect indication of triplet excimer formation comes from the decrease of the triplet lifetime of o-xylene with increasing concentration as estimated by butene-2 quenching studies[129].

Most of the above evidence does not appear unambiguous especially because of the possibility of photoproducts in halogenated aromatic hydrocarbons and in the cases where high energy electron beams are used. Moreover it does not seem to be any systematic approach to the search for the triplet excimer. In the following we will try to understand why the observation of triplet excimers is so scarce and propose appropriate conditions for its observation.

Mechanisms of Triplet Excimer Formation

I. Association of a triplet excited molecule with another ground state molecule

$$^3M^* + {}^1M \longrightarrow {}^3D^* \qquad (105)$$

Reaction 105 requires the mutual diffusion of $^3M^*$ and ^1M. On the other

hand it is a well known fact that triplet states are very effectively quenched in fluid solutions and phosphorescence can only be observed in crystals or frozen glassy solutions at low temperature. In this way by freezing the solution to prevent collisional quenching we prevent the triplet excimer formation. We should note here that if the $^3D^*$ formation requires a minimal configurational change this may be achieved even at a highly viscous solution because of the long lifetime of the triplet state.

The temperature was considered above as acting only through changes in the viscosity of the medium. Hoytink et al.[130] suggest that there is an intrinsic (apart from diffusion) activation energy for triplet excimer formation. This activation energy $\sim 400\ cm^{-1}$ although small will be important at 77°K. Different interpretations have been discussed by Baldwin[131] and Siebrand[132].

II. Generation of triplet excimer through intersystem crossing from the singlet excimer state.

$$^1M^* + {}^1M \longrightarrow {}^1D^* \xrightarrow{isc} {}^3D^* \qquad (106)$$

Indirect evidence for the existence of this process comes the study of the temperature dependence of the singlet excimer lifetime. This dependence in most cases has been reproduced by the inclusion of a single temperature-dependent rate parameter k_{ID} in the form

$$k_{ID} = A_{ID} \cdot \exp(-E_{ID}/RT)$$

The computed frequency factors A_{ID} are some orders of magnitude lower than characteristic values in the range 10^{12}-$10^{14}\ s^{-1}$ for unimolecular reactions and the process has been described as a spin-intercombination process or $k_{ID} = k_{ISC\ D}$[15]. Mechanism II depends on the formation of a singlet excimer formation process is again diffusion controlled and in fact is expected to be much more sensitive to the fluidity of the medium because of the short

lifetime of the singlet state.

Another complication may be that the intersystem crossing may be followed by dissociation

$$^1D^* \xrightarrow{isc} {}^3D^* \longrightarrow {}^3M^* + M \qquad (107)$$

This behavior has been reported for pyrene in ethanol at 20°C by Melinger and Wilkinson[334] who measured the instantaneous population of the molecular triplet state by flash kinetic spectrophotometry. Although these authors treat the over-all process as one of dissociative intersystem crossing

$$^1D^* \longrightarrow {}^3M^* + M \qquad (108)$$

their results are consistent with an excimer intersystem crossing yield of 0.12 and a rate constant of 2.3×10^6 s^{-1}[15]. If process 107 takes place in a viscous environment, recombination of the products can give $^3D^*$.

Finally it has been suggested that the geometrical requirements for singlet and triplet excimers are different and probably in a rigid matrix the necessary spatial rearrangement is not possible to take place[133]. It is almost obvious, but after overlooked, that in order to observe triplet excimer formation the viscosity of the medium should be high enough such that triplet quenching is minimized and low enough such that diffusion of the excited triplet chromophore to form an excimer dimer is probable during the lifetime of the excited state. A way to enhance the possibility of triplet excimer formation is the use of a "double molecule" like 1,3DPP. Toluene has quite a long triplet lifetime (in rigid media ~6 sec.). The combination of long lifetime and the enhanced collision probability are ideal. Since the optimum viscosity is unknown one should scan a large range of viscosities (temperatures).

A degassed 10^{-3}M solution of 1,3DPP in 3-methylpentane (3MP) at 77°K exhibits a toluene type emission with fluorescence maximum at 285 nm and

phosphorescence maximum at 390 nm with typical vibrational structure. It should be noted here that the viscosity of 3MP at 77°K ($\sim 10^{12}$ cp) is high enough to prevent diffusional relaxation before emission. The lifetime of this phosphorescence is 6.5 sec. similar to that of toluene. The relative intensities of fluorescence and phosphorescence are also similar.

The emission observed from a 10^{-3}M degassed solution of 1,3DPP in isopentane(iP) at 77°K ($\sim 10^{6}$ cp) varied somewhat depending on the rate of formation of the glass. Usually a monomer fluorescence M_F and a monomer phosphorescence M_P are observed as in 3MP, however the phosphorescence spectrum is relatively diffuse compared to that observed in 3MP at 77°K.

Figure 9 shows both spectra together with the emission spectrum recorded after the sample was allowed to warm up slightly; the estimated temperature is about 115°K. The phosphorescence spectrum in the latter case is shifted to longer wavelengths with a maximum at 420 nm. When the sample was allowed to further warm up and the viscosity of the solution decreased the intensity of phosphorescence decreased rapidly until it was completely quenched and only monomer fluorescence is emitted. At such viscosities, diffusional relaxation leading to singlet excimer formation during the lifetime of the excited monomer singlet state does not occur. Excimer fluorescence at 330 nm (D_F) began to appear and dominated the spectra in the neighborhood of room temperature at appreciably lower viscosities. The energy gap between the maximum of D_P and the 0,0 of M_P is ~ 5000 cm^{-1}. The 420 nm emission was interpreted as excimer phosphorescence. The mechanism of the excimer formation in this case (singlet excimer is not present) is obviously the direct association of a triplet excited phenyl ring with a singlet ground state one:

$$^3M^* + {}^1M \longrightarrow {}^3D^*$$

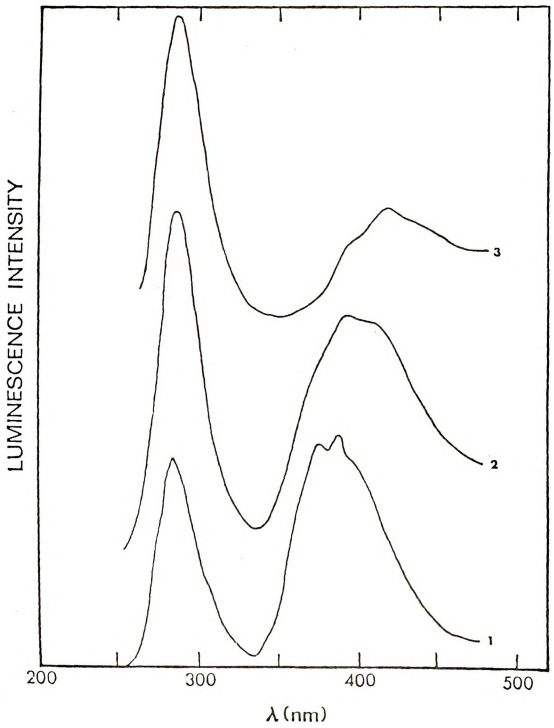

Figure 9. Total Emission Spectra of 1,3-diphenylpropane; (1) 3MP Glass at 77°K, (2) iP Glass at 77°K, and (3) After the iP Glass Was Allowed to Melt (Estimated Temperature 115°K).

Since the emission is observed during the softening of the glass matrix and disappears upon warming, photoproducts could not be responsible for it. This maximum correlates with electron-beam induced emissions from alkyl benzene liquids. It is also consistent with Castro and Hochstrasser's reported emissions from halobenzene crystals. These were disputed by Lim and Chakrabarti as photoproducts however the maximum of the emission reported by Lim is far too low in energy (8000 cm^{-1} from the 0,0 of M_p) to correspond to triplet excimers.

Singlet and Triplet Intramolecular Excimers of 1,3-Diphenylpropane at 77°K

Concentrated solutions of 1,3DPP in rigid glass or iP at 77°K under conditions where microcrystals are formed exhibit an excimer fluorescence at 340 nm and excimer phosphorescence at 425 nm, Figure 10. Upon slight warming the phosphorescence band maximum shifts to 420 nm similar to that observed in fluid media. Phosphorescence decay measurements at different wavelengths show that there are two components a long-lived one at short wavelengths and a short-lived component at longer wavelength. This appears to be a unique case where both singlet and triplet excimers are observed. In the following we will try to analyze the mechanism of excimer production in a disordered solid, like the microcrystalline solid we used.

I. Singlet excimer:

There are may kinds of defects that can be realized in a disordered crystals, such as vacancies which are regions of lower density than the bulk material, or overcrowded regions of higher density. The initially produced singlet exciton wave will propagate till it meets such a defect. The loss of translational symmetry and the loss of the strict phase relations of the excited regular lattice result to the immobilization of the exciton. Grain boundaries may also have the same effect.

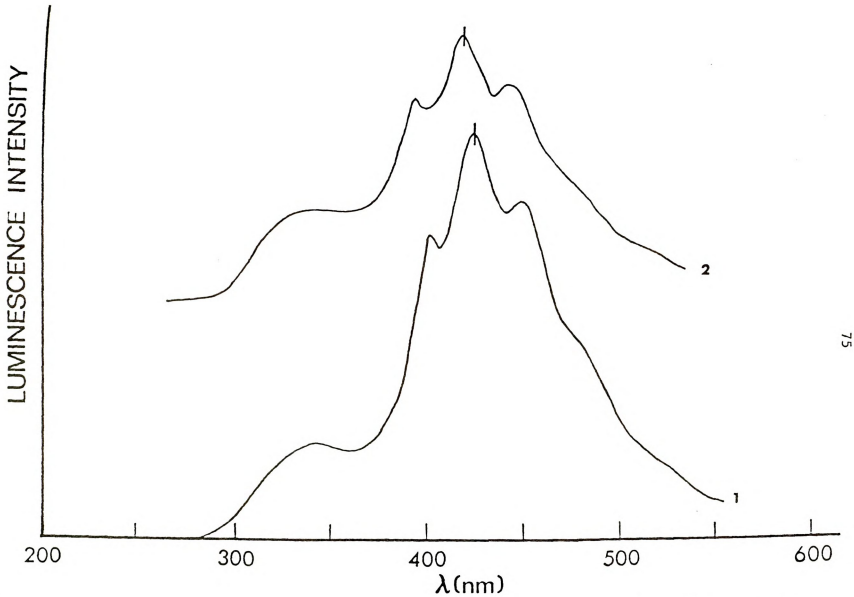

Figure 10. Emission of Concentrated Solutions of 1,3DPP in iP. (1) Microcrystals at 77°K, (2) After Sample was Allowed to Warm Up Slightly.

An important type of defect will be an excimer site that is two molecules forced in close proximity and held by the strong crystal packing forces.

There are obviously two ways that the singlet excimer can be formed:
(1) Free propagation of the exciton till it meets the appropriately oriented molecular pair then the energy decreases adiabatically and the exciton is trapped with the formation of a singlet excimer.
(2) Trapping of the exciton at another defect site with subsequent longer range energy transfer to the excimer site. This mechanism which is considered more effective for impurity trapping at low temperatures by Hochstrasser[134] can only operate in our case if the "excimer pair" is strongly interacting in the ground state and the transition energy is appreciably reduced.

We believe that trapping of singlet excitons of either the Frenkel or the Forster-Dexter type at the "excimer site" is the reason for observing only excimer emission in our microcrystalline system. We also believe that an analogous situation appears in various polymers like polystyrene where the emission appears almost completely excimeric.

II. Triplet exciton:

Although the probability of intersystem crossing in crystals of aromatic hydrocarbons is lower than in the free molecule (solution) case still a significant amount of the absorbed quanta will ultimately reside in the lowest triplet state[135].

Analogously to the singlet exciton the triplet excitation can propagate in the crystal in the form of a triplet exciton. This was shown by studies of Avakian and Merrifield[136] and by the dynamic experiments of Ern et al.[137]. The motion of the triplet exciton can be best characterized

by a relatively slow random-walk, hopping mechanism[138]. In this way trapping of the triplet exciton may give rise to triplet excimers.

Another possibility of course is direct intersystem crossing from the singlet excimer state. In this case even if the triplet excimer state is dissociative at the ISC energy recombination may be expected to take place.

CHAPTER 3

INTRAMOLECULAR EXCIPLEX-CHARGE TRANSFER INTERACTIONS IN THE SYSTEMS (PHENYL)-$(CH_2)_n$-(PYRIDINE) AND AROMATIC CARBOXYLIC ACIDS

INTRODUCTION

In this chapter we are studying intramolecular exciplex interactions. Initially we study the systems 4-(3-phenylpropyl)-pyridine ⟨⬡⟩-$(CH_2)_3$-⟨⬡⟩N (1,3PyPP) and 4-benzylpyridine ⟨⬡⟩-CH_2-⟨⬡⟩N ($PyCH_2P$). These systems depending on the solvent properties display a variety of interactions. In neutral alcohol solution, the absorption spectra of 1,3PyPP do not show signs of ground state interactions while the room temperature fluorescence spectrum shows intramolecular excimer formation completely analogous to the 1,3DPP case. As the hydrogen bonding ability or acidity of the solvent increases (H_2O, EtOH + $HClO_4$, H_2O + $HClO_4$) strong hydrogen bonding or protonation of the pyridinic nitrogen changes the interaction drastically. Analysis of the absorption spectra of 1,3PyPP and $PyCH_2P$ shows significant ground state interactions while the broad emissions show extremely large Stokes shifts of~14,000-15,000 cm^{-1}. Since upon protonation of the pyridinic nitrogen the electron affinity of the pyridine segment is expected to increase drastically (see also INDO calculations) the interaction is now of the charge-transfer type. This fact is also verified by the out of plane polarization of the fluorescence. Thermodynamic arguments lead us to believe that in certain cases complete electron transfer is possible.

It is interesting to note that while Py^+CH_2P shows strong CT-exciplex

interaction, no excimers are observed in diphenylmethane, illustrating the difference in geometric requirements of excimer and CT-exciplex interactions.

Upon changing the excitation wavelength, shifts are observed in the emission. The emission bands arise from molecules associated in the ground state (charge transfer interaction) or from molecules associated in the excited state (exciplex interaction). This fact is also proved by study of the excitation spectra of these emissions. Although one would expect that the relaxed exciplex and charge-transfer states to be the same, the rotational barriers of the connecting chain appear to inhibit this relaxation resulting to a composite emission. Finally the emission spectra at low temperature show the importance of solvent relaxation in these systems. The phosphorescence of 1,3PyPP and $PyCH_2P$ under all conditions is arising from the lowest locally excited toluene triplet state suggesting that the ^3CT state is dissociative. It is interesting that the emission of the relaxed singlet state appears at lower energy than the triplet state emission.

In the even-odd system 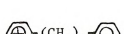 unlike 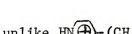 the two structures where the positive charge is on either ring, are degenerate and charge-resonance is expected. This phenomenon is manifested in the difference of fragmentation patterns of butylbenzene and 1,3DPP in the gas phase inside the mass spectrometer.

Finally exciplex interactions may not be manifested by the appearance of new emission bands but may show up in a more subtle way. Aromatic carboxylic acids of the general form 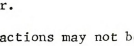 show enhanced intersystem crossing and changes in fluorescence/phosphorescence intensity ratios and lifetimes compared to the compound lacking the carboxyl group. This

phenomenon has been interpreted as an enhancement of spin-orbit coupling as a result of exciplex interactions[204]. In order to test further this point, namely, that the effect is due to the intramolecular exciplex interaction of carboxyl group and the aromatic ring, compounds that have the carboxyl group rigidly held and do not allow for intramolecular relaxation are studied. The observed fluorescence and phosphorescence quantum yields and lifetimes support the above mechanism.

I. (PHENYL)-$(CH_2)_n$-(PYRIDINE) SYSTEM

Electronic States and Spectral Properties of Pyridine and Pyridinium Ion

The spectroscopic properties of pyridine have been under investigation for many years. The sharp absorption, in the vapor phase, that starts at 2800 Å was assigned by Kasha[139] to an n,π^* transition. This transition overlaps the lowest π,π^* absorption which starts around 2600 Å[140]. The presence of many progressions built on a strong 0,0 band in the case of the n,π^* transition, indicate a dipole allowed transition B_1. The low intensity of this band was attributed by Orgel[141] to the small overlap of the n and π orbitals. Finally the rotational fine structure of the 0,0 band is consistent with a B_1 state[142]. Sponer and Rush[140] place the $^1B_2(^1L_b)$ state at 38,350 cm^{-1} and finally El-Sayed[143] places the $^1A_1(^1L_a)$ at 49,750 cm^{-1}.

An interesting feature of the pyridine absorption spectra is the dramatic changes induced by the solvent (hydrocarbon vs hydrogen bonding protonic solvents)[144]. The n,π^* band disappears (blue shift in hydrogen bonding solvents is a characteristic of n,π^* states) and the $\pi\pi^*$ absorption intensifies and apparently sharpens[145]. This subject will be discussed in more detail later.

In an acidic environment the lone pair on the nitrogen is protonated

to give the pyridinium ion. E. Clementi[146] showed that the lone pair on the nitrogen is partly delocalized on the neighboring carbon atom but retains 1.41 electrons in the sp^2 hybrid on the nitrogen nucleus. The energy of the $^1A_1$ state of pyridinium was placed at 5.5 eV and that of $^1B_2$ at 4.8eV by Brown and Heffernan[147].

In Figure 11, we show the relative positions of the lowest states of benzene, pyridine and pyridinium. The energies of the benzene states are those given by D. S. McClure[148].

Considering the emission properties, we find that pyridine is a non-fluorescing compound. Cohen and Goodman[149] suggest that the fluorescence quantum yield is less than 10^{-5}. On the other hand the intersystem crossing yield for pyridine is about 0.3[150]. The most probable deactivation process of the lowest singlet seems to be internal conversion to the ground state. Pyridine besides being non-fluorescent is also non-phosphorescent. Singlet-triplet absorption studies by Evans[151] using high pressure oxygen as a perturbation, indicate that the observed triplet state of pyridine is $\pi\pi^*$ in nature. This state should correlate with the lowest triplet state of benzene (a molecule that exhibits strong phosphorescence).

Pyridium ions, like pyridine, are not emitting[152]. This is true for cases where there is no charge-transfer interaction between the pyridinium cation and the associated anion (like in the case of perchlorates). Kosower[153] has shown that the absorption spectrum of 1-methyl-pyridinium iodide shows an additional shoulder at long wavelength which is interpreted as a charge-transfer absorption of a complex between the pyridinium cation (acceptor) and the iodide ion (donor).

Briegleb et al.[154] found an emission from the above compound which they ascribed to the reverse charge-transfer process.

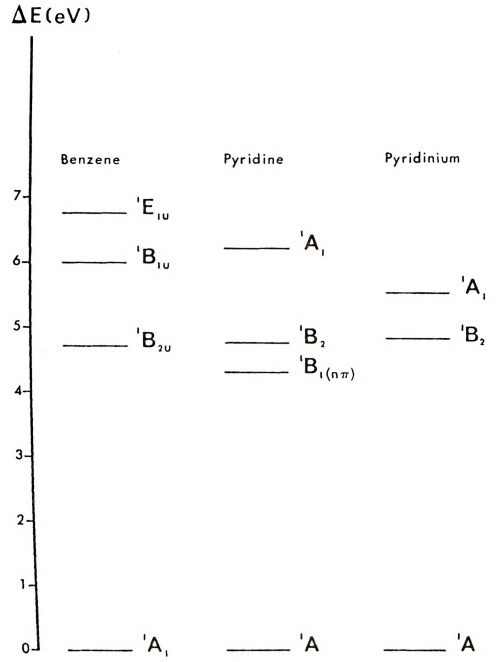

Figure 11. Symmetries and Energies of the Lowest Singlet States of Benzene, Pyridine and Pyridinium Ion.

The above discussion on the spectral properties of pyridine apply to its methyl derivatives (picolines) and especially to the 4-methyl-pyridine (γ-picoline) which represents more accurately our system.

Absorption Spectra

(A) Absorption Spectra of γ-Picoline (4-Methyl-Pyridine)

As we see from Figures 12 and 13 the $^1B_1(n\pi^*) \leftarrow {}^1A_1$ transition which appears as a long wavelength tail in the hydrocarbon solution is blue shifted and disappears under the $^1B_2(\pi\pi^*) \leftarrow {}^1A_1$ transition in water. An assumed hydrogen bond strength of ~6 kcal/mole might be expected to correspond to a shift of around 2000 cm^{-1}[145].

Hochstrasser[155] has measured the dipole moment of pyridine in the $^1B_1(n\pi^*)$ state to be -1.0D to be compared with the ground state dipole moment of +2.19D (opposite direction)[156]. Simonetta[157] considers the dipole-dipole interactions to be important in blue-shifting the $^1B_1(n\pi^*)$ state. Let us now consider the behavior of the $\pi\pi^*$ states as a function of solvent polarity and nitrogen protonation. Table 5 shows this behavior.

The $^1B_2(\pi\pi^*)$ is formally allowed in C_{2V} symmetry but still is quite weak which shows that the replacement of a C-H group (toluene) by a N (γ-picoline) is a small perturbation. Therefore we expect that the intensity of a such a transition will be sensitive to an environmental perturbation. The intensity increases on going from hydrocarbon to water to acid and the extent of perturbation increases in the same way. The intensity increase is also accompanied by a small blue shift. At this point we do not know if this shift is real or it is artificially caused by the blue shift of the overlaping $^1B_1(n\pi^*)$. An important thing to note is that no new bands or long wavelength tails appear as a result of nitrogen protonation.

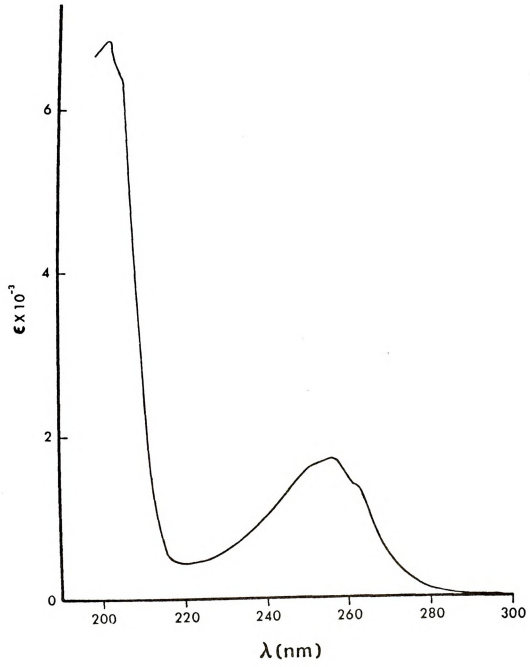

Figure 12. Absorption Spectrum of γ-Picoline in Methylcyclohexane.

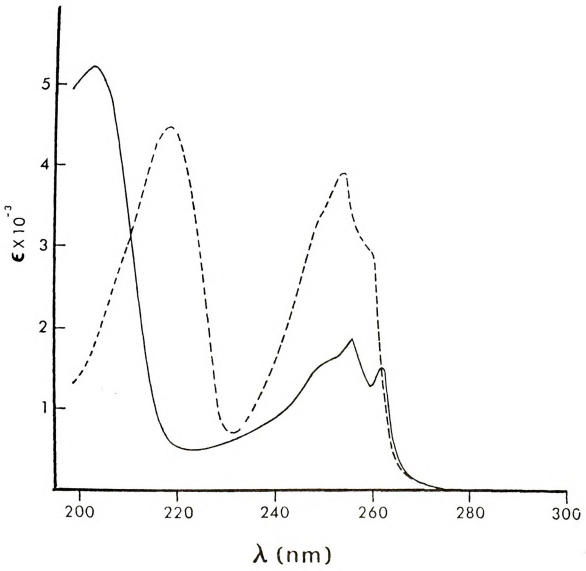

Figure 13. Absorption Spectrum of γ-Picoline in Water (__), Absorption Spectrum of γ-Picolinium Perchlorate in Water (--).

Table 5. Effect of the Medium on the Frequency and Intensity of the γ-Picoline Absorption Spectrum.

Solvent	$\tilde{\nu}_{max}$ (cm^{-1})	ϵ_{max}
$^1B_2 \leftarrow {}^1A_1$		
MCH	39,039	1705
H_2O	39,139	1844
H_2O + $HClO_4$	39,573	3898
$^1A_1 \leftarrow {}^1A_1$		
MCH	49,652	6815
H_2O	49,383	4759
H_2O + $HClO_4$	45,872	4481

This spectroscopic behavior has also been predicted theoretically by Mataga and Mataga[158] using a semiempirical SCF MO technique involving only the π electrons, and later by Janet Del Bene and H. H. Jaffe[159] by an all electron CNDO method. Del Bene and Jaffe ascribe the above effects to the polarization of the π system induced by the hydrogen bond or protonation. In pyridine, the charge density on the nitrogen atom is 5.24 electrons, of which 1.16 belong to the π system. In the pyridinium ion, the total charge density on nitrogen decreases to 4.94 electrons, even though the π electron density increases to 1.46. The tendency of the system to relieve the positive charge on the nitrogen atom that results from the addition of a proton gives rise to a highly polarized π cloud.

Another interesting feature of the spectra is the apparent sharpening on going from hydrocarbon to hydrogen bonding solvents. In the $n\pi^*$ state an electron is removed from the lone pair so the hydrogen bond is expected to dissociate or to greatly weaken[160]. If the hydrogen bonded $n\pi^*$ state is dissociative for the N...H bond then the absorption to the $^1B_1(n\pi^*)$ will be continuous with no discrete vibronic bands. Since $^1B_2(\pi\pi^*)$ and $^1B_1(n\pi^*)$ are overlapping and in protic media $^1B_2$ is increased in intensity then one may expect a "sharper" structure.

The behavior of the $^1A_1(\pi\pi^*) \leftarrow {}^1A_1$ band is the opposite of the $^1B_2(\pi\pi^*) \leftarrow {}^1A_1$ band. Increasing the polarity and acidity of the medium we observe a considerable red shift and a decrease in intensity. This behavior has been also observed by Zanker[161].

Another molecule that we should study before examining the spectra of our systems for ground state interactions is of course toluene. Table 6 shows some numbers.

The 0,0 transition of the ^1L_b state of toluene was placed by Ginsburg[162]

Table 6. Effect of the Medium on the Frequency and Intensity of the Toluene Absorption Spectrum.

	Solvent	$\tilde{\nu}_{max}$ (cm^{-1})	ϵ_{max}
^1L_b	MCH	38,100	260
	EtOH	38,197	290
^1L_a	MCH	48,100	7900
	EtOH	47,985	8400

at 37,477 cm^{-1} while the 0,0 for the ^1L_b state of γ-picoline was placed by Stephenson[145] at around 38,500 cm^{-1}.

From the above data we see that toluene's absorption extends to the red of the γ-picoline absorption and that in the case of the 2500 Å band of the systems that we are interested in (phenyl)-$(CH_2)_n$-(pyridine), toluene's contribution to the extinction coefficient is small while in the case of the 2000 Å band toluene's absorption is most important.

Finally let us consider the absorption spectra of 1,3-diphenylpropane as a model system where there are no specific ground state interactions between the two aromatic rings (Table 7).

Table 7. Effect of the Medium on the Frequency and Intensity of the 1,3DPP Absorption Spectrum.

	Solvent	$\tilde{\nu}_{max}$ (cm^{-1})	ϵ_{max}
^1L_b	EtOH	38,197	473
^1L_a	EtOH	48,309*	17,000

*The vibronic component with the largest Franck-Condon factor in the spectrum of toluene appears at 47,619 cm^{-1} in the case of 1,3DPP.

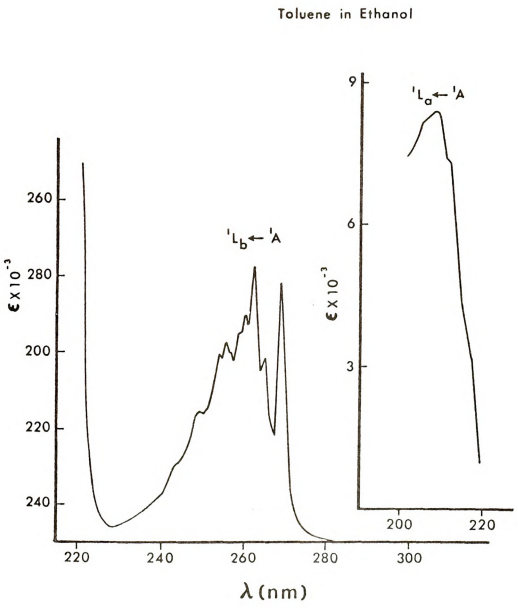

Figure 14. Absorption Spectra of Toluene in Ethanol.

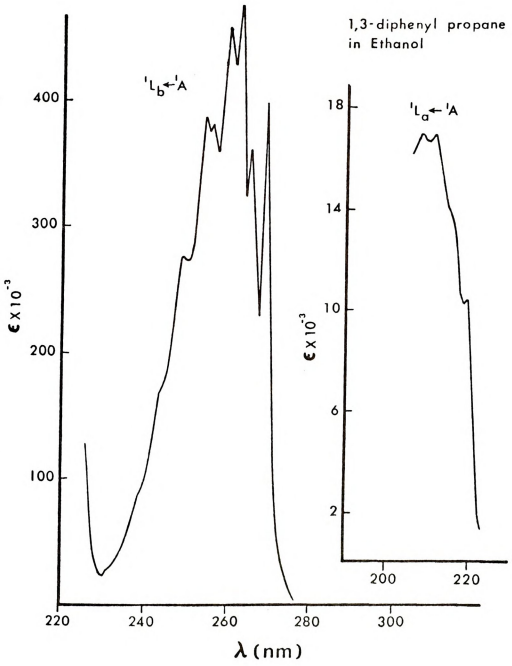

Figure 15. Absorption Spectra of 1,3-Diphenylpropane in Ethanol.

The first absorption band in 1,3DPP is not shifted compared to toluene but shows a hypochromic effect ϵ_{max}(1,3DPP) = 473 to be compared $2\epsilon_{max}$(toluene) = 580. More important is the reduction in intensity of the 0,0 band, $I_{max}/I_{0,0}$ = 1.19 in 1,3DPP and $I_{max}/I_{0,0}$ = 1.08 in toluene. Since the intensity of the 0,0 band is a measure of the diviation of the electronic symmetry from D_{6h}(benzene) this may mean that the introduction of the second phenyl group counterbalances to some extent the effect of the side carbon chain. The second absorption band of 1,3DPP shows a better resolved vibronic structure, a slightly altered vibronic structure and a small red shift (~360 cm^{-1}). One would expect some differences between 1,3DPP and toluene in the $^1B_2$ state. If we consider the polarization of the ^1L_b ($^1B_1$) state we find that it is X polarized while the ^1L_a ($^1B_2$) is Y polarized (see cooridinate system) so any difference between the model (toluene) and the actual system (1,3DPP) will be accentuated in the $^1B_2$ state. Also the dispersive interactions will be stronger in the more polarizable $^1B_2$ (exciton interaction will show the same behavior). The sharpening may be due to the relative rigidity of the 1,3DPP rotamers (steric interactions, selection of the TT configuration) compared to the free rotating group of toluene.

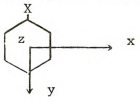

(B) Absorption Spectra of (Phenyl)-$(CH_2)_n$-(Pyridine), n = 1,3.

Table 8 shows the effect of solvent and protonation on the spectra of 4-(3-phenylpropyl)-pyridine (1,3PyPP).

The first band of neutral 1,3PyPP appears normal a superposition of the absorptions of toluene and γ-picoline. There is a slight hypochromicity in MCH which seems to be an inductive effect and a slight hyperchromicity in H_2O which may be due to mixing of local states with charge-transfer states.

Table 8. Effect of the Medium on the Frequency and Intensity of 1,3PyPP and 1,3Py$^+$PPC1O$_4^-$ Absorption Spectra.

		1st absorption band		2nd absorption band	
Compound	Solvent	$\tilde{\nu}_{max}(cm^{-1})$	ϵ_{max}	$\tilde{\nu}_{max}(cm^{-1})$	ϵ_{max}
1,3PyPP	MCH	39,139	1760	48,660	15,325
	EtOH	39,060	1860	48,640	13,229
	H_2O	39,139	2300	48,540	15,180
1,3Py$^+$PP	EtOH	39,535	5180	48,160	10,400
	H_2O	39,620	6020	48,146	12,145

The second band appears again normal, the band is composite of transitions of γ-picoline and toluene in this region. The most dramatic changes appear in the spectrum of 1,3Py$^+$PP. Looking at the spectrum of 1,3PyPP in water and water + $HClO_4$ we see then in the acid medium the absorption has a weak but obvious red tail. Also the hyperchromicity is considerable (ϵ_{max} expected aroung 4200). The second absorption band appears anomalously blue shifted and hypochromic.

The spectra of benzylpyridine show the same behavior:

Table 9. Effect of the Medium on the Frequency and Intensity of the PyCH$_2$P and Py$^+$CH$_2$PC1O$_4^-$ Absorption Spectra.

Compound	Solvent	$\tilde{\nu}_{max}(cm^{-1})$	ϵ_{max}
Py-CH$_2$-P	EtOH	39,000	2290
	H_2O	38,986	2580
Py$^+$-CH$_2$-P	EtOH	39,308	5835
	H_2O	39,370	5940

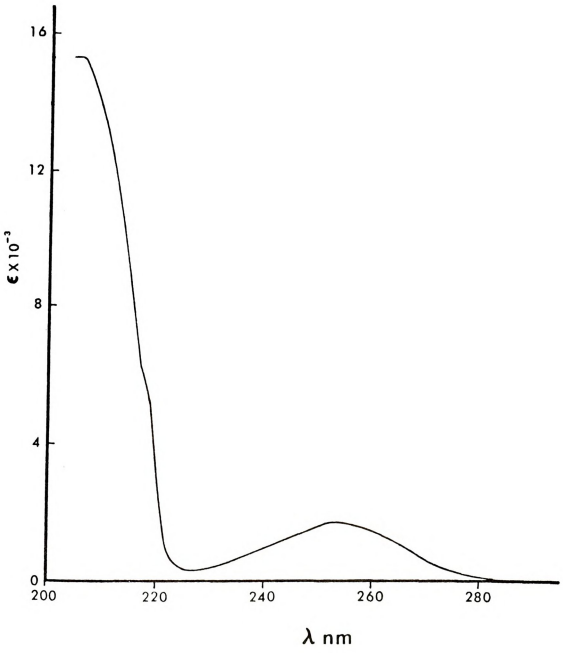

Figure 16. Absorption Spectrum of 4-(3-Phenyl-propyl)-Pyridine in Methylcyclohexane.

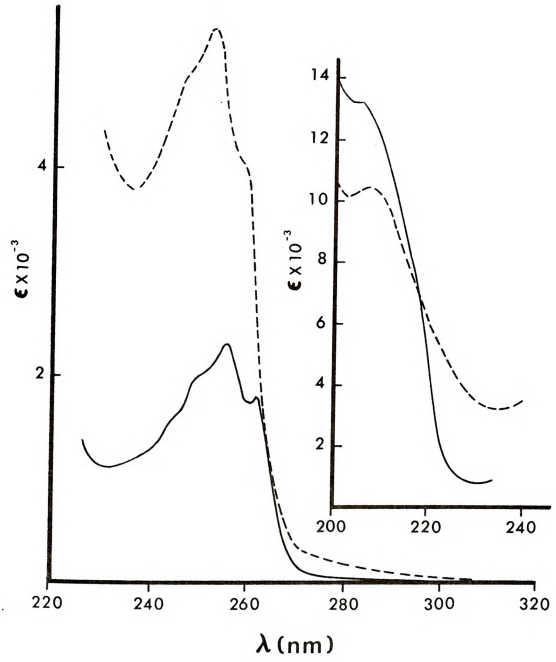

Figure 17. Absorption Spectra of 4-(3-Phenyl-Propyl)-Pyridine (__) and the Corresponding Pyridinium Perchlorate (--) in Water.

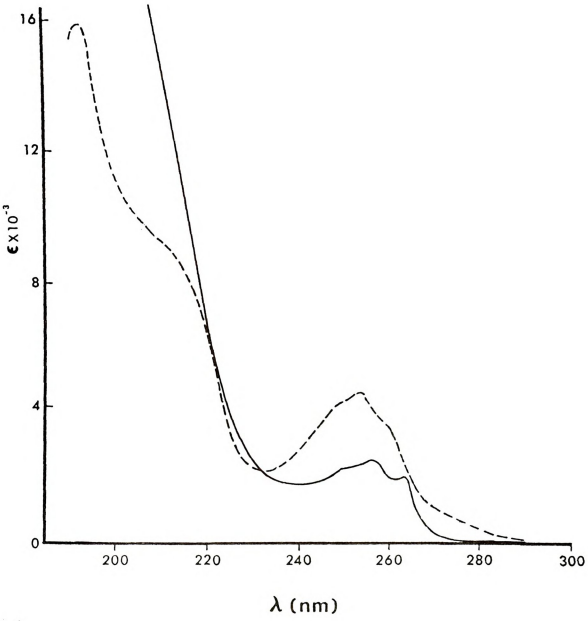

Figure 18. Absorption Spectra of Benzylpyridine (__) and Benzylpyridinium Perchlorate (--) in Water.

The second band of benzylpyridine was not studied because it extented further to the blue beyond our instrumental capacity.

The red tail in the case of benzylpyridinium is even more pronounced. We assign this red shifted band to an intramolecular charge-transfer transition from the phenyl ring to the pyridinium cation. This intramolecular charge-transfer transition appears stronger in the case of Py^+-CH_2-P than in $1,3Py^+PP$, at 280 nm the apparent extinction coefficients are as follow:

$1,3Py^+PP$	in	H_2O	$\epsilon = 144$
		EtOH	$\epsilon = 96$
Py^+CH_2P	in	H_2O	$\epsilon = 560$
		EtOH	$\epsilon = 468$

This difference in intensity may be due to a stronger CT interaction in benzylpyridinium and/or a higher association (conformational restrictions). Also the interaction appears to be stronger in the more polar water.

The blue shift of the second band may be due to perturbation by the CT state.

A literature search showed that similar behavior have been reported in related systems. Kosower[163] noticed a long wavelength shoulder (~3090Å) in the absorption spectrum of 1-(4-methoxabenzyl)-4-carbomethoxypyridinium perchlorate

Later, S. Shifrin[164] studied the absorption spectra of N-(β-p-x-phenylethyl)-3-carbamoylpyridinium chlorides with x various electron donating groups (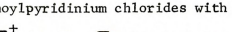) and observed red shifted shoulders which ascribed to CT transitions. Finally de Boer[165] studied a series of compounds of the general formula x- 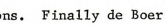 (n = 1,2,3) and found CT bands with maxima between 280-290 nm.

The appearance of the charge-transfer transition in acid media only, we believe, is a manifestation of the increased electron affinity of the pyridine ring upon protonation. To test this idea further we performed some all-electron semiempirical SCF calculations using the INDO (intermediate neglect of differential overlap)method of Pople[166]. The description and analysis of the technique can be found in J. A. Pople and D. L. Beveridge, "Approximate Molecular Orbital Theory", McGraw-Hill, 1970. We used the same nuclear geometry for pyridine as that used by Clementi in his ab-initio SCF calculation[167]. The N···H distance in the case of hydrogen bonded pyridine-water was assumed to be 1.75 Å following Hoffmann[168]. Finally the N^+-H distance was found by energy minimization to be 1.08 Å. Figure shows the net charges and the energies of the lowest unoccupied orbital $6b_2(\pi_4)$ in various situations.

As we see from Figure 19, the first antibonding orbital of pyridine $6b_2(\pi_4)$ has a positive energy which in good agreement with the value calculated by Clementi. Hydrogen bonding lowers somehow the orbital energy by ~0.4 eV (9 kcal/mole). Finally protonation has a dramatic effect giving an orbital energy of -5.15 eV. Of course this result is probably quite high but it is indicative of the large change of orbital energies upon protonation. Another interesting result is that the positive charge in the pyridinium ion is spread to the ring on the ortho and para positions while the nitrogen still remains slightly negative. Hydrogen bonding appears to delocalize about 4% of a positive charge to the ring, this is in good agreement with experimental results from ^{14}N nuclear magnetic resonance experiments where the positive charge was estimated to be $7 \pm 3\%$ of an electronic charge[169].

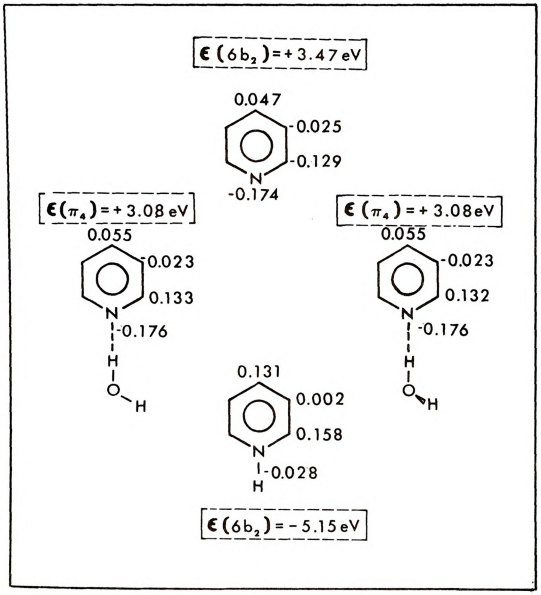

Figure 19. INDO Calculations. Energies of the Lowest Unoccupied MO and Charge Densities. Pyridine, Pyridine-Water Complex (Two Configurations) and Pyridinium Ion.

Emission Spectra-Fluorescence

Figure 20 shows the emission spectrum of 4-(3-phenyl-propyl)-pyridine in neutral ethanol solution. The spectrum appears to be quite similar to the spectrum of 1,3DPP. The emission at around 284 nm is the emission from the toluene part of the molecule while the broad and structureless emission at 325.5 nm appears to be arising from an intramolecular "heteroexcimer" state. The shift of the heteroexcimer emission is $\bar{\nu}^{M}_{0,0} - \bar{\nu}^{D}_{max} = 6520\ cm^{-1}$, blue shifted by around 460 cm^{-1} from the excimer maximum of 1,3DPP. This heteroexcimer emission is also viscosity dependent: addition of glycerol to the solution drastically reduces the dimer to monomer ratio and at about 70% glycerol (n = 80 cp) the dimer emission disappears. Under the same conditions excimer emission in 1,3DPP still occurs. This is easily understood because of the polarity of the pyridine and glycerol and the possibility of hydrogen bonding (solvation, reduction of mobility). Dispite the similarities with 1,3DPP there are certain important differences. First the emission from 1,3PyPP is blue shifted. According to Chandross[170] one would expect stronger interaction between two molecules with different electron affinities. The electron affinity of pyridine is about 1.7 times larger than that of benzene[171] and so the charge-transfer interaction may be expected to be stronger. Since the states of pyridine and benzene are almost degenerate one may expect also a molecular exciton interaction. If the lowest state of pyridine is the n,π^* state and since it is well known that the n,π^* is out of plane polarized there will be no exciton interaction in a face to face configuration. (The exciton interaction of course would have been negligible because of the small oscillator strength). We believe that the lowest state in ethanol is a $\pi\pi^*$ because when 1,3PyPP is disolved in hydrocarbon where the n,π^* state is known to be the lowest state no emission

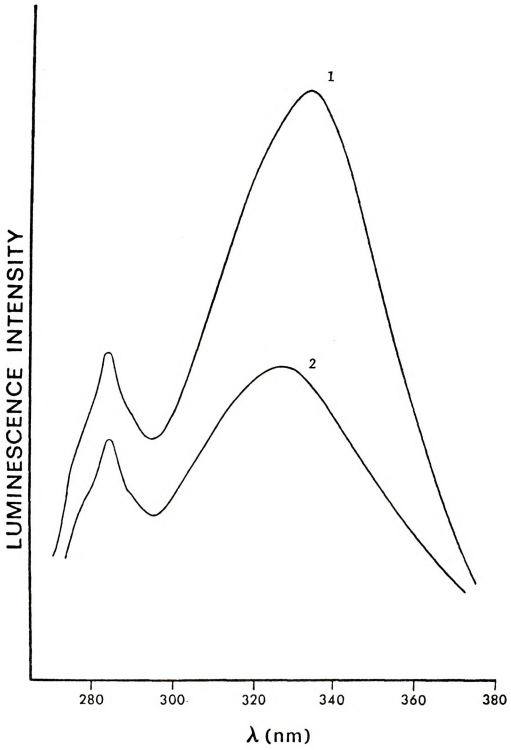

Figure 20. Room Temperature Fluorescence Spectra of (1) 1,3-Diphenylpropane in Ethanol (2) 4-(3-Phenyl)-Pyridine in Ethanol.

was observed. Apparently an exoenergetic energy transfer from the toluene to the nonemitting γ-picoline part is taking place. We believe that the difference in ionization potentials and electron affinities may be important in cases where electron transfer is taking place while in our case the interaction is of the charge-exchange type and resonance between the CT states may be important.

Looking at the emission spectra of 1,3DPP and 1,3PyPP in EtOH, we see that the dimer to monomer ratios are different.

$$I_D/I_M(1,3DPP) = 1.8 \quad \text{(Air equilibrated)}$$

$$I_D/I_M(1,3PyPP) = 1.3 \quad \text{(Air equilibrated)}$$

A similar behavior has been observed by Hirayama[172] for a series of intramolecular excimers. We list some of his results:

System	I_D/I_M	
Phenyl-$(CH_2)_3$-Phenyl	2.45	
O-Tolyl-$(CH_2)_3$-O-Tolyl	1.14	(Nitrogenated solutions)
Phenyl-$(CH_2)_3$-O-Tolyl	0.48	
Phenyl-$(CH_2)_3$-M-Tolyl	0.30	

Again we observe a lower I_D/I_M ratio in the case of mixed (hetero-) excimers.

In the case of 1,3PyPP intramolecular excimer we may have expected a high I_D/I_M ratio. Let us consider the possible mechanisms of excimer formation in this system:

I. $P^* + Py \rightleftharpoons (PPy)^*$; $P^* \rightarrow P + h\nu_M$; $P^* \rightarrow P + \text{heat}$; $(PPy)^* \rightarrow P + Py + \text{heat}$; $(PPy)^* \rightarrow P + Py + h\nu_D$

II. $P + Py^* \rightleftharpoons (PPy)^*$; $Py^* \rightarrow Py + \text{heat}$; $(PPy)^* \rightarrow P + Py + \text{heat}$; $(PPy)^* \rightarrow P + Py + h\nu_D$

Since the pyridine part of the molecule is responsible for the largest part

of the absorption and since pyridine is not emitting then if mechanism II is operating the I_D/I_M ratio should be quite high. From our results it appears that mechanism II is not operating because the excimer formation can not compete with the efficient non-radiative processes in pyridine.

Birks[173] discusses the previously mentioned results of Hirayama and concludes that the observed I_D/I_M ratios reflect the fact that the binding energies of the mixed excimers are less than those of the excimers. It is interesting to note that in the systems studied by Hirayama $\tilde{\nu}^D_{max}$ is always the same.

In our case we observe both spectral blue shifts and decreased I_D/I_M compared to 1,3DPP. These phenomena may just result from weaker interaction (binding) due to the out of resonance conditions. The same results seem to us that may be produced by another cause. It is expected that if one of the partners in the mixed excimer is not emitting then the mixed excimer non-radiative mechanisms may be enhanced. Cherkasov[174] verified this idea experimentally. Efficient non-radiative decay of the excimer would obviously decrease the I_D/I_M but also may lead to blue shifts. Usually we assume that emission results from an equilibrium state where the solvent has relaxed completely. This is usually true because of the very short dielectric relaxation times of the common solvents. Ethanol has a relatively long relaxation time $\sim 10^{-10}$ sec., and one can visualize the case where the dielectric relaxation time and the lifetime of the molecule are comparable. In this case the solvent relaxation may not be complete and this will result in a blue shifts. Very recently this idea was tested experimentally by Weber[175] who studied derivatives of naphthalene and indole under high oxygen pressures and in deoxygenated solutions. The oxygen quenched the molecular fluorescence and decreased significantly the lifetime. As a result of incomplete relaxation the oxygenated solutions showed blue shifts of ~ 8 nm. It would be

interesting to test this possibility in our system by attempting to measure the mixed excimer lifetime.

Benzylpyridine (Py-CH_2-P) under the same condition (neutral ethanol) gave no emission. A model for benzylpyridine will be diphenyl methane. As it was shown by Watson and El-Bayoumi[176] diphenylmethane does not show any excimeric emission but only changes of the P/F ratio and the intersystem crossing rate constant compared to toluene. Earlier Hirayama[49] had established the "three carbon chain" rule for excimer formation. So it is not surprising that benzylpyridine does not show any excimer emission. The very low quantum yield of monomer emission is undoubtly a result of energy transfer to pyridine.

Figure 21 shows room temperature emission spectra of 1,3PyPP in ethanol solution after addition of perchloric acid. The different curves correspond to different excitation wavelengths. The change is dramatic. The spectra are very broad and structureless and show a huge Stokes-shift. There is also an excitation wavelength dependence.

1,3Py^+PP in EtOH at room temperature

Excitation (nm)	$\tilde{\nu}_{max}$ emission (cm^{-1})
265	23,810
280	23,946
300	24,414

The shift expressed as $\tilde{\nu}^M_{0,0} - \tilde{\nu}^D_{max} \sim 13{,}400\ cm^{-1}$ (at 265 nm). The shift between the maxima of the spectra excited at 265 nm and 300 nm is $\sim 600\ cm^{-1}$.

Benzylpyridine (Py^+-CH_2-P) in ethanol + $HClO_4$ shows the same behavior and the shifts are even larger:

Py^+-CH_2-P in EtOH at room temperature

Excitation (nm)	$\tilde{\nu}_{max}$ emission (cm^{-1})
260	22,727

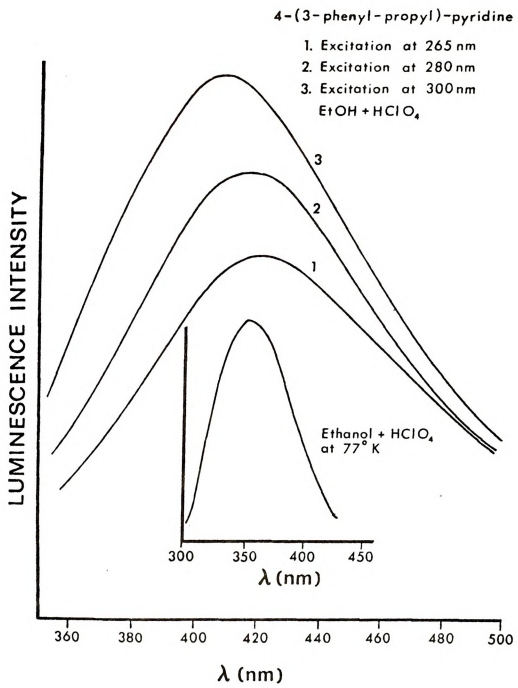

Figure 21. I. Room Temperature Fluorescence Spectra of 4-(3-Phenyl-Propyl)-Pyridine in Ethanol + $HClO_4$. 1. Excitation at 265 nm, 2. Excitation at 280 nm, 3. Excitation at 300 nm.
II. Total Luminescence Spectrum of the Above Solution at 77°K (Excitation at 265 nm).

Excitation (nm)	$\tilde{\nu}_{max}$ emission (cm^{-1})
270	22,830
280	22,988
290	23,364

$\tilde{\nu}^{M}_{0,0} - \tilde{\nu}^{D}_{max} \sim 14,500\ cm^{-1}$ (at 260 nm) and $\tilde{\nu}^{D}_{max}(290) - \tilde{\nu}^{D}_{max}(260) \sim 640\ cm^{-1}$.

From our study of the absorption spectra we know that upon addition of the acid a charge-transfer interaction is becoming important. It is natural therefore to ascribe these red shifted emissions to charge-transfer fluorescence.

The shifts are unusually high. There are very few reports on charge-transfer fluorescence at room temperature. Rosenberg and Eimutis[177] studied the CT fluorescence of several methylbenzene complexes with pyromellitic dianhydride at room temperature, the observed shifts were about 8000 cm^{-1}.

The largest shifts observed were in a system involving again a pyridinium moiety. Briegleb et al.[154] observed very large Stokes shifts 10,000-20,000 cm^{-1} for the CT fluorescence of the systems $MePy^{+}X^{-}$ where X^{-} various electron donating anions like I^{-}, SCN^{-}, N_3^{-} etc. The temperature range was -120° to -170°C(glass). Briegleb's interpretation for this enormous Stokes shift was "the result of an intermolecular configuration transformation in the excited state".

Figure 22 shows the emission spectra of 1,3PyPP in water. The spectra resemble the spectra in acidic ethanol.

1,3PyPP in water

Excitation (nm)	Emission $\tilde{\nu}_{max}$ (cm^{-1})
260	22,727
270	22,883
280	23,810

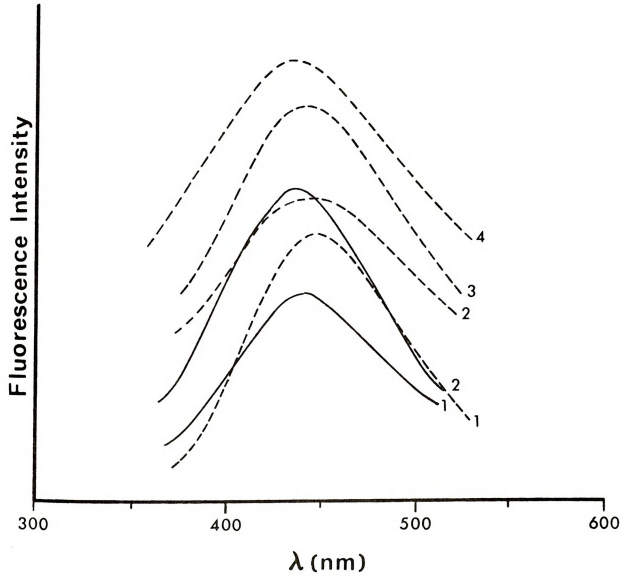

Figure 22. Room Temperature Fluorescence Spectra of 1,3PyPP in Water (__). 1. Excitation at 260 nm, 2. Excitation at 270 nm. Room Temperature Fluorescence Spectra of $1,3Py^{+}PPClO_4^{-}$ in Water (--). 1. Excitation at 260 nm, 2. 270 nm, 3. 280 nm, 4. 290 nm.

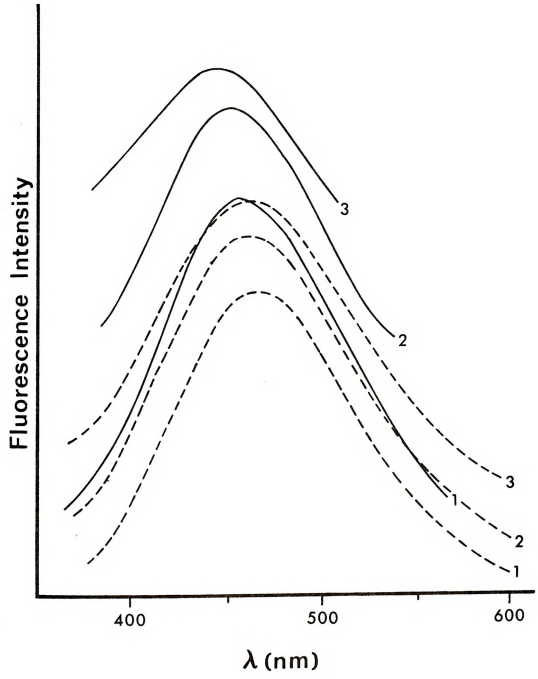

Figure 23. Room Temperature Fluorescence Spectra of Benzylpyridine in Water (__). Excitation 1. 260 nm, 2. 270 nm, 3. 280 nm. Room Temperature Fluorescence Spectra of Benzylpyridinium Perchlorate in Water (--). Excitation 1. 260 nm, 2. 270 nm, 3. 280 nm.

$\tilde{\nu}^{M}_{0,0} - \tilde{\nu}^{D}_{max} \sim 14,500\ cm^{-1}$ and $\tilde{\nu}^{D}_{max}(280) - \tilde{\nu}^{D}_{max}(260) \sim 1100\ cm^{-1}$.

The same behavior is displayed by Py-CH_2-P in water, Figure 22.

Py-CH_2-P in water

Excitation	Emission $\tilde{\nu}_{max}(cm^{-1})$
260	21,930
270	22,222
280	22,624

$\tilde{\nu}^{M}_{0,0} - \tilde{\nu}^{D}_{max} \sim 15,300\ cm^{-1}$ and $\tilde{\nu}^{D}_{max}(280) - \tilde{\nu}^{D}_{max}(260) \sim 690\ cm^{-1}$.

Finally we added acid ($HClO_4$) to the water solutions of 1,3PyPP and Py-CH_2-P and Figures 22 and 23 show the results.

1,3Py^{+}PP in water

Excitation (nm)	Emission $\tilde{\nu}_{max}(cm^{-1})$
260	22,371
270	22,472
280	22,624
290	22,988

$\tilde{\nu}^{M}_{0,0} - \tilde{\nu}^{D}_{max}(260) \sim 14,900\ cm^{-1}$, $\tilde{\nu}^{D}_{max}(280) - \tilde{\nu}^{D}_{max}(260) \sim 250\ cm^{-1}$.

Py^{+}-CH_2-P in water

Excitation	Emission $\tilde{\nu}_{max}(cm^{-1})$
260	21,520
270	21,692
280	21,739

$\tilde{\nu}^{M}_{0,0} - \tilde{\nu}^{D}_{max}(260) \sim 15,700\ cm^{-1}$, $\tilde{\nu}^{D}_{max}(280) - \tilde{\nu}^{D}_{max}(260) \sim 220\ cm^{-1}$.

From the absorption spectra study we found evidence of charge-transfer interaction in the case of 1,3PyPP and $PyCH_2P$ in EtOH + $HClO_4$ and in H_2O + $HClO_4$. Weak charge-transfer interactions in neutral water solutions can not excluded since the low sensitivity of the absorption spectra compared to the emission spectra does not allow detection of small interactions.

Further the blue shift of the n,π* state, which appears as a red tail in non protic media, tends to obscure such weak interactions. In the excited state the charge transfer interaction is expected to be stronger. Leonhardt and Weller[178] pointed out that electronically excited molecules have a lower ionization potential and a higher electron affinity than molecules in the ground state. The following diagram helps to clarify this point.

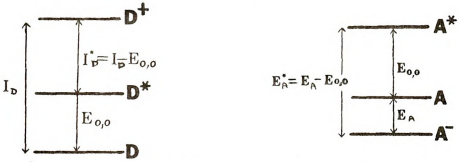

Experimental studies by the same authors confirmed this idea. A flash-spectroscopic investigation of the system perylene-⟨⊙⟩$\overset{+}{N}$H in methanol showed formation of perylene cations. Using for perylene I_D = 7 eV and $E_{0,0}$ = 23,000 cm^{-1} or 2.85 eV[179], we get a lower limit of the pyridinium electron affinity of -4.2 eV. In the same way for toluene I_D = 8.8 eV and $E_{0,0}$ = 4.6 eV which leads again to a lower limit of the electron affinity of -4.2 eV. The observation of perylene cations makes us believe that electron transfer is also possible in the systems we are considering. From the above discussion one may expect the existence of both charge-transfer complexes and exciplexes in the systems under study. Excitation spectra (uncorrected) support this idea. The excitation spectra of 1,3PyPP and $PyCH_2P$ in water + $HClO_4$ acid solutions show two excitation bands, one corresponding to the molecular absorption and the other to the CT absorption. The ratio of the intensities (maxima) I_{CT}/I_M for the two compounds is different. For example, observing the emission at 450 nm, in the case of 1,3PyPP the ratio is 1.4 while in the case of $PyCH_2P$ is 3.1. This seems to suggest

that the 1,3PyPP system is less associated probably due to the steric restrictions that lower the probability of association especially since the interaction potential (charge exchange) is a short-range one. Further the energetics of the binding are not expected to be favorable in the ground state of this system since there is no Coulombic interaction of the kind present in the usual D^+A^- complexes. In the case of $PyCH_2P$ the phenyl and pyridine rings are held in close proximity and association and dissociation are less meaningful. The importance of water in increasing the intramolecular interaction can be easily understood if we consider its acid properties, high polarity and finally high surface tension (hydrophobic bonding).

The large observed Stokes-shifts in CT complexes and exciplexes are considered as a result of large configuration changes in the excited state plus solvent shifts due to the polar nature of the excited state. In our case we expect large configuration changes, especially changes in the solvent cage created by the electron transfer and the production of a phenyl cation from the hydrophobic and apolar phenyl group. The counter-ion (ClO_4^-) may play a role too. The INDO calculations discussed earlier indicated that the positive charge in the pyridinium moeity is delocalized on the ring carbons. If this is true then we may expect that on the average the anion will be situated above the ring in the "ground state" of the exciplex and probably in the case of the ground state weak CT complex. In the excited state the positive charge will be mainly on the phenyl creating a large effective dipole(cation-anion) leading to farther relaxation.

The importance of relaxation is also shown by the low temperature, rigid glass spectra. Figure 24 and 25 show the total emission spectra of 1,3PyPP and $PyCH_2P$ in acidic ethanol glass at 77°K. In the rigid glass, relaxation is greatly prevented and thus the considerable blue shift compared to fluid solution. The fluorescence is overlapping with donor

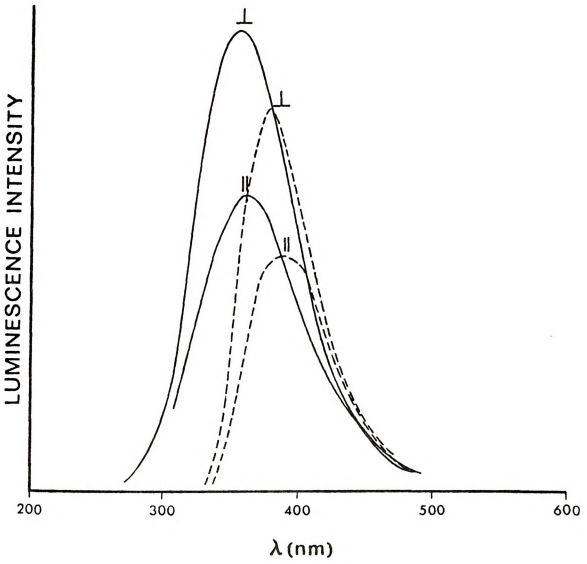

Figure 24. Total Luminescence Polarization Spectrum of $1,3Py^{+}PPClO_4^{-}$ in Ethanol at 77°K (__). Phosphorescence Polarization Spectrum of $1,3Py^{+}PPClO_4^{-}$ in Ethanol at 77°K(--).

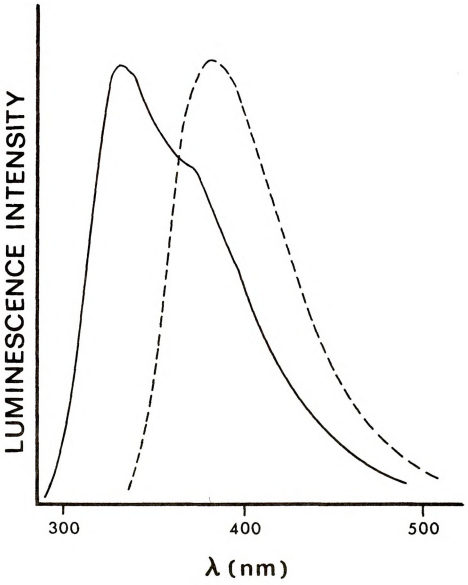

Figure 25. (__) Total Luminescence Spectrum of Benzylpyridinium Perchlorate in Ethanol at 77°K. (--) The Phosphorescence Spectrum under the Same Conditions.

phosphorescence as we will see later.

The apparent maximum in the case of 1,3PyPP is at 350 nm a blue shift of ~4800 cm^{-1}. In the case of $PyCH_2P$ the apparent maximum is at 330 nm which means a blue shift of ~7600 cm^{-1}. This seems to suggest that relaxation is more important in $PyCH_2P$ while the binding energy of the CT complex is less.

This most probably is associated with the larger average distance of the phenyl and pyridine ring in $PyCH_2P$ compared to 1,3PyPP (assumed in a "sandwich" configuration). This larger distance will reduce the covalent character of the CT state. Note also that the absorption CT band is situated at ~290 nm in acidic water solution of 1,3PyPP (maximum of excitation spectra) while the corresponding band for $PyCH_2P$ is at ~275 nm.

Polarization spectra at 77°K give additional evidence for the nature or the excited state. Figure 24 shows the polarization spectrum of 1,3PyPP in ethanol + $HClO_4$. The polarization ratio is

$$(I_{\parallel} - I_{\perp})/(I_{\parallel} + I_{\perp}) = -0.22$$

(fluorescence + overlapping red shifted, phosphorescence). By the use of a phosphoroscope the phosphorescence (donor phosphorescence, see later) was isolated. The polarization ratio of this phosphorescence is -0.23. Since as it is well known, the phosphorescence of π systems is out of plane polarized, the fluorescence from 1,3PyPP under the above conditions appears to be out of plane polarized (The theoretical polarization for perpendicular absorbing and emitting states is -0.33) which is in agreement with the assigned CT character of the emission.

The blue shift accompanying progreesive red excitation is somehow puzzling. From our absorption and emission data we observe that conditions that favor strong interaction or higher association (water + $HClO_4$ as solvent and in the case of $PyCH_2P$) the shifts are less pronounced.

Table 10. Stokes Shifts and Effect of Excitation Wavelength on the Emission Maxima of 1,3PyPP and $PyCH_2P$ in Different Solvents (in cm^{-1}).

Solvent	Compound	$\bar{\nu}_{max}(280)-\bar{\nu}_{max}(260)$	Stokes Shift(260nm)
H_2O	1,3PyPP	1100	14,500
	$PyCH_2P$	694	15,300
EtOH + acid	1,3PyPP	600	13,400
	$PyCH_2P$	260	14,500
H_2O + acid	1,3PyPP	250	14,900
	$PyCH_2P$	220	15,700

This may suggest that the shift is associated with excitation of different species. Shifts of the emission spectra with excitation wavelength were observed in various cases, especially for quinine and related compounds.[180,181]

Note that in all cases red excitation resulted in red shifted emissions. The interpretations suggested usually involve emissions from slightly different species like rotomers or differently solvated species.

Itoh and Azumi review these various possibilities and suggest that the shift arises from incomplete relaxation of the solvent Franck-Condon state[182]. The authors note that the "shift is more prominent in solvents which are capable of hydrogen bonding or protonation" although they don't accept protonation as the cause of the shift.

In the case under study it is natural to believe that if the emission is resulting from closely related species, these species are "exciplex like" or "charge-transfer complex like" species. As we progressively excite with longer wavelength light the importance of CT complexes over exciplexes is expected to increase. One may expect that in a usual intermolecular complex the CT excited state and the exciplex state arising from

the same molecular pair are the same. This may not be true for an intramolecular case. Recently Itoh et al.[112] studied the intramolecular exciplex and charge-transfer complex formations in (9,10-Dicyanoanthracene-$(CH_2)_3$-(Naphthalene) DCAN system. Their conclusion was that there are two fluorescent states in the potential energy surface of DCAN. The authors rationalized this as follows: the electronic interaction and therefore the geometrical arrangement between the DCA and naphthalene moieties are different from each other in the Franck-Condon excited states of the exciplex and the CT complex, because the exciplex formation is the photochemical process but the formation of the latter is really the thermal process followed by the photoexcitation. The internal or geometrical conversion from their Franck-Condon states to the identical fluorescent state, if it is correct, is forbidden in our compounds by the steric factor concerned with the trimethylene chain. Such a reasoning could be helpful in our case if we assume that the CT state is blue shifted relative to the exciplex state. The reason for this being so is not easy to visualize however, especially because besides the geometrical reorganization of the solute itself the solvent reorganization is very important. This may explain why shifts (although smaller) are observed in the case of $PyCH_2P$ and the large shifts in plain water where a variety of solute-solvent interaction centers (different degrees of solvation,hydrogen bonding) are expected.

Phosphorescence from 1,3PyPP and $PyCH_2P$

Figure 26 shows the phosphorescence spectrum of 1,3PyPP in (1) neutral ethanol glass at 77°K and (2) in acidic ethanol glass. As we see no shifts are produced by the addition of the acid and the position of the phosphorescence maximum is the same as that of toluene's phosphorescence (~380 nm).

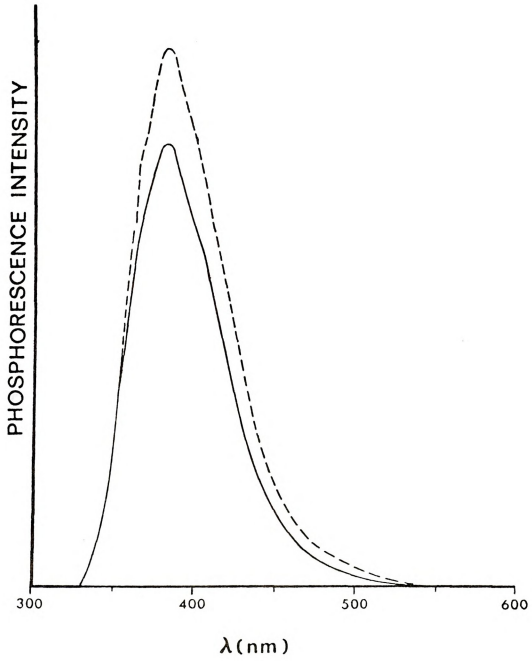

Figure 26. (__) Phosphorescence Spectrum of 1,3Py^{+}PP in Ethanol at 77°K.
(--) Phosphorescence Spectrum of 1,3Py^{+}PPClO$_4^{-}$ under the Same Conditions.

As we already have seen the charge-transfer fluorescence and the phosphorescence are strongly overlapping at 77°K. This appears to be quite a common case. In fact in the first systems to be studied, namely 1,3,5-trinotrobenzene complexes of polycyclic aromatic hydrocarbons in glasses at -180°C, a phosphorescence emission band of the donor virtually coincided with the charge-transfer fluorescence band[183,184]. So the very resonable postulate was made that the total emission of complex was the phosphorescence transition of the donor.

As discussed by Nagakura and coworkers[185], the case where the ^{3}LE state of the donor is lower energetically than the ^{3}CT is the most common case. McGlynn and his associates[186,187,188] accounted for the donor phosphorescence by proposing that the energy of the excited ^{1}CT state could be lost by transfer to a lower ^{3}CT state. Since this triplet level is dissociative at the energy of the intersystem crossing, McGlynn suggested that probably the complex would largely dissociate to yield the acceptor in the ground state and the donor in its lowest excited triplet state. Clearly in our systems the ^{3}CT state is dissociative since there is no covalency (unparied spins) and no ion-pair Coulombic interactions but only the usual intermolecular forces.

Measurements of the phorphorescence lifetime of $1,3Py^+PPClO_4^-$ in ethanol glass gave a τ_p = 6.8 sec. in good agreement with the phosphorescence lifetime of toluene (6.5 sec.) under the same condition. The phosphorescence of $PyCH_2P$ is again donor phosphorescence.

II-MANIFESTATIONS OF CHARGE-RESONANCE INTERACTIONS IN THE CASE OF ϕ-$(CH_2)_3$-ϕ^+ IN THE GAS PHASE

From our previous discussions on the system 1,3Py$^+$PPC1O$_4^-$, we concluded that complete electron transfer may take place in the excited state. Badger and coworkers[189,190] studied the absorption spectra of benzene cation ($C_6H_6^+$) and discovered long wavelength bands which they assigned as follows: 1.80μm^{-1} $C_6H_6^+$; 1.08μm^{-1} $(C_6H_6)_2^+$ (charge-resonance band); 2.15μm^{-1} $(C_6H_6)_2^+$ (corresponding to the 1.80μm^{-1} transition in the monomer). The monomer IR band was assigned to a $\sigma \rightarrow \pi$ transition. The similarity between the bands ascribed to the benzene dimer cation and the bands of (2,2) paracyclophane cation led the authors to suggest a sandwich structure for $(C_6H_6)_2^+$. In a subsequent paper Badger and Brocklehurst[191] studied the diphenyl propane and diphenylmethane cations. Both compounds gave absorption bands characteristic of the intramolecular charge resonance band. The interaction in diphenylmethane show again the difference between the geometrical requirements for excimer and CR interaction.

The charge resonance in species of the form $(C_6H_6)_2^+$ has also been demostrated by E.S. R.[192].

In this section we will study this intramolecular charge resonance interaction in 1,3-diphenylpropane cation in the gas phase as is manifested in the mass spectra of 1,3-diphenylpropane.

Mode of Fragmentation of Alkyl-Benzenes in the Mass Spectrometer

The mass spectra of aromatic hydrocarbons show several characteristic features that reflect the influenece of the aromatic nucleus. Thus ionization of alkylbenzene gives rise to parent ions of formula $C_nH_{2n-6}^+$. Decomposition produces chiefly ions of the type $C_nH_{2n-7}^+$, corresponding to phenylalkyl ions; such data suggest that the benzene ring itself is stable

to electron bombardment and survives in many fragment ions[193].

The most characteristic cleavage of alkylbenzenes occurs β to the aromatic ring, i.e., by rupture of the benzylically activated bond. In toluene, this results in the loss of one hydrogen atom to yield the ion $C_7H_7^+$(m/e = 91), which is also obtained in the higher homologs (ethyl-, propyl-, butyl-,... benzenes) by elimination of a methyl, ethyl, propyl, ..., etc. radical. So,

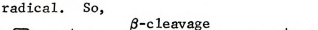

The most obvious formulation for $C_7H_7^+$ would be that of a benzyl cationI but extensive studies using appearance potentials and isotope labeling

I II

have shown that the actual structure is that of tropylium cation II. If the side chain is propyl or larger, another fragmentation process accompanies this simple β-cleavage, namely β-fission accompanied by rearrangement of one hydrogen atom, which results in the production of a neutral olefin molecule and the $C_7H_8^+$(m/e = 92)

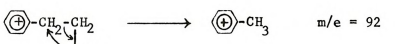

III

or

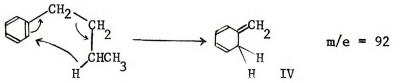

H IV

Since the energy requirements for the further decomposition of the $C_7H_8^+$ ion differ from those of toluene, the methylenecyclohexadiene formulation IV may be preferred. Another mode of fragmentation is the γ-cleavage

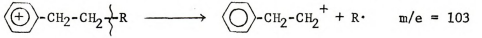

Table 11. Relative Intensities of Various Fragments of Butylbenzene and 1,3DPP in the Mass Spectrometer.

Compound	Ion (m/e)	Relative Intensity I_I/I_M^+
n-Butylbenzene	134 (Molecular ion, M^+)	1.00
	91	3.73
	92	1.84
	103	0.12
1,3-diphenylpropane	196 (M^+)	1.00
	91	1.50
	92	2.90
	103	0.21

The comparison of the butylbenzene and 1,3-ciphenylpropane mass spectra is shown in Table 11.

Discussion

The most intense peak in the mass spectrum of n-butylbenzene is the one corresponding to the ion with m/e = 91 resulting from the previously mentioned β-cleavage. The most abundant ion in the case of 1,3DPP is the ion with m/e = 92 resulting from β-fission and accompanied hydrogen rearrangement.

This process is energetically more favorable in the case of 1,3DPP than in the case of BuΦ because in the former the resulting double bond is stabilized through conjugation with the phenyl ring in the resulting styrene molecule.

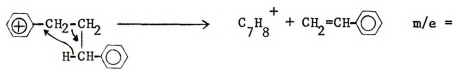

The ion with m/e = 103 is resulting from γ-cleavage. Again this process is energetically favored in the case of 1,3DPP because the resulting radical (benzyl radical) is stabilized through resonance with the phenyl ring.

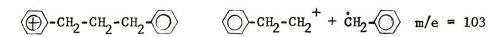

The most important ion for our purpose is the ion m/e = 91. As we see this ion is more abundant in the case of n-butylbenzene than in the case of 1,3DPP. Since its formation should not depend on the nature of the substituent on the γ-carbon one may suggest that its reduced rate of formation from the parent ion in the case of 1,3DPP may be due to some stabilization of the parent ion by the presence of the second phenyl group. From our previous discussion an obvious explanation is the formation of an intramolecular complex of the type (A) which is stabilized by charge-

(A)

resonance between the two phenyl rings.

The ratio of the rate constants of fragmentation of 1,3DPP and n-butylbenzene to the various ions is given by the ratio of the relative abundances of the particular ion in the two compounds

$$\frac{k(m/e=91)1,3DPP}{k(m/e=91)Bu} = 0.40$$

$$\frac{k(m/e=92)1,3DPP}{k(m/e=92)Bu} = 1.57$$

$$\frac{k(m/e=103)1,3DPP}{k(m/e=103)Bu} = 1.81$$

In a magnetic sector mass spectrometer a typical ion will spend about one microsecond in the ionization chamber between the instant of formation and its departure through the exit slit. It is accelerated to an energy

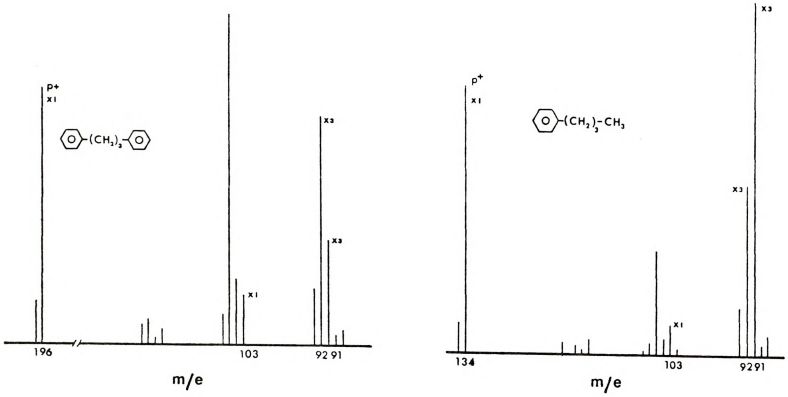

Figure 27. Portions of the Mass Spectra of 1,3-Diphenylpropane and Butylbenzene. Energy of the Electron Beam 70 eV.

of three kilovolts in the next seven microseconds, spends about four microseconds traversing the field-free region and the magnitic field, and in another two microseconds it arrives at the collector. Of course all the above times are estimates. For fragment ions to be formed in the ion source it is necessary that the decomposition reaction proceed with a rate 10^{+6} sec^{-1} or faster. If the rate of the reaction is in the neighborhood of 10^{5} sec^{-1} the decomposition will occur in transit, and that part occurring in the field-free region between the electrostatic accelerating and the magnetic deflecting fields produces the metastable ions.

We looked in the spectrum of 1,3DPP for metastable ions $m/e = m_f^2/m_i$ where m_i = parent ion, m_f = m/e = 91 (β-cleavage) and we did not find them which means that the rate of formation of the m/e = 91 ion from the parent ion is 10^{6} sec^{-1} or higher.

In order that the proposed stabilization be effective the rate of intramolecular phenyl-phenyl collision must be comparable or higher to the rate of β-cleavage which put a lower limit at $\sim 10^{6}$ sec^{-1}.

III-INTERSYSTEM CROSSING ENHANCEMENT THROUGH CHARGE-TRANSFER INTERACTIONS

Introduction

Exciplex (CT) interaction need not be associated with the appearance of a new emission band. The phenomenon of impurity quenching is considered as arising from the formation of non fluorescent exciplexes (dynamic quenching) or non fluoresced charge transfer complexes (static quenching).

One of the most important quenching mechanisms upon complexation is an enhancement of intersystem crossing. Christodouleas and McGlynn[186] have studied the intersystem crossing process in donor-acceptor complexes

of naphthalene with sym-trinitrobenzene (TNB), tetrachlorophthalic anhydride (TCPA) and tetrabromo (TBPA)- and tetraiodo-phthalic anhydrides (TIPA), in rigid ether-isopentane solutions at 77°K. They compared the ratio Φ_P/Φ_F of the naphthalene (donor) phosphorescence and fluorescence yields with that of a similar solution of naphthalene. Φ_P/Φ_F increased by a factor of ~30 in the naphthalene-TNB complexes, an increase attributable to CT interaction since there are no heavy atoms in the acceptor (TNB). Φ_P/Φ_F increased by a factor of 10^3-5 x 10^4 in TCPA, TBPA and TIPA complexes, increasing in the order of the atomic number of the heavy atoms in the acceptor.

Since that time numerous investigations have verified that charge-transfer interactions enhance the intersystem crossing. In several cases it has been shown, through laser photolysis studies, that the triplet state is generated "immediately" after the laser pulse and before the exciplex reaches the excited thermally equilibrated state. This for example has been shown for anthracene and pyrene quenched by diethlaniline[194] for pyrene and 1,2-benzanthracene quenched by dimethylaniline[195]. Independent support for the occurrence of this fast ISC mechanism comes from comparison of temperature effects on the triplet yields with those on the yields of exciplex fluorescence (nonpolar solvents) and ion formation (polar solvents).[196]

Regarding the mechanism by which the charge-transfer interaction enhances ISC, McGlynn has proposed the following scheme[197].

The initially formed locally excited state (A^1D^*) can be described in a first approximation by the wavefunction

$$^1\Psi_{LE} \approx a\,^{1,3}\Phi(A^-D^+) + b\,^1\Phi(A^1D^*) \qquad b \gg a$$

in which $^{1,3}\Phi(A^-D^+)$ and $^1\Phi(A^1D^*)$ represent the contributions of the corresponding zero-order charge-transfer and locally excited states. Fast

internal conversion to the singlet CT state may subsequently take place.

$$^1\Psi_{CT} = c^{1,3}\Phi\,(A^-D^+) + d^1\Phi\,(A^1D^*) \qquad c \gg d$$

Finally ISC will lead to

$$^3\Psi_{CT} = e^{1,3}\Phi\,(A^-D^+) + f^3\Phi\,(A^3D^*)$$

The efficiency of the $^1\Psi_{CT}$ - $^3\Psi_{CT}$ coupling arises from the mixing of the $^1\Phi\,(A^-D^+)$ and $^3\Phi\,(A^-D^+)$ states. Matrix elements of the form $\langle ^1\Phi\,(A^-D^+)|H_{SO}|^3\Phi\,(A^-D^+)\rangle$ may be quite large mainly because the plane of symmetry which negates significant spin-orbit coupling of $^3\Phi_{\pi\pi^*}$ states of planar aromatics is destroyed by the very process of CT complexing. Some $p\sigma$ character is mixed into the pi-MO's of D or A; one-center spin-orbit matrix elements are no longer zero and, in fact, should become dominant. In addition the perturbation gap between the two states is quite small, a factor that enhances the mixing. Finally for the same reasons $^3\Phi\,(A^-D^+)$ may mix significantly with other local singlets $^1\Phi_i$. Second order mixing involving vibronic interactions is also contributing.

Intramolecular Exciplex-CT Interactions in Aromatic Carboxylic Acids

It is known that the absorption and emission properties of an aromatic chromophore incorporated in an amino acid molecule, are greatly influenced by the presence of amino and carboxylic groups even though these substituents are separated from the chromophore by two methylene groups. In aqueous solutions this effect was manifested[198,199,200,201] by the pH effects on the yields of fluorescent aromatic amino acids (phenylalanine, tyrosine, tryptophane) at room temperature. Addition and removal of a proton at the substituent occur due to changes in pH and are responsible for the observed changes in the fluorescence yields. This reflects an interaction between the carboxylic (or amino group) and the aromatic ring which is the emitting moiety.

El-Bayoumi and coworkers have undertaken a study of this quenching effects through various model compounds.

Tournon and El-Bayoumi[202] have studied the absorption and fluorescence spectra of a number of phenylcarboxylic acids of the general form ϕ-$(CH_2)_n$-COOH (n = 1 phenylacetic up to n = 4 phenylvaleric). It was found that the acids in their conjugate base forms have essentially the same fluorescence yields as toluene. When the pH is decreased, the fluorescence yield undergoes a sharp drop at a pH value of about 4.5, corresponding to the appearance of the un-ionized form of the carboxyl group. The extent of this fluorescence quenching decreases with increasing the separation between the phenyl and the carboxylic group, i.e., with increasing the number of methylene groups. The ratio of phosphorescence to fluorescence is higher for the protonated form than that for the corresponding anion form. The most dramatic effects are exemplified by phenylacetic acid. In going from phenylacetic anion to phenylacetic acid the oscillator strength of the $^1B_{2u} \leftarrow {}^1A_{1g}$ benzene transition decreases by $\sim$22% while the fluorescence yield decreases by $\sim$70%. Since singlet-singlet nonradiative transitions from the lowest singlet to the ground state are expected to be negligible in these molecules, this decrease in fluorescence yield was considered by the authors as an indication that proronation of the carboxylate group increases the intersystem crossing rate. This is further supported by the larger phosphorescence/fluorescence intensity ratio for phenylacetic acid compared to toluene, the measured phosphorescence/fluorescence ratios in ethanol glass being 2.05 and 0.96 respectively.

The possibility that the quenching is due to some proton transfer reaction was eliminated by observing that the ethyl ester of phenylacetic acid has a similar fluorescence yield as phenylacetic acid.

The most reasonable interaction appears to be of charge-transfer

nature. Considering the values of ionization potential and electron affinities of toluene and acetic acid molecules, the electron transfer would be from the aromatic group to the carboxylic acid group. Observation of charge-transfer absorption in phenylacetic acid would provide direct evidence for intramolecular interaction between the phenyl ring and the carboxyl group. Benzoic acid, where the carboxyl group is directly conjugated to the phenyl ring, a charge-transfer band appears at 228 nm. By comparing the $^1B_{1u} \longleftarrow {}^1A_{1g}$ absorption bands of toluene, phenylacetic acid and phenylvaleric acids we see that a shoulder on the long-wavelength side of the absorption band appears in the case of phenylacetic acid (between 220 and 235 nm). This shoulder may be due to a CT transition. In a recent flash photolysis experiment[203] of these acids, intramolecular interactions between the carboxyl and phenyl groups were also implied.

The carboxylic acid is expected to have a higher electron affinity than the carboxylate anion. This would make the energy of the charge-transfer state lower for the phenylcarboxylic acid compared to the corresponding anion.

In a subsequent paper Tournon and El-Bayoumi[204] studied the fluorescence and phosphorescence yields in media of different viscosities. Table 12 shows some interesting results.

The stronger fluorescence quenching in lower viscosity media at the same temperature indicates that intramolecular relaxation occurs during the lifetime of the excited singlet state. This is similar to intramolecular exciplex interaction[205] reported for naphthylalkyl amines, although in that case exciplex emission was observed.

An additional evidence for the charge-transfer nature of the quenching mechanism came from the study of the luminescence properties of

Table 12. Effect of Viscosity on the Fluorescence and Phosphorescence Quantum Yields and ISC Rates of Toluene and Ethyl-Phenyl Acetate.

Compound	Solvent	$\Phi_F^{300°K}$	$\Phi_F^{77°K}$	$\Phi_P^{77°K}$	$(\Phi_P/\Phi_F)^{77°K}$	$k_{ISC}^{77°K} \times 10^{-6} s^{-1}$
Toluene	3MP(2.6×10^{12})	0.14	0.27	0.29	1.08	13.2
	iP(8.9×10^{5})	0.14	0.23	0.17	0.75	16.2
Ethyl-phenyl-acetate	3MP(2.6×10^{12})	0.04	0.17	0.33	2.00	18.8
	3MP+iP(10^{7}) (1:3)	0.03	0.12	0.11	2.09	28.0
	iP(8.9×10^{5})	0.02	0.02	0.06	3.00	188

The number in parenthesis after the solvent is the viscosity at 77°K in poise.

compounds of the form x--CH_2-COOH[206]. By changing the substituent x, the ionization potential of the donating moiety is varied. If a charge-transfer mechanism is operating an increase in quenching is expected as the ionization potential of the donating moiety is lowered[207], i.e., in the series x = H, CH_3, OH, OCH_3. Table 13 shows the results in water at room temperature.

Table 13. Effect of the Substituent X on the Absorption and Emission Properties of X-  -CH_2-COOH.

x	$f_{COO^-}(\times 10^{-3})$	$\Delta f/f(\%)$	Φ_{COO^-}	Φ_{COOH}	$\Delta\Phi/\Phi(\%)$	I.P.(eV)
-H	5.3	18	0.06	0.02	68	9.24
$-CH_3$	12	17	0.14	0.03	75	8.82
-OH	22	10	0.03	0.03	90	8.50
$-OCH_3$	20	10	0.03	0.03	90	8.20

f = oscillator strength

The expected correlation is found and moreover it is shown that $\Delta\Phi/\Phi$ and $\Delta f/f$ vary in opposite directions. This indicates that the inductive effect is mainly responsible for the variation of $\Delta f/f$ and the charge-transfer interaction for the variation of $\Delta\Phi/\Phi$.

In order to provide some more evidence for the importance of steric factors in determing the extent of intramolecular interactions between the phenyl and carboxyl groups and separate out the inductive effects we have studied some model systems. The study involves a comparative study of the luminescence properties at room and liquid nitrogen temperature of phenylacetic indan-1-carboxylic, phenylpropionic, indan-2-carboxylic acids as well as the parent hydrocarbons toluene and indan.

The carboxyl group is separated by one or two methylene groups in these acids but while rotation is free around C-C bonds involving the methylene groups in phenylacetic and phenylpropionic acids, no rotation around these bonds can occur in indan-carboxylic acids due to the five membered ring. This prevents the carboxyl group from assuming conformations that may bring it close to the ring in indan derivatives. The results are summarized in Table 14.

From the study of the results in Table 14 the following observations are made:

(1) The remarkable (70%) fluorescence quenching observed when phenylacetate anion is protonated does not occur in the case of indan-1-carboxylic acid although both acids have one methylene carbon between the phenyl and carboxyl groups. This indicates that the carboxyl group in the indan derivative can not approach the phenyl group in a conformation favorable for charge-transfer interaction which may lead to fluorescence quenching.

(2) The small but measurable fluorescence quenching effect of the carboxyl

Table 14. Luminescence Properties of Rigid and Non-Rigid Phenylakylcarboxylic Acids in Ethanol.

Compound	Formula	Φ_F 300°K	Φ_F 77°K	Φ_P 77°K	(Φ_P/Φ_F) 77°K	τ_P	τ_P°
Toluene		0.13	0.27	0.26	0.96	7.7	21.5
Phenylacetic		0.04 (0.13)	0.17	0.35	2.1	5.0	12.0
Phenylpropionic		0.10 (0.13)	0.26	0.32	1.22	7.0	16.0
Indan		0.27	0.43	0.16	0.37	8.0	28.5
Indan-1-carboxylic		0.20 (0.20)	0.38	0.21	0.55	6.8	20.0
Indan-2-carboxylic		0.27 (0.27)	0.41	0.17	0.41	7.7	26.5

Φ_F 300°K, Φ_F 77°K are quantum yields of fluorescence at room temperature and at 77°K, respectively.

Φ_P 77°K the quantities in brackets are room temperature yields of the anions.

τ_P 77°K is the observed phosphorescence lifetime.

τ_P° is the natural phosphorescence lifetime, $\tau_P^\circ = \tau_P(1 - \Phi_F)/\Phi_P$.

group in the case of phenyl propionic acid (23%) is absent in indan-2-carboxylic acid. In both cases the phenyl and carboxyl groups are separated by two methylene groups.

(3) The ratio of the fluorescence yield at liquid nitrogen temperature to that at room temperature is the same for indan and indan-2-carboxylic acid but is slightly different for indan-1-carboxylic acid indicating some but insignificant relaxation effects of the carboxyl group in the excited singlet state of indan-1-carboxylic acid.

(4) For indan-1-carboxylic acid the room temperature fluorescence yield is lower than that of indan by about 26% and there is a slight phosphorescence lifetime, indicating some interaction between the carboxyl and phenyl group.

(5) From the absorption spectra we find that the oscillator strength of the first absorption band decreased by 23% in indan-1-carboxylic acid and by 17% in indan-2-carboxylic acid compared to indan. These results are similar to changes in oscillator strength in phenyl acetic and phenyl propionic acids compared to toluene and are interpreted in terms of the inductive effect of the carboxyl group.

CHAPTER 4

EXCITED STATE PROTON TRANSFER REACTIONS INVOLVING THE 7-AZAINDOLE MOLECULE

INTRODUCTION

Excited state proton transfer reactions along with excimer/exciplex interactions comprise the most common adiabatic photoreactions; that is, reactions in which the products are generated in an excited state. This fact allows the study of these phenomena by fluorescence spectroscopy.

In this chapter, we are concentrating on the various kinds of proton transfer reactions in which a model biological molecule 7-azaindole (7AI) is involved. Initially the acid-base properties of the molecule are discussed in terms of its absorption spectra and from absorption and emission measurements the excited state pK_a^* and pK_b^* are determined. As it was first shown by Taylor, El-Bayoumi and Kasha[208] hydrogen bonded dimers of 7AI upon excitation show biprotonic phototautomerism. The technique of time resolved spectroscopy is applied here to study the dynamics of this double proton transfer. 7AI deuterated in the N_1 position is studied in a frozen 3-methylpentane matrix at 77°K. Time resolved spectra in the nanosecond time range show clearly the time evolution of the phenomenon (development of the emission corresponding to tautomeric species). Analysis of the nonexponential character of the decay curves gives the rate constants of the forward and backward reactions. The rates for plain (non deuterated) 7AI are calculated through the observed isotope effect on fluorescence

spectra. Finally from the invariance of the relative intensities of dimer and tautomer fluorescence at 77°K and 4°K and the kinetic results at 77°K, is concluded that the reaction at low temperatures proceeds through quantum mechanical tunneling and not by a thermally-activated process.

When 7AI is dissolved in alcohols a new emission band appears that has been ascribed to a tautomeric species arising from a double proton transfer involving the 7AI molecules and an alcohol molecule. Through the effect of solvent deuteration on the fluorescence quantum yields of 7AI, N-methyl-7-azaindole and a model compound for the tautomeric species strong evidence is found in favor of the tautomerism mechanism.

Finally the more subtle interactions between 7AI and water (no new emission appears) are studied through solvent isotope effects, temperature and pH studies.

THE HYDROGEN BOND

(I) Theoretical Models of the Hydrogen Bond

Electrostatic Model

The hydrogen bond in this model is regarded as a special case of donor-acceptor interaction. In order to form a stable hydrogen bond A-H···B, the essential requirement of the acceptor is that the charge distribution of the A-H bond orbital is such as to leave the proton sufficiently unscreened. The essential condition to be met by the donor is that it have lone-pair electrons. Attempts have been made to represent the energy of electrostatic interaction of the hydrogen bond in terms of dipole interactions[209,210] or in terms of the interaction of point-charge models[211,212].

It has been known that the directional properties of lone-pair

orbitals, like those of bonding orbitals in the first row elements, are due primarily to the directional characteristics of the atomic p orbitals, and the directional properties of bonding orbitals and lone-pair orbitals centered on the same atom are closely interdependent. Accordingly, hybridization of atomic orbitals, which nearly always occurs to some degree in bonding orbitals, will also cause hybridization of the lone-pair atomic orbitals. An important consequence of hybridization which has been pointed out by Coulson[213,214] is that the charge distribution of the orbital relative to the nucleus is therby made unsymmetrical, giving rise to an effective orbital dipole (or atomic dipole). The magnitude of the lone-pair orbital dipole can be obtained by determining the centroids of the charge of the hybridized lone-pair orbital. If the wave function for the hybridized orbital is given by

$$\Psi = (1 + \lambda^2)^{-\frac{1}{2}}\left[\Phi(s) + \lambda\Phi(p_x)\right]$$

where λ is a hybridization parameter and $\Phi(s)$ and $\Phi(p_x)$ are the usual one-electron atomic functions, then the centroid of charge distribution is expressed by the following relation:

$$\bar{x} = 2\lambda\int\Phi(s)x\,\Phi(p_x)d\tau/(1+\lambda^2) = 2\lambda/(1+\lambda^2)\cdot 5/z(3)^{\frac{1}{2}} \qquad (109)$$

x in equation 109 is measured relative to the nucleus in the direction of the orbital. Slater's values for the effective nuclear charge z are used. If the hydrogen bond is regarded as resulting from an H-A group of a second molecule directed at a lone-pair orbital, then the dominant term in the interaction energy could be considered to be the interaction of the proton with the lone pair dipole. The values of the dipoles corresponding to the individual lone-pair hybrid orbitals are obtained by multiplying $\bar{x}$ by the total charge -2e.

	Centroids of lone-pair orbitals $\bar{x}$(Å)	
N	0.339	Tetrahedral
O	0.290	
F	0.254	

For example, considering the central hydride molecules NH_3, H_2O and HF, if the lone-pairs may be represented approximately by tetrahedral hybrid orbitals; and using the above values for the centroids, one would conclude that, relative to a common H-A group, the NH_3 lone-pair would form stronger hydrogen bonds than the HF lone-pair, with the H_2O lone-pair intermediate. For the quantitative calculation of the hydrogen bond energy, it is assumed that the total electronic charge of each localized orbital (either a bonding or lone-pair orbital) is concentrated at a point at the centroid of the orbital. To fix the centroid of the bonding orbitals, the observed dipole moment of the molecule is used and the charges are placed so as the give the correct dipole moment.

The electrostatic description of the hydrogen bond based on point-charge model gives the correct order of magnitude for the energy of the hydrogen bond. It should be noticed though that calculations of the hydrogen bond energies based on the electrostatic model do not offer a severe test because there is parametric freedom in the placement of the point charges, and furthermore, the overlap energy as well as the dispersion energy and polarization energy have been neglected. The deficiencies of electrostatic model in explaining several experimental aspects of the hydrogen bond have been pointed out by Coulson[215].

Valence-Bond Theory

Coulson and Danielson[216] gave a semi-quantum mechanical treatment of the hydrogen bonding O-H···O as a four-electron problem. They considered

the following resonance structures for the hydrogen bonded system:

$\overset{-}{O}_A\text{-}H \quad O_B \qquad \Phi_1$ (pure covalent, no charge transfer)

$\overset{-}{O}_A \quad H^+ \quad O_B \qquad \Phi_2$ (pure ionic, no charge transfer)

$\overset{-}{O}_A \quad H\text{-}\overset{+}{O}_B \qquad \Phi_3$ (charge transfer, ions H-O bonding)

The wavefunction for this hydrogen-bonded system takes the form

$$\Psi = c_1\Phi_1 + c_2\Phi_2 + c_3\Phi_3$$

where the wavefunctions for the component structures are

$$\Phi_1 = N_1 \left\{ |\chi_A(1)\bar{\chi}_H(2)\chi_B(3)\bar{\chi}_B(4)| - |\bar{\chi}_A(1)\chi_H(2)\chi_B(3)\bar{\chi}_B(4)| \right\}$$

$$\Phi_2 = N_2 \; |\chi_A(1)\bar{\chi}_A(2)\chi_B(3)\bar{\chi}_B(4)|$$

$$\Phi_3 = N_3 \left\{ |\chi_A(1)\bar{\chi}_A(2)\chi_H(3)\bar{\chi}_B(4)| - |\chi_A(1)\bar{\chi}_A(2)\bar{\chi}_H(3)\chi_B(4)| \right\}$$

where χ_A and χ_B are oxygen atomic orbitals and χ_H is a hydrogen atomic orbital.

For the choice of atomic orbitals, the 1s orbital is used for the hydrogen atom. For the oxygen orbitals hybrids of the s and p orbitals are used. The appropriate values of the coefficients c_i and the energy E of the system are determined as usual by the variational method. The Hamiltonian is just an effective four-particle Hamiltonian. In the solution of the problem experimental information is also used.

The calculation is performed as follows:

(a) The overlap matrix is calculated nonempirically using Slater's orbitals.

(b) The diagonal elements of the Hamiltonian are calculated semiempirically taking into account the fact that H_{ii} is just the energy of the pure state Φ_i. H_{ii} is composed of the following terms: (1) the covalent bond energy expressed by the familiar Morse formula; (2) the short-range repulsion energy expressed by the help of the empirical formula $Kexp(-br)$; (3) the energy associated with the transfer of an electron from atom x to

an atom y; (4) the polarization energy.

This is the Coulson-Danielson method. The methods used by Sokolov[217] and Tsubomura[218] differ in many points. Nevertheless, the conclusions reached by all these theories are similar and can be stated as follows:
(I) The electrostatic forces(1), the short-range repulsion forces(2), and the charge-transfer forces(3), are all of the same order of magnitude but of different sign. Often effects (2) and (3) cancel each other which explains the success of electrostatic theories.
(II) The amount of charge transferred from O_B to O_A is found to be non-negligible (but small) for short bonds and negligible for long bonds; thus the long bonds are essentially electrostatic.

Charge-Transfer Theory

This theory is developed in analogy to the charge-transfer theory of molecular complexes that we have already outlined. Since in both cases the charge migration is an important factor it may be hoped that the theories applicable to the study of charge-transfer interactions are, mutatis mutandis, applicable to the study of hydrogen bonding. The theory in the form put by Bratoz[219] is as follows: again the system O_A-H$\cdots O_B$ is considered. The four electrons in the hydrogen bonding are distributed over three orbitals the bonding and the antibonding OH orbitals, $\varkappa_1$ and $\varkappa_2$ and the O_B lone-pair orbital $\varkappa_3$. The wavefunction representing the hydrogen bond is

$$\Psi = c_1\Phi_1 + c_2\Phi_2$$

where

$$\Phi_1 = N_1 |\varkappa_1\bar{\varkappa}_1\varkappa_3\bar{\varkappa}_3|$$

$$\Phi_2 = N_2\{ |\varkappa_1\bar{\varkappa}_1\varkappa_2\bar{\varkappa}_3| - |\varkappa_1\bar{\varkappa}_1\bar{\varkappa}_2\varkappa_3| \}$$

The first term Φ_1, describes the situation where two electrons are placed on O_AH and two on O_B (no bond function). This accounts for the electrostatic

and shrot-range repulsion interactions. The second function Φ_2, describes the situation in which charge transfer has taken placé from the O_B lone-pair orbital $\varkappa_3$ to the antibonding O_AH orbital $\varkappa_2$. This function confers on the hydrogen bond a partially convalent character (dative bond function). The energy E and the coefficients c_1 and c_2 are obtained by the variational method. The diagonal elements are calculated again semiempirically. Although different authors have different computational approach, the results are similar:

(a) The hydrogen bond energy can be decomposed as postulated by the VB theory. Al remarks concerning the relative importance of its components remain valid.

(b) The contribution of the charge-transfer term increases as the ionization potential of the lone-pair becomes smaller.

(c) The special role of the hydrogen in the hydrogen bond formation is due to the smallness of the short-range repulsion term. This reflects the small "size" of the hydrogen.

(d) In the charge-transfer process a fraction of an electron is placed on the antibonding O_AH orbital ν_2. The O_AH bond is thus weakened, its length increased, and the force constant $k_{\nu_{OH}}$ decreased. This is just what is observed experimentally.

(e) The charge migration increases the polarity of the O_A-H$\cdots O_B$ systems and intensifies the ν_{OH} IR bands.

SCF-MO Theory

In this theory the complex AH$\cdots$B is considered as a single large molecule and is treated by the SCF-MO and CI techniques. The problem has been approached from a direct ab initio approach or by introducing drastic approximations. In the non-empirical valence bond calculations,

the nonrelativistic Schroedinger equation is solved using a nonorthogonal atomic basis in a multideterminant wavefunction. This approach has been used for the study of H-bonds[220,221]. However, this method is very difficult to apply to larger systems in which the number of determinants for a minimal calculation becomes enormous and the resultant wavefunction difficult to interpret. It appears that as a starting point in understanding hydrogen bonds, molecular orbital theory is the most satisfactory approach. The literature on the subject up to 1971 has been reviewed by Allen[222]. For more recent references see for example the work of Del Bene[223].

There are several generalizations that have been produced by these studies:

(1) The stabilization of an H-bonded dimer appears to arise primarily from the electrostatic interactions between the proton and the lone-pair of electrons. For example in the dimers $ROH\cdots O{=}CH_2$, the order of increasing hydrogen bond strength parallels the order of increasing sigma electron withdrawing ability of R.

(2) The hydrogen bonds (open chain dimers) are almost linear.

(3) Although the electrostatic interaction appears to be the principal interaction, the dipole-dipole term is also important. Thus, in the dimers $ROH\cdots O{=}CH_2$ there is a tendency for the permanent dipole moments of the proton donor and acceptor molecules to approach a somewhat antiparallel alignment, in so far as possible within the orientational requirement for the directed lone-pair.

(4) There is a small transfer of charge which takes place from the proton acceptor to the proton donor molecule, and it occurs through the sigma electron system.

A very interesting investigation, through ab initio techniques, of the

double well picture of the hydrogen bond was performed by Clementi et al.[224] The study was on the DNA base pair Guanine-Cytosine and the motivation was the theory put forward by Lowdin[225] on the possible importance of quantum mechanical tunneling for the interconversion between different tautomeric forms.

Although there was a noticeable shoulder where the second minimum might have been expected no second minimum was found. Clementi and coworkers gave various possible sources of error in their prediction of the lack of a doulbe minimum.

The most important is that no simultaneous motion of two hydrogen bridges was considered. To test this possible error source, Clementi and coworkers carried out calculations on the formic acid dimer, which has two hydrogen bonds. First only the motion of a single hydrogen bridge was considered. Using the Guanine-Cytosine basis set only a single minimum was found. When a much larger double-zeta-plus polarization basis was used, a very pronounced shoulder was predicted but no minimum. It was only when the coupled motion of the two hydrogen bridges was considered and a double-zeta basis set was used that the calculation yielded a double minimum.

(II) Potential Energy Curves

The Double Minimum Potential

The bulk of physicochemical evidence presently available indicates that the H atom is localized near the donor atom in the majority of H bonds, even when A and B are similar atoms. This situation is represented by an unsymmetrical potential energy curve (Figure 28) where the lower of the two minima is located near the donor atom. The first experimental evidence for an unsymmetrical double minimum potential in a H bonded

system, was provided by (A) vibrational spectroscopy. In 1959 Bell and Barrow[226] showed that the first and second overtone O-H stretching vibrations of ethanol, phenol, and p-nitrophenol exhibit a pair of bands in the presence of bases. The height of the second potential minimum was shown to depend on the strength of the proton donor and the acceptor strength of the base[227]. The same concept was used to interpret the splitting of the first overtone of the NH_2 symmetric stretching vibration band in a number of intramolecularly H bonded ortho-anilines[228]. Some of the basic criteria for the existence of a double minimum potential in a H bonded system, with the second minimum at about the $v = 2$ level, are (1) splitting of the ν_{02} but not the ν_{01} band; (2) an increase in the magnitude of the splitting with increase in the strength of the H bond; (3) a reduction of the splitting on deuteration; (4) a temperature independent intensity ratio for the pair of bands resulting from the splitting of ν_{02}, since both transitions originate in the ground state. The band splitting is concentration independent in an intramolecularly H-bonded system, since the effect originates in the monomer.

Some of the strongest supporting evidence for a double minimum potential comes from (B) neutron diffraction studies. Hydrogen possesses only a single scattering electron and accordingly exerts rather an insignificant effect on the X-ray scattering. With neutrons, however, the scattering is by the nuclei of the atoms and it happens that the scattering by a proton is not much below the average of all the elements. As a result of it is possible by studying the diffraction of neutrons to produce projections of "neutron scattering density" in which the protons are quite accurately located in relation to the other atoms in the structure. For example neutron diffraction studies of KH_2PO_4 show the proton

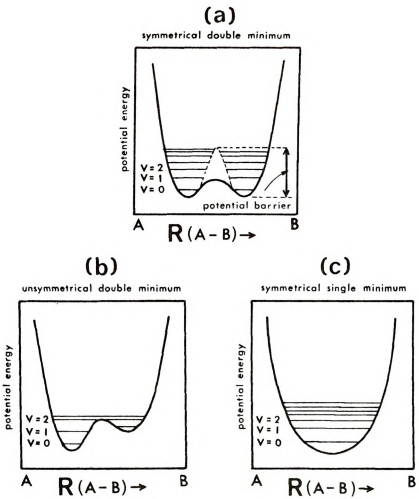

Figure 28. Potential Energy Diagrams for the Motion of the Proton in a Hydrogen Bond A-H···B.

as an elongated shape between the two oxygen atoms which are separated by 2.49 Å[229]. This distribution could be interpreted in either of two different ways: as a centrally located proton with very anisotropic motion or, more likely as a disordered distribution of the protons between two possible positions, one on each side of the mid-point between the oxygen atoms. In the case of ice the O-O distance is much longer, being 2.76 Å and the two possible hydrogen possitions are much farther apart (about 0.74 Å) so that the disordered protons appear as separate well-defined peaks. In the study of Peterson and Levy[230] on deuterated ice, the magnitude of the deuteron peaks on the neutron-diffraction projections is consistent with a half-deuteron being associated, on the average, with each of two possible positions on the lines joining the pairs of oxygen atoms. Other indirect evidence comes from (C) dielectric saturation experiments[231]. Piekara studied alcohol dimers and found a positive saturation effect. His explanation was as follows: in a system of dimers, transitions both from state 1 (left well) to state 2 (right well) and the inverse transitions leading from state 2 to 1 occur, as a result of which equilibrium $1 \rightleftarrows 2$ ($O\text{-}H\cdots O \rightleftarrows O^{-}\ldots H\text{-}O^{+}$) is established, so that the system contains a number of dimers with the proton shifted. When an external electric field is switched on, the dimers whose $O\text{-}H\cdots O$ bonds are directed approximately in accordance with the field produce $1 \longrightarrow 2$ transitions more readily, since for them the barrier height is smaller. This leads to a new state of equilibrium $1 \rightleftharpoons 2$ more to the advantage of state 2, "field-stimulated proton shift". As state 2 possesses an electric moment due to the hydrogen bond μ_2 that is greater than the moment μ_1 in state 1, the shift in equilibrium necessarily involves an increase in the dielectric permittivity due to the external electric field. In dimers, this increase greatly prevails

over the decrease from the usual saturation effect due to alignment of dipoles and, as a result, there is a positive saturation effect.

Other indirect evidence on the double well picture comes from data on (D) compressibility[232], (E) thermal expansion[233,234], the change in bond energy[235] change of intermolecular distance on deuteration[236] and N.M.R. studies[237].

At this point it should be mentioned that the interpretation of the above experiments is not as decisive as might be desired. For example even one of the best evidence the split of the IR bands can be due to an overtone of the AH bending mode, enhanced by Fermi resonance with γ_{str}[238].

One of the early views of H bonding was the concept of "mesohydric tautomerism" according to which the H was thought to resonate very rapidly between two equally probable positions, one near the donor atom, and the other near the acceptor atom. This concept would require that the potential energy function for the H atom either posses two equal potential minima with a low barrier between the two (Figure 28-b) or be symmetrical, with one broad minimum (Figure 28-c).

Hadzi and collaborators[239] have classified hydrogen bonds of the O_A-H$\cdots O_B$ type into four groups. In group A are included the symmetric single minimum H bonds; in group B, the symmetric double minimum H bonds with a small potential barrier; in group C, the symmetric double minimum H bonds with a potential barrier higher than in group B; and in group D, the H bonds with an asymmetric double minimum potential curve. The H bonds of type A and B are uniformly very short, with $R(O_A \cdots O_B)$ varying from 2.4 to 2.6 Å. Some typical single minimum H bonds are observed in KH maleate, NaH diacetate, KH dibenzoate, KH bisphenylacetate. The IR spectra are characterized by the absence of a γ_{01}(O-H) band in the region

above 1800 cm^{-1}; the PMR signals are narrow and weak and remain unchanged at low temperature. The H bonded compounds belonging to type B (KH_2AsO_4, $NH_4H_2PO_4$, $CaHPO_4$, $NaHCO_3$) exhibit two O-H bands in the 1900-3000 cm^{-1} region, separated by 300-500 cm^{-1}; the PMR signals are strong and narrow at room temperature and only slightly broader at -180°C[240,241].

(III) The Hydrogen Bond in the Excited State

A molecule in its lowest excited electronic state has a different electronic distribution than the molecule in its ground state. If the chromophoric portion of the molecule is involved in H-bonding one would expect changes in its strength. In this way electronic absorption or emission spectroscopy may provide experimental evidence about the H-bonding. Kasha[242] first discussed the effect of hydrogen bonding on absorption spectra, pointing out that absorption bands corresponding to $n\pi^*$ transitions should be "blue shifted" in hydrogen-bonding media. Bayliss and McRae[182] considered hydrogen-bonding interactions to be a special case of dipole-dipole interactions. However, Pimentel[243] pointed out that dipole-induced dipole and dipole-dipole interactions produce small solvent shifts compared with those due to hydrogen bonding. He discussed the importance of hydrogen-bonding effects compared with other solvent effects and pointed out the role of the Franck-Condon principle in hydrogen bonding. In the case when hydrogen bonding is stronger in the ground state than in the excited state (Figure 29) the hydrogen bond energy $W_e < W_g$ and the excitation energy implied by the Franck-Condon Prindiple is labeled w. In the case where the hydrogen bonding is weaker in the ground state then $W_e > W_g$.

Solvent shifts due to hydrogen bonding can be formulated as follows:

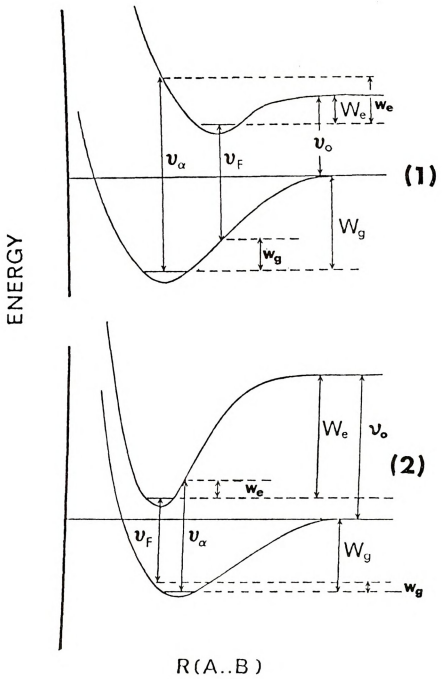

Figure 29. Hypothetical Potential Energy Curves for the Formation of a H-Bond A-H···B in Ground and Excited States, (1) $W_g \rangle W_e$, (2) $W_g \langle W_e$.

$$\nu_a - \nu_0 = \Delta\nu_a = W_g - W_e + w_e$$

$$\nu_f - \nu_0 = \Delta\nu_f = W_g - W_e - w_g$$

When hydrogen bonding is stronger in the ground state $W_e < W_g$ so $\Delta\nu_a > 0$, i.e., a blue shift which exceeds $W_g - W_e$ by w_e will be observed in absorption. Similarly in emission a shift less than $W_g - W_e$ by w_g will be observed (either a red or blue shift). When hydrogen bonding is weaker in the ground state $W_g < W_e$, both emission and absorption spectra will show red shift. The well characterized H bonds have energies in the range 1-7 kcal/mole (350-2500 cm^{-1}). According to the above discussion, a blue shift in absorption may exceed the ground state hydrogen bonding energy, hence, the blue shift is expected in the range of 350-2500 cm^{-1} or larger than 2500 cm^{-1}. But a red shift in absorption should never be as large as W_g, so should not be larger than 2500 cm^{-1}.

So a red shift in the absorption spectrum indicates that the hydrogen bonding is stronger in the excited state. This indicates that the base strength of the acceptor has increased in the excited state. The spectra of nitrogen heterocyclic bases in which the lowest transition is $\pi\pi^*$ have been found to undergo red shifts upon hydrogen bonding. This is because of electron redistribution around the hydrogen bonded nitrogen, increase in charge density, which increases its basicity in the excited state.

PROTON TRANSFER REACTIONS IN HYDROGEN-BONDED SYSTEMS: GROUND AND EXCITED STATES

A proton transfer reaction in which a proton involved in a hydrogen bond A-H···B is transferred from A to B, belongs to the broad classification of acid-base reactions. The transfer may occur along a potential energy curve similar to the ones depicted in Figure 28 by two mechanisms, direct transfer over the barrier and/or through quantum mechanical tunneling

through the potential barrier separating the two minima. The phenomenon of tunneling will be discussed more extensively later. The transition from a H bonded complex A-H···B to a proton transfer complex $A^-\cdots H\text{-}B^+$ in a nonpolar solvent is accompanied by significant changes. For example, in the IR spectra, the disappearance of ν_{OH}(A-H) bands and the appearance of $\nu_{OI}(B^+\text{-}H)$ bands have been observed in the IR spectra of mixtures of some carboxylic acids ranging from acetic (the weakest, $pK_a = 4.76$) to trifluoroacetic (the strongest, $pK_a = 0.23$) with pyridine in $CHCl_3$[244].

Evidence for ground-state proton transfers has also been found in ultraviolet absorption studies. Baba et al.[245] investigated the absorption spectra of the p-nitrophenol-triethylamine system as a function of amine concentration and found absorption bands corresponding to a hydrogen-bonded complex and a proton transfer complex.

The first observation of excited state proton transfer seems to have been made by Weber[246] who noticed that the fluorescence of 1-naphthylamine-4-sulfonate changed color as the pH of the solution was altered, although no corresponding change was observed in the absorption spectrum. These observations were later explained[247] as an excited-state ionization of the compound due to the fact that it becomes more acidic in the excited state. At low pH values, the cation of the molecule fluoresced; at high pH, the anion was the emitting species. Since ionization occured only in the excited state, the absorption spectrum remained the same. Since Forster's observation numerous cases have been found of excited state proton transfer. For example it has been found[248] that the shift of the fluorescence maximum of beta-naphthol in C_6H_6 brought about by the addition of triethylamine is quite large (4000 cm^{-1}) and is almost equal to that due to the ionic dissociation in aqueous solution (4200 cm^{-1}). On

the other hand, the shift of the absorption spectrum (^1L_b) of beta-naphthol caused by hydrogen bonding with TEA is only 370 cm^{-1}. These results suggest strongly that ion pair formation, due to complete proton transfer rather than a hydrogen bond formation, occurs in the fluorescent equilibrium state.

Intramolecular proton transfers in the excited state have also been observed. Weller[249] found two fluorescence bands in salicylic acid and its esters, one of which corresponded to a normal fluorescence. The other fluorescence was shifted to much longer wavelengths; he attributed this band to emission from a proton transfer tautomer in which the hydroxyl proton is transferred to the carbonyl group. Stokes shifts, which have been attributed to excited state intramolecular proton transfer, have also been reported for the hydroxynaphthoic acids[250,251,252].

Weller[253,254,255] has performed a number of experiments concerned with the kinetics of proton transfer in the excited state. He discussed methods of determining the excited-singlet-state dissociation constants, pK*, from spectroscopic data.

Jackson and Porter[256] have applied the same techniques to determine the pK of molecules in the lowest excited triplet state. Their results showed that the pK of the lowest triplet is usually close to that of the ground state rather than to that of the lowest excited singlet state. Recently nanosecond time-resolved spectroscopy has been used to investigate the kinetics of excited-state proton transfers. Brand et al.[257] studied the excited state ionization of beta-naphthol. Proton transfer rates of the order of 10^7 s^{-1} (room temperature) were found and the results agree very well with results obtained using Weller's photostationary experiments technique. Ware et al.[258] applied the same technique to study the intramolecular proton transfer in the excited singlet state of 3-hydroxy-2-naphtholic acid.

PROTON TUNNELING

One of the most unusual and interesting results of quantum mechanics is the prediction of tunneling, i.e., the ability of a particle to exist in, or pass through, a region of space where its total energy is less than its potential energy. According to classical mechanics, such a phenomenon is impossible.

The physical importance and consequences of tunneling have been recognized since the very earliest days of quantum mechanics. Hund[259] discussed the probability of intramolecular rearrangements via tunneling in 1927. As early as 1932, Wigner[260] discussed tunneling with a view aimed at chemical kinetics; in the same year, the tunneling mechanism responsible for the doubling of certain spectral bands of ammonia was clarified[261]. When proton transfer is very fast, such as in acid-base reactions in aqueous solutions, there exists the possibility that the proton in the incipient H bonded complex A-H···B tunnels through the potential barrier between the two minima. This possibility was pointed out by Bell in 1935. Since then, a great deal of indirect evidence has been accumulated which indicates the occurrence of proton tunneling in ultrafast proton transfer[262,263]. Johnston[264] and Caldin[265] have provided reviews of various aspects of proton tunneling in ordinary chemical reactions, and the significance of tunneling to the understanding of the hydrogen bond has been well-described[227,266,267]. Lowdin[268] has discussed tunneling from a biological viewpoint.

In the following we will outline a simplified approach for obtaining the transmission coefficient for an arbitrary shape potential. To do so we use the so called JWKB method (after its proponents in quantum mechanics, Jeffrey, Wentzel, Kramer and Brillouin). Let us start from the 1-dimentional

Schroedinger equation*:

$$(-h^2/8\pi^2 m)\partial^2\Phi/\partial x^2 + V(x)\Phi = E\Phi$$

We introduce the notation

$$p(x) = (2m(E - V(x))^{\frac{1}{2}}$$

and

$$k(x) = 2\pi p(x)/h$$

According to JWKB scheme, an approximate solution may now be presented by:

$$Ak^{-\frac{1}{2}}\exp(i\int^x k dx) + Bk^{-\frac{1}{2}}\exp(-i\int^x k dx)$$

(see for example E. Merzbacher: "Quantum Mechanics" Wiley 1970, chapter 7)

A point where k = 0 is a turning point. The JWKB solution has oscillatory behavior in the "permitted" region and an exponential behavior in the "forbidden" region. Of fundamental importance is the Jeffreys-Kramers formula which connects the solutions on both sides of a turning point $x = x_1$ or $x = x_3$.

For real functions, one obtains:

$$c_1 k^{-\frac{1}{2}}\sin(\int_x^{x_1} k dx + \pi/4 + \gamma_1) \longleftrightarrow$$
$$c_1 |k|^{-\frac{1}{2}} \left\{\tfrac{1}{2}\cos\gamma_1 \exp(-\int_{x_1}^{x} |k| dx) + \sin\gamma_1 \exp(+\int_{x_1}^{x} |k| dx)\right\} ,$$
$$c_3 |k|^{-\frac{1}{2}} \left\{\tfrac{1}{2}\cos\gamma_3 \exp(-\int_{x}^{x_3} |k| dx) + \sin\gamma_3 \exp(+\int_{x}^{x_3} |k| dx)\right\} \longleftrightarrow$$
$$c_3 k^{-\frac{1}{2}}\sin(\int_{x_3}^{x} k dx + \pi/4 + \gamma_3)$$

For complex functions, one obtains instead:

$$a_1 k^{-\frac{1}{2}}\exp\left[-i(\int_x^{x_1} k dx + \pi/4)\right] + \beta_1 k^{-\frac{1}{2}}\exp\left[+i(\int_x^{x_1} k dx + \pi/4)\right] \longleftrightarrow$$
$$a_2 |k|^{-\frac{1}{2}}\exp(+\int_{x_1}^{x} k dx) + \beta_2 |k|^{-\frac{1}{2}}\exp(-\int_{x_1}^{x} k dx)$$

with connection formulae:

$$a_2 = a_1 + \beta_1$$
$$\beta_2 = -\tfrac{1}{2}i(a_1 - \beta_1)$$

* The JWKB method can also be applied to three-dimentional problems, if the potential is spherically symmetric and a radial differential equation can be separated.

Similarly one has around the other turning point:

$$\alpha_3 k^{-\frac{1}{2}} \exp\left[i\left(\int_{x_3}^{x} k\,dx + \pi/4\right)\right] + \beta_3 k^{-\frac{1}{2}} \exp\left[-i\left(\int_{x_3}^{x} k\,dx + \pi/4\right)\right]$$

$$\alpha_2' |k|^{-\frac{1}{2}} \exp\left(+\int_{x}^{x_3} |k|\,dx\right) + \beta_2' |k|^{-\frac{1}{2}} \exp\left(-\int_{x}^{x_3} k\,dx\right)$$

with connection formulae:

$$\alpha_2' = \alpha_3 + \beta_3$$

$$\beta_2' = \tfrac{1}{2} i(\alpha_3 - \beta_3)$$

In order to derive a formula for the transmission coefficient in general, we will consider a single incident wave hitting a barrier with two turning points (Figure 30). In region I, there is an incident wave

$$\alpha_1 k^{-\frac{1}{2}} \exp\, i\left(\int_{x_1}^{x} k\,dx + \pi/4\right)$$

which is partially transmitted into region III in the form of a right-going wave

$$\alpha_3 k^{-\frac{1}{2}} \exp\, i\left(\int_{x_3}^{x} k\,dx + \pi/4\right)$$

where as $\beta_3 = 0$. The transmission coefficient is now defined by the fraction

$$g = |\alpha_3|^2 / |\alpha_1|^2$$

Introducing the symbol

$$K = \int_{x_1}^{x_3} |k|\,dx = 2\pi/h \int_{x_1}^{x_3} (2m(V(x) - E))^{\frac{1}{2}} dx \qquad (110)$$

and using the connection formulae:

$$\alpha_2' = \alpha_3 \qquad \beta_2' = \tfrac{1}{2} i \alpha_3$$

$$\alpha_2 = \beta_2' e^{-K} \qquad \beta_2 = \alpha_2' e^{+K}$$

$$\alpha_2 = \alpha_1 + \beta_1 \qquad \beta_2 = -\tfrac{1}{2} i(\alpha_1 - \beta_1)$$

This gives immediately the relations

$$\alpha_3/\alpha_1 = -2i(\tfrac{1}{2} e^{-K} + 2e^{+K})^{-1}$$

and

$$g = |\alpha_3|^2 / |\alpha_1|^2 = e^{-2K}/(1 + \tfrac{1}{4} e^{-2K})^2 \approx e^{-2K}$$

If the barrier is parabolic at its top (Figure 30), one can easily evaluate the integral in equation 110

$$K_0 = (\tfrac{1}{2}\pi 2\pi/h\ a_0)(2m(V_2 - E_0))^{\frac{1}{2}}$$

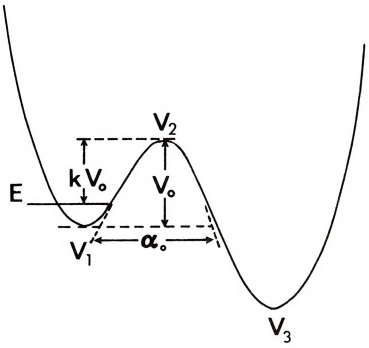

Figure 30. Model Barrier for Proton Tunneling Calculations.

The factor $\pi/4$ comes here from the shape of the hill.

If one measures the energy from the top in fractions k of V_0, so that $E = V_2 - kV_0$ one obtains

$$K = kK_0$$

and

$$g = \exp(-k\pi^2/ha_0)(2m(V_2 - E_0))^{\frac{1}{2}}$$

ISOTOPE EFFECTS

Primary Kinetic Isotope Effect

The basic principle which underlies most theoretical considerations of isotope effects is the Born-Oppenheimer approximation. This approximation states that one can separate the quantum mechanics of molecules into a problem of electronic motion with the nuclei in fixed positions and a separate problem of nuclear motion. In the electronic motion problem, the only property of nuclei which appears is their charge. The potential energy for the nuclear motion problem is the electronic energy (including the repulsion between nuclei) as a function of nuclear configuration; this potential energy is then independent of the isotopic masses of the nuclei. The kinetic energy expression of the nuclear motion problem does, of course, contain the masses of the nuclei. Thus, the study of isotope effects on reaction kinetics is a study of how different masses of nuclei affect motion on the same poetntial surfaces on which molecules move and so on the mechanism of chemical reactions.

The formalism of the kinetic isotope effect (primary when the bond in which the isotopic atom is involved is broken during the reaction) has been given by Bigeleisen and Wolfsberg[269], Bigeleisen[270] and Bigeleisen and Goepper-Mayer[271]. An alternative and independent approach was taken by Melander[272]. For a comprehensive treatment of isotope effects see "Isotope

Effects in Chemical Reactions" ACS Monograph 167, Edited by Collins and Bowman, Van Nostrand Reinhold 1970.

In the following we will follow a simplistic approach to the problem which never the less will give use the essential features of the effect.

Within the framework of transition-state theory the ratio of the rate constants for say a hydrogen/deuterium abstraction reaction will be

$$AH + B \rightleftharpoons [AHB]^{\ddagger} \longrightarrow A^{\cdot} + BH^{+}$$

$$AD + B \rightleftharpoons [ADB]^{\ddagger} \longrightarrow A^{\cdot} + BD^{+}$$

$$k_H/k_D = (kT/h)K_H^{\ddagger}/(kT/h)K_D^{\ddagger} = Q_D Q_H^{\ddagger}/Q_H Q_D^{\ddagger} \qquad (111)$$

where the Q's and the $Q^{\ddagger}$s are the partition functions for the molecules AH and AD and for the activated complexes $AHB^{\ddagger}$ and $ADB^{\ddagger}$. The Q's for each molecule or activated complex may be expanded as the product of translational, rotational and vibrational partition functions (but with neglect of tunneling).

$$Q = Q_{trans} \cdot Q_{rot} \cdot Q_{vib} \cdot Q_{el}$$

The quotients of the translational and rotational partition functions for isotopic molecules may be expressed in terms of vibrational frequencies and the masses, m_i, of the various atoms by equating the classical and quantum-mechanical partition functions at high temperatures.

$$\frac{Q_{classical}(H)}{Q_{classical}(D)} = \frac{h^{3r}\int_{\infty}^{\infty}\cdots\int_{\infty}^{\infty}\exp\left(-\sum_i^{H} p_i^2/2m_i^H kT\right)dp_1^H\cdots dp_{3r}^H}{h^{3r}\int_{\infty}^{\infty}\cdots\int_{\infty}^{\infty}\exp\left(-\sum_i^{D} p_i^2/2m_i^D kT\right)dp_1^D\cdots dp_{3r}^D} \times \frac{\int_{\infty}^{\infty}\cdots\int_{\infty}^{\infty}\exp(-V^H(q_1^H\cdots q_{3r}^H))dq_1^H\cdots dq_{3r}^H}{\int_{\infty}^{\infty}\cdots\int_{\infty}^{\infty}\exp(-V^D(q_1^D\cdots q_{3r}^D))dp_1^D\cdots dp_{3r}^D} \qquad (112)$$

Since the potential functions for isotopic molecules are the same, the ratio of the total classical partition functions will be

$$Q_{classical}(H)/Q_{classical}(D) = \prod_i (m_i^H/m_i^D)^{3/2} \qquad (113)$$

and when T is large (room temperature and above), the ratio of vibrational partition functions

$$\frac{Q_{vib}(H)}{Q_{vib}(D)} = \prod_i \frac{e^{-h\nu_i^H/2kT}}{1-e^{-h\nu_i^H/kT}} \Big/ \prod_i \frac{e^{-h\nu_i^D/2kT}}{1-e^{-h\nu_i^D/kT}} \qquad (114)$$

reduces to $\prod_i \nu_i^D/\nu_i^H$. Then equating classical and quantum-mechanical partition functions we get

$$Q^H_{trans}Q^H_{rot}/Q^D_{trans}Q^D_{rot} = \prod_i(\nu_i^H/\nu_i^D)\prod_i(m_i^H/m_i^D)^{3/2} \qquad (115)$$

For the vibrational partition function of the transition state of ordinary, nonlinear molecules, only 3n-7 vibrations may be included, since one degree of freedom has already been taken specifically into account in the derivation of Eyring's equation. Since however, the ordinary translational and rotational motions are not specially treated in the absolute rate theory, the quotient in equation 115 must therefore include not only 3n-7 real vibrations of each transition state but the imaginary vibrations $\nu^{*\ddagger}_H$ and $\nu^{*\ddagger}_D$ as well. So from equations 115 and 111, we get

$$k_H/k_D = \nu^{*\ddagger}_H/\nu^{*\ddagger}_D \prod^{3n-6}\nu_D/\nu_H \prod^{3n-7}(\nu^{\ddagger}_H/\nu^{\ddagger}_D)(Q^D_{vib}Q^{H\ddagger}_{vib}/Q^H_{vib}Q^{D\ddagger}_{vib}) \qquad (116)$$

On substituting the vibrational partition functions from equation 114 to 116 the equation for the ratio of the rate constants is obtained. However, the transition state $AHB^{\ddagger}$ has only one real vibration and the Group A and B are assumed structureless. Furthermore, for this particular case, the quotient of the form 1 - exp(-$h\nu_i$/kT) may be approximated by unity, since the frequencies of stretching bonds involving hydrogen are high.

With these simplifications, equation 116 easily reduces to equation 117,[273]

$$k_H/k_D = \nu^*_H/\nu^*_D \cdot \nu_{AD}/\nu_{AH} \cdot \nu_H/\nu_D \cdot \exp(\text{ZPE}/RT) \qquad (117)$$

where $\nu^{*\ddagger}_H$ and $\nu^{*\ddagger}_D$ are the frequencies of the vibrations of the transition state which become translational motion (a) ν_{AH} and ν_{AD} are the stretching

frequencies of the one-dimensional molecules AH and AD, and $\nu_H^{\ddagger}$ and $\nu_D^{\ddagger}$ are the frequencies of the real vibration in the transition states of AHB and ADB (b)

(a) $\longleftarrow$ A H B $\longrightarrow$ symmetric

(b) $\longleftarrow$ A H$\rightarrow\leftarrow$B anti-symmetric

ZPE = ZPE (reactants, hydrogen) - ZPE (reactants, deuterium) - ZPE (activated complex, hydrogen) - ZPE (activated complex, deuterium), where ZPE = zero point energy.

Westheimer has shown that if $k_1 = k_2$, i.e., if the force constants binding H (or D) to A and B are equal then

$$\nu_H^{*\ddagger}/\nu_D^{*\ddagger} \cong (2)^{\frac{1}{2}}; \qquad \nu_{AD}/\nu_{AH} \cong (\tfrac{1}{2})^{\frac{1}{2}} \quad \text{and} \quad \nu_H^{\ddagger}/\nu_D^{\ddagger} = 1$$

so the entire preexponential term of equation 117 is unity. If $k_1 \gg k_2$ then again the preexponential factor is approximately unity, since the ratio of the frequencies of the "symmetric" vibration now "cancels" the ratio of the frequencies of AH and AD and the ratio $\nu_H^*/\nu_D^* = 1$. Regardless, then, of the ratio of the force constants, the preexponential factor estimated for this simplified model is near unity. The factor that determines the isotope effect is then just the difference between the zero point energies.

Solvent Kinetic Isotope Effect

"Solvent isotope effect" is a term frequently used in discussions of kinetic and equilibrium processes in light and heavy water for the part of the total isotope effect which is attributed to isotopic substitution of the solvent. It has been said to be due primarily to differences in structure of the two waters[274,275,276]. That differences exist is evident from differences in thermodynamic properties of the two liquids, in the heats of hydration and solubilities of salts in the two waters[277,278]. Swain

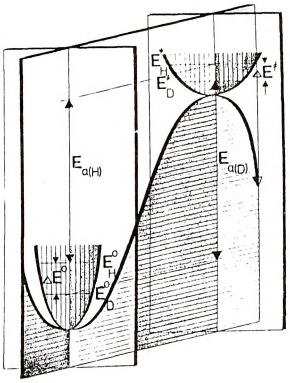

$$E_{a(D)} > E_{a(H)} \qquad \frac{k_H}{k_D} > 1$$

The vibrational origin of the effect of deuterium substitution on reaction rates.

Figure 31. Primary Kinetic Isotope Effect. The Vibrational Origin of the Effect of Deuterium Substitution on Reaction Rates.

and Bader[279,280] proposed a model where the solvent isotope effect is explained in terms of zero point energies associated with the hindered translations and hindered rotations (librations) of H_2O and D_2O (as well as the internal vibrations). The hindered translations are of very low frequency (~170 cm^{-1}) and are treated classically. The librational frequencies of H_2O and D_2O are different for example at 10°C $\tilde{\nu}_{H_2O}$ = 710 cm^{-1} and $\tilde{\nu}_{D_2O}$ = 530 cm^{-1}.

The conclusion is that solvent isotope effects can be calculated rather accurately by (1) determining the internal vibrations of any molecules which have protons which would exchange with water and become deuterons in D_2O solution, (2) determining the librational frequencies of the water molecules solvating each molecule appearing in the reaction. As a crude generalization, it can be expected that ion-forming reactions will have a solvation isotope effect contribution to $k_{H_2O}/k_{D_2O} > 1$, corresponding to a net increase in structure breaking (net decrease in librational frequencies) on going from reactants to transition state, while effects < 1 are expected for ion-destroying reactions, and effects close to unity are expected for reactions which do not produce or destroy ions. Solvation isotope effects will generally be small, probably no more 20-30% except for small ions which can have a considerable effect on the water structure (librational frequencies).

Deuterium Isotope Effects on the Rates of Non-Radiative Transitions

There are two general approaches in the literature to the problem of non-radiative transitions[281]. In the time dependent approach, initially a set of zeroth-order states is selected which are not the true stationary states of the system, but which are eigen functions of an inexact Hamiltonian. The difference between the true Hamiltonian and the inexact Hamiltonian provides a perturbation which causes "radiationless transitions"

between this initial set of states. According to the stationary state approach absorption occurs not to a non-stationary state but to a stationary state of the system. Any mixing of states due to an intramolecular perturbation would occur before interaction with an external field. The most important theory using the time dependent approach is the theory of Robinson and Forsch[282]. The popularity of this theory is mainly due to its simplicity. An account of the stationary state approach has been given in detail in a review article by Jortner, Rice and Hochstrasser[283].

In order to understand the effect of deuterium substitution on the rates of non-radiative transitions, we will give a very brief account of the theory of Robinson and Frosch.

We consider a molecule interacting with a solvent. The electronic states of the system (for fixed nuclei) are Φ_ℓ and Φ_u with energies $E_\ell < E_u$, and with corresponding vibrational states $\chi_\ell(E)$ and $\chi_u(E)$ where E is the vibrational energy measured relative to the zero-point energies E_ℓ and E_u respectively. Initially the system is in the state $\Phi_u\chi_u(0)$ which is an exact eigenstate in the Born-Oppenheimer approximation. If we go beyond this approximation there is a non-zero matrix element of the form

$$H_{\ell u} = \langle \Phi_\ell \chi_\ell(E) | T_N | \Phi_u \chi_u(0) \rangle$$

where T_N is the nuclear kinetic energy operator. $H_{\ell u}$ is negligible, except when $E \simeq E_u - E_\ell$. Its main effect is that it induces radiationless transition from Φ_u to Φ_ℓ. In polyatomic molecules, where one has a large number of states $\Phi_\ell\chi_\ell(E)$ and these are broadened by solvent interactions, they merge into a continuum of state density ρ_E. According to Robinson and Frosch the radiationless transition probability per unit time is then given by

$$k^{nr}_{\ell u} = 4\pi^2 \rho_E |H_{\ell u}|^2 / h^2 \qquad (118)$$

$H_{\ell u}$ can be separated into electronic and vibrational components by writing

$$H_{\ell u} = \langle \Phi_\ell(E) | T_{\ell u} | \Phi_u(0) \rangle \qquad T_{\ell u} = \langle \chi_\ell | T_N | \chi_u \rangle$$

So equation 118 can be written as

$$k_{\ell u}^{nr} = 4\pi^2 \rho_E J_{\ell u}^2 F/h^2$$

where $J_{\ell u}^2$ is the electronic factor and F is the Franck-Condon factor, describing the square of the overlap of the continuum of vibrational states $\Phi_\ell(E)$ with $\Phi_u(0)$. So while a radiative transition is a vertical transition between the potential surfaces corresponding to different electronic states, a radiationless transition is a horizontal transition, which involves crossing or tunneling from the potential surface of the initial electronic state u to the continuum of isoenergetic vibrational levels of the potential surface associated with the final electronic state ℓ.

The deuterium effect on the rate of non-radiative transitions is hidden in the Franck-Condon factor. Since F depends on vibrational overlap it is sensitive to any isotopic substitution in the molecules which modifies the vibrational frequencies. Siebrand[284] has derived the so-called "isotope rule"

$$(\partial \log F_i(E)/\partial E)_{E'} = (\mu_i/\mu)^{\frac{1}{2}} (\partial \log F(E)/\partial E)_{E'}$$

where i denotes the isotope (deuterium) and μ is the reduced mass of the oscillator governing F(E) for E = E'. The lower Franck-Condon factor for molecules where H has been replaced by D (C-H $\longrightarrow$ C-D) is due to lower frequency of the C-D vibrations relative to C-H vibrations so it takes more C-D vibrational quanta to make up a given energy gap with a poorer vibrational overlap as a result. This is of course true in cases where the C-H vibrations are important in accepting the energy. For aromatic hydrocarbons it has been shown that when the energy gap is larger than $\sim$4000 cm^{-1}, C-H vibrations are important but when $<$ 4000 cm^{-1} the C-C stretching modes dominate and the isotope effect disappears.

The most well studied non-radiative transition is the $T_1 \longrightarrow S_0$ intersystem crossing and this process is also the most sensitive to deuterium substitution. The result of deuteration being an increase of the phosphorescence quantum yield and lifetime. For example Lim and Laposa[285] found:

	$(\tau_T)_D/(\tau_T)_H$
Phenanthrene	4.13
Naphthalene	8.13
Triphenylene	1.49

The same authors and also Laposa, Lim and Kellogg[286] did not find any change in the fluorescence lifetime and quantum yield. Due to the large energy gap between S_1 and S_0 one would expect a very large isotope effect if internal conversion is important. The absence of an isotope effect shows that at least in aromatic hydrocarbons the $S_1 \longrightarrow S_0$ non-radiative transition is not important. This observation has been generalized to other classes of molecules although there are not experimental data for the proof of this assumption. In cases of partial deuteration of aromatic hydrocarbons it has been found that the triplet lifetime shows a significant dependence on the position of the substitution[287,288,289].

A deuterium isotope effect appears also in cases where not the molecule itself is deuterated but the medium in which the molecule is situated. The first case reported is by Hirota and Hutchison[290] who found that the triplet lifetime of naphthalene (guest) in deuterated durene (host) is longer that in the case of protonated durene. Very large solvent isotope effects on the luminescence of metal ions were found by Kropp and Winsdor[291,292,293]. For example for $Eu(NO_3)_3$ the quantum yield increases 18 times going from H_2O to D_2O.

These solvent isotope effects have been explained within the frame of

Robinson and Frosch theory as a slowing of the radiationless transitions in the deuterated solvent due to smaller overlap integrals between the molecular vibrations and the solvent vibrations which eventually will accept the energy. Recently Ermolaev[293] has used the Forster-Dexter theory of energy transfer[295,296] to explain solvent isotope effects. The electronic energy degradation process was supposed to occur due to inductive-resonant interaction between and excited molecule (ion) and the vibrations of the solvent molecule[297]. Solvent isotope effects on the fluorescence quantum yields of several polar molecules were reported by Stryer[298]. The effect was attributed to excited state prototropic reactions.

This interpretation has been challenged for at least some of the molecules studied by several investigators[299,300]. This point will be discussed later in more detail.

PROTON TRANSFER REACTIONS IN 7-AZAINDOLE HYDROGEN BONDED SYSTEMS

Introduction-Absorption Spectra

The spectra of aromatic nitrogen heterocyclic compounds show a general resemblance to the spectra of corresponding aromatic hydrocarbons. Systems whose spectra are being compared must have the same number and geometrical arrangement of π electrons[301]; thus, an imino nitrogen in a heterocyclic molecule is equivalent to -CH=CH- group in an aromatic hydrocarbon. The spectra of aromatic hydrocarbons have been compared and classified by Platt[302]; his notation is used for electronic transitions in heterocyclic systems, also.

An aza-substitution does not change the spectrum of an aromatic hydrocarbon very much; the most general difference seems to be an increase in the intensity of the ^1L_b band. This feature is demonstrated very

clearly in the case of quinoline as compared to naphthalene[301]. Similar effects are noted in the comparison of other heterocyclic and hydrocarbon systems. In Figures 32 and 33, we display the vapor phase absorption spectra of indole and 7-azaindole. The lowest energy transition of indole has been assigned as $^1A \rightarrow {}^1L_b$, and the second transition was assigned to be $^1A \rightarrow {}^1L_a$. The ^1L_b is more intense in indole than in naphthalene spectrum. In 7-azaindole the $^1A \rightarrow {}^1L_a$ transition is approximately short axis polarized and so the aza-substitution at the 7 position is expected to perturb the ^1L_a transition more than the ^1L_b causing the two bands to be closer together in 7-azaindole than in indole. Further, the aza-substitution might be expected to increase further the intensity of the ^1L_b band. Both phenomena can be seen in the displayed spectra. A more detailed analysis of the vapor spectra of these compounds has been performed by R. W. Wagner[303].

Wagner also performed Pariser-Parr-Pople calculations on these molecules, and in Figures 34 and 35, we reproduce his results on indole and 7-azaindole showing the π electron charge densities in the ground, ^1L_b and ^1L_a states. We also give the charge density differences with plus sign as increase and minus sign as decrease. These results will be useful in interpreting the excited state acid-base properties of these molecules.

Indole

Absorption spectra have been recorded in the gas phase, hydrocarbon (3MP), diethyl ether, alcohol and water. The data $\tilde{\nu}_{0,0}$ and $\tilde{\nu}_{max}(^1L_a)$ are shown in Table 15.

Considering hydrocarbon (3MP) as a reference, there is a red shift in ether and ethanol solution but a blue shift in water. The interaction of

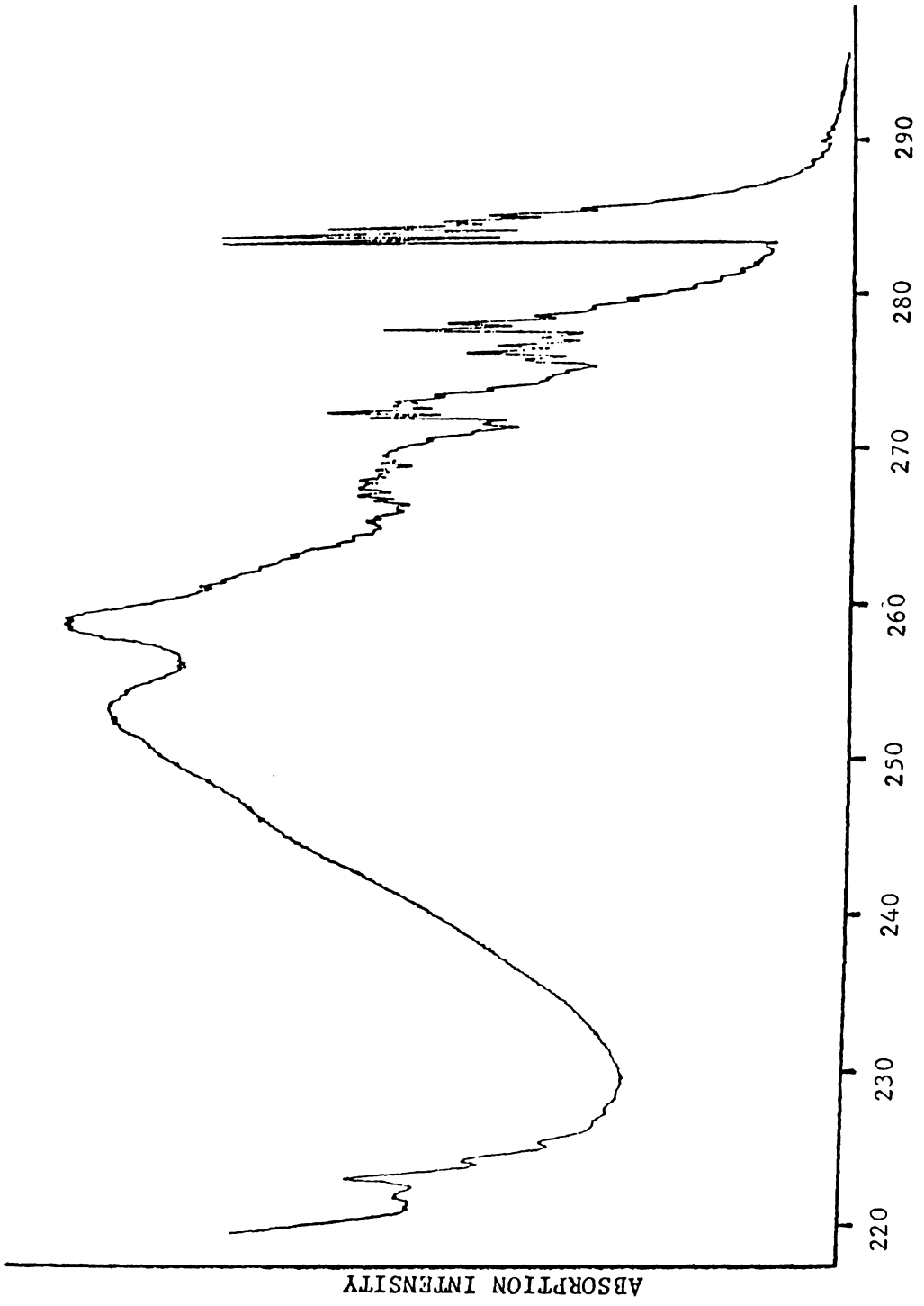

Figure 32. Indole Vapor Absorption Spectrum.

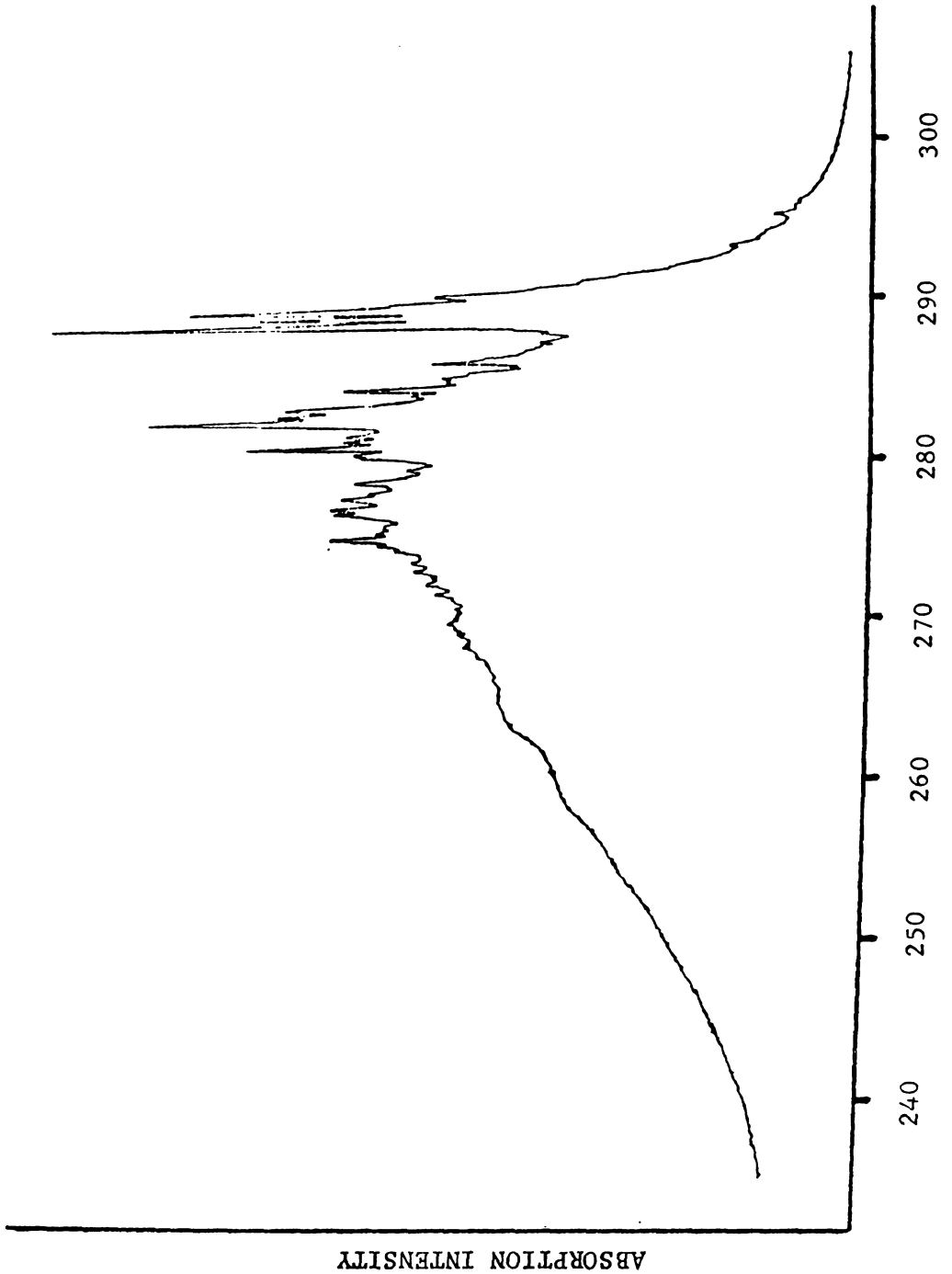

Figure 33. 7-Azaindole Vapor Absorption Spectrum.

Figure 34. Calculated Charge Densities for Indole

34a. Numbers at each atomic position denote π -electron charge densities in electron units for ground state (top number), ^1L_a state (middle number), and ^1L_b state (bottom number).

34b. Numbers at each atomic position denote π -electron charge density differences from ground state (in electron units) for ^1L_a state (top number), and ^1L_b state (bottom number) with plus sign indicating an increase in electron density and minus sign indicating a decrease in electron density.

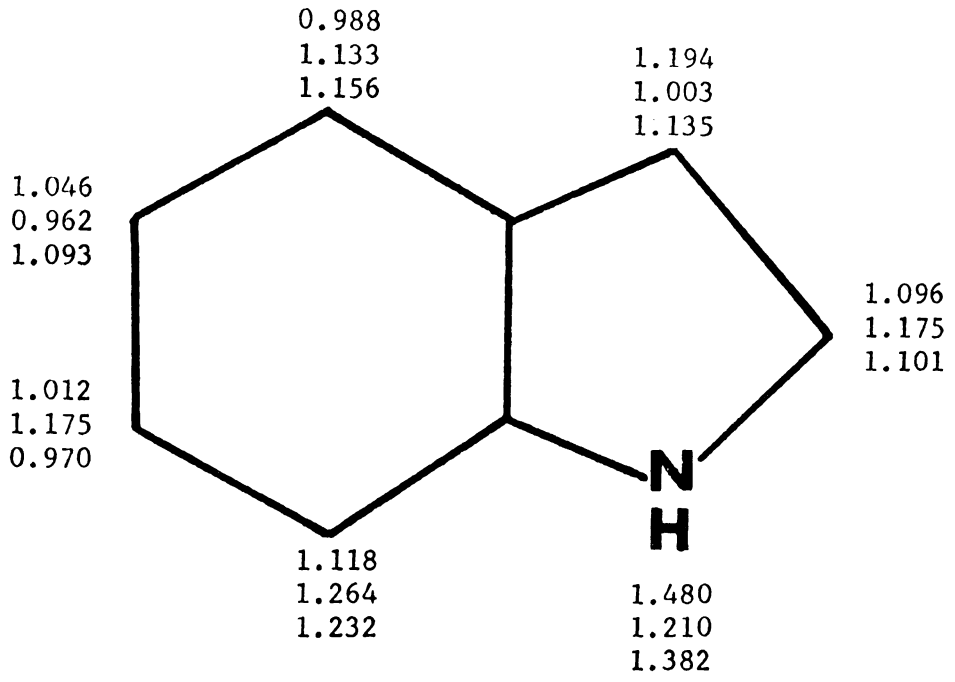

Figure 34a

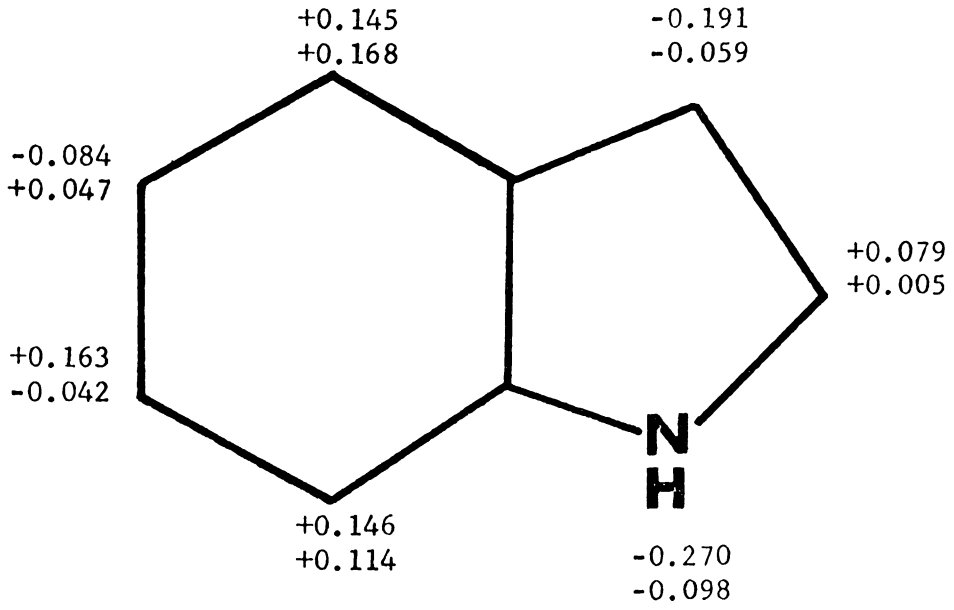

Figure 34b

Figure 35. Calculated Charge Densities for 7-Azaindole.

35a. Numbers at each atomic position denote π -electron charge densities in electron units for ground state (top number), ^1L_b state (middle number), and ^1L_a state (bottom number).

35b. Numbers at each atomic position denote π -electron charge density differences from ground state (in electron units) for ^1L_b state (top number), and ^1L_a state (bottom number) with plus sign indicating an increase in electron density and minus sign indicating a decrease in electron density.

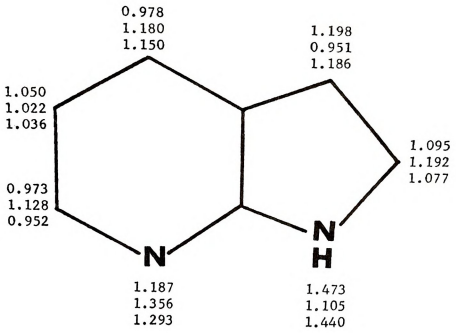

Figure 35a

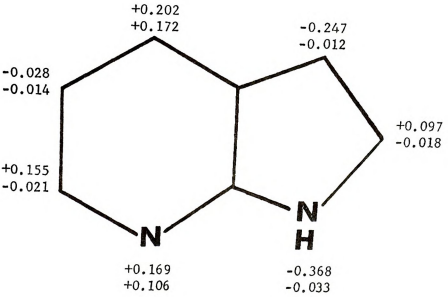

Figure 35b

Table 15. Absorption Spectral Shifts for Indole in Different Media (cm^{-1})

Solvent	$\tilde{\nu}_{0,0}(^1L_b)$	$\tilde{\nu}_{max}(^1L_a)$
3MP	34843	37594
Ether	34722	36832
EtOH	34782	36832
H_2O	34965	37105

solvent with the solute in 3MP since indole is polar (μ = 2.3D) is mainly of the dispersion type plus dipole-induced dipole interaction. Both interactions should cause red shift compared with vapor phase.

In ether besides the dispersion and dipole-induced dipole interaction, dipole-dipole interaction is important because ether has a dipole moment of 1.3D. A further shift arises from hydrogen bonding of the pyrrolic hydrogen with ether's oxygen. In ethanol and water, an additional hydrogen bond may be formed with the pi-electron of pyrrolic nitrogen. If this nitrogen is less basic in the excited state, a blue shift will be seen. Table 16 shows the shifts (in cm^{-1}) of the absorption maxima of the $^1A \longrightarrow {}^1L_b$ and $^1A \longrightarrow {}^1L_a$ transitions with respect to the hydrocarbon solution.

Table 16. Absorption Spectral Shifts (cm^{-1}) for Indole in Different Media Relative to 3MP.

State	vapor	ether	EtOH	H_2O	CH_2Cl_2
^1L_b	+501	-121	- 61	+122	-122
^1L_a	+897	-762	-762	-489	-694

Wagner's calculations show that the electronic density on position 1 (pyrrolic nitrogen) decreases in the excited state and that the decrease is larger in the ^1L_a state than in the ^1L_b state. The absorption spectra (blue shifts in water) support this conclusion and give further evidence for the increased acidity of the pyrrolic hydrogen in the excited state.

7-Azaindole

Table 17 shows the absorption maxima of 7-azaindole in several solvents.

In hydrocarbon (3MP) the spectrum shows a red shift for both ^1L_a and ^1L_b compared to the vapor which is a manifestation of the dispersion forces. In ether we observe a further red shift which appears to be mainly due to the hydrogen bonding with the pyrrolic hydrogen. The red shift seems to indicate that this hydrogen is more acidic in the excited state. In ethanol there is further red shift which may be due partly to increased dipole-dipole interactions and also as Wagner's calculations suggest due to hydrogen bonding with the pyridinc nitrogen. In water we observe a blue shift compared to ethanol although one would expect a red shift

Table 17. Absorption Spectral Shifts for 7-Azaindole in Different Media(cm^{-1}).

Solvent	$\tilde{\nu}_{0,0}(^1L_b)$	$\tilde{\nu}_{max}(^1L_a)$
Vapor	34495	36258
3MP	34013	34843
Et_2O		34722
EtOH		34482
H_2O		34602

at least because of the higher dielectric constant of water. The effect seems to be associated with the higher acidity of water this causes a blue shift because of the solvent hydrogen interaction with the pi-electron charge density at the pyrrolic nitrogen.

Excited-State Acid-Base Properties

As we already pointed out in the introduction Forster[247] and Weller[253] were the first to show that electronic excitation may change drastically the acid-base properties of a molecule.

If equilibrium is estalished during the excited state lifetime then the pK_a^* and pK_b^* can be determined in a way analogous to the spectrophotometric determination of the ground state pK's, by fluorometric titration.

For this reason we have studied the fluorescence intensity as a function of pH (corrections were made for changes in the absorption spectra) for indole and 7-azaindole. Figures 36 and 37 show the results.

Indole

As we see both at low and high pH the indole fluorescence is quenched. In the high pH region the quenching is ascribed to the ionization of the pyrrolic hydrogen according to the reaction

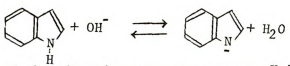

From the midpoint of the titration curve one gets a $pK_b^* = 12.3$. Exactly the same number was obtained by E. Vander Donckt[304]. The excited state $pK_b^* = 12.3$ should be compared to the ground state $pK_b = 16.97$[305] which shows that indeed the pyrrolic hydrogen acidity has considerably increased in the excited state.

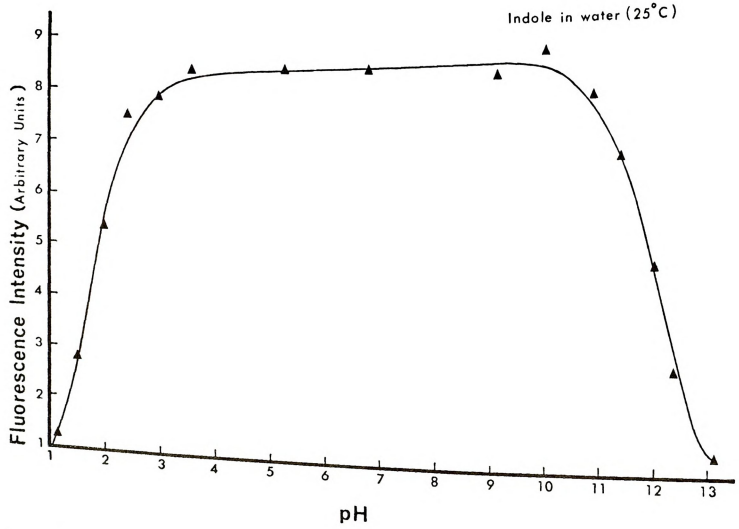

Figure 36. Effect of pH on the Fluorescence of an Aqueous Solution of Indole at 25°C.

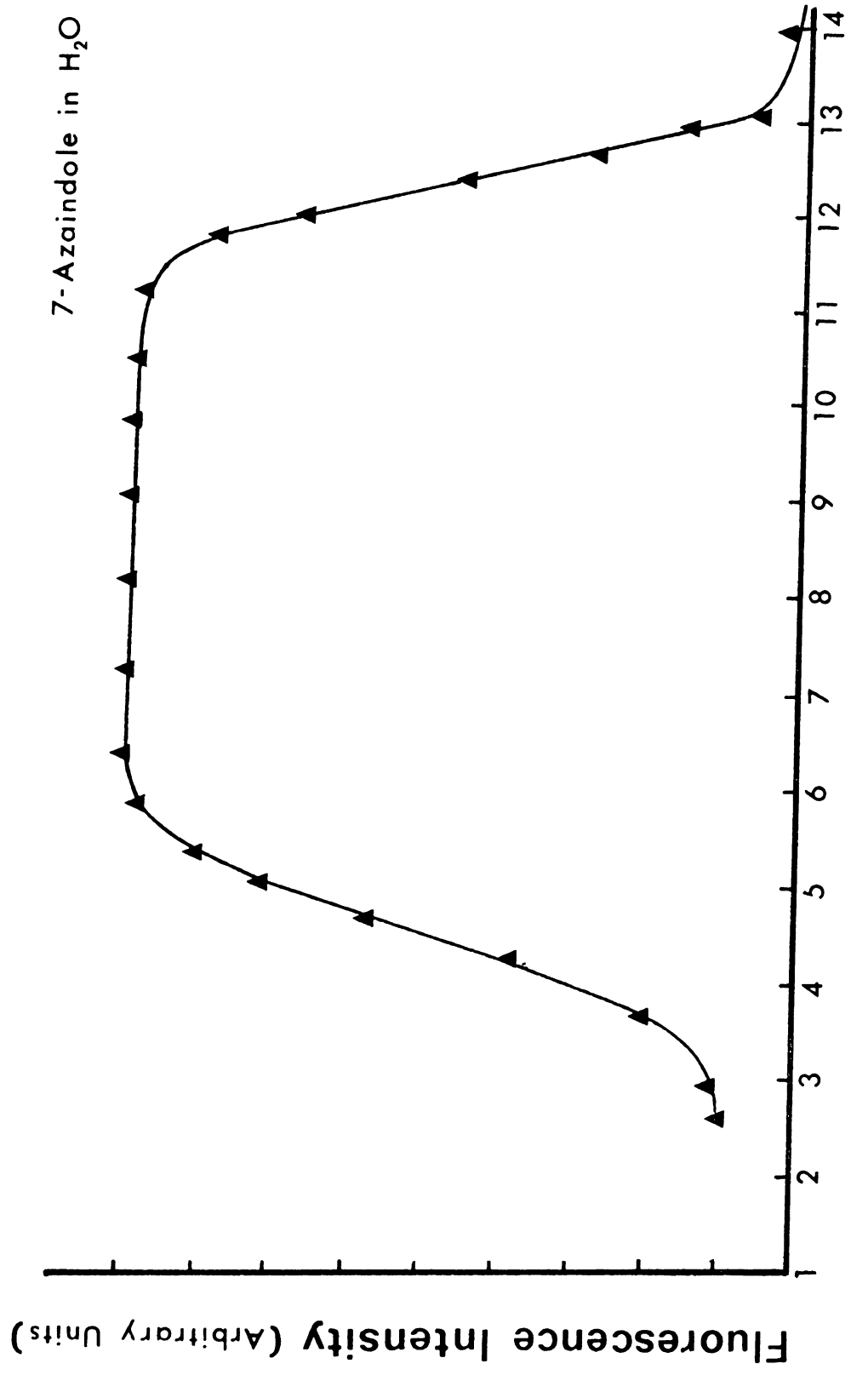

Figure 37. Effect of pH on the Fluorescence of an Aqueous Solution of 7-Azaindole at 25°C.

In the low pH region the quenching is considered to be due to protonation of the pyrrolic nitrogen according to the reaction

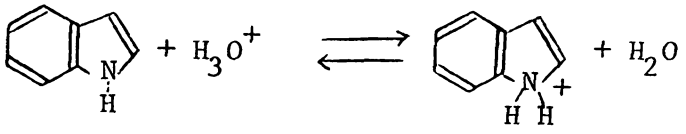

In the same way one gets a $pK_a^* = 1.8$, in very good agreement with the value $pK_a^* = 1.7$ by Bridges and Williams[306].

7-Azaindole

From the fluorometric titration of 7-azaindole we get a $pK_a^* = 4.7$. Besides the quenching upon increase of the concentration of H_3O^+ and approximately below pH = 4, a new fluorescence band appears with a maximum around 450 nm which is ascribed to the cation resulting from the protonation of the N_7 position. Since the cation is emitting it provides us with an opportunity to test if equilibrium is really established in the excited state and if a $pK_a^* = 4.7$ is really representing the true thermodynamic pK_a^*.

We did this following the method of Weller[253] which is based on a thermodynamic cycle shown below:

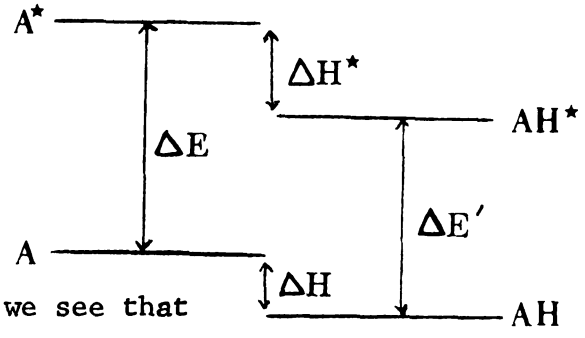

From the figure we see that

$$\Delta E + \Delta H = \Delta E' + \Delta H^*$$

where ΔE and $\Delta E'$ are the energy changes for the transition from the ground state to the first singlet levels of the base and its conjugated aicd, respectively. While ΔH and ΔH^* are the heats of reaction in the ground and

excited state. We can further write

$$\Delta H - \Delta H^* = (\Delta G + T\Delta S) - (\Delta G^* + T\Delta S^*)$$

Assuming that the entropy changes should be about equal in the ground and excited states $\Delta S \simeq \Delta S^*$, then

$$\Delta G - \Delta G^* = -RT(\ln K_a - \ln K_a^*) = \Delta E - \Delta E'$$

and

$$pK_a - pK_a^* = (\Delta E - \Delta E')/2.303RT$$

The energy changes ΔE and $\Delta E'$ can be estimated from the frequencies measured at the maxima of absorption and fluorescence by means of

$$\Delta E = h\nu = (h\nu_{abs} + h\nu_{fluo})/2$$

$$\Delta E' = h\nu' = (h\nu'_{abs} + h\nu'_{fluo})/2$$

Using our data we find (25°C) that $pK_a - pK_a^* = 3.1$. This result coupled with Albert and Adler's ground state $pK_a = 4.59$[308] gives us a thermodynamic $pK_a^* = 7.7$. This shows that the rate of protonation is slow compared to the deactivation rate of the excited state and so in the excited state the ground state equilibrium is insignificantly perturbed.

The fluorometric titration result for the $pK_b^* = 12.3$, the same as the one found for indole. Longworth et al.[307] gave a $pK_b = 7.5$ for indole. If we accept the pK_b as being the same for 7-azaindole as for indole, which appears reasonable, then the thermodynamic $pK_b^* = 9.5$ to be compared with the titrimetric $pK_b^* = 12.3$. This indicates that the ground state equilibrium is perturbed significantly (pK = 17) during the excited state lifetime but complete thermodynamic equilibrium is not attained.

DYNAMICS OF BIPROTONIC PHOTOTAUTOMERISM IN 7-AZAINDOLE HYDROGEN-BONDED DIMERS: TIME RESOLVED SPECTROSCOPY STUDIES

Biprotonic phototautomerism in 7-azaindole hydrogen-bonded dimers was first discovered by Taylor, El-Bayoumi, and Kasha[208] when they examined

the fluorescence spectrum of 7-azaindole in 3-methylpetane (3MP) as a function of concentration. It was known from earlier work by El-Bayoumi[309] that in carbon tetrachloride an appreciable fraction of the 7-azaindole (7AI) molecules is present in the form of doubly hydrogen bonded self-dimers.

In Figure 38, the room-temperature fluorescence spectrum of 7-azaindole in 3MP is seen to consist of two fluorescence bands. The first band F_1 has a maximum at about 325 nm and is attributed to the normal fluorescence of the monomer with possibly a small contribution from the dimer. The second band F_2, has a maximum at about 480 nm and an intensity relative to F_1 which depends on concentration, excitation wavelength and temperature. This second band was attributed by the authors to fluorescence from a new tautomeric species which forms in the excited state of the dimer by the simultaneous intermolecular transfer of the two pyrrolic hydrogens, as shown in Figure 38. The authors took great care in eliminating alternative explanations of F_2 such as impurities, excimers, and photodecomposition products.

Further evidence supporting this mechanism was provided by Ingham et al.[310]. It was shown that the F_2 emission is identical to the emission of 7-methyl-7H-pyrrolo(2,3-b) pyridine, "7-methyl-tautomer". The structure of this compound corresponds to the 7-methyl derivative of the proposed tautomer.

Here we are studying the kinetics of excited state double proton transfer using nanosecond time-resolved fluorescence spectroscopy technique. Because this proton transfer is extremely fast at room temperature, the experiment was conducted at 77°K. The N_1-H hydrogen was replaced by deuterium N_1-D, in order to further slow down the reaction as

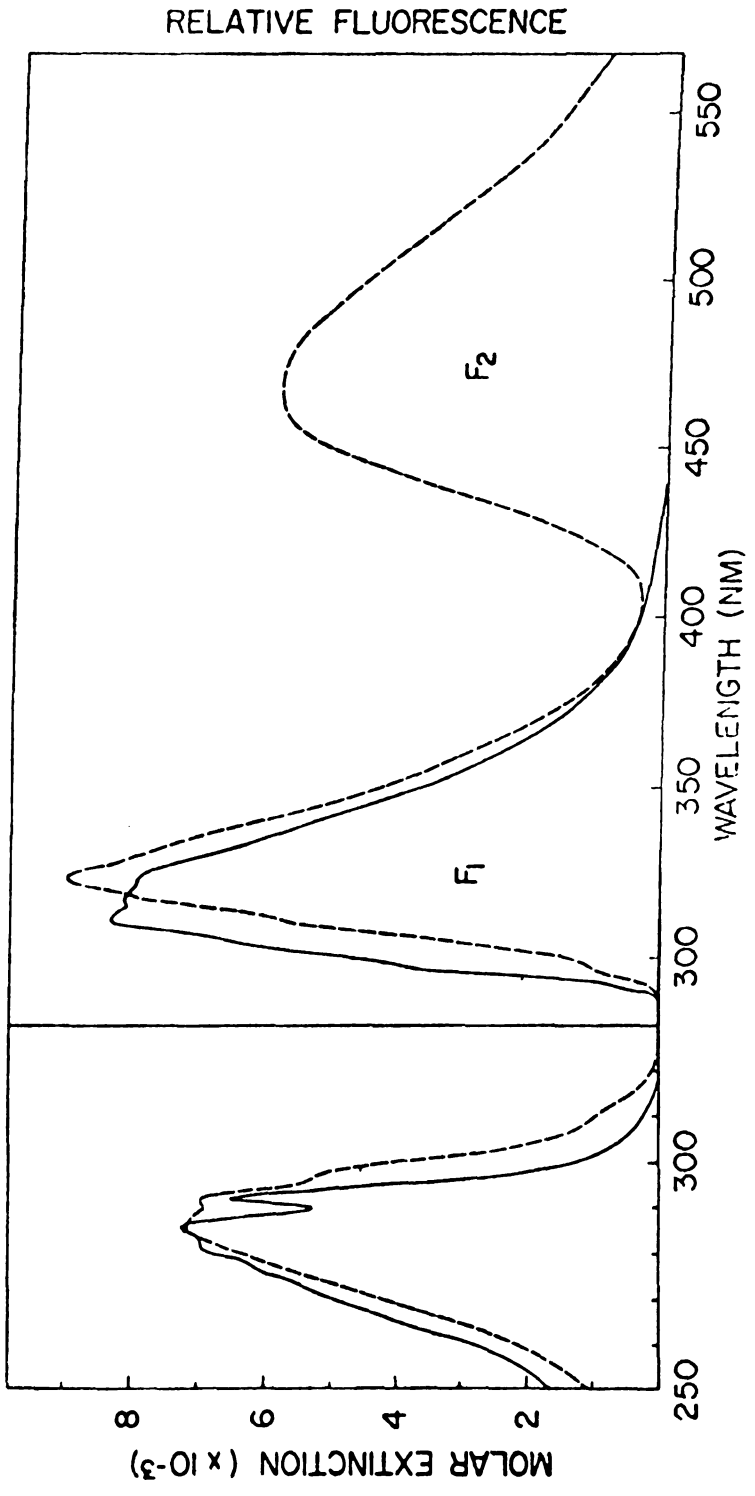

Figure 38. Room Temperature-Absorption (Left) and Fluorescence (Right) of 7-Azaindole in 3MP at $1.0x10^{-5}$M (—) and $1.0x10^{-2}$M(--). Excitation Wavelength 285 nm. Front Surface Excitation Was Used for the Concentrated Sample. The Signals Were Arbitrarily Adjusted to Give Comparable Intensity in the F_1 Region.

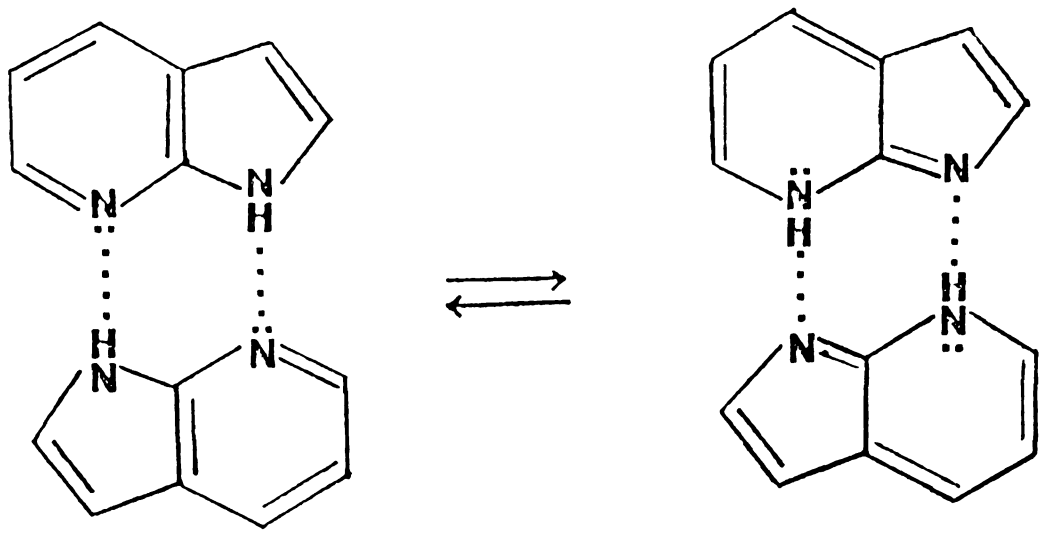

Figure 39. Biprotonic Phototautomerism in 7-Azaindole Hydrogen-Bonded Dimers.

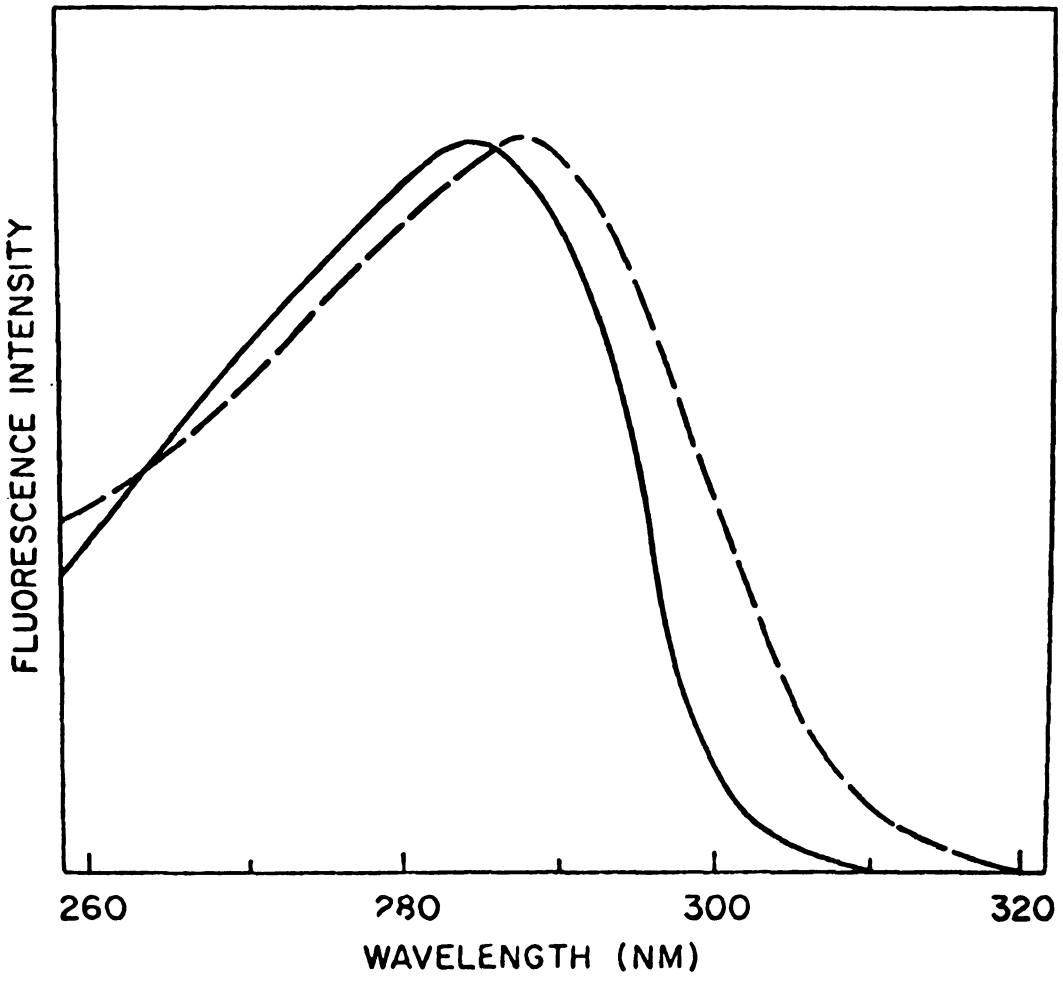

Figure 40. Corrected Fluorescence Excitation Spectra of 7-Azaindole in 3MP at 25°C. The Fluorescence Wavelengths Were 325 nm (Solid Curve, F_1) and 475 nm (Dashed Curve, F_2).

a result of a primary kinetic isotope effect. The sample used was a 10^{-2}M solution of 7-azaindole (N_1-D) in 3MP cooled slowly to 77°K. Under these conditions, virtually all 7-azaindole molecules are present as dimers since ΔH and equilibrium constant K for dimerization at room temperature are -9.6 kcal/mole and $1.8 \times 10^{3} M^{-1}$ respectively.

By studying the kinetics of the excited state reaction we hope to be able to comment on the mechanism of the thermal reaction vs tunneling and on the shape of the potential well in which the protons are located.

Excitation Delocalization in 7AI Dimer

Before attempting the kinetic analysis of the double proton (deuteron) transfer we have to resolve an important question. Namely if during the time scale of the proton transfer the excitation is localized on one 7-azaindole molecule or is delocalized (spread) over the pair comprising the dimer. The significance of this question is that in the case that the excitation is localized, the two proton transfers are inequivalent while if the proton transfer happens from a stationary state involving both 7-azaindoles then both protons are facing the same energy barrier. To answer this question let us consider two identical molecules, a and b, in proximity in a rigid amorphous solution. If molecule a alone is excited at t = 0, the system is then in a non-stationary state where the excitation will oscillate between the moieties. The probability of finding the excitation on b at time t is:

$$\rho_{ab}^{*} = \sin^2 2a \cdot \sin^2(\pi/2 \cdot 4u/ht \cdot 1/\sin 2a)$$

where $2a = \arctan(2u/\delta)$; δ is the difference (if any) in energy of the 0,0 bands of the two identical molecules. This difference may arise because of the possibility of interactions with different microenvironments. For the kind of environments used in our experiments (hydrocarbon matrices)

the interactions of the solute with the solvent is weak and mainly of the dispersion force type. In such a case δ is expected to be very small at least compared with the interaction $u = \langle \Phi_a^* \Phi_b | V_{ab} | \Phi_a \Phi_b^* \rangle$ between molecules a and b. If $\delta = 0$ then we obtain the familiar expression:

$$\rho_{ab}^* = \sin^2(\pi/2 \cdot 4u/ht)$$

where the probability of finding the excitation on molecule b oscillates between zero and one with a half period of $t = h/4u$. Although we realize that the transfer is oscillatory and, therefore, different from a kinetic first order process, we may consider the reciprocal value of that time as the "transfer rate" of this process:

$$k = 4|u|/h \ (s^{-1}) \qquad (119)$$

As we have already discussed the usual spectroscopic practice is to express the intermolecular interaction operator V_{ab} in a multipole series and keep the first non-vanishing term in this case the dipole term. The interaction then is considered as arising from the coupling of the two transition dipoles M,

$$u = \kappa |M|^2 / R^3$$

κ is a numerical factor which depends on the mutual orientation of both molecules,

$$\kappa = \cos\theta_{ab} - 3\cos\theta_a \cdot \cos\theta_b$$

where θ_{ab} is the angle between the transition moment vectors of both molecules while θ_a and θ_b are the angles between these respective vectors and the direction $a \longrightarrow b$. If the lowest energy state of 7-azaindole in the dimer is the ^1L_b state then $k \simeq -1$ while if there is a state interchange as suggested by Taylor, El-Bayoumi and Kasha[208] then $k \simeq -2$. Although in the point dipole approximation R is not well defined an approximation value of $R = 5\text{Å}$ seems appropriate. In this way u can be approximated to be of the order of 10^3 cm^{-1}. Using equation 119, we calculate a "transfer rate" of 10^{14} s^{-1}. Even in the case that u has been overestimated by say

an order of magnitude still the state of the dimer is a stationary state involving both 7-azaindole moieties.

Kinetic Analysis

Let us now consider the kinetic analysis of the double proton transfer. The kinetic scheme considered is the following:

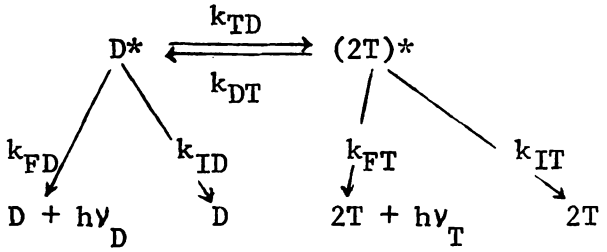

In the scheme we have pictured the two tautomers arising from the double deuteron transfer as sharing the excitation and constituting a single entity. Although this may be true by the same arguments used for the dimer it is not necessary for the following kinetic treatment (this applies to dimer too) since the reverse deuteron transfer is independent of concentration since the two tautomers are trapped in the same cavity of the rigid medium. So the two macroscopic rate constants k_{TD} and k_{DT} are first order rate constants. The kinetic equations after a δ-pulse excitation will be completely analogous to the ones describing the intramolecular excimer interaction in 1,3DNP.

$$d[D^*]/dt = -x[D^*] + k_{DT}[(2T^*)] \tag{120}$$

$$d[(2T^*)]/dt = -y[(2T^*)] + k_{TD}[D^*] \tag{121}$$

where

$$k_D = k_{FD} + k_{ID}$$

$$k_T = k_{FT} + k_{IT}$$

$$x = k_D + k_{TD}$$

$$y = k_T + k_{DT}$$

Solving equations 120 and 121 with the initial condition that $[(2T^*)] = 0$ at $t = 0$, we obtain

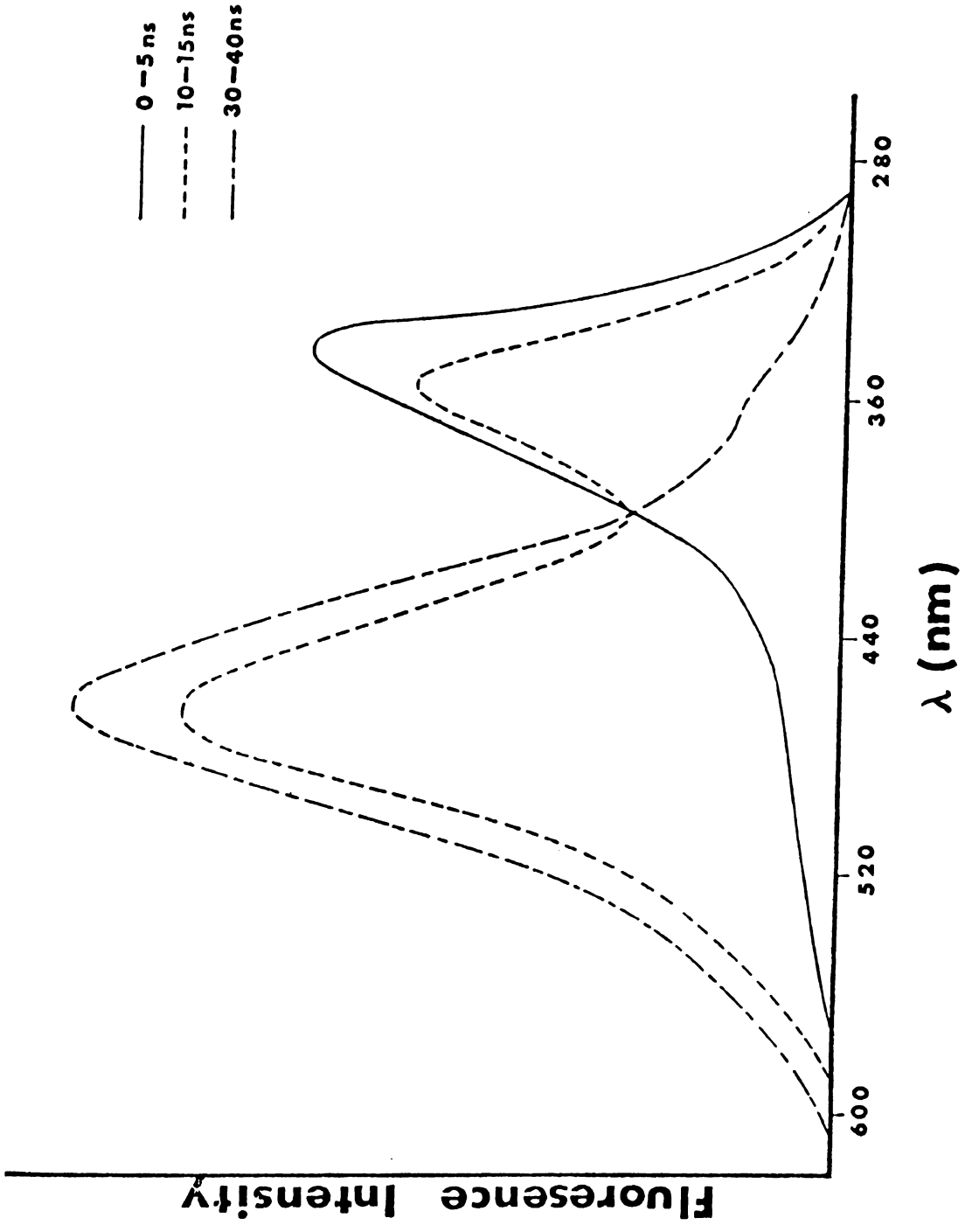

Figure 41. Time Resolved Emission Spectrum of 7AI-d_1 in 3MP at 77°K.

$$[D^*] = [D^*]_0/(\lambda_2-\lambda_1)\left[(\lambda_2 - x)e^{-\lambda_1 t} + (x - \lambda_1)e^{-\lambda_2 t}\right]$$

$$[(2T)^*] = [D^*]_0 k_{TD}/(\lambda_2 - \lambda_1)\cdot(e^{-\lambda_1 t} - e^{-\lambda_2 t})$$

where $$\lambda_{1,2} = \tfrac{1}{2}(x + y \mp \sqrt{(y-x)^2 + 4k_{TD}k_{DT}}) \qquad (122)$$

and as usual changing to intensities we obtain

$$I_D(t) = k_{FD}[D^*]/[D^*]_0 = k_{FD}(\lambda_2-x)(e^{-\lambda_1 t}+Ae^{-\lambda_2 t})/(\lambda_2-\lambda_1)$$

where $$A = (x - \lambda_1)/(\lambda_2 - x)$$

$$I_T(t) = k_{FT}[(2T)^*]/[D^*]_0 = k_{FT}k_{TD}(e^{-\lambda_1 t}-e^{-\lambda_2 t})/(\lambda_2-\lambda_1)$$

From equation 122 we get that

$$\lambda_1 + \lambda_2 = k_D + k_T + k_{DT} + k_{TD} \qquad (123)$$

$$\lambda_1 \cdot \lambda_2 = k_{TD}k_T + k_D k_{DT} + k_D k_T \qquad (124)$$

Rate Constants for Proton Transfer

The dimer decay is found to be described (as expected) as the sum of two exponentials with unequal amplitudes. The values of λ_1 and λ_2 found after deconvolution of the dimer decay are:

$$\lambda_1 = 3.33 \times 10^8\ s^{-1}$$

$$\lambda_2 = 1.11 \times 10^8\ s^{-1}$$

The decay part of the tautomer fluorescence is described by a single exponential $k_T = 1.0 \times 10^8\ s^{-1}$.

The only unknown quantity that we should obtain in order to be able to use equations 123 and 124 and thus obtain the proton transfer rates is k_D, the dimer decay constant in the absence of proton transfer. Since we can not prohibit the proton transfer from happening after the dimer is excited we have to use a model. As such we chose N-methyl-7-azaindole which can not form dimers, and therefore no proton transfer can take place.

The observed lifetime of N-methyl-7-azaindole of 3.8 ns does not correspond directly to the lifetime of the dimer. The reason for this lies in the fact that the excitation is spread to both members of the

dimer. Since the Einstein A coefficient for a transition between states u and 1 is given by

$$A_{u1} = 1/\tau^\circ = 8\pi h\nu^3 g_1 B_{u1}/g_u$$

where B_{u1} is the Einstein B coefficient for induced emission and g_1 and g_u are the degeneracies of the lower and upper states respectively and τ° the radiative lifetime, then $\tau^\circ \propto g_u/g_1$ and one therefore expects the radiative lifetime of the hydrogen bonded dimer ($g_u = 2$) to be approximately twice the radiative lifetime of the model N-methyl-7-azaindole ($g_u = 1$). The dimerization may affect the non-radiative rates to some extent also but this effect will be assumed negligible.

The radiative lifetime of N-methyl-7-azaindole is 19 ns, this value is obtained from the observed lifetime τ_F of 3.8 ns and the quantum yield Φ_F of 0.2 using the relation $\tau_F^\circ = \tau_F/\Phi_F$.

The total decay rate constant of N-methyl-7-azaindole $1/\tau = k_{total}$ is 2.6×10^8 s^{-1}. This can be decomposed to a radiative rate constant $k_F = 5.0 \times 10^7$ s^{-1} and a non-radiative one $k_{NR} = 2.1 \times 10^8$ s^{-1}. The radiative constant of the dimer will then be $k_F(\text{dimer}) = \frac{1}{2}k_F(\text{N-methyl-7-azaindole}) = 2.5 \times 10^7$ s^{-1} and so the total rate constant for the dimer (no deuteron transfer) will be

$$k_{total}(\text{dimer}) = k_F + k_{nr} = 2.3 \times 10^8 \text{ s}^{-1}$$

which corresponds to a lifetime of $\tau_D = 4.2$ ns. Using the value of 2.3×10^8 s^{-1} for k_D and equations 123 and 124 we obtain the transfer rates shown in Table 18.

Table 18. Rate Constants for the Double Proton Transfer in 7-Azaindole Dimers at 77°K.

$k_D = 2.3 \times 10^8$ s^{-1}	$k_T = 1.0 \times 10^8$ s^{-1}
$k_{TD} = 8.6 \times 10^7$ s^{-1}	$k_{DT} = 1.8 \times 10^7$ s^{-1}

The rate constants for the forward and backward deuteron transfer are exceptionally large if one considers that the temperature of the experiment is 77°K ($kT \sim 50\ cm^{-1}$) and comparison is made with rate constants of thermal reactions. This is consistent with the fact that the proton transfer competes successfully with the other processes deactivating the excited molecule which are of the same order of magnitude. Moreover the forward and reverse deuteron transfer rate constants are of the same order of magnitude. This result is important in the effort to determine the shape of the potential well in which the two deuterons are moving.

Activation Energies for Proton Transfer

The large rate of the double deuteron transfer points to a very low activation energy for the process. Ingham, Abu-Elgheit and El-Bayoumi[301] studied the effect of temperature on the ratio F_2/F_1 measured from the relative intensities of the corresponding band maxima. The curve of F_2/F_1 vs T was found to proceed through a sharp maximum near 200°K. In a more recent paper Ingham and El-Bayoumi[311] made a more extensive study of the temperature dependence and explained the shape of the F_2/F_1 vs T curve as resulting from the competition of two phenomena the increasing association of 7-azaindole with lowering of the temperature and the simultaneous decrease of proton transfer as the thermal energy is decreased. Using a limited temperature range (200°K to 130°K) they plotted $\log F_2/F_1$ vs 1/T and obtained a linear plot (there is a certain scatter of data). From the slope of this plot they obtained an apparent activation energy of 1.4 kcal/mole ($500\ cm^{-1}$). Due to certain assumptions inherent to their treatment the authors consider the above value of $500\ cm^{-1}$ as a lower limit to the activation energy. This value for the activation is very small and is indicative of the very small binding of the proton in the excited state.

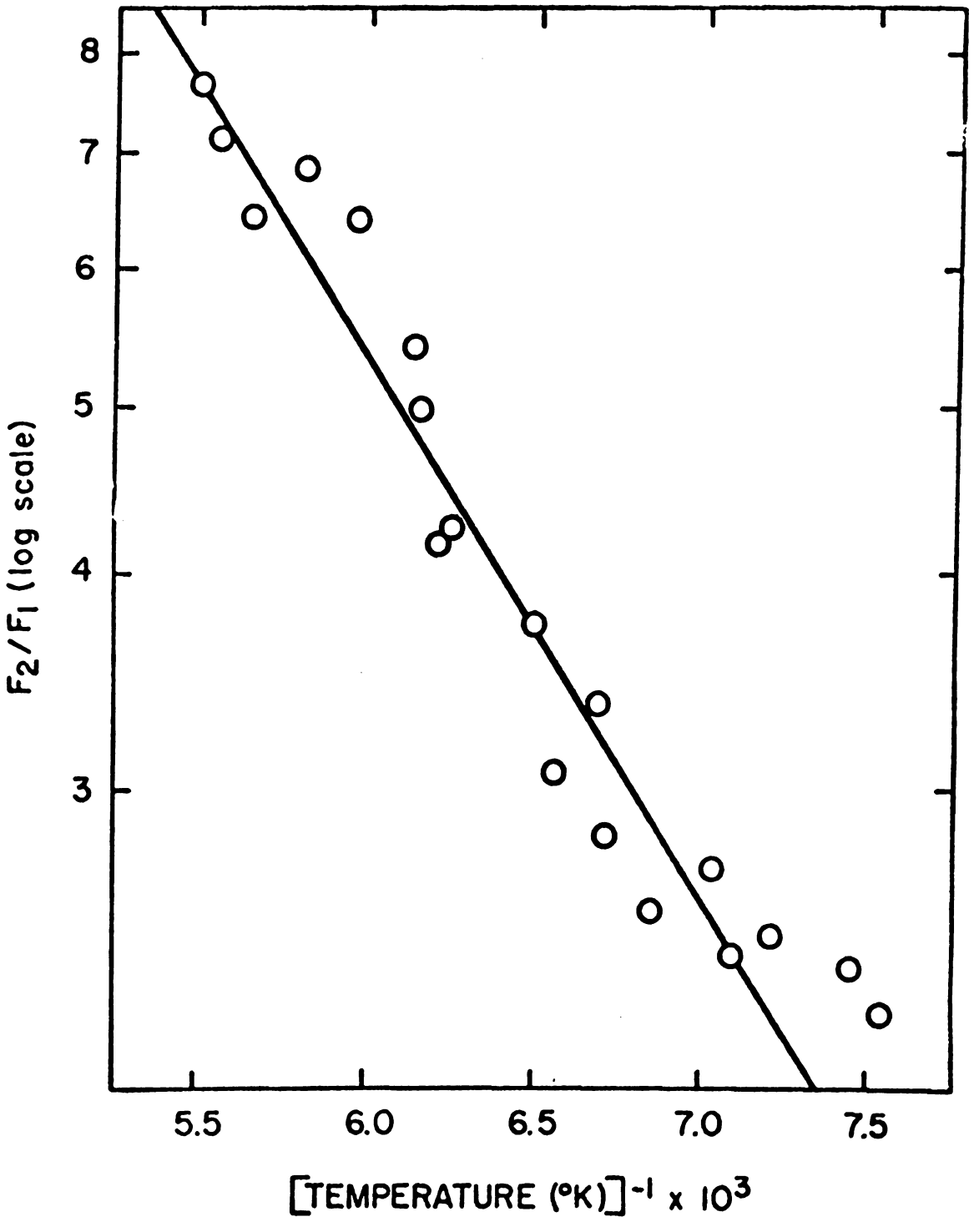

Figure 42. Arrhenius Plot for Estimation of the Barrier to Double Proton Transfer in 7AI Dimers. The Straight Line Has a Correlation Coefficient of 0.93.

At this point it is interesting to try determine if the reaction is a thermal one or proceeds through tunneling. Using the results of the kinetic analysis and assuming a thermal reaction one obtains

$$k_{TD}^{d} = A \cdot \exp(-E^{d}/RT)$$

The preexponential factor will be of the order of 10^{12}-10^{13} (frequency of N-D stretching vibration). In this way one obtains an activation energy of

$$E^{d} = 500 \text{ cm}^{-1} \quad (A = 10^{12})$$

$$\text{or } E^{d} = 600 \text{ cm}^{-1} \quad (A = 10^{13})$$

This is the activation energy for the double deuteron transfer which is to be compared with the experimental value of 500 cm^{-1} for the double proton transfer. One way to relate the results of double deuteron transfer to the case of double proton transfer is through the kinetic isotope effect.

Kinetic Isotope Effect

The kinetic description of the system under conditions of continuous illumination is as follows:

$$\begin{aligned} d[D^*]/dt &= I_0 - (k_D + k_{TD})[D^*] + k_{DT}[(2T)^*] \\ d[(2T)^*]/dt &= k_{TD}[D^*] - (k_T + k_{DT})[(2T)^*] \end{aligned} \tag{125}$$

Under steady state conditions $d[D^*]/dt = d[(2T)^*]/dt = 0$. Using the definitions for the quentum yields

$$\Phi_{FD} = k_{FD}[D^*]/I_0 \qquad \text{and} \qquad \Phi_{FT} = k_{FT}[(2T)^*]/I_0 \tag{126}$$

and since after correction for different instrumental sensitivity in the two different spectral regions

$$\Phi_{FT}/\Phi_{FD} = F_2/F_1 \tag{127}$$

we obtain from equations 125, 126 and 127

$$F_2/F_1 = (k_{FT}[(2T)^*])/(k_{FD}[D^*]) = (k_{FT}k_{TD})/(k_{FD}(k_{DT}+k_T))$$

$$\text{So} \qquad (F_2/F_1)_H/(F_2/F_1)_D = k_{TD}^{h}/k_{TD}^{d} \cdot (k_{DT}^{d} + k_T^{d})/(k_{DT}^{h} + k_T^{h}) \tag{128}$$

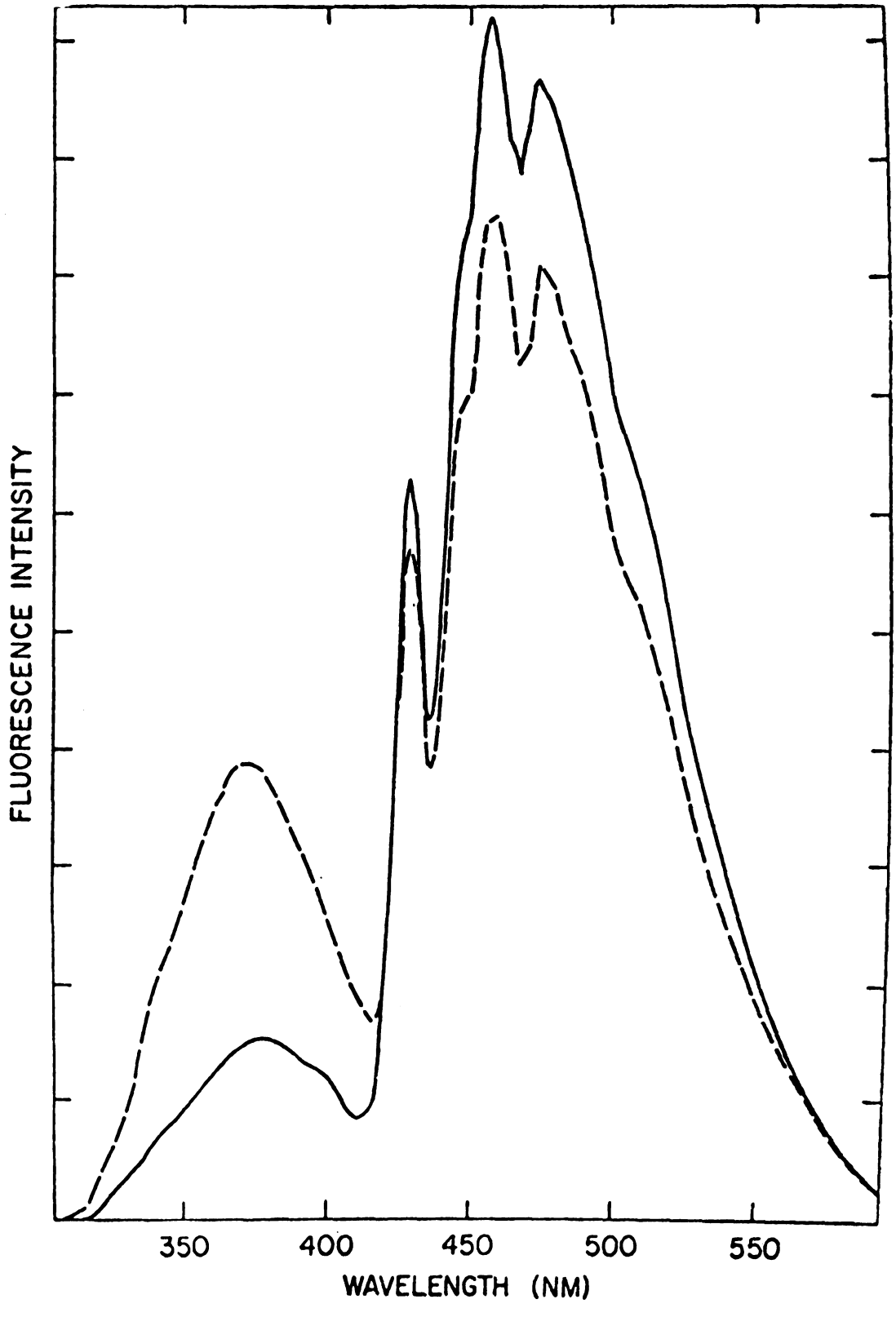

Figure 43. Effect of Deuterium Substitution on the Fluorescence of 7AI (10^{-2}M) in 3MP at 77°K. The Degassed Solutions Were Excited at 285 nm Using Front Surface Excitation. Solid Curve 7AI and Dashed Curve 7AI-d_1.

Since the isotopc substitution is not expected to change the radiative lifetimes. Further since $k_T + k_{DT} \simeq k_T$ and since $k_T = k_{FT} + k_{nr}$, k_T^h is expected to be equal to k_T^d except in the improbable case of a very large and specific effect of one H/D atom on the non-radiative rates. Under these assumptions equation 128 can be simplified to

$$(F_2/F_1)_H/(F_2/F_1)_D = k_{TD}^h/k_{TD}^d \qquad (129)$$

The experimental isotope effect measured as in equation 129 as the ratio of F_2/F_1 for protonated and deuterated 7-azaindole in 3MP matrix at 77°K is 2.9 so $(k_{TD}^h/k_{TD}^d)_{77°K} = 2.9$

Using our result for k_{TD}^d we obtain a $k_{TD}^h = 2.5 \times 10^8\ s^{-1}$. Further as we discussed in the introduction this kinetic isotope effect is connected to the zero-point energy difference so:

$$k_{TD}^h/k_{TD}^d = \exp(-\ ZPE/RT)$$

where $k_{TD}^h/k_{TD}^d = 2.9$

The ZPE thus obtained is around 60 cm^{-1}. If the activation energy for the double proton transfer is 500 cm^{-1} then the activation energy for the double deuteron transfer is around 560 cm^{-1}. This is in good agreement with the estimated activation energy of 500-600 cm^{-1} considering the double deuteron transfer at 77°K as a thermal process. It appears that a mechanism that involves motion of the deuterons over the potential barrier can explain the experimental data at 77°K because of very small energy barrier.

Tunneling vs Proton Transfer

Ingham and El-Bayoumi[311] have reported that F_2/F_1 does not change significantly even at 4°K (the authors cite various difficulties preventing accurate evaluation of the ratio). Under the assumption that the radiative and non-radiative rates do not change from 77°K to 4°K, which is reasonable

since any vibronic effects responsible for these changes will be the same at 77°K and 4°K, one gets that $(k_{TD})_{77°K} \simeq (k_{TD})_{4°K}$. For the reaction to be a thermal one at this temperature (4°K) the activation energy should be around 30 cm^{-1} a result which points strongly to quantum mechanical tunneling. In the following we will try to build a simple model for the case that the tautomerism is following a tunneling mechanism.

In the introduction we discussed briefly the phenomenon of proton tunneling and we derived a formula for the transmission coefficient through a parabolic barrier. This derivation implied a free particle striking the barrier from the left. In the case of the hydrogen bonded dimer the hydrogen (deuterium) is initially oscillating in the left-hand well between its two turning points with a characteristic frequency ν, that is now we are dealing with tunneling of a bound particle. If the oscillation frequency is ν then the particle hits the barrier from the left $\frac{1}{2}\nu$ times per second and each time it hits the barrier the probability of getting through is g, the transmission coefficient. In this way we can define a tunneling rate constant as $k_{tun} = \frac{1}{2}\, g(s^{-1})$ and a characteristic time, tunneling time, as $\tau_{tun} = 1/k_{tun}$. One important question is if the vibrational levels of the well are occupied in a way dictated by Boltzmann statistics or tunneling occurs from a non-thermal distribution of states prepared by the action of light. In our case the tunneling time is of the order of 10^{-7} s while the vibrational relaxation times are of the order of 10^{-12} s, obviously we have a Boltzmann distribution and more over because of the low temperature (77°K) we can safely assume that only the zeroth vibrational levels are populated. Let us now try to estimate the "hit frequency" . If one assumes that the bottom of the well is approximately parabolic one can make an estimate of ν. A parabolic well is characterized

by a potential of the form

$$V = a(x - x')^2/2$$

A quantum-mechanical wave packet is then going to oscillate with the same frequency as a classical particle. The Hamiltonian may be expressed in the form $H = p^2/2m + \frac{1}{2}a(x - x')^2$

Consequently, if 2b is the distance between the two classical turning points, one has the relation

$$E = \tfrac{1}{2}ab^2 = \tfrac{1}{2}h\nu \qquad \text{and since} \qquad a = 4\pi^2 m\nu^2$$

$$\nu = h/(4\pi^2 mb^2)$$

For b in Å and for deuterons

$$\nu = 5 \times 10^{11}/b^2 \ \text{sec}^{-1}$$

For hydrogen bonded systems a value of 2b = 0.6 Å seems reasonable and gives a frequency of $\nu = 5.6 \times 10^{12}\ s^{-1}$.

In the case of the 7-azaindole dimer both deuterons must change positions in order that tautomerization happens. From the previous discussion on the delocalization of the excitation we can say that the two deuterons are moving in two identical potential wells presumably independently. If both hit the barrier on the correct side the probability that both tunnel through is g^2. Since we assumed that the motions of the two deuterons are not coupled the phase difference of their vibrational motions will be random. It is reasonable to propose that only particles that are both moving toward the correct side of the barrier can give rise to tautomers. Since there are four possibilities the tunneling rate constant will be $k_{tun} = \frac{1}{4}\nu g^2$

As we show in the introduction g can be written as

$$g = \exp(-\pi^2 \kappa a_0 (2mV_0)^{\frac{1}{2}}/h)$$

At 77°K, κ can be taken as one. So g for deuteron can be written as

$$g = \exp(-48.825 a_0 V_0^{\frac{1}{2}})$$

where a_0 is in Å and V_0 in eV. So the tunneling rate constant will be given by

$$k_{tun} = 1.4 \times 10^{12} \exp(-2 \times 48.825 a_0 V_0^{\frac{1}{2}}) \ s^{-1} \qquad (130)$$

If we substitute the experimental value of k_{TD} in equation 130 then $a_0 V_0^{\frac{1}{2}} = 0.099$. If one assumes some reasonable values for a_0, V_0 can be estimated:

$a_0 = 0.4$ Å then $V_0 = 500\ cm^{-1}$

$a_0 = 0.5$ Å then $V_0 = 320\ cm^{-1}$

$a_0 = 0.6$ Å then $V_0 = 220\ cm^{-1}$

Despite the crudeness of the model one can see that the results are reasonable and tunneling can be a possible mechanism contributing to the proton/deuteron transfer at 77°K and higher temperatures while it has to be the only path for proton/deuteron transfer at 4°K. Considering the depth of the second well where the proton/deuteron is situated we can say that approximately should be the same as the first one (symmetric double well). This is indicated by the closeness of the values of k_{TD} and k_{DT}. To get an idea of the ΔH^*, the heat of the reaction, one can again consider the reaction at 77°K as thermal and then the activation energy for the back transfer will be $E_{DT} = E_{TD} + \Delta H^*$ for $A = 10^{12}$, $\Delta H^* = 80\ cm^{-1}$. Since the emission maxima of the dimer and tautomer are shifted by 10,000 cm^{-1} (3MP) and since the excited state double well appears almost symmetric then the large shift is due to the fact that in the ground state the second well is 10,000 cm^{-1} higher in energy than the first. An interesting experiment will be to study the overtones of the N-H/N-D stretchings in 7-azaindole dimers in the ground state. Preliminarly one would expect that splittings (doublets) will appear in the third overtone for the H compound and in the 4th overtone for the D compound.

EXCITED STATE COMPLEX OF 7-AZAINDOLE WITH ALCOHOLS: EVIDENCE OF EXCITED STATE DOUBLE PROTON TRANSFER

As it was first shown by Taylor et al.[208] the room temperature emission spectrum of 7-azaindole in ethanol is composed of two emission bands. Besides the molecular fluorescence band of 7-azaindole (7AI), F_1, another broad (excimer like) fluorescence band, F_2, appears with a maximum at 540nm. It can be easily shown that this new emission band (F_2) is not due to excimers. First the ratio F_1/F_2 is independent of the 7-azaindole concentration unlike the normal excimer behavior and second upon addition of ether F_2 decreases and finally disappears in pure ether solution of the same concentration. Taylor et al. attributed the F_2 band as arising from a tautomer resulting from a double proton transfer in the excited state between 7AI and an alcohol molecule in a completely analogous way to the tautomerization of H-bonded 7-azaindole dimers in hydrocarbon solvents. The tautomer is the same in both cases and only the mechanism of its production is different.

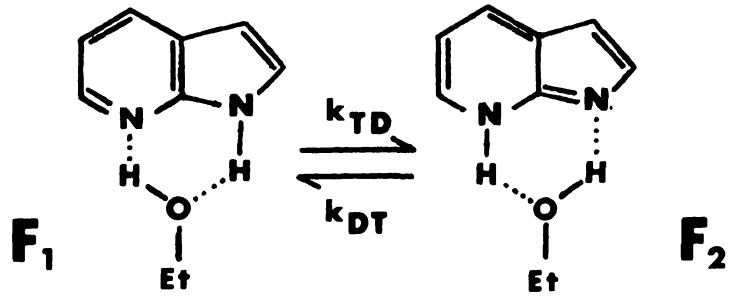

We will now present some more evidence supporting the above mechanism of excited state double proton transfer between a 7-azaindole molecule and an alcohol molecule. First we studied the emission spectra of 7AI in EtOH and EtOD. The total quantum yields in the two solvents are:

$$\Phi_{Total}(EtOH) = 1.3\ (\pm\ 0.1) \times 10^{-2}$$

$$\Phi_{Total}(EtOD) = 3.3\ (\pm\ 0.2) \times 10^{-2}$$

$$\Phi(EtOD)/\Phi(EtOH) = 2.5$$

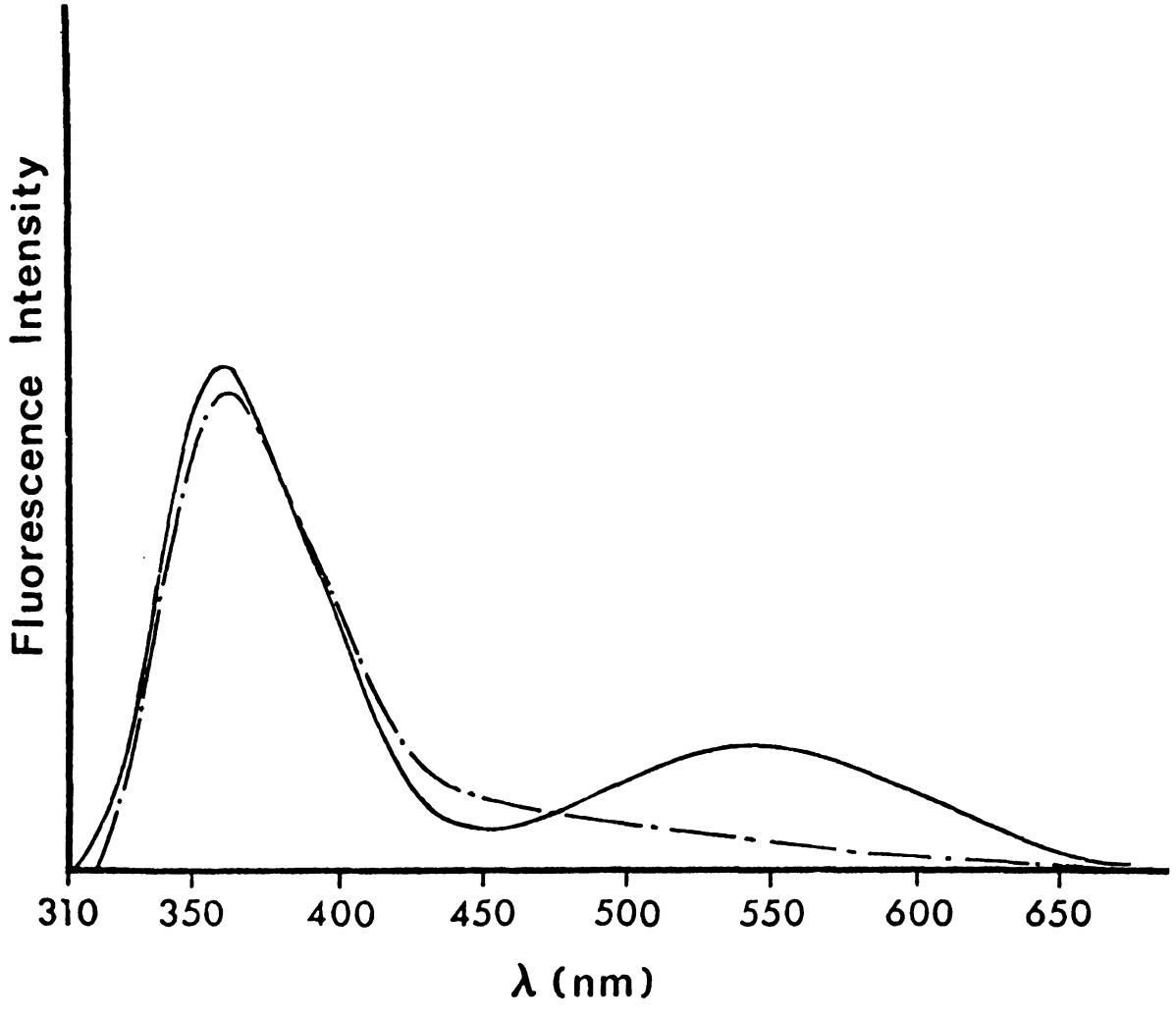

Figure 44. Corrected Room Temperature Fluorescence Spectra of 7AI in EtOH (__) and 7AI in EtOD (-·-·).

Also $(F_2/F_1)_{EtOH} = 0.313$ and $(F_2/F_1)_{EtOD} = 0.072$. If we use the same kinetic treatment as that for the 7AI dimers under continuous illumination, equation 129, we obtain:

$$(F_2/F_1)_{EtOH}/(F_2/F_1)_{EtOD} = k^h_{TD}/k^d_{TD} = 4.35$$

This isotope effect is too large to be just a kinetic solvent isotope effect (see introduction) and must be a primary isotope effect where the H/D of the OH/OD group is abstracted in the excited state of the 7AI-ethanol complex. The excited state basic pK suggests protonation of N_7.

We further studied the quantum yield of N-methyl-tautomer in EtOH and EtOD solutions and found that $\Phi_{EtOD}/\Phi_{EtOH} = 1.53$.

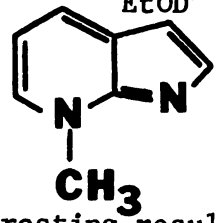

This is a very interesting result since it appears to be a genuine solvent isotope effect on the fluorescence quantum yield and may mean that internal conversion is important in this compound.

We also studied the quantum yields of N_1-methyl-7-azaindole in EtOH and EtOD and we found that $\Phi_{EtOD}/\Phi_{EtOH} = 1.0$. These results seem to suggest the following:

(1) Since the emission yield of N_7-methyl-tautomer increases in EtOD while that of N_1-methyl-7-azaindole remains unchanged, the kinetic isotope effect as measured by the F_2/F_1 ratio in EtOH compared to EtOD is actually higher than the observed 4.35 ratio. This supports a primary isotope effect.

(2) The 7-aza-nitrogen and the pyrrolic hydrogen N_1-H are both involved in producing species that emit F_2. Indole and N-methyl-7-azaindole do not exhibit any F_2 fluorescence.

(3) Simple protonation of the 7-aza-nitrogen or proton-abstraction of the pyrrolic hydrogen are not responsible separately for F_2 fluorescence. The

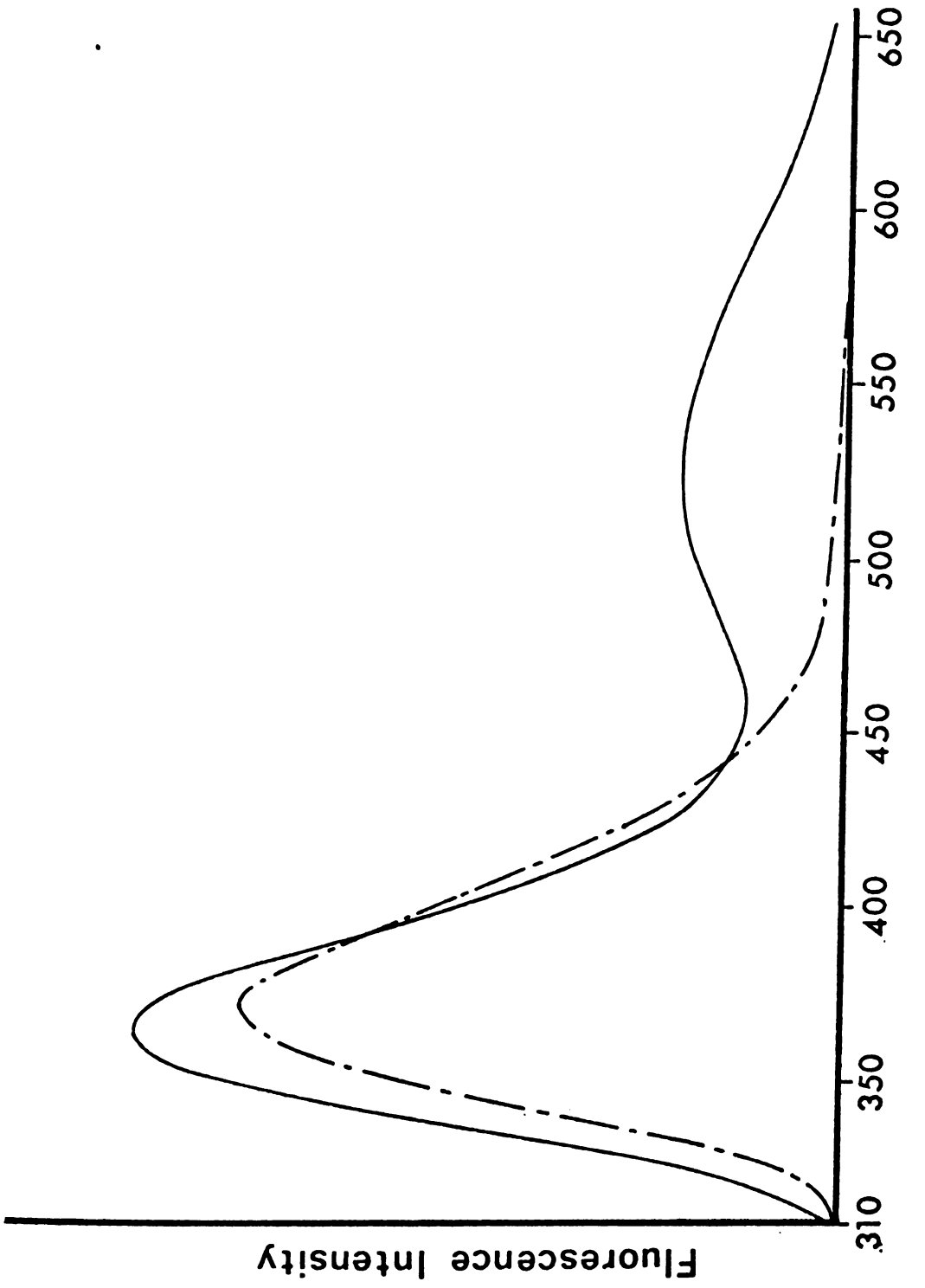

Figure 45. Room Temperature Fluorescence Spectra of 7AI in Ethanol (—) and N-Methyl-7AI in Ethanol (-·--).

emission of 7AI in alcohol solution acidified by HCl exhibits a band at 450 nm which lies between F_1 and F_2. Addition of sodium ethoxide to ethanol solution of 7AI leads to quenching of F_1 fluorescence with no spectral alterations. This quenching is due to abstraction of the pyrrolic proton which is more acidic in the excited state.

(4) The N_1-methyl-7-azaindole is insensitive to solvent deuteration.

(5) The protonation of 7-aza-nitrogen and proton abstraction of the pyrrolic hydrogen are coupled in the process of producing the tautomer responsible for F_2.

Another important question is if the complex is a 1:1 cyclic complex as suggested by Taylor et al., or 1:2 complex where two alcohol molecules are complexed with one molecule of 7AI.

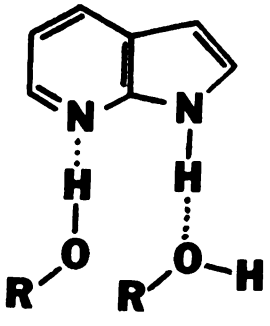

1:2

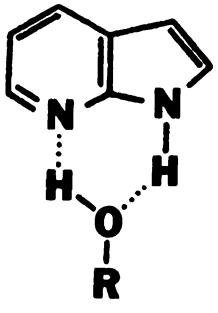

1:1

When small amounts of ethanol are added to a dilute (1.0×10^{-4} M) solution of 7AI in 3MP at room temperature the absorption spectra are perturbed in the same way as during 7AI dimerization (red shifts). The absorption at 310 nm is due primarily to the complex and can be used to determine the stoichiometry and the association constant of the complex, as was shown by H. A. Benesi and J. H. Hildebrand[312] and Scott[313]. For a 1:1 complex the following equation is valid

$$C_A/A = C_A/C_I\epsilon l + 1/\epsilon l K C_I$$

where C_A is the ethanol concentration, C_I is the 7AI concentration, l is

the path length, ϵ is the molar extinction coefficient of the complex at 310 nm and K is the association constant. A plot of C_A/A vs C_A is shown in Figure 46 for data obtained at room temperature and 310 nm[310]. The good linearity of the plot confirms the assumption of a 1:1 complex since higher order complexes would produce a curvature. Further from the ratio of intercept to slope an equilibrium constant of $K = 49\ M^{-1}$ is obtained.

THE INTERACTION OF 7-AZAINDOLE WITH WATER

Quenching Mechanisms-Solvent isotope Effects

The problem of the nature of the non-radiative processes that quench indole's fluorescence in water solutions is an old one. Despite the very intensive study by many authors the problem has not been clarified completely.

First Stryer[298] found that the ratio of the fluorescence quantum yields of indole in D_2O and H_2O was $\Phi_{D_2O}/\Phi_{H_2O} = 1.29$ while that of 1-methyl-indole was 1.09. Stryer explained these results as indicating that deprotonation of the pyrrolic nitrogen in the excited state is a major quenching mechanism of indole's fluorescence and that this deprotonation is easier in H_2O. 1-methyl-indole lacking the hydrogen does not show any significant isotope effect.

Forster and Rokos[299] have excluded proton-transfer as being responsible for the solvent isotope effect on the fluorescence yield of some aromatic amines as suggested by Stryer in the same article. They suggest that solute-solvent interaction is directly responsible for internal conversion in these molecules.

Bowen and Seamen[314] have noted a relationship between the fluorescence shift and fluorescence quantum yield for several analogous amines in polar

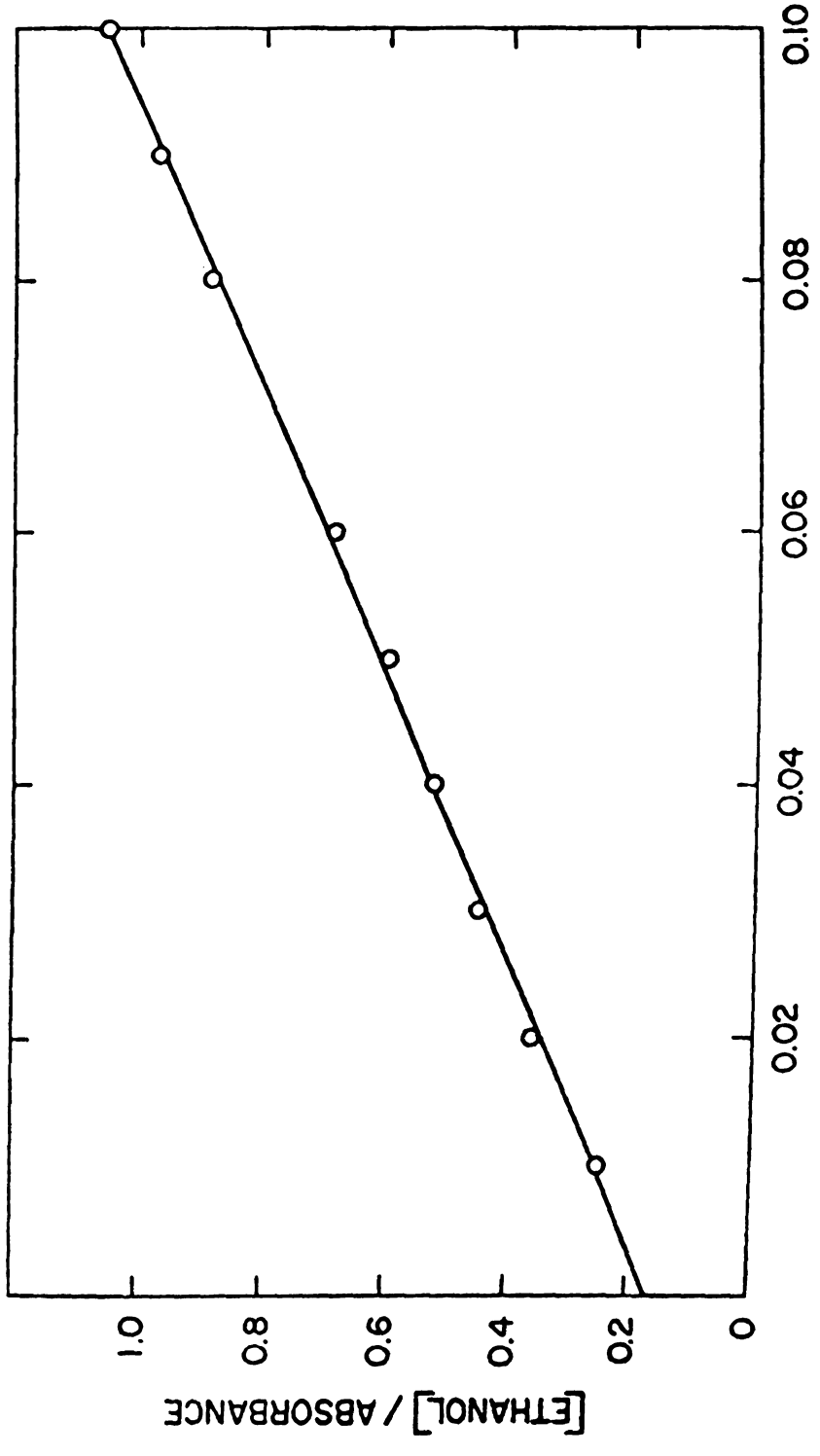

Figure 46. Application of the Benesi-Hildebrand Equation in the Determination of the 7AI-Ethanol Complex at 25°C. Absorbance Values Were Determined at 310 nm. The 7AI Concentration Was 1.0 x 10^{-4}M.

solvents which Forster and Rokos regard as evidence for a direct relation between the mechanism responsible for the red shift and that responsible for the quantum-yield change. A similar correlation has been reported by Viktorova[315] for several organic fluors in both single and bicomponent solvents, the quantum yield passing through a maximum value with increasing Stokes shift in the emission. The author explained this phenomenon in terms of discrete centers in mixed solutions corresponding to molecules of the fluor associated with different numbers of solvent molecules. Eisinger and Navon[300] have suggested that the predominant non-radiative relaxation process for indole is a tunneling process between the potential surface corresponding to the fluorescent state and that corresponding to the ground state, followed by rapid vibronic relaxation. The authors give an isotope effect of Φ_{D_2O}/Φ_{H_2O} = 1.30 for indole and 1.19 for 1-methyl-indole, which they attribute to the internal conversion process.

Walker et al.[316] suggested the important non-radiative path may be electron transfer to the solvent. This possibility was suggested by the results of Grossweiner and Joschek[317]. Walker et al. ascribed the isotope effect to "differences in the solvation state of electrons in D_2O and H_2O".

Ricci[318] gives a Φ_{D_2O}/Φ_{H_2O} = 1.49 for indole and = 1.19 for 1-methyl-indole. The fact that the ratio is not unity for 1-methyl-indole was attributed by the author as due to a tunneling type interaction in which the highly energetic carbon to hydrogen stretching vibrations transfer energy via coupling to the OH and OD stretching vibrations of the solvent molecules. In D_2O the lower frequency OD stretching vibrations cannot dissipate the vibrational energy as effectively as a fluorescence quencher as H_2O resulting in 19 per cent more fluorescence in D_2O than H_2O. Ricci also found that the isotope effect increases as the methylation of the indole ring increases

reaching a value of 3.46 in the case of 2,3,6-trimethyl indole. The author suggests that as the number of methyl groups on the indole ring are increased the importance of non-radiative decay through the CH stretching vibrations decreases resulting in a proportional increase in the importance of the isotopically dependent deprotonation mode of non-radiative decay. He considers two possibilities for the deprotonation step: (a) rate limiting proton transfer followed by a fast non-radiative decay of the anion

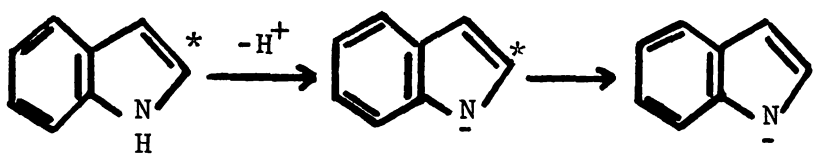

or (b) proton loss as part of the internal conversion process:

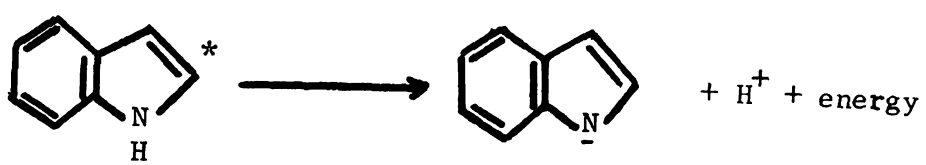

Several other authors support the one or the other explanation (see for example E. P. Busel et al.[319]; M. S. Walker et al.[320] and E. P. Kirby et al.[321]),but no clear answer has been given yet.

We have found that 7AI's fluorescence is quenched considerably in water. For example the fluorescence quantum yield of 7AI in a dilute solution in 3MP (no F_2) is 0.24 while the fluorescence quantum yield in water is 0.03, an eightfold decrease. We also found that 7AI's fluorescence is greatly enhanced in D_2O being 3.63 times higher than in H_2O. Some results are summarized in Table 19. By looking at the results in Table 19, we immediately see that the isotope effect is connected to some non-radiative deactivation path. The larger the quenching, the larger the isotope effect. So $\Phi_F(7AI, H_2O) < \Phi_F(\text{indole}, H_2O)$ and $(\Phi_{D_2O}/\Phi_{H_2O})_{7AI} > (\Phi_{D_2O}/\Phi_{H_2O})_{\text{indole}}$. Second we see that when we replace the pyrrolic hydrogen with a methyl

group the quantum yield increases with a simultaneous decrease of the isotope effect and that actually

$$\Phi_{\text{N-methyl-7-azaindole}} \simeq \Phi_{\text{N-methyl-indole}}$$

and

$$(\Phi_{D_2O}/\Phi_{H_2O})_{NM7AI} \simeq (\Phi_{D_2O}/\Phi_{H_2O})_{NMI}$$

The above result shows very clearly the importance of the pyrrolic hydrogen for the quenching path. In the case of 7AI the isotope effect difference between 7AI and NM7AI is very large. In the case of indole vs 1-methyl-indole the difference is small and many authors have argued (Eisinger and Navon primarily) that the differences between indole and NMI may be just due to different coupling with the medium. This does not seem likely at least for 7AI. So at this point we can conclude that the N-H group participates in the quenching. Further, by comparing indole and 7AI quantum yields we can say that the quenching function of the pyridinic nitrogen can only be exemplified in the presence of the pyrrolic hydrogen or in other words the deactivation mechanism involves interaction with both sites.

We also studied the fluorescence intensity of 7AI in D_2O as a function

Table 19. Fluorescence Quantum Yields of Indole, 7-Azaindole and Methyl Derivatives in Water and Deuterium Oxide.

Compound	$\Phi_F(H_2O)$	$\Phi_F(D_2O)/\Phi_F(H_2O)$
Indole	0.45	1.41
N-methyl-indole	0.62	1.19
7-azaindole	0.03	3.63
N-methyl-7-azaindole	0.64	1.18

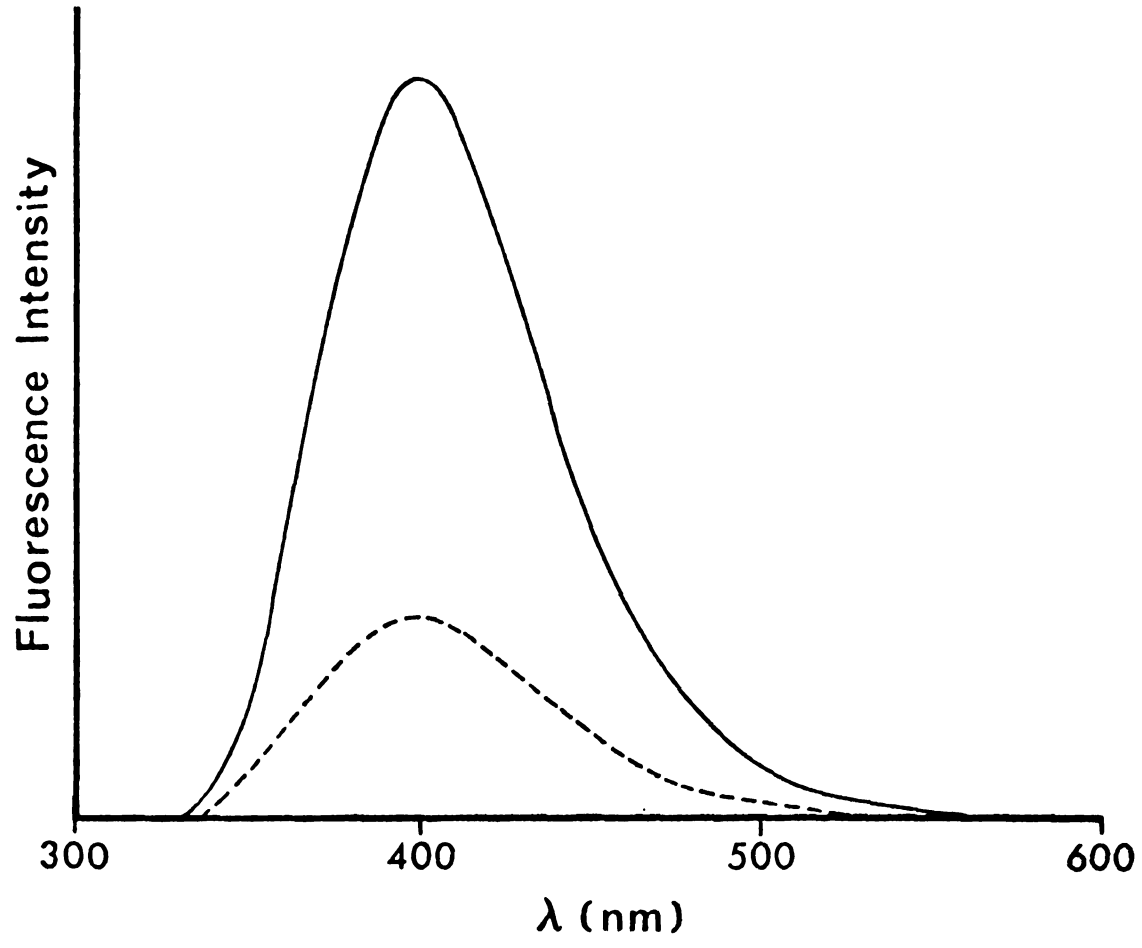

Figure 47. Room Temperature Fluorescence Spectra of 7AI in H_2O (--) and D_2O (__). Both Solutions Have the Same Optical Density.

of pD. As was shown by Glasoe and Long[322], pD can be measured using a glass electrode by appling the correction

$$pD = \text{pH meter reading} + 0.40$$

where the "pH meter reading" is obtained with an apparatus standardized to read pH in H_2O solutions.

From the fluorimetric titration curve in D_2O, we obtain a $pK_b^* = 13.1$ in D_2O. Although excited state pK's cannot be determined very accurately, it appears that the ionization of the pyrrolic hydrogen is suppressed somehow in D_2O (compare with $pK_b^* = 12.3$ in H_2O).

Martin[323] has proposed an equation, used to predict pK_D from pK_H of ground state acids

$$pK_D - pK_H = 0.45 + 0.015pK_H - 0.12Z$$

where Z denotes the net charge on the acid form of the conjugate acid-base pair being considered. Using a $pK_H^* = 12.3$, we obtain a $pK_D^* = 13$ in reasonable agreement with what we observe. Such good correlations for excited state acids have been reported by Wehry and Rogers[324]. An interesting correlation was found by considering the variation of the isotope effect $\Phi_{(D_2O)}/\Phi_{(H_2O)}$ with pH(pD). The results are displayed in Figure 49. As it is seen from the figure the isotope effect appears to remain constant in the pH range around 7-11 while it decreases at lower pH and increases at higher pH. The sharpest changes appear around the $pH = pK_a^*$ and $pH = pK_b^*$. This shows that the isotope effect depends on the quenching mechanism (quenching by H^+ low pH, or quenching by OH^- high pH). In the high pH region the isotope effect is the highest. In this pH range undoubtly the ionization of the pyrrolic hydrogen is significant. Since the ionic product of water $k_w = a_{H^+}a_{OH^-}$ at 25°C is $k_w = 10^{-14}$ then $\log a_{OH^-} = pH - 14$, where the activities a are approximately equal to concentrations. We have used

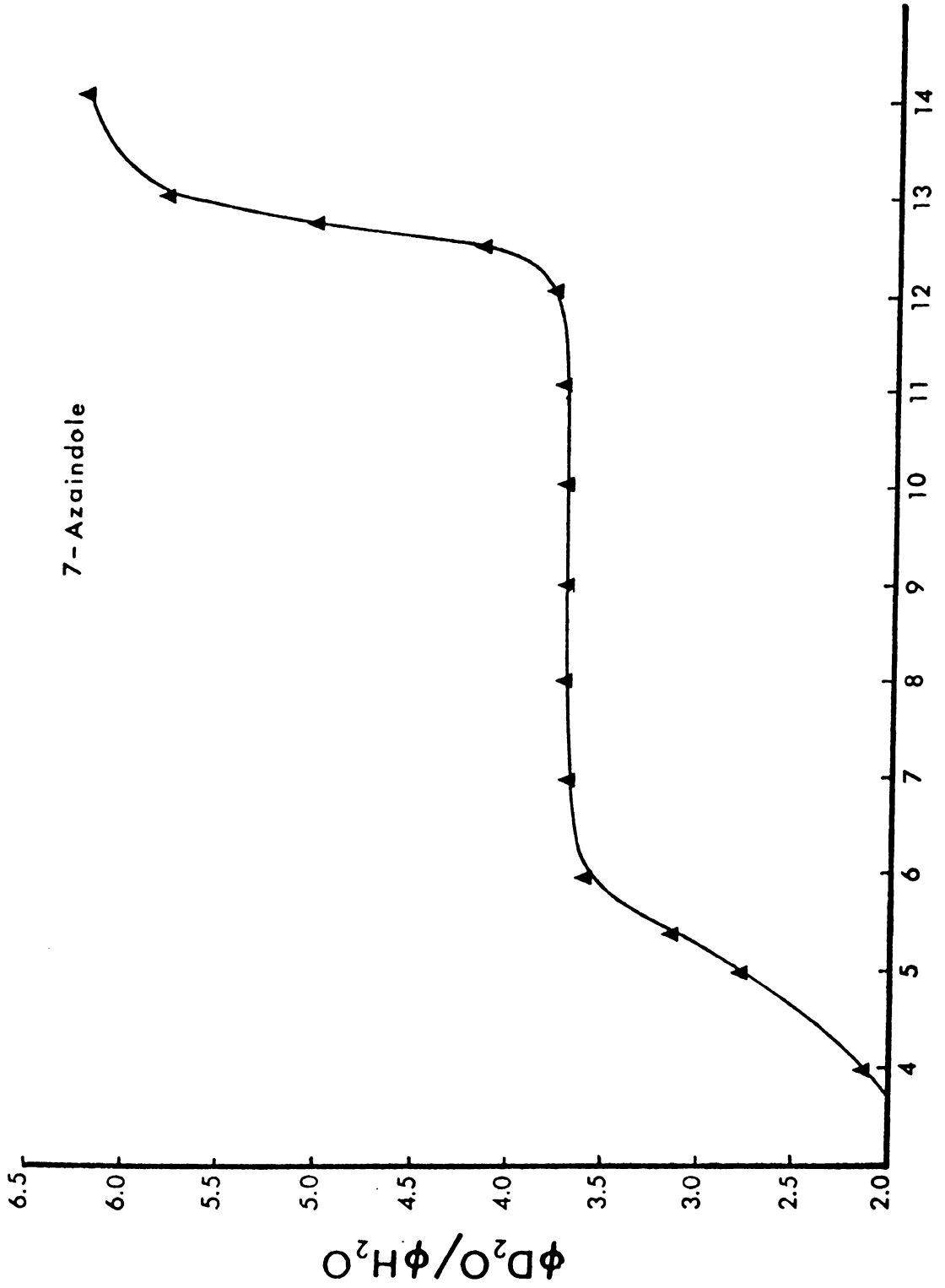

Figure 48. Variation of the Solvent Deuterium Isotope Effect Measured by the Ratio of the Room Temperature (25°C) Fluorescence Quantum Yields of 7AI in H_2O and D_2O as a Function of pH(pD).

the well known Stern-Volmer equation

$$I_0/I = 1 + k_Q [Q]$$

where I_0 is the fluorescence intensity at neutral pH, k_Q is the quenching rate constant ($\ell mole^{-1}\ s^{-1}$), τ is the lifetime at neutral pH and Q (quencher), in this case is the OH^-.

Figure 49 shows a plot of $\log(I_0/I)$ vs $-\log a_{OH^-}$. The plot has two linear sections intersecting at approximately the titrimetric pK_b^*. The sudden change in slope may mean a change in quenching mechanism. If in the high pH range the quenching is due to acid dissociation then this result may be considered as supporting the idea that at "neutral" pH the quenching involves a more complicated mechanism involving both the $\diagdown$N-H and $\diagup\!\!\diagup$N: sites.

Bowen[325] was the first to show the existence of activated quenching. That is:

$$k_{nr} = A\exp(-E_A/RT) \qquad (131)$$

The quantum yield of fluorescence is given by

$$\Phi_F = k_F/(k_F + k_{nr}) \qquad \text{or} \qquad \Phi_F^{-1} = 1 + k_F^{-1}k_{nr}$$

or using equation 131 for k_{nr}

$$(\Phi_F^{-1} - 1) = k_F^{-1}A\exp(-E_A/RT) \qquad (132)$$

Equation 132 provides a means for determining the acrivation energy E_A by plotting $(\Phi_F^{-1} - 1)$ vs $1/T$.

We have studied the temperature dependence of 7AI's fluorescence in H_2O and D_2O solutions (neutral pH). Absolute fluorescence quantum yields at different temperatures were calculated by comparing the fluorescence intensity at a particular temperature with that at room temperature(Φ_F = 0.031).

The results are displayed in Figure 51. The activation energy for both H_2O and D_2O is about the same 6 kcal/mole while the preexponential factors

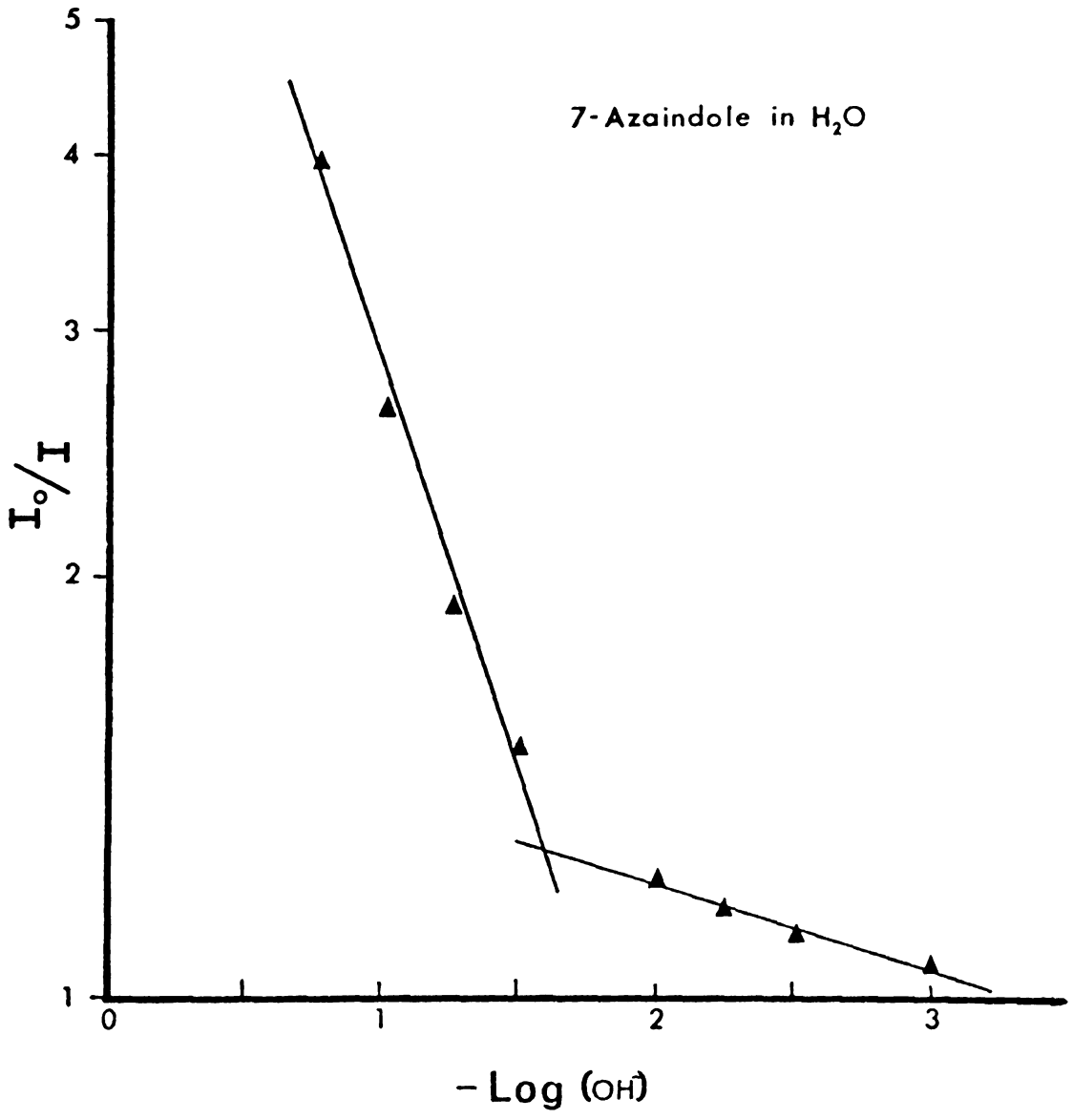

Figure 49. Quenching of 7AI's Fluorescence in Water by Hydroxyl Ions. I_0/I vs $-\log(OH^-)$ Where I_0 is the Intensity at Neutral pH.

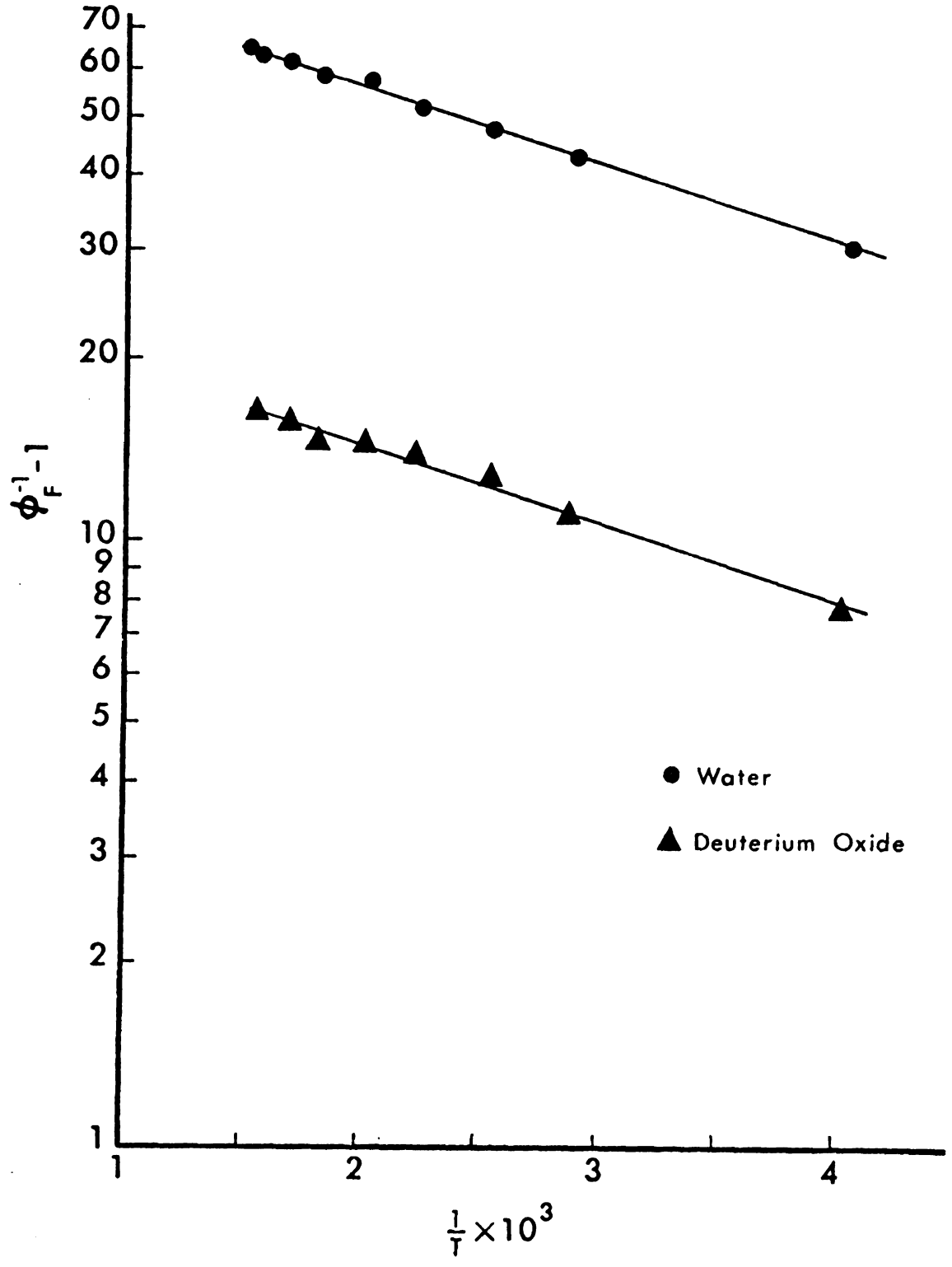

Figure 50. Determination of the Activation Energies for the "Activated Quenching" of 7AI's Fluorescence in Water. Circles: Water, Triangles: Deuterium Oxide.

A_{H_2O} and A_{D_2O} are different. Eisinger and Navon[300] performed exactly the same analysis for tryptophan and found that again the activation energies (7 kcal/mole) were the same in both H_2O and D_2O and that the isotope effects can be traced to the frequency factors of the acrivated quenching. In this way a better expression for the isotope effect is:

$$(\Phi_F^{-1} - 1)_{H_2O}/(\Phi_F^{-1} - 1)_{D_2O} = A_{H_2O}/A_{D_2O} = 3.92$$

provided of course that the radiative lifetime does not change from H_2O to D_2O which has been shown to be valid for indole. The fact that the activation energies appear the same in H_2O and D_2O should not be taken as absolute because minor, but significant, changes may be masked by experimental error. Since k_F is of the order 10^7 s^{-1} then the preexponential factors are of the order 10^{12}. If the activated quenching is due to an activated intersystem crossing[326], one may expect a spin prohibition factor of about 10^{-4}-10^{-6} which would result in producing a preexponential factor of 10^7-10^9 (A for unimolecular processes, is usually 10^{13}). The observed preexponential factors seem to disfavor an intersystem crossing process while solvent induced internal conversion process as suggested by Eisinger and Navon can not be excluded.

Kirby and Steiner[321] and Busel et al.[319] have also studied the activated quenching of indole and indole derivatives in water. In their treatment they included a temperature independent deactivation mechanism so that equation 132 was generalized to

$$(\Phi_F^{-1} - 1) = k_F^{-1}A\exp(-E_A/RT) + k_F^{-1}k_{nr}'$$

where k_{nr}' does not depent on temperature.

Their analysis showed that the activation energies and the temperature independent quenching k_{nr}' were the same in H_2O and D_2O. The temperature independent process has been attributed to an $S_1 \longrightarrow T_1$ process while the temperature dependent process was Busel et al. to excited state acid-base

reactions while Kirby and Steiner do not give a specific assignment for the process although they disfavor the electron ejection idea.

As we have seen the problem is very complex and probably it is not just one quenching mechanism as it is usually assumed but more than one operating simultaneously. In the case of 7AI in water solutions of different pH we can visualize the following kind of complexes

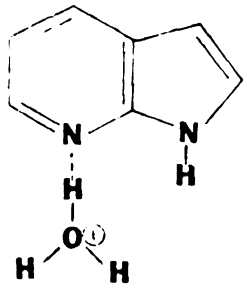

I

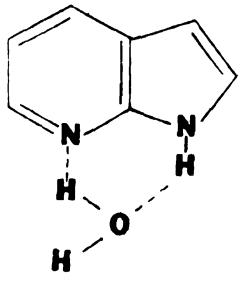

II

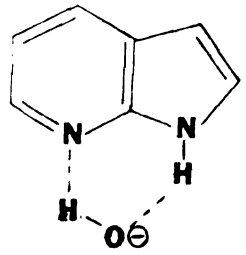

III

Complexes II and III predominating at medium and high pH respectively can revert upon light absorption to either the anion or a tautomeric species IV. Internal conversion from the anion and the tautomer may be efficient in water solutions. The isotope effect may be due to both kinetic isotope effects on the deprotonation of N-H and protonation of $\rangle N:$ (probably more important for structure III) and to suppression of the internal conversion process in the deuterated solvent (effect of O-D vibrations).

At low pH, structure I would quench in a different way than the ones considered above. While studying the quenching of 7AI fluorescence by acids we assumed that the quenching was due to protonation of N_7. Although this might be true, we have noticed that the quenching is not followed by the appearance of the cationic fluorescence except at very low pH. A very similar case has been observed by Forster[327], in his study of 2-naphthylamine in water-sulfuric acid mixtures. He postulated a third species (besides the $-NH_2$ and $-NH_3^+$) where the proton is shared between the amine and the solvent. Weller have suggested that a ring-protonated molecule (carbon

protonation) can play the role of the third species. In our case protonation in position 3 is possible. Schulman and Liedke[328] have formulated this third species as a stoichiometric complex (exciplex) between the amino group and the hydronium ion 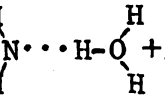 . Their explanation for the quenching resulting from such a complex formation is that secondary hydrogen bonding between the hydronium ion and the aqueous solvent could provide an efficient quenching mechanism, the electronic excitation energy being taken up by the vibrations of the solvent structure. It appears quite likely that quenching by such a complex is important in 7AI at moderately low pH.

We have studied some other aza-aromatics (see structures below) in H_2O and D_2O solutions. None of them showed any significant isotope effect supporting the idea of the cooperativity of the two sites in 7-azaindole.

CHAPTER 5

EXPERIMENTAL

(I) Experimentally Studied Molecules

1. 1,3-Bis-(α-naphthyl)propane (1,3DNP). 1,3DNP was provided by Prof. M. Szwarc. It was synthesized according to the procedure described by Chandross and Dempster[56]. The product was analysed with Mass Spectra, NMR, Stoichiometric analysis. Finally we compared the absorption and emission spectra of the received sample with those reported by Chandross and Dempster and found no difference.

2. 1,3-Diphenylpropane (1,3DPP). 1,3DPP was synthesized by Prof. D. Farnum through reduction of 1,3-diphenylpropanone-2. The product was extensively purified by fractional vacuum distillation and was tested by gas chromatography and comparison with the reported emission spectra of 1,3DPP by F. Hirayama[49].

3. 4-(3-Phyenlpropyl)-pyridine (97%) (1,3PyPP), and 4-Benzylpyridine (99+%) ($PyCH_2P$). 1,3PyPP and $PyCH_2P$ were obtained from Aldrich Chemical Company and were further purified by repeated fractional vacuum distillations. The lower absorption band in 3MP was essentially that of γ-picoline.

4. Phenylacetic, Phenylpropionic and Indan-1-Carboxylic Acids were obtained from Aldrich Chemical Company. They were further purified by repeated recrystallizations and vacuum sublimation.

5. Indan was also obtained from Aldrich and was distilled under reduced pressure.

6. Indan-2-Carboxylic Acid was synthesized according to the procedure of

Perkin and Revay[329]. The compound was identified by absorption spectroscopy, NMR and mass spectroscopy. The purification involvent several recrystalizations and sublimations.

7. Indole was purchased from Calbiochem and was recrystallized once from an alcohol-water mixture then vacuum sublimed slowly for one day.

8. 1-Methylindole was purchased from Eastman Organic Chemicals and was purified by fractional distillation under reduced pressure.

9. 7-Azaindole was purchased from Aldrich and was recrystallized from cyclohexane three times.

10. N_1-d-7-Azaindole was prepared by refluxing 7-azaindole in alkaline D_2O for one hour. Mass spectral analysis gave an isotopic purity of 91%.

11. N_1-Methyl-7-Azaindole and 7-Methyl-7H-pyrrolo(2,3-b)pyridine (N_7-Methyl-Tautomer were prepared according to the method of Robison and Robison[330]. NM7AI was purified by vacuum distillation and NMT was purified by paper chromatography.

(II) Solvents

Water. Only doubly-distilled water was used.

Ethanol. 200 proof ethanol was distilled through a 1 meter vacuum jacket column. The distillation rate was adjusted such that a very slow rate (about 5 drops per minute) was maintained. Distillation continued until the benzene-alcohol azeotrope was no longer present as determined by an absorption spectrum of the distilled alcohol in a 10 cm cell. That is, the characteristic benzene UV absorption was no longer apparent. Ethanol was then distilled and used as needed.

3-Methylpentane (3MP). A modified version of the purification method of Potts[331] was used. Phillips Pure Grade 3-methylpentane (3MP) was shaken

for 30 minutes with a 50:50 mixture of concentrated sulfuric acid and concentrated nitric acid. It was then shaken 3 times for 30 minutes each with concentrated sulfuric acid. This was followed with several shakings using sodium carbonate solutions until the CO_2 production ceased. The 3MP was then shaken several times with water until the water remained clear compared to the initial yellow color it attained with the first shaking. After storing the 3MP overnight over anhydrous calcium sulfate it was placed in a flask and sodium ribbon was added. It was refluxed through a vacuum jacketed 1m column and distilled for use as needed. Passing the distillated through a 1m column of activated Silica Gel did not alter its absorption characteristics so this step was not required in the purification process.

Methyl Cyclohexane, 2-Methyl-Butane (Isopentane), Dichloromethane, Glycerol, and p-Dioxane were spectroquality solvents by Matheson Coleman and Bell (MC/B).

Methyl Sulfoxide. Spectrophotometric Grade by Aldrich Chemical Company.

Deuterium Oxide. 99.81 atom %, 0.2 uc Tritium/ml. International Chemical and Nuclear Coorporation (ICN).

Ethyl Alcohol-d. 99% Aldrich Chemical Company.

(III) Spectral Measurements

Absorption Spectra. All reported absorption spectra were obtained with a Cary 15 spectrophotometer.

Emission Spectra. Most of the fluorescence spectra were obtained with an Aminco-Keirs spectrophosphorimeter equipped with a high pressure xenon arc lamp and a EMI 9781 R photomultiplier tube. All the phosphorescence spectra were obtained with the above instrument equipped with a rotating can phosphoroscope. 0.5 mm slits were used.

The emission spectra of 1,3DPP were obtained with a component system for higher resolution. Excitation wavelengths were selected by a B & L 10 cm grating blazed at 3000 Å in a B & L 500 mm monochromator. The excitation illumination was focused on the sample whose emission was detected at a right angle relative to excitation. The emission monochromator was a Spex 1700-II which utilized a 10 cm B & L grating blazed at 5000 Å. The emission spectrum was detected with a EMI 9558 QA photomultiplier tube. The tube's high voltage was maintained by a Fluke 412B power supply which was normally operated at 1100 V. Signals from the detected emission were fed to a PAR HR-8 Lock-in Amplifier whose reference was provided by a light chopper. Finally the amplified emission signal was displayed on a strip-chart recorder.

Some of the solution samples were degassed prior to their use in luminescence studies. This procedure consisted of attaching the sample tube with closed stopcock to the vacuum line, freezing the tube with liquid nitrogen, opening the stopcock to evacuate the tube above the frozen sample to a pressure of 10^{-6} Torr, closing the stopcock, allowing the sample to thaw, refreezing, evacuating the tube and continuing this freeze-thaw cycling until the vacuum line ionization gauge did not quiver when the stopcock was opened after a freeze.

Quantum Yields. Luminescence quantum yields for the phenyl carboxylic acids and indan derivatives were determined by comparison with toluene's fluorescence. The fluorescence quantum yield of toluene at 300°K in cyclohexane is 0.14 using diphenylanthracene with a quantum yield of 0.84 as a standard[176]. If two solutions absorbing the same number of photons in the same solvent emit N_1 and N_2 photons, respectively, the ratio of their luminescence quantum yields is equal to the ratio of the number of photons emitted, which are proportional to the areas under the fluorescence

bands, plotted on an energy scale:

$$\Phi_2/\Phi_1 = N_2/N_1$$

To obtain the same number of exciting photons absorbed by the two solutions, we adjust the concentrations so that they have the same optical density at the exciting wavelength. The wavelength of the excitation light was taken at 260 nm, in the $^1A_{1g} \longrightarrow {}^1B_{2u}$ absorption band. No corrections for the Aminco-Keirs response are necessary, since the emission spectra are in the same wavelength range.

If quantum yields are to be compared in different solvents, correction must be made for refraction in the solvents. In a solvent with a refractive index n, there will be a broadening of the angle of aperture of the excited light beam by n^2. Hence if n_1 and n_2 are the indices of refraction of the solvents corresponding to the two measurements, the ratio of the quantum yields will be

$$\Phi_2/\Phi_1 = N_2/N_1(n_2/n_1)^2$$

Quantum yields measurements at 77°K were performed by comparing the areas of the emission curves A_F(77°K)/A_F(room temperature) and correcting for the contraction and the change of the refractive index of the solvent as the result of cooling. The refractive indices at 77°K were deduced from those at room temperature by consideration of the specific refractivity (n-1)/d which is temperature invariant (where d is the density).

Quantum yields for indole derivatives in various solvents at room temperature were obtained by utilizing a double beam quantum yield instrument interfaced with a PDP 11 computer[332].

This instrument measures both emission and absorption and corrects for both monochromator and phototube response. It is programmed to correct for inner-filter effects for solutions with optical densities up to 1.

The quantum yield standard used was 10^{-6}M quinine sulfate in 1N H_2SO_4 for which the quantum yield is accepted as 0.54.

Temperature Variation Studies. A quartz dewar with a flat quartz excitation window and a 1 cm square suprasil cuvette were used. The temperature of the sample was controlled by boiling liquid nitrogen using a power resistor and allowing the N_2 gas to flow into the sample dewar. The temperature of the sample was monitored through a thermocouple (copper, constantan) attached to the outside of the cuvette immediately above the point of excitation. Comparing readings of thermocouple on the outside and inside of a cuvette containing solvent, one finds not more than 1° difference between thermocouples over wide ranges of temperature.

Fluorescence Decay and Time-Resolved Spectral Studies

Single Photon Time Correlation Spectrometer

The essential parts of the apparatus are a nanosecond flash lamp, special photomultiplier where individual photons are detected. A time-to amplitude converter (TAC) where the fluorescence photons are timed relative to the flash lamp, and a multichannel analyser (MCA) where the data are stored.

A block diagram of the instrument is shown in Figure 51. The nanosecond lamp is essentially a relaxation oscillator where the voltage across two electrodes is increasing through charging a capacitor till the breakdown voltage of the gas filling the lamp (H_2 was used) is reached where upon the lamp discharges and the cycle is repeated. Such a free-running lamp was used for the 1,3DNP experiment (ORTEC 9352). The width at half maximum (whm) was $\sim$ 4 ns. In the proton transfer study a gated lamp was used (Photochemical Assodiates, University of Western Ontario) which employs a Thyratron which acts as an ultrafast switch and allows the lamp to discharge

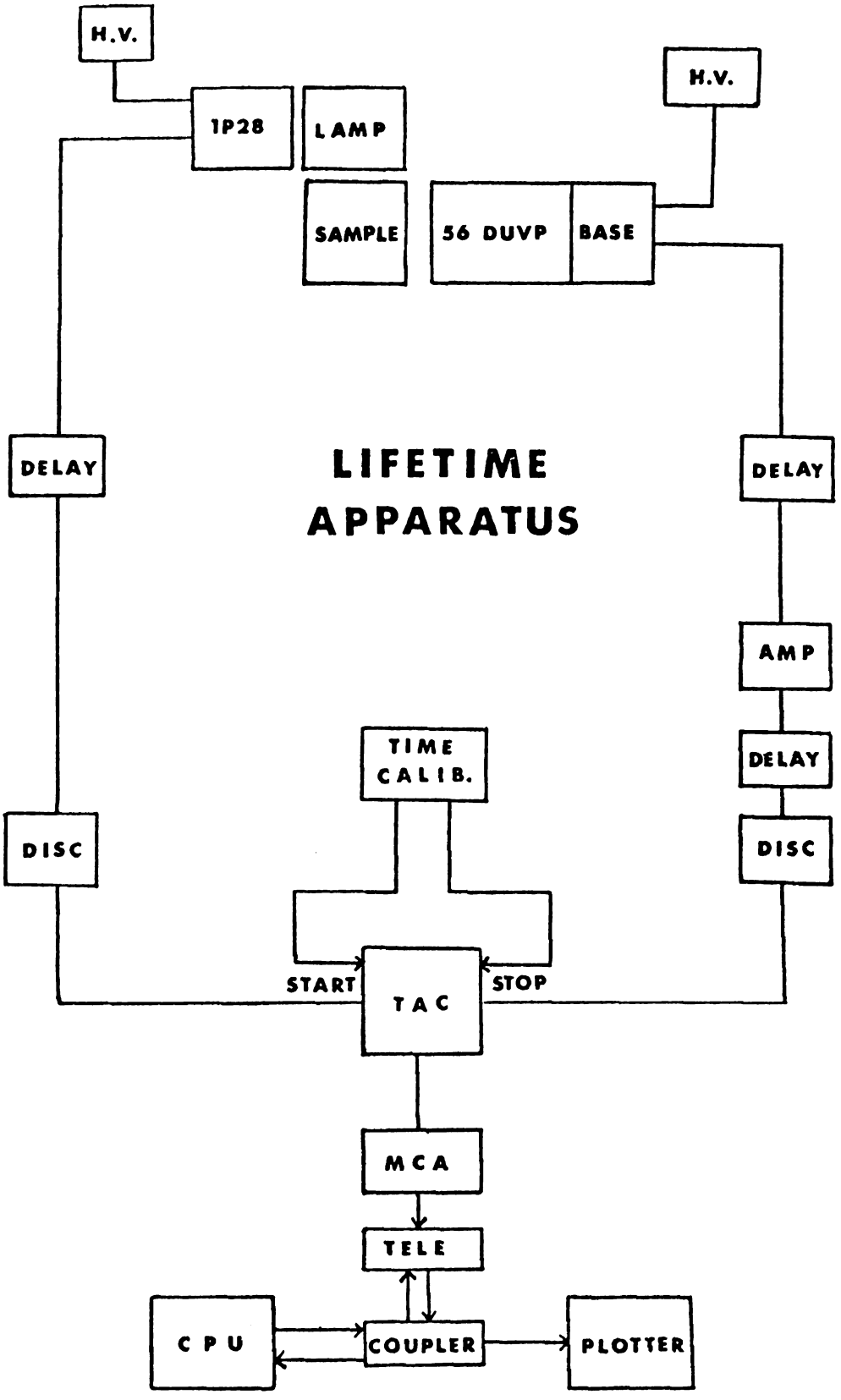

Figure 51. Block Diagram for Time Resolved Spectrophotometer.

when the thyratron grid is triggered with a pulse. A typical pulsing rate is 50 KHz. The whm was $\sim$ 2 ns and the lamp intensity is $\sim 10^7$-10^8 photons/flash. The lamp flash is detected with the IP28 phototube and the resulting analog pulse, after discrimination against low-level noise (ORTEC Model 436) is used to start the TAC. The IP28 anode pulse times the occurrence of the lamp flash in less than 100 picoseconds.

Fluorescence photons are detected by a fast photomultiplier 56DUVP. (Time resolution 800 picoseconds). This tube is capable of amplifying a single photon into an electrical pulse of several volts. This pulse is used to stop the TAC.

The time resolution of the apparatus depends upon the uncertainty of timing the detection of single-photon pulses relative to the flash-lamp pulse. The principal time jitter arises from the fact that the amplitude of single-photon pulses is not constant but covers a broad range in pulse heights. The jitter associated with timing by single-level crossing was eliminated by using a "constant fraction timing" discriminator (ORTEC Model 463). In this type of instrument the input pulse is split into two channels; one channel is inverted and delayed and the other channel is simply attenuated. The channels are added such that the resultant bipolar pulse has the desired fractional trigger threshold associated with its zero crossing point. This effectively eliminates the time jitter.

The heart of the instrument is the TAC (ORTEC Model 457), the operation of which is illustrated in Figure 52. Each time the lamp flashes, a synchronization pulse is sent to the TAC and initiates its time sweep (start). If a stop pulse is received from the photomultiplier during the time sweep, a TAC output pulse is generated with amplitude proportional to

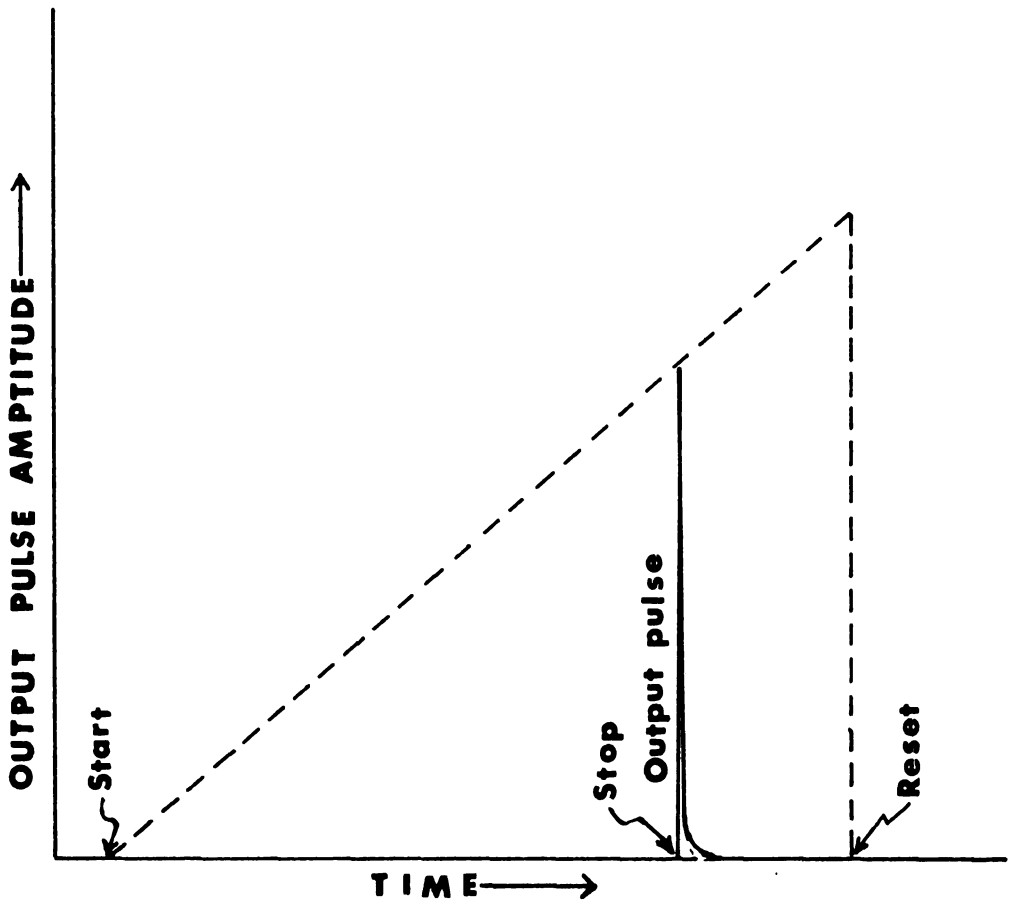

Figure 52. The Basic Idea of Time-To-Amplitude Conversion. The Output Pulse Amplitude is Proportional to $t_{stop} - t_{start}$.

the time (t_{stop}-t_{start}).

The calibration of the TAC is performed with the ORTEC 462 Time Calibrator. The time base is a precision 100-MHz crystal-controlled oscillator that is calibrated against WWV, the National Bureau of Standards frequency, and is temperature-compensated for accuracy throughout the normal operating range of 0 to 50°C.

The TAC output is fed to the MCA. The MCA (NUCLEAR DATA Model 1100) takes this voltage V and converts it to an appropriate channel number C. The final result is a count stored in channel number C which is a record of the time at which the photon was observed by the photomultiplier. The analyzer channels now represent increments in time, and the counts in each channel are proportional to the probability for fluorescence emission from the sample between t and $t + \Delta t$, where t is measured from an arbitrary but fixed point each flash. Note that each pulse of the lamp can produce only one count since the TAC only seeks one photon after it is started. By collecting many of these single photon events we eventually build in the analyzer the decay curve of the emitting species.

The contents of the memory of MCA can be displayed on an oscilloscope (HEWLETT-PACKARD Model 130 BR) on an XY plotter or can be fed to a teletype equipped with a tape punch. Through use of an accustic coupler, the teletype is connected with the CDC 6500 computer where the data are processed. The processed data are plotted through a digital plotter (HEWLETT-PACKARD 7200 A).

The lamp pulsing rate and the photon counting rates are monitored through two digital counters (MONSANTO Model 150A).

For this method to produce true decay curves, the rate of detecting photons must be less than 10% of the lamp-repetition rate. Faster collection

of fluorescence photons results in what is called "pulse pile-up", biasing of the decay curve in favor of early events. Typically the lamp repetition rate was 50 KHz and the count rate 100 counts/sec. The count collection was continued until typically 10^4-10^5 counts were collected in the channel corresponding to the maximum in the curve. The standard deviation of each point is given by Poisson statistics; i.e., $\sigma = (N)^{\frac{1}{2}}$ where N is the number of counts in the channel in question.

It can be shown by Laplace transform techniques that the instrument output is given by the convolution integral

$$I_F^{obsd}(t) = \int_0^t G(t')F(t-t')dt'$$

or for digital data with time divided into channels

$$I_F^{obsd}(t_i) = \int_0^{t_i} G(t')F(t_i-t')dt'$$

where G(t) is the time response of the fluorescence system when excited with the delta pulse of light, and F(t) is the time dependence of the lamp distorted by the detection system. To obtain the desired function G(t), one must solve this integral equation a process called deconvolution. The various deconvolution techniques have been reviewed by Ware[333].

We have used the deconvolution procedure suggested by Ware et al.[62]. According to this procedure G(t) is expressed as

$$G(t) = \sum_{k=1}^{n} a_k \exp(-t/\gamma_k)$$

where γ_k have fixed values selected to span certain range. Least-squares techniques are used to obtain the best weighting factors for each exponential in order to minimize the sum of the squares of the deviations between the observed decay curve and that calculated from the lamp curve and this empirical function:

$$I_F^{calcd}(t_i) = \int_0^{t_i} \sum_k a_k \exp(-t_i/\gamma_k)F(t_i-t')dt'$$

The residual ρ_i for the i^{th} data point (i^{th} channel) is given by

$$\rho_i = I_F^{obsd}(t_i) - I_F^{calcd}(t_i)$$

The deconvolution problem then reduces to obtaining the coefficients a_k such that

$$\sum_i \rho_i \partial\rho_i/\partial a_j = 0 \qquad j = 1,2,\ldots,n$$

Time Resolved Spectra. Time resolved spectra were obtained by measuring the emission spectrum through a time window. In practice, the instrument is first operated in the single-photon lifetime mode, and the upper and lower discriminator levels of the multichannel pulse-height analyser are adjusted in order to obtain the desired time window, that is only pulses between E and E + ΔE are allowed to pass and so events occurring only between t and t + Δt after excitation are recorded. This can be seen visually on the oscilloscope during the collection of the decay curve, since the upper and lower level discriminators will block out the leading and trailing edges of the decay curve and can be used to create a window with any time size. The instrument is then switched to multichannel scalling and a spectrum is obtained through the time window created by the analyser discriminators.

BIBLIOGRAPHY

BIBLIOGRAPHY

1. T. H. Lyman, Astrophs. J., 60, I (1924).

2. L. A. Sommer, Proc. Natl. Acad. Sci. (U. S.), 13, 213 (1927).

3. Lord Rayleigh, Proc. Roy. Soc., A125, 1 (1929).

4. S. Mrozowski, Z. Physik, 106, 458 (1937).

5. Th. Forster, and K. Kasper, Z. Physik. Chem. (Frankfurt), 1, 275 (1954).

6. J. B. Birks, Acta Phys. Polon., 26, 367 (1964).

7. H. Leonhardt and A. Weller, Ber. Bunsenges. Phys. Chem., 67, 791 (1963).

8. O. Cheshnovsky, A. Gedanken, B. Raz, and J. Jortner, Chem. Phys. Lett., 22, 23 (1973).

9. B. Stevens, Spectrochim. Acta, 18, 439 (1962).

10. J. Tanaka, Bull. Chem. Soc. Japan, 36, 1237 (1963).

11. P. F. Jones and M. Nicol, J. Chem. Phys., 48, 5440 (1968).

12. M. T. Vala, J. Haebig, and S. A. Rice, J. Chem. Phys., 43, 886 (1965).

13. Th. Forster, Angew. Chem. Intern. Ed., 8, 333 (1969).

14. J. B. Birks, Progress in Reaction Kinetics, 5, 181 (1970).

15. B. Stevens, Advances in Photochemistry, 8, 161 (1971).

16. A. Dalgarno and J. T. Lewis, Proc. Phys. Soc., (London) A69, 57 (1956).

17. F. London, Trans. Faraday Soc., 33, 8 (1937).

18. B. Pullman, P. Claverie, and J. Caillet, Proc. Natl. Acad. Sci. (U.S.), 55, 904 (1966).

19. R. J. W. LeFevre and K. M. S. Sundaram, J. Chem. Soc., 4442 (1963).

20. J. Frenkel, Phys. Rev., 37, 17 (1931); ibid, 37, 1276 (1931).

21. A. S. Davydov, J. Exptl. Theor. Phys. (U. S. S. R.), 18, 210 (1948).

22. A. S, Davydov, Theory of Molecular Excitons, Translation by M. Kasha and K. Oppenheimer, McGraw-Hill, N. Y., 1962.

23. M. R. Philpott, Adv. in Chem. Phys., I. Prigogine and S. A. Rice editors, John Wiley, 1973, p. 227.

24. H. Margenau and N. R. Kestner, Theory of Intermolecular Forces, Second Edition, Pergamon Press 1969, p. 318.

25. A. W. Overhauser, Phys. Rev., 101, 1702 (1956).

26. P. Avakian and R. E. Merrifield, Mol. Crystals, 5, 37 (1968). R. E. Merrifield, Acc. of Chem. Research, 1, 129 (1968).

27. R. S. Mulliken, J. Amer. Chem. Soc., 74, 811 (1952).

28. S. P. McGlynn, Chem. Rev., 58, 1113 (1958).

29. G. Briegleb, Elektronen-Donator-Acceptor Komplexe Springer-Verlag, Berlin-Gottingen-Heidelberg, 1961.

30. J. N. Murrel, Quart. Rev., 15, 191 (1961).

31. R. S. Mulliken and W. B, Person, Ann. Rev. Phys. Chem., 13, 107 (1962).

32. R. S. Becker and E. Chen, J. Chem. Phys., 45, 2403 (1966).

33. R. S. Mulliken and W, B, Person, Molecular Complexes: A Lecture and Reprint Volume. Wiley N. Y., 1969.

34. Th. Forster, Pure Appl. Chem., 4, 121 (1962).

35. M. A, Slifkin, Nature,200, 766 (1963).

36. R. M. Hedges and F. A. Matsen, J. Chem. Phys., 28, 950 (1958).

37. J. R. Hoyland and L. Goodman, J. Chem. Phys., 36, 12, (1962). ibid, 36, 21 (1962).

38. T. Azumi and S. P. McGlynn, J. Chem. Phys., 41, 3131 (1964).

39. E. Doller and Th. Forster, Z. Physik. Chem. N. F., 31, 274 (1962).

40. E. Konijnenber, Thesis, University of Amsterdam, 1963.

41. J. N. Murrel and J. Tanaka, Mol. Phys., 7, 363 (1964).

42. T. Azumi, A. T. Armstrong, and S. P. McGlynn, J. Chem. Phys., 41, 3839 (1964).

43. R. J. Buenker and S. D. Peyerimhoff, Chem. Phys. Lett., 3, 37 (1969).

44. W. von Niessen, J. Chem. Phys., 55, 1948 (1971).

W. von Niessen, Theor. Chim. Acta (Berlin), 31, 111 (1973). ibid., 32, 13 (1973).

45. T. Azumi and H. Azumi, Bull. Chem. Soc. Japan, 40, 279 (1967).

46. A. K. Chandra and E. C. Lim, J. Chem. Phys., 48, 2589 (1968).

47. F. Hirayama, "Energy Transfer and Quenching in Plastic Scintillators", Thesis, University of Michigan.

48. S. S. Yanari, F. A. Bovey, and R. Lumry, Nature, 200, 242 (1963).

49. F. Hirayama, J. Chem. Phys., 42, 3163 (1965).

50. D. H. Phillips and J. C. Schug, J. Chem. Phys., 50, 3297 (1969).

51. J. Eisinger, M. Gueron, R. G. Shulman and T. Yamane, Proc. Not. Acad. Sci., 55, 1015 (1966).

52. N. J. Leonard, J. Iwamura, and J. Eisinger, Proc. Nat. Acad, Sci., 64, 352 (1969).

53. B. Stevens, Advances in Photochemistry, Vol. 8, 1971, pp. 216-217.

54. J. Ferguson, J. Chem. Phys., 28, 765 (1958).

55. J. B. Birks, Nature, 214, 1187 (1967).

56. E. A. Chandross, and C. J. Dempster, J. Am. Chem. Soc., 92, 3586 (1970).

57. H. J. Pownall and L. C. Smith, J. Am. Chem. Soc., 95, 3136 (1973).

58. H. J. Galla and E. Sackmann, Biochim. Biophys. Acta, 339, 103 (1974).

59. J. B. Birks, T. A. King and I. H. Munro, Proc. Phys. Soc., 80, 355 (1962).

60. I. Isenberg and R. D. Dyson, Biophys. J., 9, 1337 (1969).

61. R. Schuyler and I. Isenberg, Rev. Sci. Instrum., 42, 813 (1971).

62. W. Ware, L. J. Doemeny and T. L. Nemzek, J. Phys. Chem., 77, 2083 (1973).

63. J. B. Birks, Photophysics of Aromatic Molecules, Wiley-Interscience, 1970, p. 70.

64. P. Claverie, in "Molecular Associations in Biology" Pullman editor, Academic Press, 1968.

65. A. I. R. Rae and R. Mason, Proc. Roy. Soc., A304, 487 (1968).

66. M. T. Vala, J. H. Hillier, S. A, Rice and J. Jortner, J. Chem. Phys., 44, 23 (1966).

67. A. I. Kitaygorodsky, Tetrahedron 14, 230 (1961).

68. G. Favini and M. Simonetta, Theor. Chim. Acta, 1, 294 (1963).

69. M. J. Mantione, Theor. Chim. Acta, 15, 141 (1969).

70. O. K. Rice and H. C. Ramsperger, J. Amer. Chem. Soc., 49, 1617 (1927).

71. L. S. Kassel, J. Phys. Chem., 32, 225 (1928).
ibid, 32, 1065 (1928).

72. S. W. Benson, in "Foundations of Chemical Kinetics" McGraw-Hill 1960, pp. 245-246.

73. F. W. Schuler and G. W. Murphy, J. Amer. Chem. Soc., 72, 3155 (1950).

74. J. B. Aladekomo and J. B. Birks, Proc. Roy. Soc., A284, 551 (1965).

75. B. K. Selinger, Austral. J. Chem., 19, 825 (1969).

76. J. B. Birks, M. D. Lumb and I. H. Munro, Proc. Roy. Soc., A280, 289 (1964).

77. R. B. Cundall and D. A. Robinson, Chem. Phys. Lett., 13, 257 (1972).

78. R. L. Barnes and J. B. Birks, Proc. Roy. Soc. A291, 570 (1966).

79. E. Doller and Th. Forster, Z. Phys. Chem. (N.F.) 48, 58 (1965).

80. B. Stevens and M. I. Ban, Trans. Faraday Soc., 60, 1515 (1964).

81. Th. Forster and H. P. Seidel, Z. Phys. Chem. (N. F.), 48, 58 (1965).

82. E. A. Moelwyn-Hughes, J. Chem. Soc., 850 (1940).

83. J. B. Birks, M. D. Lumb and I. H. Munro, Acta Phys. Polon., 26, 379 (1964).

84. C. Lewis and W. R. Ware, Mol. Photochem., 5, 261 (1973).

85. F. Hirayama and S. Lipsky, J. Chem. Phys., 51, 1939 (1969).

86. G. J. Hoijtink, Z. Elektrochem., 64, 156 (1960).

87. J. B. Birks, M. D. Lumb and I. H. Munro, Proc. Roy. Soc., (London), A280, 289 (1964).

88. R. L.Barnes and J. B. Birks, Proc. Roy. Soc. (London), A291, 570 (1966).

89. T. Azumi and H. Azumi, Bull. Chem. Soc. Japan, 39, 1829 (1966)
ibid, 39, 2317 (1966).

90. N. Mataga, M. Tomura, and H. Nishimura, Mol. Phys., 9, 367 (1965).

91. R. B. Cundall, L. C. Pereira and D. A. Robinson, Chem. Phys. Lett., 13, 253 (1972).

92. E. A. Chandross. J. Chem. Phys., 43, 4175 (1965).

93. J. R. Greenleaf, M. D. Lumb and J. B. Birks, J. Phys. B, 1, 1157 (1968).

94. M. Mataga, Y. Torihashi and Y. Ota, Chem. Phys. Lett., 1, 385 (1967).

95. J. B. Birks, D. J. Dyson, and I. H. Munro, Proc. Roy. Soc., A275, 575 (1963).

96. N. Mataga, Chem. Phys. Lett., 1, 385 (1967).

97. W. H. Melhuish and W. S. Metcalf, J. Chem. Soc., 480 (1958).

98. P. Debye, Trans. Electrochem. Soc., 82, 205 (1942).

99. R. M. Noyes, Prog. Reaction Kinetics, 1, 131 (1961).

100. E. Fisher, Z. Elektrochem. 53, 16 (1949).

101. A. Gieser, A. Spernal and K. Wirtz, Z. Naturforsch. 8A, 522 (1953) ibid, 8A, 532 (1953).

102. K. Kawaoka, A. U. Khan and D. R. Kerns, J. Chem. Phys., 46, 1842 (1967).

103. F. W. Robinson and R. P. Frosch, J. Chem. Phys., 37, 1962 (1962).

104. G. J. Hoytink, Accounts Chem. Res., 2, 114 (1969).

105. R. W. Nicholls, P. A. Fraser, W. R. Jarmain and R. P. McEachran, Astrophys. J., 13, 399 (1960).

106. M. D. Lumb and D. A. Weyl, J. Mol. Spectroscy., 23, 365 (1967).

107. J. B. Aladekomo and J. B. Birks, Proc. Roy. Soc.,A284, 551 (1965).

108. J. Langelaar, R. P. H. Rettschnick, A. M. F. Lambooy and F. J. Hoytink, Chem. Phys. Lett., 1, 609 (1968).

109. J. Langelaar, Thesis, University of Amsterdam (1969).

110. R. D. Nelson, D. R. Lide, A. A. Maryott, in "Selected Values of Electric Dipole Moments for Molecules in the Gas Phase", National Bureau of Standards (NSRDS-NBS 10).

111. Handbook of Chemistry and Physics, The Chemical Rubber Company.

112. M. Itoh, T. Mimura, H. Usui, and T. Okamoto, J. Am. Chem. Soc., 95, 4388, (1973).

113. J. Kirkwood, J. Chem. Phys., 2, 351 (1934).

114. R. G. Pearson. J. Chem. Phys., 20, 1478 (1952).

115. J. Timmermans, in "Physico-Chemical Constants of Pure Organic Compounds", Elsevier Publishing Company 1950.

116. M. B. Ledger and P. Suppan, Spectrochim. Acta, 23A, 3007 (1967).

117. J. B. Birks, in "Photophysics of Aromatic Molecules" pp. 439-441.

118. Mohyi-Eldin M. Abu-Zeid, Prodeeding of the 6th International Symposium on Atomic, Molecular and Solid-State Theory and Quantum Biology, Interscience Publishers 1972.

119. J. Beens, H. Knibbe, and A. Weller, J. Chem. Phys., 47, 1183 (1967).

120. D. J. Witt and C. R. Estee, Proc. S. Dakota Acad. Sic., 31, 229 (1952).

121. M. Hanack, in "Conformation Theory", Academic Press 1965.

122. W. B. Person and G. C. Pimentel, J. Am. Chem. Soc., 75, 5321 (1953).

123. K. S. Pitzer, J. Chem. Phys., 8, 711 (1940).

124. O. S. Khalil, R. H. Hofeldt and S. P. McGlynn, J. Luminescence, 6, 229 (1973).

125. G. Castro and R. M. Hochstrasser, J. Chem. Phys., 45, 4352 (1966).

126. E. C. Lim and S. K. Chakrabarti, Mol. Phys., 13, 293 (1962).

127. I. H. Hillier, L. Glass and S. A. Rice, J. Chem. Phys., 45, 3015 (1966).

128. L. G. Christophorou, M. E. M. Abu-Zeid and J. G. Carter, J. Chem. Phys., 49, 3775 (1968).

129. R. B. Cundall and A. J. R. Voss, Chem. Commun., 116 (1969).

130. J. Langelaar, G. Jansen, R. P. H. Rettschnick and G. J. Hoytink, Chem. Phys. Lett., 12, 86 (1971).

131. B. A. Baldwin, J. Chem. Phys., 50, 1039 (1969).

132. W. Siebrand, J. Chem. Phys., 50, 1040 (1969).

133. Chandross, J. Am. Chem. Soc., 92, 704 (1970).

134. R. M. Hochstrasser, Rad. Research, 20, 107 (1963).

135. R. M. Hochstrasser and T. F. Hunter, J. Chem. Phys., 40, 2739 (1964).

136. P. Avakian and R. E. Merrifield, Phys. Rev. Lett., 13, 541 (1964).

137. V. Ern, P. Avakian and R. E. Merrifield, Phys. Rev., 148, 862 (1966).

138. R. E. Merrifield, Acc. of Chem. Res., 1, 129 (1968).

139. M. Kasha, Discuss. Faraday Soc., 9, 14 (1950).

140. H. Sponer and J. H. Rush, J. Chem. Phys., 20, 1847 (1952).

141. L. E. Orgel, J. Chem. Soc., 121 (1955).

142. L. Salem, in "Molecular Orbital Theory of Conjugated Systems" W. A. Benjamin, Inc., N. Y. 1966 p. 462.

143. M. A. El-Sayed, J. Chem. Phys., 36, 552 (1962).

144. M. Kasha, in "Light and Life" W. D. McElroy and B. Glass, eds. The Johns Hopkins Press, Baltimore, 1961 p. 31.

145. H. P. Stephenson, J. Chem. Phys., 22, 1077 (1954).

146. E. Clementi, J. Chem. Phys., 46, 4731 (1967).

147. R. D. Brown and M. L. Heffernan, Austral. J. Chem. 12, 554 (1959).

148. D. S. McClure, Electronic Spectra of Molecules and Ions in Crystals, Solid State Physics, Academic Press, Vol. 8-9 1959.

149. D. J. Cohen and L. Goodman, J. Chem. Phys., 46, 713 (1967).

150. R. B. Cundall, F. J. Fletcher and D. G. Milne, Trans. Faraday Soc., 60, 1146 (1964).

151. D. F. Evans, J. Chem. Soc., 3885 (1957).

152. Th. Forster, Fluoreszenz Organisher Verbindungen, Vandenhoeck and Ruprecht, Gottingen, 1951, p. 105.

153. E. M. Kosower and P. E. Klinedinst Jr., J. Am. Chem. Soc., 78, 3493 (1956).

154. G. Briegleb, J. Trencseni and W. Herre, Chem. Phys. Lett., 3, 146 (1969).

155. R. M. Hochstrasser and J. W. Michaluk, J. Chem. Phys., 55, 668 (1971).

156. R. D. Nelson Jr., D. R. Lide Jr., and A. A. Maryott, Natl. Std. Ref. Data Ser., Natl. Bur. Std. (US) 10, 29 (1967).

157. P. Cremaschi, A. Gamba, and M. Simonetta, Theor. Chim. Acta (Berlin) 31, 155 (1973).

158. S. Mataga and N. Mataga, Z. Physik. Chem. N. F. 19, 231 (1959).

159. J. Del Bene and H. H. Jaffe, J. Chem. Phys., 49, 1221 (1968).

160. V. S. Krishna and L. Goodman, J. Am. Chem. Soc., 83, 2042 (1961).

161. V. Zanker, Z. Physik. Chem. (Frankfurt) 2, 52 (1954).

162. N. Ginsburg, W. W. Robertson, and F. A. Matsen, J. Chem. Phys., 14, 511 (1946).

163. E. M. Kosower, D. Hofmann, and K. Wallenfels, J. Am. Chem. Soc., 84, 2755 (1962).

164. S. Shifrin, Biochim. Biophys. Acta, 96, 173 (1965).

165. J. W. Verhoeven, I. P. Dirkx and Th. J. de Boer, Tetrahedron Lett., 4399 (1966).

166. J. A. Pople, D. L. Beveridge, and P. A. Dobosh, J. Chem. Phys., 47, 2026 (1967).

167. E. Clementi, J. Chem. Phys., 46, 4731 (1967).

168. W. Adam, A. Grimison, R. Hoffmann, and C. Z. de Ortiz, J. Am. Chem. Soc., 90, 1509 (1968).

169. H. Saito and K. Nukada, Tetrahedron Lett., 111 (1965).

170. E. Chandross, J. Chem. Phys., 45, 397 (1966).

171. R. O. Loutfy and R, W. Yip, Can. J. Chem., 51, 1881 (1973).

172. F. Hirayama, J. Chem. Phys., 42, 3163 (1965).

173. J. B. Birks, in "Photophysics of Aromatic Molecules", Wiley Interscience 170, p. 424.

174. F. N. Nezmaiko, I. E. Obyknovennaya and A. S. Cherkasov, Opt. Spectry., 21, 23 (1966).
ibid, 21, 285 (1966).

175. G. Weber and J. R. Lakowicz, Chem. Phys. Lett. 22, 419 (1973).

176. F. H. Watson and M. Ashraf El-Bayoumi, J. Chem. Phys., 55, 5464 (1971).

177. H. M. Rosenberg and E. C. Eimutis, J. Phys. Chem., 70, 3494 (1966).

178. H. Leonhardt and A. Weller, Ber. Bunseges. Physik. Chem. 67, 791 (1963).

179. J. B. Birks, in "Photophysics of Aromatic Molecules" pp. 72 and 460.

180. G. Weber and M. Shinitzky, Proc. Natl. Acad. Sci., U.S. 65, 823 (1970).

181. K. Itoh and T. Azumi, Chem. Phys. Lett., 22, 395 (1973).

182. N. S. Bayliss and E. G. McRae, J. Phys. Chem. 58, 1002 (1954).

183. C. Reid, J. Chem. Phys., 20, 1212 (1952).

184. M. M. Moodie and C. Reid, J. Chem. Phys., 20, 1510 (1952).

185. S. Iwata, J. Tanaka and S. Nagakura, J. Chem. Phys., 47, 2203 (1967).

186. N. Christodouleas and S. P. McGlynn, J. Chem. Phys., 40, 166 (1964).

187. S. P. McGlynn and J. D. Boggus, J. Am. Chem. Soc., 80, 5096 (1958).

188. S. P. McGlynn, J. D. Boggus and E. Elder, J. Chem. Phys., 32, 357 (1966).

189. B. Badger, B. Brocklehurst and R. D. Russel, Chem. Phys. Lett., 1, 122 (1967).

190. B. Badger and B. Brochlehurst, Trans. Faraday Soc., 65, 2576 (1969).

191. B. Badger and B. Brocklehurst, Trans. Faraday Soc., 65, 2582 (1969).

192. O. Edlund, P. O. Kinell, A. Lund and A. Shimizu, J. Chem. Phys., 46, 3679 (1969).

193. F. W. McLafferty, Mass Spectrometry of Organic Ions, Academic Press, New York, 1963.

194. C. R. Goldschmidt, R. Potashnik, and M. Ottolenghi, J. Phys. Chem., 75, 1025 (1971).

195. E. J. Land, J. T. Richards, and J. K. Thomas, J. Phys. Chem. 76, 1025 (1971).

196. N. Orbach, R. Potashnik, and M. Ottolenghi, J. Phys. Chem., 76, 1133 (1972).

197. S. P. McGlynn, T. Azumi, and M. Kinoshita, Molecular Spectroscopy of the Triplet State, Prentice-Hall Englewood Cliffs, N. J., 1969, pp. 284-325.

198. A. White, Biochem. J. 71, 217 (1959).

199. R. W. Cowgill, Arch. Biochem. Biophys., 100, 36 (1963).

200. J. Feitelson, J. Phys. Chem., 68, 391 (1964).

201. F. Bishai, E. Kuntz, and L. Augenstein, Biochim. Biophys. Acta, 140, 381 (1967).

202. J. Tournon and M. A. El-Bayoumi, J. Am.Chem. Soc., 93, 6396 (1971).

203. L. J. Mittal, J. P. Mittal and E. Hayon, J. Am. Chem. Soc., 95, 6203 (1973).

204. J. Tournon and M. A. El-Bayoumi, J. Chem. Phys., 56, 5128 (1972).

205. E. A. Chandross and A. T. Thomas, Chem. Phys. Lett., 9, 393 (1971).

206. J. Tournon, E. Kuntz, and M. A. El-Bayoumi, Photochem. Photobiol. 16, 425 (1972).

207. K. Watanabe, J. Chem. Phys., 26, 542 (1957).

208. C. A. Taylor, M. A. El-Bayoumi, and M. Kasha, Proc. Nat. Acad. Sci. U.S., 63, 253 (1969).

209. G. Briegleb, Z. Physik. Chem., (Leipzig) B51, 9 (1941).

210. J. S. Rowlinson, Trans. Faraday Soc., 47, 120 (1951).

211. J. Lennard-Jones, Proc. Roy. Soc., A14, 198 (1949).

212. J. Lennard-Jones and J. A. Pople, Proc. Roy. Soc., A205, 155 (1951).

213. C. A. Coulson, Trans. Faraday Soc., 38, 433 (1942).

214. C. A. Coulson, Proc. Roy. Soc., A207, 63 (1951).

215. C. A. Coulson, Research (London) 10, 149 (1957).

216. C. A. Coulson and V, Danielsen, Arkiv. Fysik. 8, 205 (1955).

217. N. D. Sokolov, Zh. Eksperim, i Teor. Fiz. 23, 315 (1952).

218. H. Tsubomura, Bull. Chem. Soc., Japan, 27, 445 (1954).

219. S. Bratoz, Symp. Forces Intermoleculaires, Bordeaux, 1965.

220. G. Bessis and S. Bratoz, J. Chim. Phys., 57, 769 (1960).

221. P. A. Kollman and L. C. Allen, J. Am. Chem. Soc., 92, 6101 (1970).

222. P. A. Kollman and L. C. Allen, Chem. Rev., 72, 283 (1972).

223. J. E. Del Bene, J. Chem. Phys., 58, 3139 (1973).

224. E. Clementi, J. Mehl, and W. von Niesen, J. Chem. Phys., 54, 508 (1971).

225. P. O. Lowdin, Rev. Mod. Phys., 35, 724 (1963).

226. C. L. Bell and G. M. Barrow, J. Chem. Phys., 31, 1158 (1959).

227. G. M. Barrow, Spectrochim. Acta 16, 799 (1960).

228. Krueger, Can. J. Chem., 42, 201 (1964).

229. G. E. Bacon, in D. Hadzi (editor), Hydrogen Bonding, Pergamon London, 1959 p. 23.

230. S. W. Peterson and H. A. Leby, Acta Cryst., 10, 70 (1957).

231. A. Piekara, J. Chem. Phys., 36, 2145 (1962).

232. A. R. Ubbelohde and K. J. Gallagher, Acta Cryst., 8, 71 (1955).

233. Y. Imry, I. Pelah and E. Wiener, J. Chem. Phys., 43, 2332 (1965).

234. S. Ganesan, Nature, 185, 757 (1960).

235. A. Grimison, J. Phys. Chem., 67, 962 (1963).

236. C. C. Costain and G. P. Srivastava, J. Chem. Phys., 41, 1620 (1964).

237. R. Blinc and M. Pintar, J. Chem. Phys., 35, 1140 (1961).

238. J. L. Wood, J. Mol. Structure, 13, 141 (1972).

239. R. Blinc, D. Hadzi and A. Novak, Z. Elektrochem., 64, 567 (1960).

240. R. Blinc and D. Hadzi, Spectrochim. Acta, 16, 852 (1960).

241. D. Hadzi, Pure and Appl. Chem. 11, 435 (1965).

242. M. Kasha, Disc. Faraday Soc., 9, 14 (1950).

243. G. C. Pimentel, J. Am. Chem. Soc., 79, 3323 (1957).

244. G. M. Barrow, J. Am. Chem. Soc., 78, 5802 (1956).

245. H. Baba, A. Matsuyama, and H. Kokubum, J. Chem. Phys., 41, 895 (1964).

246. K. Weber, Z. Physik. Chem. (Leipzig) B15, 18 (1931).

247. Th. Forster, Z. Elektrochem., 54, 42 (1950).

248. N. Mataga and Y. Kaifu, Mol. Phys., 7, 137 (1963).

249. A. Weller, Naturwiss., 42, 175 (1955); Z. Elektrochem., 60, 1144 (1956).

250. K. Z. Hirota, Physik. Chem. (Frankfurt) 35, 222 (1962).

251. Y. V. Noboikin, B. A. Zadorozhnyi, and E. N. Povlova, Opt. Spectry. 9, 347 (1960).

252. Y. V. Noboikin, B. A. Zadorozhnyi, and E. B. Povlova, Opt. Spectry. 6, 312 (1959);
ibid, 6, 231 (1959).

253. A. Weller, Z. Elektrochem., 56, 662 (1952).

254. A. Weller, Z. Physik. Chem., 18, 163 (1958).

255. A. Weller, in "Progress in Reaction Kinetics", Vol. 1, Pergamon Press, London, 1961, Chap. 7.

256. G. Jackson and G. Porter, Proc. Roy. Soc., (London), A260, 13 (1961).

257. M. R. Loken, J. W. Hayes, J. R. Gohlke, and L. Brand, Biochem., 11, 4779 (1972).

258. W. R. Ware, P. R. Shukla, P. J. Sullivan, and R. V, Bremphis, J. Chem. Phys., 55, 4048 (1971).

259. F. Hund, Z. Physik, 43, 805 (1927).

260. E. P. Wigner, Z. Phys. Chem. (Leipzig), B19, 203 (1932).

261. D. M. Dennison and G. E. Uhlenbeck, Phys. Rev., 41 313 (1932).

262. E. Grunwald, in "Progress in Physical Organic Chemistry".

263. Cohen, Streitwieser, and Taft, eds. Wiley, N. Y. 1965 Vol 3.

264. H. S. Johnston, Adv. Chem. Phys., 3, 131 (1961).

265. E. F. Caldin, Chem. Rev., 69, 135 (1969).

266. C. Haas and D. F. Horning, J. Chem. Phys., 32, 1763 (1960).

267. D. Hadzi, J. Chem. Phys., 34, 1445 (1961).

268. P. O. Lowdin, Adv. Quantum Chem. 2, 213 (1965).

269. J. Bigeleisen and M. Wolfsberg, Adv. Chem. Phys., 1, 15 (1958).

270. J. Bigeleisen, J. Chem. Phys., 17, 675 (1949).

271. J. Bigeleisen and M. Goeppert-Mayer, J. Chem. Phys., 15, 261 (1947).

272. L. Melander, Arkiv. Kemi, 2, 211 (1950).

273. F. H. Westheimer, Chem. Rev., 61, 265 (1961).

274. P. M. Laughton and R. E. Robertson, Can. J. Chem. 34, 1714 (1956).

275. R. E. Robertson, Can. J. Chem. 35, 613 (1957).

276. R. E. Robertson and P. M. Laughton, Can J. Chem., 35, 1319 (1957).

277. F. D, Rossini, J. W. Knowlton and H. L. Johnston, J. Res. Natl. Bur. Stand., 24, 369 (1940).

278. W. M. Jones, J. Chem. Phys., 48, 207 (1968).

279. C. G. Swain and R. F. W. Bader, Tetrahedron 10, 182 (1960).

280. C. G. Swain, A. D. Ketley and R. F. W. Bader, J. Am. Chem. Soc., 18, 2353 (1959).

281. R. B. Henry, M. Kasha, Ann. Rev. Phys. Chem., 19, 161 (1968).

282. G. W. Robinson and R. P. Frosch, J. Chem. Phys., 37, 1962 (1962); ibid, 38, 1187 (1963).

283. J. Jortner, R. S. Berry and R. M. Hochstrasser, Adv. Photochem., 7, 149 (1969).

284. W. Siebrand and D. F. Williams, J. Chem. Phys., 46, 403 (1967).

285. E. C. Lim and J. D. Laposa, J. Chem. Phys., 41, 3257 (1964).

286. J. D. Laposa, E. C. Lim and R. E. Kellogg, J. Chem. Phys., 42, 3025 (1965).

287. R. Watts and S. J. Strickler, J. Chem.Phys., 49, 3867 (1968).

288. T. Gierke, R. J. Watts and S. J. Strickler, J. Chem. Phys., 50, 5425 (1969).

289. B. R. Henry and J. L. Charlton, J. Am. Chem. Soc., 95, 2782 (1973).

290. N. Hirota and C. A. Hutchison, J. Chem. Phys., 46, 1561 (1966).

291. J. L. Kropp and M. W. Winsdor, J. Chem. Phys., 42, 1599 (1965).

292. R. Borkowski, H. Forest and D. Grafstein, J. Chem. Phys., 42, 2974 (1965).

293. J. Kropp and W. Dawson, J. Chem. Phys., 45, 2419 (1966).

294. V. L. Ermolaev and E. B. Sveshnikova, Chem. Phys. Lett., 23, 349 (1973).

295. Th. Forster, Ann. Physik, 2, 55 (1948).

296. D. L. Dexter, J. Chem. Phys., 21, 836 (1953).

297. V. L. Ermolaev and E. B. Sveshnikova, Opt. i Spektroskopiya 30, 379 (1971).

298. L. Stryer, J. Am. Chem. Soc., 88, 5708 (1966).

299. Th. Forster and K. Rokos, Chem. Phys. Lett. 1, 279 (1967).

300. J. Eisinger and G. Navon, J. Chem. Phys. 50, 2069 (1969).

301. J. R. Platt, J. Chem. Phys., 19, 101 (1951).

302. H. B. Klevens and J. R. Platt, J. Chem. Phys., 17, 470 (1949).

303. R. W. Wagner, Ph. D. Thesis, Michigan State University, 1971.

304. E. Vander Donckt, Bull. Soc. Chim. Belges, 78, 69 (1969).

305. G. Yagil, J. Phys. Chem., 71, 1034 (1962).

306. J. W. Bridges and R. T. Williams, Biochem. J. 107, 225 (1968).

307. J. Longworth, R. Rahn, and R. Shulman, J. Chem. Phys., 45, 2930 (1966).

308. T. K. Adler and A. Albert, J. Chem. Soc., 1794 (1960).

309. M. A. El-Bayoumi, Ph. D. Thesis, Florida State University, 1961.

310. K.C. Ingham, M. Abu-Elgheit and M. A. El-Bayoumi, J. Am. Chem. Soc., 93, 5023 (1971).

311. K. C. Ingham and M. A. El-Bayoumi, J. Am. Chem. Soc., 96, 1674 (1974).

312. H. A. Benesi and J. H. Hildebrand, J. Am. Chem. Soc., 71, 2703 (1949).

313. R. L. Scott, Rec. Trav. Chim., Pays-Bas, 75, 787 (1956).

314. E. Bowen and D. Seaman, Luminescence of Organic and Inorganic Materials, Kaleman and Spruch Editors, Wiley N. Y. 1962.

315. E. V. Viktorova, Opt. Spectry. 22, 206 (1967).

316. M. S. Walker, T. W. Bednar, and R. Lumry, in "Molecular Luminescence", E. C. Lim editor, Benjamin, N. Y. 1969.

317. L. I. Grossweiner and H. I. Joschek, Adv. Chem. Ser., 50, 279 (1965).

318. R. W. Ricci, Photochem. Photobiol., 12, 67 (1970).

319. E. P. Busel, T. L. Bushaeva, and E. A. Burshein, Optics and Spectry., 29, 268 (1970).

320. M. S. Walker, T. W. Bednar, R. Lumry and F. Humphries, Photochem. Photobiol., 14, 147 (1971).

321. E. P. Kirby and R. F. Steiner, J. Phys. Chem., 74, 4480 (1970).

322. P. K. Glasoe and F. A. Long, J. Am. Chem Soc., 64, 188 (1960).

323. R. B. Martin, Science, 139, 1198 (1963).

324. E. L. Wehry and L. B. Rogers, J. Am.Chem. Soc., 88, 351 (1966).

325. E. J. Bowen, Disc. Faraday Soc., 27, 40 (1959).

326. E. C. Lim, J. D. Laposa, and J. M. H. Yu, J. Mol. Spectry., 19, 412 (1966).

327. Th. Forster, Chem. Phys. Lett., 17, 309 (1972).

328. S. G. Schulman and P. Liedke, Z. Physik. Chem., N. F. 84, 317 (1973).

329. W. H. Perkin and G. Revay, J. Chem. Soc., 228 (1894).

330. M. M. Robinson and B. L. Robinson, J. Am. Chem. Soc., 77, 6554 (1955).

331. N. S. Potts, J. Chem. Phys., 20, 809 (1952).

332. J. F. Holland, R. E. Teets, and A. Timnick, Anal. Chem., 45, 145 (1973).

333. W. R. Ware, in "Creation and Detection of the Excited States" Vol. 1A, A. Lamola Ed. Marcel Dekka, N. Y. 1971.

334. T. Melinger, and F. Wilkinson, Trans. Faraday Soc., 62, 1785 (1966).